Applications of

Dispersive Optical Spectroscopy Systems

Applications of Dispersive Optical Spectroscopy Systems

Wilfried Neumann

SPIE PRESS
Bellingham, Washington USA

Library of Congress Cataloging-in-Publication Data

Neumann, Wilfried.
Applications of dispersive optical spectroscopy systems / Wilfried Neumann.
pages cm
Includes bibliographical references and index.
ISBN 978-1-62841-372-4
1. Optical spectroscopy. 2. Optical spectrometers. I. Title.
QC454.O66N478 2015
543'.5–dc23

2014032115

Published by

SPIE—The International Society for Optical Engineering
P.O. Box 10
Bellingham, Washington 98227-0010 USA
Phone: +1 360 676 3290
Fax: +1 360 647 1445
Email: spie@spie.org
Web: http://spie.org

Printed in the United States of America
First printing

SPIE.

Table of Contents

Preface

My search for universal and comprehensive literature on dispersive optical spectroscopy revealed many gaps. The books with very basic information are rather theoretical and dig deep into arithmetic derivations to calculate spectrometers, illumination, and detection. The majority of books about the different applications of optical spectroscopy are either very theoretical or are "cookbooks" that do not explain the rationale for doing something a certain way. Even though several books bridge the gap between background knowledge and instrumental realization, I found none that combines the different techniques. The books with comprehensive content (available from the vendors of dispersers, spectrometers, detectors, and applied systems) naturally feature the advantages of the supported products, but they rarely offer an overall view.

For more than twenty years, I have calculated and delivered special dispersive spectroscopy systems for different applications. In the time between inquiry and decision, customers wanted to justify my presentation and compare it. A common problem was finding useful references to verify my calculations and predictions. So, I often wrote long letters combining the different parameters of the project. Several of my customers—industrial project managers as well as researchers—not only acknowledged the proposals but also often used the papers to check the instrumental performance at delivery. Because the proposals fit the requirements, and the predictions were at least reached, their confidence was earned. Customers used my papers for internal documentation and teaching.

Several asked me to provide the knowledge in a general, written database in order to encompass the theory, practice, and applications. After my retirement from regular work, I did just that and published my writing on my homepage (www.spectra-magic.de). The content has since been improved and extended into a pair of books, the second of which you are reading now.

This volume complements my previous book, *Fundamentals of Dispersive Optical Spectroscopy Systems* (SPIE Press, 2014), which describes and evaluates the parameters relevant to spectrometer systems, as well as the most important equations and their interpretation for dispersion elements, basic spectrometer concepts, illumination, light transfer, and detection. In principle, it also

combines the parameters of the components into function groups (building blocks) and performance curves; however, it only briefly touches on the requirements of the multiple, and very different, applications in optical spectroscopy. Separating the fundamentals and applications was necessary to keep the topics manageable and concise.

It is not the goal of this book to introduce the chemistry, biology, or physics behind applications. The theory is only discussed if it is required to discuss spectrophotometric parameters. Like every other kind of technical equipment, a certain solution benefits the user the better it fits the application requirements. Thus, it is useful to connect measurement needs and the available technology.

The aim of this book is to supply students, scientists, and technicians entering the field of optical spectroscopy with a complete and concise tutorial; to offer background knowledge, perspective, and technical details to system designers for reference purposes; and to provide an easy-to-read compendium for specialists familiar with the details of optical spectroscopy. The technical requirements are developed and converted or compared with existing solutions. In some cases, nonexistent "ideal" or "optimal" systems are defined because they will help determine what compromise must be made for the planned system. These comparisons can help estimate whether an experiment is possible by dispersive optical spectroscopy and within what limits. Engineers and laboratory technicians may support their work with background information about typical systems or—if required—justify existing systems with respect to other applications.

Acknowledgments

My thanks are first addressed to my wife, Heidi, for her patience during the months spent investigating, reviewing, and writing. I also thank those who urged me to start writing in the first place and who collected data and calculations. It is my pleasure to thank the numerous customers who challenged me with requirements not fulfilled by systems offered on the market, and their trust to buy systems without possible previous tests. I also appreciate the companies that employed me for over 30 years and supported my ideas and plans to implement the special systems. After the manuscript was given to SPIE, external reviewers spent much effort on the content, providing corrections and suggestions for improvement; that valuable support came from Mr. Robert Jarratt and Dr. Alexander Scheeline. Last but not least, I'd like to thank Tim Lamkins, Scott McNeill, and Kerry McManus Eastwood at SPIE for the work they invested into the project. I hope that readers will find useful details that further their interest or work.

Wilfried Neumann
December 2014

Glossary of Symbols and Notation

A	Absorbance (extinction) in photometric absorption measurements
A	Geometric area
A	Light angle inside a prism
ADC (A/D-C)	Analog-to-digital converter
A_{iG}	Effective disperser area at a given disperser angle
A_{iM}	Illuminated area of the focusing mirror
B	Bandwidth
C	Capacity
C	Contrast; ratio of useful signal/disturbance
c_0	Speed of light
CCD	Charge-coupled device
d	Deflection angle at the prism
d	Dispersed beam after a grating
D^*	Numeric capability of an IR detector for the recovery of low signals
dB	Decibel
d_x	Focus displacement after thermal change
d_y	Focus increase after thermal change
e	Base of the natural logarithm
E	Deformation factor at the exit of a spectrometer
$\bar{e}$	Electron
$E_{(\lambda)}$	Irradiance of a light beam on a normalized surface
el	Elbow angle
eV	Electron volt
f	Focal length
f	Frequency
f_c	Angular frequency
FSR	Free spectral range
FWHM	Full width at half maximum
h	Planck's constant (6.626×10^{-34} Js)

h	Slit height
H	Total aberration
hb	Number of pixels binned together
I	Parallel incident beam to grating or prism
i_1	Angle of the prism's incident light related to N
J	Joule
k	Absorption coefficient of a material
k	Boltzmann's constant (1.381×10^{-23} JK^{-1})
k	Grating constant for the distance of the grating lines
K	Kelvin
K	Thermal dilatation coefficient
L	Inductivity
L	Luminosity, light flux in spectrometers
$L_{(\lambda)}$	Radiance
LN	Liquid nitrogen
m	Modulation factor in lifetime measurements by phase/modulation
m	Spectral order number
M	Magnification factor
M	Radiant emittance/exitance
MCP	Microchannel plate; also, microchannel-plate image-intensifier system
m_s	Minimum slit width
n	f-number
n	Refractive index
n	Total number of lines in a grating
N	The normal of a grating or prism
O	Aberration
O_1	Basic aberration
O_{ss}	Additive aberration
P	Power
PMT	Photomultiplier tube
PPS	Pulses per second; also, events per second
PSD	Phase-sensitive detector (in the lock-in); also, position-sensitive (counting) detector
Q	Energy of radiation R; also, the numerical resolution
Q	Ratio of the numerical resolution R_r/R_p
Q	Quality factor
QE	Quantum efficiency
r	Radius of curved slits; also, the distance of the slit to the instrument's center
R	Normalized reflectance of a sample
R	Numeric resolution
R	Resistance

RD	Reciprocal dispersion
ROI	Region of interest
R_p	Theoretical resolution of a dispersing element
r_p	Absolute value of parallel polarization
R_r	Real experimental resolution
r_s	Absolute values of perpendicular polarization
s	Constant of thermal diffusion
SL	Number of vertical lines of a CCD
SNR (S/N-R)	Signal-to-noise ratio
sr	Steradian
SR	Number of horizontal register pixels of a CCD
STD	Standard deviation
T	Temperature; also, thermal change
T	Normalized transmission in photometric applications
w	Median distance of a mirror to the center line or grating center axis
W	Active grating or mirror width
W	Electrical or optical work
x	Geometric dilation as a function of thermal change
x	Half the inclusion angle at the grating
y	Geometric increase of the focal spot as a function of thermal change and dilatation
α	Angle of the light illuminating the grating or prism with respect to N
β	Angle of the diffracted or refracted light leaving the disperser with respect to N
δ	Inclusion angle of the light at the disperser originating from the lateral distance and width of the mirrors
δ	Phase angle or phase shift ellipsometry (SE)
Δ	Imaginary part of ellipsometric data
ε_1	Angle of the grating-impinging beam
ε_2	Angle of the beam leaving the grating
ι	Internal off-axis angle
ι_h	Horizontal off-axis angle in a spectrometer
ι_v	Vertical off-axis angle in a spectrometer
λ	Wavelength
ν	Oscillation frequency of a light wave
$\tilde{\nu}$	Frequency of a light wave presented as a wavenumber
ρ	Complex result of ellipsometric data
σ	Statistical parameter often used for deviations
τ	Time constant
Φ	Angle of sample illumination in ellipsometry
Φ	Median grating angle

Φ	Phase angle/phase shift in phase/modulation lifetime measurements
Φ	Radiant power/flux
Ψ	Real part of ellipsometric data
ω	Angular frequency
ω	Normalized cone angle of illumination
Ω	Acceptance angle
Ω	Real and normalized aperture of a spectrometer; also, light-guiding factor

Chapter 1
Transmission, Absorption, and Reflection Measurements

1.0 Introduction

The interaction between light and matter may lead to the following effects:

1. Transmission without interaction;
2. Reflection without absorption effects;
3. Transmission and/or reflection, where the light changes the energetic state of the sample; and
4. Transmission and/or reflection with light scattering effects at the sample.

The law of conservation of energy states that the light transmitted through any sample, plus the sum of reflections by the sample, results in the factor 1 of the energy introduced:

$$T + R = 1. \tag{1.1}$$

The law does not account for the fact that transmitted light may be refracted, diffracted, or scattered by the sample. It also does not consider that absorbed energies may appear in the beam as luminescent signals. Similar effects can modify the reflected light beam. If one precisely measures both the transmission and reflection of a sample, the sum may be <1, having no error in measurement; however, if the result turns out to be >1, one would have a *perpetuum mobile* (perpetual motion machine).

1.0.1 Principles

A measurement of the integrated or wavelength-dependent light flux in front of and after a sample will reveal no difference in case 1. From a practical perspective, this scenario does not always apply, as shown in Fig. 1.1.

The figure illustrates the interactions between light and matter. The left side shows the possible effects of a light beam impinging a transmitting sample. A beam of collimated light e_0 hits the sample or the sample

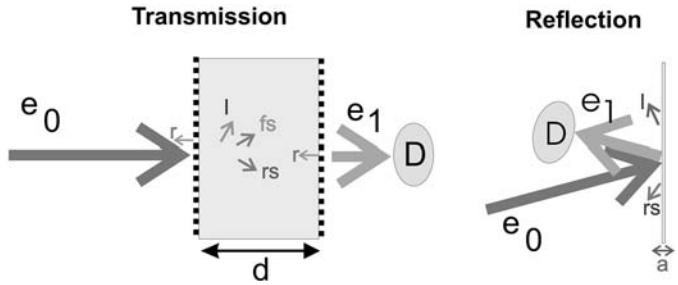

Figure 1.1 Interactions of light and matter.

container at a perpendicular angle. Reflections *r* may occur at the front surface and again at the rear. Besides the light loss due to absorption, the sample may scatter some light without changing the photon energy *fs*. It may also scatter light at a different state of energy/wavelength *rs*. The light signal e_1, arriving at the detector, may therefore not only be modified by absorption of the primary sample, but also the absorbed optical energy will lift the sample to a higher energetic state, primarily resulting in sample heating. However, the absorbed energy may also produce a higher state of sample excitation and "later" lead to luminescent light *l* (i.e., fluorescence). In this case, it is important to remember that the part of luminescent light that travels in the direction of the measurement beam may enhance the signal e_1.

When looking at reflection experiments, the same principal effects may occur, and the deeper the experiment light penetrates into the sample surface *a*, the stronger absorption effects (light losses) will modify the signal. It is rather difficult to differentiate these effects from reflection losses. The bandwidths required for a good analysis may be very different. If the goal is the absorption of the atomic contents of the sample, analyzed qualitatively and/or quantitatively, the sample needs to be transferred into the gaseous state. The measurement then occurs only at known atomic lines, supported by light sources, such as hollow cathode lamps (HCLs), that provide only the required, extremely narrowband spectral lines. The necessary monochromators act more like a filter than a disperser. Special requirements like that are provided by special instruments, e.g., atomic absorption spectrometers (AA, AAS). If the molecular state of a sample is the subject of measurement in the molecular state, a contiguous spectral analysis is required, and spectrophotometers with a wide wavelength range and bandwidths of >0.01 nm will fit. Some of the most-prominent absorption setups are discussed in this chapter.

1.0.2 Absorption measurements

Absorption measurements are almost always used to characterize liquids and gases, whereas reflection measurements are overwhelmingly used

for solids and colloidal samples. The transmittance T (the normalized transmission) is

$$T = [(e_1 - BG)/(e_0 - BG)], \tag{1.2}$$

where e_0 is the optical measurement signal entering the sample, e_1 is the optical signal leaving the sample, and BG is the so-called background, which includes all environmental signals that occur in the detection system and the electronic channel.

The pure absorption signal is created by the absorption coefficient of the sample material at the actual optical energy (wavelength) and the pathlength of the light through the sample. Lambert and Beer have proven that the magnitude of absorption increases in a logarithmic fashion with the pathlength. They called the result *extinction* (annihilation). Unfortunately, in the U.S., the use of that expression has been replaced by the word *absorbance*, which is not ideal because of potential confusion with *absorption*. The latter is the effect, and the former is its value. In the literature before about 1960, including that from the U.K., the nomenclature was absorption for the effect, absorbance for the normalized linear value, and extinction for the normalized, inverted logarithmic value. Thus, the concepts were easily understood and separated. Regardless, the American expression will be used herein.

The calculation of absorbance is

$$A = -\log_{10}[(e_0 - BG)/(e_1 - BG)]. \tag{1.3}$$

A single measurement will not produce the value of absorbance A, which is a dimensionless number called an absorbance unit (AU). At least two data collections are required, as well as the calculation of the logarithmic ratio. A primitive setup would require two measurements with a sample change in between. Spectrum e_0 represents the behavior of the system, including the reference solution. Spectrum e_1 is the unknown sample placed in the same or identical cell and solution. The method becomes elegant when the spectrophotometer system has two sample positions and the result is directly calculated at each wavelength.

1.0.3 Reflection measurement

Measurement of the reflection is based on the theoretical case where light does not penetrate the sample surface, and thus no absorption occurs. The resulting value is therefore linear, and, if normalized to 1, is called reflectance, which is given by

$$R = [(e_1 - BG)/(e_0 - BG)], \tag{1.4}$$

where R is often presented as a percentage.

The procedure is more or less the same as that for the absorption measurement. One main difference is found in the reference sample, which will

have a known reflectance at the required spectral positions. The measurement is aggravated by three parameters:

1. It will, in reality, not be possible to bring both beams into a zero-degree configuration because guiding the beam is more complicated;
2. Reflections have an impact on the polarization of the light, which may change the result; and
3. In almost all cases, the light will slightly penetrate the sample surface, even by only a few atomic layers, which means that the result may include some minor absorption components.

1.1 Techniques for Static Absorption Measurements

A single-beam instrument is straightforward: the light source, monochromator, sample, and detector are in a row, as shown in the top-left of Fig. 1.2. The number of components is minimal, providing more efficient use of the available light power compared to double-beam systems, which are shown on the right of Fig. 1.2. Systems like the upper pair will only work with monochromatic light, taking advantage of the fact that the sample will be loaded with the minimum amount of photon energy. Because the detector is mounted rather close after the sample (collection optics may be added in between), all light passing through the sample will be recovered—even small modifications of the beam shape, created by the sample, will not be detrimental.

The lower pair of systems disperses the light after the experiment, which has the advantage that the spectrometer can be used as either a monochromator or a spectrograph; the detector will be chosen accordingly, and in some cases both techniques are provided. The trade-off for the increased flexibility is that the sample receives the full spectrum that is passed through the spectrometer. Therefore, the light power at the sample is

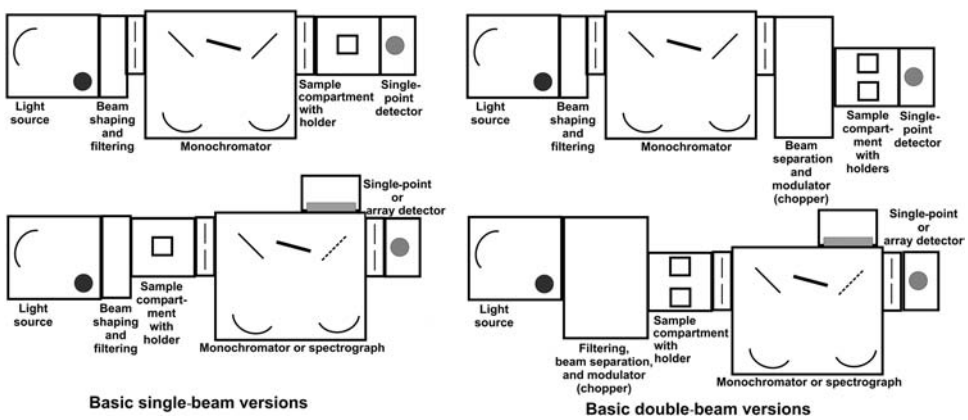

Figure 1.2 The basic spectrophotometer in four different versions.

several orders stronger than in the upper case, even when filtered. Furthermore, if the sample modifies the beam's shape or travel, the spectrometer will not be correctly illuminated, which produces errors in the measurement. The data-handling system of a single-beam instrument has enough memory for the reference measurement, sample measurement, background, and final result. A double-beam system will (in almost all cases) create the background, reference, sample signals, and the resulting data point in real time. In the course of deciding whether to use a single-beam or double-beam spectrophotometer, some basic considerations may be helpful.

Single-beam spectrophotometers use the available light better, and they provide the required SNR in less time than double-beam systems. Time-dependent measurements (such as kinetics, flowing or moving samples, etc.) often deliver better results in single-beam configurations. When a double-beam system is used for time-critical measurements, it will probably work in single-beam mode, but it will still be slower. Single-beam spectrophotometers cannot compensate for any signal change caused by the system itself during the entire routine of recording the reference and sample. That basic behavior holds true for both scanning and parallel detection.

A double-beam instrument comprises many more components, which lowers the light flux and increases the measurement time for a comparable SNR, but all signal changes that occur during data acquisition that are not created by the sample, cuvettes, solvents, etc. are compensated. If the result is in doubt, a double-beam unit can take a data set with the sample and reference transposed. The two results will only differ in the sign of the transmission or absorption (not absorbance) value. If that is not the case, something is wrong with the system or the experiment and must be sorted out. A single-beam instrument does not offer that test method. Although a single-beam system can by no means simulate a double-beam instrument, any double-beam spectrophotometer works in single-beam mode.

1.1.1 Technical realization of an optimal spectrophotometer for absorption and reflection

As shown in Fig. 1.1, the value of absorbance includes many parameters, some of which are competing with each other. Furthermore, many users are interested in a large dynamic range. The instrument should provide a wide wavelength range and be able to measure very small absorption values in the presence of very large ones.

The technically feasible wavelength ranges are defined in the *Fundamentals* book.[2] With that knowledge, it is possible to realize a range of $\sim$150$-$3200 nm with a single instrument. There is no need to look for a system in the deeper IR because that is the domain of Fourier-transform (FT-IR) systems. Below 190 nm, the absorption of air would require evacuating the entire beam travel or purging it with dry nitrogen. The range above 1100 nm suffers from the absorption of water in the air; nitrogen purging reduces that,

too. The range below 150 nm is called the extreme UV and is reserved for special instruments. The term "optimal" in this section refers to the accuracy, repeatability, and fidelity of spectral data, while time considerations follow later. Thus, to begin, double-beam systems that perform direct ratio recording (DRR) are reviewed.

1.1.2 Detection range at the wavelength and signal scale

The detection limit of an absorption spectrophotometer is defined by the smallest difference measurable and safely recorded near the zero absorbance value (0 AU, or 100% transmission). The technical limits are set by the statistics of photons and the short-term stability of the light source. On the other hand, the internal noise and stability of the detector and measurement electronics apply equally. (See the chapters on light sources and detectors in *Fundamentals*.[2]) If one wants to publish results with errors or uncertainties of less than 1%, the reproducibility must be within 10^{-4} AU, which, in turn, requires transmittance values within ± 0.00023. At the other end of the scale, high values of absorbance mean that very little light arrives at the detector. That limit is given by two parameters: (a) the variation of the background signal, created by the detector and associated electronics, can create fake signals, and (b) the stray light created by the spectrometer itself. Light of different wavelengths, effected by very different absorption, may be directed through the sample and to the detector. If that happens, additional light will arrive at the detector and produce lower absorbance values than those created by the sample at the assumed wavelength. If the system must be able to represent a linear range of 3 AU at a maximum error of 1%, the stray light must be kept below 10^{-5}, which is not possible with a single-stage monochromator covering wide wavelength ranges. The best instruments are equipped with a double monochromator (see Section 4.3 in *Fundamentals*[2]), provide stray light $<10^{-8}$, and allow absorbance ranges of up to 5 or even 6 AU. If the full-scale output of the electronic system is 1 V, then 6 absorbance units are represented by only 1 μV. To present data within 1%, the system noise must stay below 10-nV RMS, which represents the realistic limit in the best systems available.

1.1.3 Data-acquisition methods

Section 5.6.3 of *Fundamentals*[2] proves that a lock-in-based detection system, working with alternating signals, provides data stability orders better than a DC system. For the simultaneous data acquisition of two samples (sample and reference), alternating light is automatically required. In a spectrophotometer, the light is split by mechanically synchronized mirror systems and guided through two identical channels. The system incorporates a third, dark phase to capture the background *BG*. The dark phase may occur once or twice per cycle; thus, the full sequence includes "Dark = *BG*," "Reference = e_0," and "Sample = e_1." The three signals are separately integrated and stored,

and the processor creates for each single wavelength the complete result $A = -\log_{10}[(e_0 - BG) / (e_1 - BG)]$.

If the transmission or reflection data are wanted, the result becomes $R = [(e_1 - BG) / (e_0 - BG)]$. Many instruments also allow for the collection of data from only one of the optical channels, a process called single-beam acquisition, which creates $S = (e_1 - BG)$. In any mode, if AU values near 0 (100% T) are recovered, then the accuracy can be improved through the time applied per data point (integration time, or number of integrations combined with averaging) or by increasing the light flux to improve statistics. Each measurement cycle, consisting of three or four intervals—(e_0, BG, e_1) or (e_0, BG, e_1, BG)—will be collected with predefined parameters, and the optimal parameters can be found in a test run. Modern systems do not take data and change wavelength at the same time; they do one at a time (the so-called stepped scan) and work completely with digitized data. Older instruments use analog sample-and-hold circuitry and capture synchronized data with a wavelength scan. So long as the scan runs rather slowly (<0.03 bandwidths per data point), there is no disadvantage to digital systems. Thus, data created by "old" instruments are not necessarily worse. The rotating mirror system—the chopper—is probably the most-important component in the data acquisition. It splits the light symmetrically, guides it through the two channels, and blocks it in between (BG). From the chopper, an optical sensor creates the control signals, which splits the detector output and processes the signals separately. Systems of high value provide a symmetric beam configuration, comprising dual synchronized choppers, to realize optimal beam separation and efficiency. Whether the system has one or two dark phases per rotation is not important. Figure 1.3 presents one full cycle in a spectrophotometer with three-phase DRR.

The system creates three intervals: R to illuminate the reference channel, BG to capture the background with no light at all, and S to illuminate and collect the sample light. Because of the size of the light beam at the chopper, there are times between the phases with crosstalk and overlap. The active time of the signal integrator is adjusted such that data are only taken during the stable time of each phase. In the example, 25% of the theoretical channel time is lost by overlap plus some safety time. A three-phase chopper runs

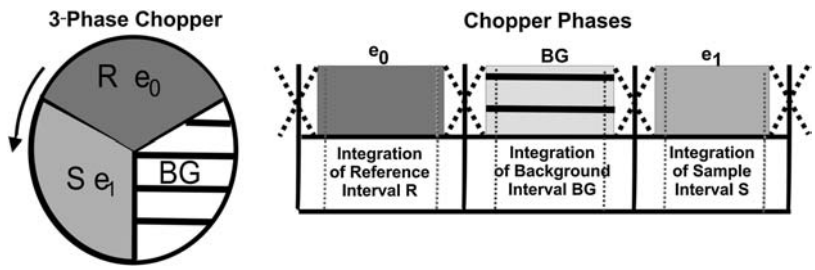

Figure 1.3 Three-phase chopper system that rotates counterclockwise.

asymmetrically, so it is harder to balance. Four-phase choppers are symmetric and easier to balance; however, the total loss in integration time is higher (e.g., 33% per phase). A cycle will start with the integration of the reference signal e_0. If that value is between 30–100% of the linear range of the detector, it will proceed and integrate the dark value *BG* in the same cycle, as well as the sample signal e_1. If the reference signal is outside the required range, a fast calculation of improved settings will follow. Several parameters can be applied. If the detector is a PMT, the high voltage (alternatively, the pre-amp gain) can be modified. If the detector is solid state, only the pre-amp gain can be changed. Some systems also offer the option to change the slitwidth, which will keep the SNR constant but is much slower and not possible within one cycle.

As soon as the reference signal is in the optimal range, the parameters are fixed, and all three or four integrations are performed and stored. The number of cycles that are required to optimize the SNR is again defined by the pre-definitions, which can be optimized for time, precision, SNR, or bandwidth. After the integrations are stored, the absorbance or transmission/reflection value is calculated and stored. The wavelength is then changed, and the whole process starts over. Therefore, it is not trivial to pre-calculate the time for a complete scan, and it turns out that all parameters of the spectrometer and detector system run into the signal and its SNR. The user will have direct control over several of the parameters, but others will be subsequently set by the program. The slitwidth, along with the lamp, defines how much light enters the spectrometer; the integration time per data point may influence the precision, and so on. The reference sample may create remarkable differences in absorption over wavelength, which combine with the light flux and detector sensitivity at a given wavelength. For special requirements, there is no disadvantage if the system provides a look-up table of the parameters used point by point or if it works according to a predefined table. If the stray light can be neglected, high absorbance values in the sample can be recorded over short wavelength intervals by applying compensation techniques. If, at strongly absorbing samples, the sample data will appear noisy and/or have bad reproducibility, and if variation of the slitwidth and integration time do not offer the required improvement, a known reference with high absorbance (called bias) can be used. This action will automatically force the control system to adapt to the low light level at the detector, and the difference between e_0 and e_1 will be minimized, leading to improved precision. The bias absorbance must be added to the measured result later.

1.1.4 Light path and spectral disturbance

The light path incorporates many optical components that interact with the light: windows, lenses, mirrors, sample cells, fiber optics, and others. If the right materials and coatings are not used, they may be the source of spectral interferences, e.g., superimposed fluorescence created in glass, fiber optics, or mirror coatings. When constructing a system, it is important to discuss

possible impacts with suppliers in order to preclude them. During operation, all of the components need protection from dirt because otherwise (besides loss of efficiency) it may be the source of fluorescence problems. Many of the materials create (by their nature) Raman and/or Brillouin signals that cannot be completely suppressed. However, the user should be aware of them and their position relative to the excitation beam. Clever selection of materials is always helpful.

1.1.5 The optimal spectrophotometer

Given what may happen at the sample and within the measurement system, a highly flexible and modular setup can address many different tasks, and a high-performance spectrophotometer is one such setup. Under the homogeneous-looking housing, different building blocks are combined; the higher the required flexibility is, the more modular the system. Naturally, the light sources, the double-monochromator components, and the detectors will be selected such that the system will provide a basic signal that is as flat as possible. But where does the double monochromator go? If it is placed in front of the sample compartment, then the sample and reference will only be burdened with a little light power from a rather small band of optical energy. That is good, and it will not be difficult to create a pair of beams that run collimated for ~12 cm through the sample housing and create data close to reality. If the sample (at the actual wavelength) is not perfectly clear, it will scatter the light, depending on the measurement requirements (if only the collimated part of the light will be collected and analyzed, or if a certain angle of scattering will be integrated). Signals created in the sample by luminescence effects are unwanted in any case. Note that systems that fulfill those requirements will not be optimized for short measurement times. The end result is a concept like that shown in Fig. 1.4.

The optimal spectrophotometer, in terms of fidelity of results, comprises two light sources, a double-illumination monochromator, a detachable and flexible sample module (including housing and beam guiding), a single-stage emission monochromator, and at least two detectors.

A system like that is not commercially available from the suppliers of analytical instrumentation; however, it is found in cleverly managed labs. The components include one D_2 lamp, one halogen lamp, and programmed switching of the mirror (MM), including the appropriate order filtering to illuminate the double monochromator that is equipped with three gratings per stage. An alternative is a combination of gratings in one stage and a prism in the other. The configuration is such that a minimum number of reflecting surfaces is required. Whether the spectrometer works additively or subtractively is not the first priority; it can be re-configured by software. The resulting module sample compartment/beam guidance will sit on a separate platform. Thus, different pre-adjusted platforms will be safe and easily detached and exchanged. The system can perform applications such as standard absorption

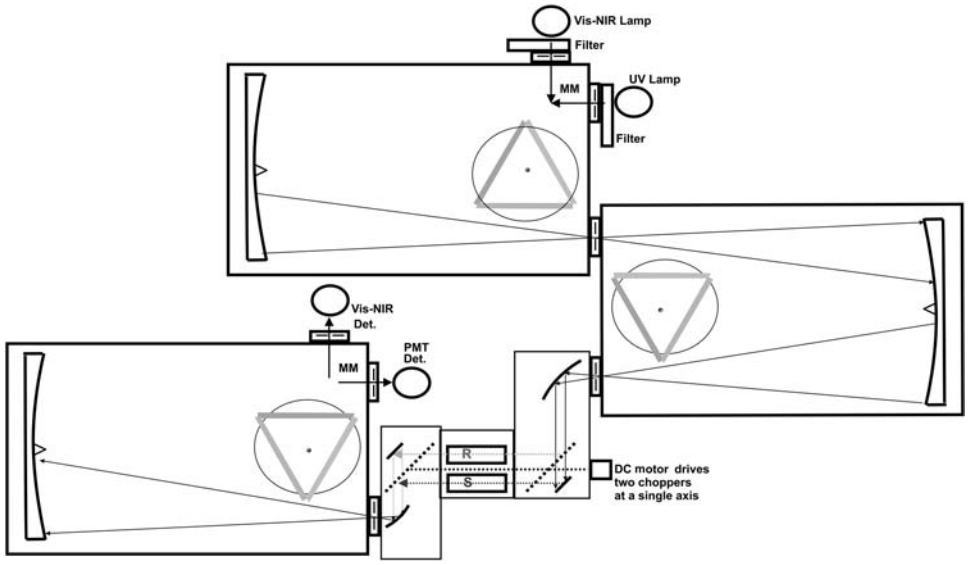

Figure 1.4 The optimal spectrophotometer.

with cell pathlengths of up to 10 cm, scattering experiments with an integrating sphere, and measurement of reflection. The sample *S* can receive extra illumination through the wall of the compartment, which is called "side illumination." This scenario may create luminescence or apply extra stress on the sample during measurement by lasers. Thermostatic control of the sample and reference, stirring, sample changers, etc. can be added.

1.1.6 A standard high-performance spectrophotometer

If a disturbance caused by luminescence or other overlaying effects, which would appear at other wavelengths than the one selected, can be neglected or does not really appear, the monochromator between the sample compartment and detectors can be removed. That will streamline the whole system and more closely match systems that are available (like that shown in Fig. 1.5).

Without the emission monochromator, the system provides higher flexibility and a better SNR. Two gratings may be sufficient to cover 190−3000 nm; the light sources and detectors stay the same. If scattering samples and/or references are the subject of measurement, the angle of light recovery after the sample compartment can be made adjustable within a much wider solid angle. This scenario is possible because of the wide acceptance angle of the detector compared to the emission monochromator in between, which partially compensates for scattering or any angular deviation of the beam in the sample. Again, the construction of the sample compartment should be very flexible. However, without extra filtering, the setup cannot discriminate wavelengths, which may lead to false measurements.

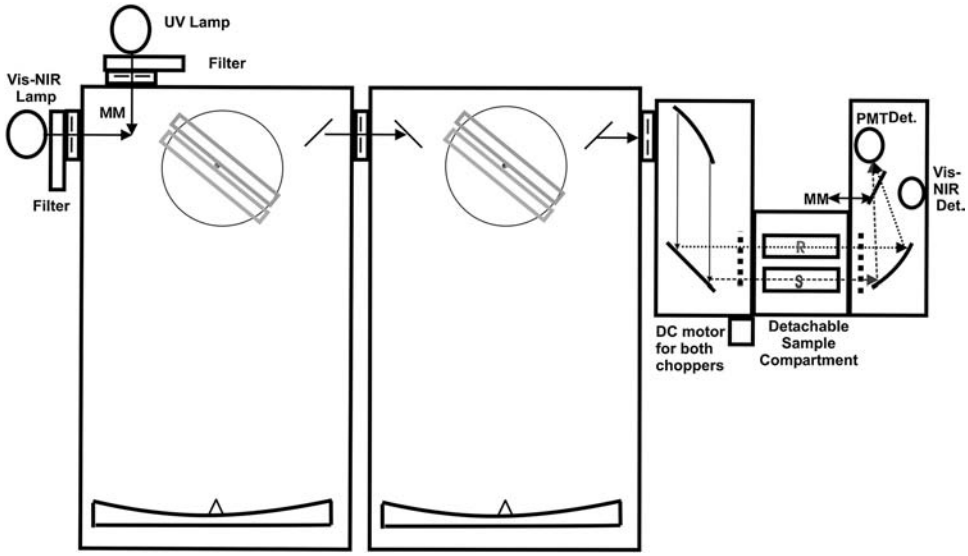

Figure 1.5 Outline of a standard double-grating spectrophotometer.

An alternative version uses a prism and gratings as dispersing elements. Applying a prism in one of the stages (often the first one) will have advantages and disadvantages:

Advantages

- The prism does not know spectral orders, and the order filter set becomes obsolete. It has a very high efficiency (80–90%) that is distributed rather homogenously over the working range. One prism can cover the range of several gratings.
- The dispersion, and thus the resolution, is much higher in the UV than in the NIR, which is good for most real experiments because they also require a higher resolution in the UV. A grating works conversely.

Disadvantages

- The prism will always disperse; it is not possible to send "white" light through the monochromator. The dispersion increases strongly from the NIR toward the UV. In order to keep the dispersion and resolution near the same value, the slitwidth must be varied during a scan.
- It is impossible to configure the subtractive mode in a double monochromator where a prism is in one stage and a grating is in the other. The grating and prism need separate drives (but that is easy with modern, computer-controlled stepper motor systems).

1.1.7 Spectrophotometer with parallel wavelength detection

To make use of the time advantage of parallel detection, several constraints must be applied. The dispersion of light will need to occur behind the sample,

which means that at least the required spectral interval will shine on the sample. The sample and reference may act like lenses, which would likely modify the beam configuration. The stray light level of a spectrograph system, compared to a similar monochromator, will be much higher (a factor of 10–100 is a good guess). Compared to a double-monochromator photometer system, the stray light level increases by several orders. The wavelength range covered in one shot (the spectral dispersion) and the resolution are coupled together and are not independent parameters. If the measured interval stays within one spectral order, it is possible to avoid order overlay and errors. If it exceeds one octave, problems will arise. If the parallel detection is within two orders, clever filtering can help. If more than two orders are the subject of parallel measurements, only order filtering at the detector surface will avoid errors. The resulting drawback is a lack of wavelength variability—everything must be fixed. Optimization of the SNR is not possible at each measured wavelength; only the maximum signal wavelength in the reference channel can be optimized. The differences in the output signal may be partially balanced by binning the detector elements in the weak areas. This action may homogenize the output signal, but it jeopardizes the spectral resolution.

Parallel-detecting photometric systems are generally well suited to the range 0.01–0.7 AU. Their main advantage is found in comparative spectroscopy, where the "true" value is not required but rather a pre-defined result within given tolerances. Time-resolved experiments, quality control, production monitoring, and similar applications are performed very well with spectrograph systems. The reference beam may be obsolete, and time may be the dominant factor for measurement, data reduction, and storage.

Figure 1.6 illustrates the components of a complete dual-beam spectrophotometer with parallel detection. The light source housing hosts a D_2 and a tungsten-halogen lamp that are controlled separately (filters and shutters are optional, depending on the application). The light is collected by separate fiber systems and delivered to a fiber optic rod, which provides homogenized light at its output. One or two more fiber cables connect to the sample chamber (or experiment location), where mirrors convert the beam in a collimated fashion. The entry light illuminates a transmitting or reflecting

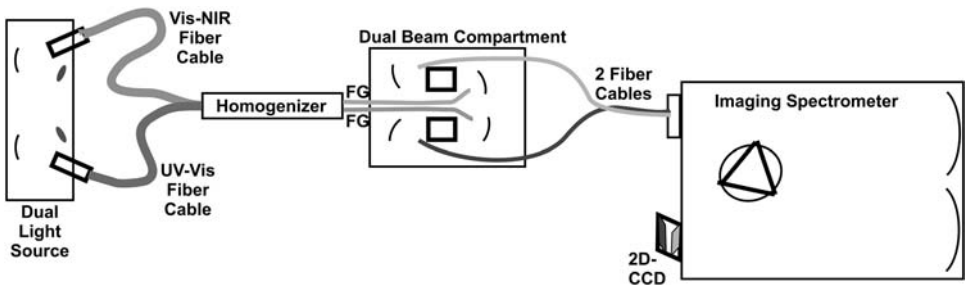

Figure 1.6 Components of an array-based spectrophotometer.

sample and probably a reference. After the sample (and reference), the light will be collected again and delivered to the spectrograph. That final fiber cable converts the cross-section. The experimental side will have a circular shape; on the spectrometer side, it will fit the shape of the entrance slit (see Section 6.7.5.1 of *Fundamentals*[2]). An optical adapter will produce the correct illumination angle for the spectrograph. In the case of dual-beam systems, the two signals will be separated in front of the spectrograph, travel along separate pathways to different areas of the 2D-CCD, and experience separate processing and storage (see Section 5.8.8).

The spectrograph may be equipped with more than one grating to allow some flexibility. The CCD will be selected for the proposed resolution, dynamic range, and read-out time. If enough light is available at the detector, actual systems will allow millisecond-scale repetition rates, which is also the time resolution of the spectra. Faster, higher time resolutions of spectra are provided by special setups, such as MCP-CCD systems, at the cost of reduced linearity.

1.1.8 Detection range on the wavelength and signal scale with parallel wavelength detection, and single-beam spectrophotometers

This section compares steady state systems (omitting phase-sensitive detection) with the high-performance systems described earlier. Steady state single-detector channel systems use the available light more efficiently than modulated systems. A shorter experiment time for the required SNR can be expected. In terms of fidelity, whether working in single- or double-beam mode, they cannot compete with chopped systems. Steady state systems suffer from all kinds of instabilities and $1/f$ noise. Furthermore, DRR spectrophotometers adjust the reference signal to be near optimal during acquisition "on the fly," something that a single-beam system cannot do. Some single-beam systems use a pre-defined matrix pattern to vary either the high voltage (HV) or the detector gain versus the wavelength to compensate for signal variations. This variation improves the SNR, but it will not compensate for transmission changes in the reference measurement.

Parallel detecting systems, either single or double beam, may also use pre-defined patterns to vary the number of pixels per data channel versus the wavelength to homogenize the reference signal, but only in very special cases can the illumination time or gain be varied by the pattern. Because the parameters involved are many, the impacts can be manifold. For both single-channel and parallel detection, it is not possible to present simulated examples and comparisons here. (The coherences are treated in Chapters 5 and 6 of *Fundamentals*.[2]) The time advantage of a single-channel/single-beam steady state system in comparison to chopped dual-beam systems can only be calculated if the required repeatability, accuracy, and tolerances are known. Therefore, this section defines the actual limits of systems with parallel detection because of their clear time advantage in comparison to the systems discussed so far.

The available detector technology limits the wavelength range and detection range of an absorption spectrophotometer with parallel detection. Under consideration are silicon arrays and CCDs for the range of ~200–1100 nm and InGaAs arrays and CCDs for 700 nm to 1650, 2100, and 2700 nm. (The key parameters of these detectors are discussed in Section 5.8 in *Fundamentals*.[2]) The important factors here are the limiting noise, the linear range, and the stray light. A typical limit for one read-out is a range of 16 bits, or 65,536 units (counts, or cts). Thus, 65,000 cts represents 100% *T*, or 0 AU. The remaining 536 cts are a reserve to mark an eventual signal overshoot. Whatever the light flux is, and the time required to produce the 65,000 cts, the noise will be the square root of it, which is 8 bits, or 256 cts. That value defines the limit of the linear range in a single read-out without further averaging. The resulting detection limit near 0 AU is 0.00167 AU, which is equal to 0.00394% *T*. If there is enough time to produce an average, that limit will improve with the square root of the number of averages; at the same time, the impact of instabilities and 1/*f* noise will increase. A final limit is not predictable—it can only be found experimentally. Typical detector systems are burdened by a total read-out and pre-amplifier noise of ~4 cts, which will not change the picture so long as the signal is reasonably high. Consider a case where the zero absorbance level is only represented by 1% of the detector's full scale, or 650 cts, which might happen at the deep-UV end in the presence of 800 nm and if the light is produced by a D_2–halogen combination. The 4 cts are still equal to only 0.6% of the signal, or 3×10^{-5} AU. The statistical noise is a source of larger counts, adding another 25 cts at a level of 650 cts, equal to 3.8% of the full scale (fs), or 1.65×10^{-4} AU uncertainty. However, if the 0-AU reference measurement was based on 65,000 cts and the absorption leads to a value of 2 AU, then the signal is also expected to equal 1% *T*. Therefore, the measured value of 650 cts would also carry a noise of 25 + 4 cts, or 4.5%. An uncertainty of 0.02 AU, or 1% of the true value, follows if no averaging is applied. If time is not the first priority, one means of improvement is to split the interval into several fractions, with different parameters, ensuring that the reference measurement creates >10% fs at every data channel. That amount may even allow for changing the gratings and filters between the intervals (at the cost of time, of course).

Even if the homogeneity of the reference signal satisfies the required accuracy and repeatability, the stray light impact may create problems. As described in Chapter 8 of *Fundamentals*,[2] the stray light at wide wavelength intervals may add fatal errors to the acquired data. It may guide light of different, unwanted, and unexpected wavelengths to the detector. That light may have experienced a very different absorption at the sample. If that happens, the measured wavelength is overlaid by additional light, leading to lower absorbance values than those created by the sample itself at the measured wavelength. If the system must be able to represent a linear range of 3 AU at a maximum error of 1%, the stray light should be kept

below 10^{-5}, which is not possible with a rather-short single-stage monochromator illuminated by wide wavelength intervals. A wideband spectrograph may suppress the stray light to a level of 10^{-3}, at best; that, in turn, would allow absorbance measurements of 1 AU at an uncertainty of 1%. Because not many spectrographs produce the mentioned stray light value of 0.1% or less, and the range of the optimal reference signal may be limited, the upper limit may instead be 0.7 AU. Again, splitting the spectral data range into several discrete intervals will be very helpful. All of the reasons listed thus far lead to the suggestion to not attempt measurements outside 0.01 and 0.7 AU with parallel detection and wide wavelength intervals in a single read-out.

1.1.9 Proposal for a universal sample chamber for dual-beam spectrophotometry

The proposed chamber, shown in Fig. 1.7, will have dimensions of 15 cm × 15 cm × 10 cm. The incoming and outgoing light must be collimated. The chamber's bottom provides adjustment pins for repeatable interchange of platforms. The design on the left is a construction for absorption measurements. The collimated beam may have a cross-section of 3–5 mm. The upper image illustrates the beam for 10–100-mm-pathlength cells; optional stirring and thermostatic control is possible. The lower image shows a platform for microcells equipped with pre-adjusted focusing lenses. The right part of the figure is a design for reflection measurements. The incoming and the outgoing beam at the sample or reference are within an angle of 15 deg to comply with the rules of specular reflection. Again, the upper part illustrates a version with parallel light, whereas the lower figure has focused light at the sample. Both top versions allow the application of two removable polarizers. Windows allow for purging of the chamber, and an extra entrance in the front wall allows for the application of "side light" on the sample.

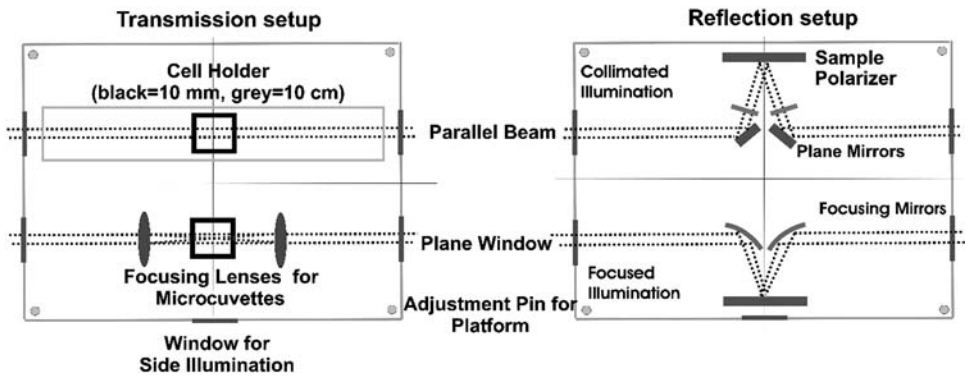

Figure 1.7 A universal sample chamber.

1.1.10 Calibration and the definition of stray light

The wavelength calibration of a spectrophotometer is identical to that of other spectrometers and is described in Chapter 7 of *Fundamentals*.[2] Sets are available to test for absorption linearity, which can be either solid state (filters) or a series of solutions. The measurement of scattered light is always proposed at the low end of the wavelength range because the probability of scattering errors is highest there, and intensities and sensitivities drop. For systems reaching below 210 nm, a cheap and easy method uses a potassium-chloride solution. A saturated, aqueous KCl solution absorbs below 220 nm but is transparent above that wavelength. In a 10-mm cell, the theoretical absorbance at 210 nm is 10 AU, which is beyond the access of any spectrophotometer. For example, if the measured value is 3 AU, the stray light is 0.1% (a value of 5 AU represents 10^{-5} stray light, and so on). If the system does not reach down to 210 nm, other solutions can be found that absorb at the low end of the wavelength range, combined with transparency above. Order-sorting and bandpass filters are not very suitable because they normally do not block better than 10^5 outside the absorbing range, which is well within the linearity range of a good double spectrometer. Regardless, special filters with better blocking are available.

1.2 Dynamic Absorption Measurements

In addition to static measurement, it is often interesting to learn how a sample behaves spectrally under external stress or what happens when two reagents are mixed. During the equilibrium and relaxation process, the spectral changes are recorded—sometimes a single wavelength provides enough information, sometimes multiple wavelengths are required to record the reactions, which are called kinetics. Typical kinetics follow *e*-functional changes over time.

Because it is often not possible to define the start and end of a kinetic function, it is helpful to note that the time constant of the function can be calculated in any region of the curve because $\log_{10}[dA/dt]$ is constant. If the absorption is recorded in AU units, it is easy to convert it into the log scale again, which is called a double logarithm. At any part of the curve that provides clear data, the kinetic parameter can be calculated. If the process was created by more than one kinetic function, it will result in a double-logarithmic curve that is not straight.

1.2.1 Typical experiments

Stopped flow

In stopped-flow experiments, two reagents are mixed in the measurement cell by flowing them through the mixing volume of the cell. After the mixture is assumed representative, the flow is suddenly stopped, hence the name. At that moment, the data acquisition of absorption data at single or multiple wavelengths starts. The "dead time"—the time between the trigger (stop of flow) and the beginning of the reaction—may need less than one or some milliseconds, while the

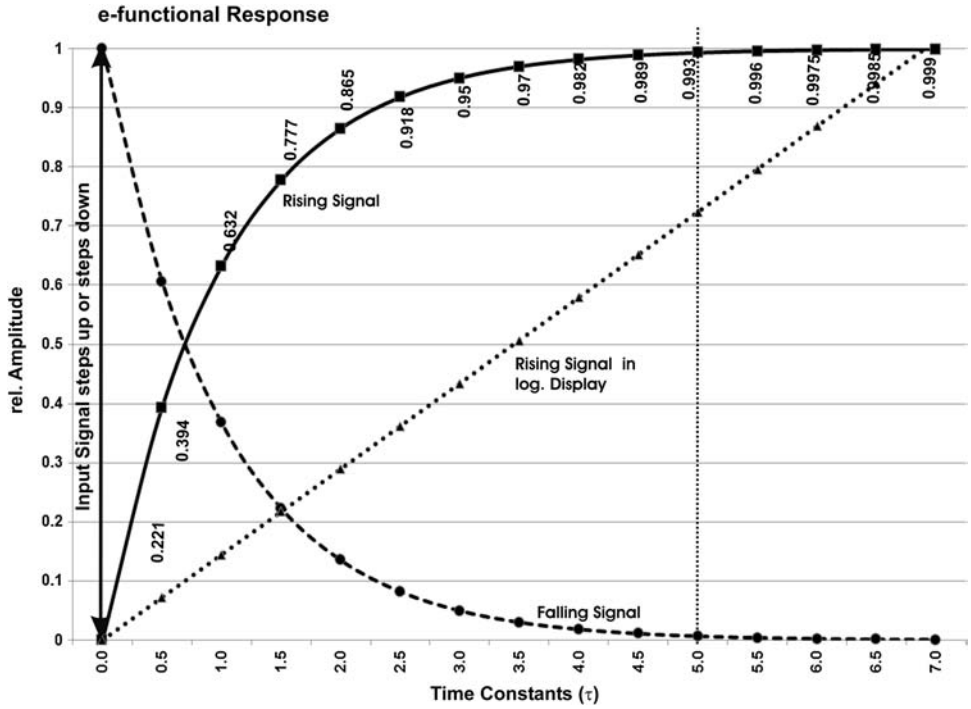

Figure 1.8 Time behavior of single kinetic processes.

reaction itself might require between <0.1 ms up to several seconds. The spectroscopic system must be versatile to adapt to that timing. A special requirement of stopped flow is that the reactions may not only happen in the standard UV–Vis range but also <190 nm. For biological samples, the polarization behavior might be even more interesting than the absorption. Most often, two or more wavelengths are required: the absorption maxima of both reacting partners. The created product may eventually have another, third maximum, and/or an isosbestic wavelength exists. The isosbestic point is a wavelength with constant absorption during the entire kinetic process. If it exists, it is an excellent reference to prove that the chemistry and data collection work well.

Stopped-flow experiments require time resolution in the microsecond range and enough memory for several hundreds of data sets. The measurement beam must be compatible with microcells sitting in an apparatus, such as thermo-jackets, magnets, or other voluminous machines. The spectrometer has a single beam with diode arrays and CCD for detection. Some setups use multiple single-channel detectors mounted to a Rowland spectrograph, as described in Section 2.5 of *Fundamentals*.[2] The single detectors provide high luminosity with fast acquisition. (Polarized deep-UV spectrophotometers are addressed in Section 11.3.2.) Because the steady state spectra of all reaction partners

and the final product can be measured in standard spectrophotometers, the photometric limitations (stray light, precision of data, spectral order overlay) of such a fast system are generally accepted.

Jump functions

These functions describe experiments wherein an external parameter changes its state quickly and the following spectral change is recorded. Typical changes are applied to the thermal status, to the externally applied magnetic or electric field, or the pH value, etc. The optical system may be identical to the one used for stopped flow; even microcells are often used. The kinetic measurements vary in the time range of microseconds to seconds.

Optically induced effects and pulse–probe measurements

If the sample is disturbed by a strong external light source and a spectral response follows, special requirements apply to the spectrophotometric system. Optically induced effects typically run fast, much faster than those described earlier. They reach down into the nanosecond range. Therefore, the measurement will need to use nanosecond-gating functions. The disturbance of the sample, in most cases, is realized by a short, intense laser or xenon-lamp pulse. To ensure that the measured absorption spectrum is loaded with a minimum (none, at best) amount of light from the external source, the optical path must be optimized. The detector's time control requires fast triggering and cleaning modes.

Technical requirements and configurations

Although static measurements in research rely on optimal precision and accuracy, it is more important in dynamic applications to recover the data quickly and accept the corresponding limits in precision. In many cases, the absolute value of the transmission or absorbance is not important but rather the change of the value over a well-defined time, such as $\Delta T/\Delta t$ or $\Delta A/\Delta t$. Thus, the configuration will become different from the static system. In the past, there were several single-wavelength spectrometers on the market equipped with a PMT. One version was the "rapid-scan" spectrometer, which was based on a grating monochromator with two identical gratings back-to-back. Quick rotation of the grating table created spectra "on the fly." Within some milliseconds, a full spectrum "flew" over the detector. A synchronized read-out system ensured that the correct wavelengths were put into an electronic multichannel analyzer for later processing. Another approach used a "dual-wavelength" spectrophotometer that was equipped with a monochromator with two gratings placed side-by-side. The beam travel guided the light along alternative pathways through the monochromator, and each one used one of the gratings. The chopper, which switched the two beams with up to 1 kHz, altered

the two wavelengths at the sample. That arrangement allowed for the recording of a pair of independent wavelengths within one millisecond. All of these systems are no longer in production, so the following will review systems with parallel detection.

The ability to detect all available wavelengths in a parallel fashion reveals a problem in the dynamic range and homogeneity of the detected range (as outlined in Section 1.1.3). A single-grating spectrograph with a silicon detector, combined with deuterium and halogen lamps and a measured range between 200−1000 nm, will barely provide a reference signal that reaches within 10−100% fs; a variation by a factor of 100 is more realistic, even if the mirrors, windows, and grating are optimized for the deep UV. Linearity and SNR problems should be expected. Splitting the wavelength range into several intervals is only an option for quick applications in rare cases because the repeatability of the experiment may not allow several measurements for one result. The shorter the required spectral interval is, the easier the spectrum can be flattened. An additional hurdle for application-oriented parameters lies in the fact that there are so many parameters involved in time-resolved absorption measurements that they can only be seen from a general perspective. There are some tools that can vary the spectral efficiency of an array, a CCD, or a CMOS device over the surface, which includes varying the size of a spectral channel by binning or by varying the height (CCD and CMOS) or the different exposure times (CMOS). However, with the exception of binning, all of these modes slow the read-out time. (The details are presented in Section 5.8 of *Fundamentals*.[2])

If the upper wavelength does not exceed 800 nm, the application of an MCP in front of the CCD or array is advantageous (see also Section 5.8). The spectral response of an S20 or S25 cathode will enhance the UV and thus partially compensate for the intensity overshot of the halogen lamp. Separating the exposure and read-out by the gating capability will improve most applications. The fact that the SNR at the highest signal may be worse compared to a bare silicon detector will, in most applications, not be critical. The diversity of applications will lead to systems that are also different in detail. The principle of a kinetic system is presented in Fig. 1.9.

The light source may be a xenon lamp or, as shown, a combination of halogen and D_2 lamps, which are combined with a 50% mirror. The light passes a 10% mirror that splits a part of the light to a reference detector to compensate for source variations. In the sample compartment, the parallel beam is focused on a very small area to illuminate a microcell. After that, the light is converted again to illuminate the spectrograph with an area detector, e.g., a diode array, a CCD, or even a CMOS device (see Section 5.8.10 of *Fundamentals*[2]). CMOS

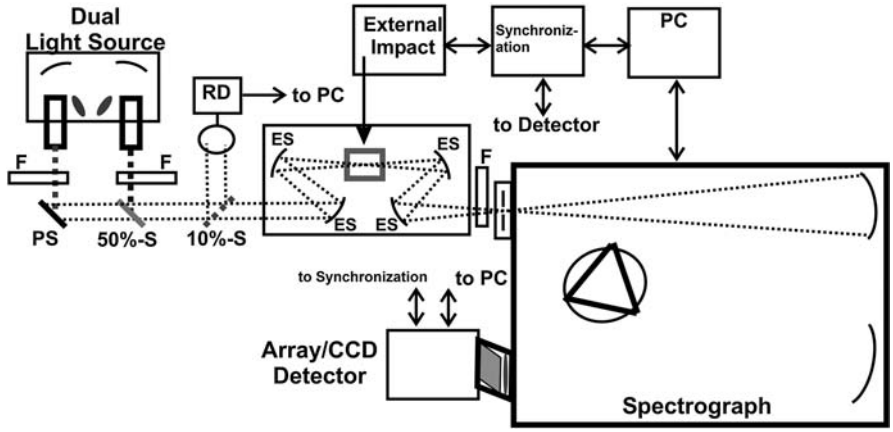

Figure 1.9 Spectrophotometer system for different fast kinetic applications.

has the theoretical advantage of direct access to each pixel, allowing different integration times at different wavelengths. As pointed out in Section 5.9 of *Fundamentals*[2], the parameters of available CMOS devices are not yet very useful for quantitative spectroscopy. For very fast measurements, gating, or for UV enhancement, an additional MCP image intensifier is used. The system timing is managed by a combination of a PC, camera controller, and the generator of the sample disturbance.

Measurements with a time resolution and illumination times >1 ms

A silicon diode array with 512 pixels can be read at a 1-MHz ADC conversion rate and 16-bit linear range, which results in a (rounded) 520-μs repetition rate (rep rate). The required light power can be estimated when the measured wavelength interval, the slitwidth, and the entrance power at the spectrograph is measured or calculated. Assuming satisfactory conditions, likely created by a 300-W halogen lamp combined with a 200-W D_2 lamp, at a used wavelength range of 250−850 nm, the resulting resolution would be ~6 nm, which is a typical value for fast data gathering. The required rep rate is then defined, and the reference spectrum (no external impact) is acquired and stored. The kinetics experiment is started, and the external impact is triggered by the array controller. It is important to understand that the illumination time = rep rate = time resolution. While pixel n is read out, pixel $n - 1$ is already illuminated again. If that disturbs the data interpretation, an MCP image intensifier can be added, as described in Section 5.8.8 in *Fundamentals*.[2]

Measurements with a time resolution and illumination times <1 ms

At illumination times in the nano- or microsecond regime, the light flux from a wideband lamp may not be enough to saturate the diode array or CCD detector in most cases. The other problem is that the

required frequency of measurements will be shorter than the read-out rate of area detectors. Depending on the experiment, the use of CCD with on-chip amplification (EMCCD, see Section 5.8.9.1of *Fundamentals*[2]) may be a solution. In most cases, the combination of a gated MCP with a 2D-CCD (see Section 5.8.9.2 of *Fundamentals*[2]) may be the better choice to realize nanosecond illumination, combined with microsecond rep rates and the acquisition of many spectra in a chain. A realized example of a millisecond dual-beam spectrophotometer system is described in Section 1.3.3.2. It performs kinetic measurements in the millisecond timeframe, compensates for scattering effects in turbid samples, and is prepared for external side illumination of the sample.

1.3 Special Absorption Techniques

1.3.1 Atomic absorption spectroscopy

The principle behind atomic absorption spectroscopy (AAS) is that atoms absorb light in a very specific manner: the absorption happens at very small spectral intervals, called lines, at bandwidths in the picometer range. The spectral position of absorption is independent of the pressure, temperature, and electric and magnetic environment. The reacting atoms must be freed from molecular conglomerates, which is the case in the gaseous phase. If the atoms are excited, they emit at the same lines that they absorb; this does not mean that the lines with the strongest absorption are automatically the most intensive emission lines. The coherence of the emission line and absorption line is used in the AAS technique. It uses light sources that only emit line spectra of one or a few elements. The most-popular source is the HCL, but resonance or glow lamps, filled with the element of interest, are also used. Ideally, they all emit only one set of spectral lines. The sample (most often a solution) must be vaporized and atomized, which primarily happens in an acetylene (ca. 2000 K) or a nitrous oxide flame (ca. 2500 K). Even-higher temperatures are reached in electrically heated graphite ovens (up to 2700 K).

In theory, the atoms in the gas phase will not correspond with each other, and no absorption background will exist besides the basic absorption of the flame itself; however, even that can reach up to 90% (1 AU), depending on the flame mixture and wavelength. Unfortunately, the theory does not often fit practical situations, and thus most AAS instruments are equipped with a background compensation device.

Unfortunately, the terms used in AAS differ from the common terms in standard absorption measurement. For example, in the latter, "background" means the dark signal created by the system itself, but in AAS, the term refers to the nonspecific absorption in the vicinity of the analyzed line. The following definitions will be used in the AAS section of this book:

- **Dark signal (zero level)** N is created by the system itself. Such is the case when the chopper is in the "dark" position and no light is transferred.

- **Background *BG*** is the nonspecific absorption signal surrounding the measured line; the background may change as soon as the solvent is loaded with the sample material.
- **Measured signal *e*** (for "element") is the sample measurement on the element-specific line with an appropriate source. It is typically split into two different data: with (e_1) and without (e_0) the sample material in the atomization and beam. Because all technical systems undergo variations over time, a dual-beam system setup can be used to compensate. If so, the reference beam bypasses the entire experimental system and provides an unattended time-dependent signal of the light used for measurement. That signal is discriminated by the signal of the atom-specific source e; thus, it is named R_e, and its counterpart for background detection is R_{BG}. Both are the denominator of the normalization process if referencing is applied in a dual-beam system.

Therefore, in a dual-beam AAS, one must deal with five different signals in a single measurement: N (dark), BG_S (nonspecific absorption in the sample beam), BG_R (nonspecific absorption in the reference), e_S (element-specific absorption in the sample beam), and e_R (element-specific absorption in the reference beam). Two of the data sets—one with the sample material in the atomization zone, the other without—produce the final result. If all of the data are used, the result will be corrected for dark signals, for nonspecific absorption, and for all system drift.

1.3.1.1 The principle of an atomic absorption spectrometer

An AAS system essentially works with only one light source (the atomic line source) and sends a beam in a straight line to the monochromator, passing the atomizer station in between and requiring some beam-shaping (BS) elements. The elements to realize this minimal setup are marked in bold in Fig. 1.10. Many systems utilize a reference beam to limit drift. In contrast to absorption spectrophotometers for liquid samples, the reference beam remains empty; it is only used for drift correction. The sample beam will ideally travel in a perfectly collimated manner with a diameter of 2 or 3 mm through the place of absorption. Parallel to the atom-specific absorption, the system shown obtains data on the nonspecific absorption (the BG). Because most AAS measurements occur between 190 and 600 nm, a D_2 lamp is commonly applied.

To control all routing, the system works with two chopper systems that are synchronized by a phase-locked loop (PLL); the phase shift between the two is always 90 deg. Chopper 2 consists of two equal blades on a single axis. The blades are mounted such that one blade is open while the other reflects. In dual-beam mode with background correction, the light is chopped twice, and five independent signals are recorded. At time t_0, the dark phase N has just ended, and the element-specific beam e opens. Because chopper 2 is also open, the beam travels the reference path, and the integrated signal is used to stabilize the HCL signal:

- At t_1, chopper 2 blocks, and a dark signal N is recorded.

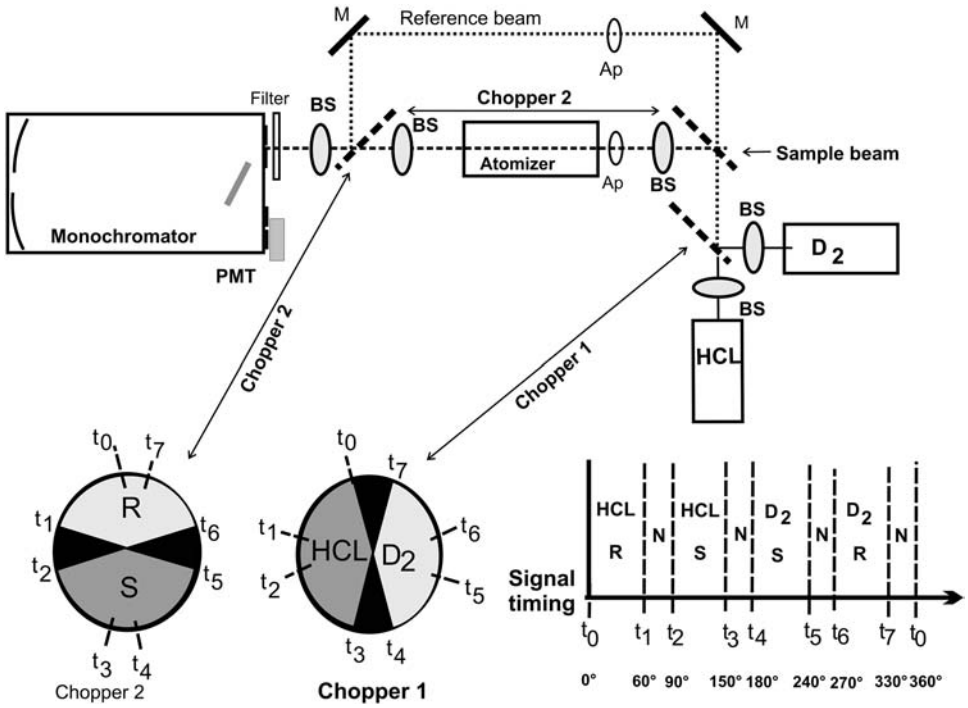

Figure 1.10 Principal components of a dual-beam AA spectrometer and timing.

- At t_2, chopper 2 guides the HCL beam *e* through the atomizer area, and the sole signal is recorded.
- At t_3, chopper 1 blocks the beam, and another part of *N* is integrated.
- At t_4, chopper 1 reflects the nonspecific light (*BG*, D_2) into the path. Because chopper 2 is still in the sample position, the D_2 light runs through the atomization area and is recorded.
- At t_5, the third part of the dark signal is recorded,
- At t_6, D_2 light travels along the reference path to create the comparison signal for stability.
- Finally, upon t_7, the final part of *N* is recorded.

From the five signals stored, all required calculations can be performed to produce one of the required two absorption signals (with or without the sample material). Beam shaping is required several times. HCL and D_2 lamps both emit a cone of light, which can be converted rather easily into collimated light (see Section 6.4.2 of *Fundamentals*[2]). In front of the place of atomization, another beam shaper might be required to produce a slender parallel beam. If required, the diameter may be reduced by the variable aperture (*Ap*) to avoid interaction of the light with the atomizer itself. The aperture in the reference beam can be used to adjust the intensity close to that of the sample beam. The two final BS are required to fit the cone of the beam to the spectrometer's needs. The function of the monochromator is that of a

variable bandfilter with very steep edges in order to keep stray light low. Typical monochromators have a 0.3–0.7-m focal length and incorporate gratings of 1200 mm^{-1}. A 0.5-m instrument will provide a dispersion of ~1.5 nm/mm, producing perhaps a 1-nm resolution at a 1-mm slitwidth. This design meets the requirement to transport the focus of the typical light sources (<3 mm) as completely as possible into the monochromator and to reach high SNR values. A second reason to make the bandpass not too narrow is the background measurement, which will measure the nonspecific absorption in the vicinity of the line. Because the line also absorbs light from the nonspecific light, the measurement should be integrated over an interval many times wider than the line. To avoid order overlay problems, a set of order filters may be mounted on the entrance slit. The detector of choice is a PMT. All sources (HCL and broadband) are mounted on different revolvers or sleighs for quick changes.

A system like the one discussed here can work in several modes to fit diverse analytical requirements. Using both light sources and both beam channels enables drift correction, wherever it occurs during the experiment time, plus compensation for nonspecific absorption. If the light beams are stable enough, chopper 2 can be stopped in the required position, at which point only chopper 1 will run and switch between *N*, *e*, and *BG* signals. This setup provides twice as long integration times per turn for the *e* and *BG* signals compared to dual-beam mode, improving SNR by $\sqrt{2}$. If no *BG* is required, the D_2 lamp is turned off, and the calculations are simpler, but no gain in time or SNR is earned. Regardless of correction for nonspecific absorption or dual-beam stabilization, a typical measurement only takes a few seconds. If a flame is used for atomization, only the solvent will be soaked in the flame and measured in front of and after the original sample solution. The ($e_0 - N$), or the single- or double-corrected data, lead to **zero** absorbance (0 AU, equal to 100% *T*). Next, the complete sample—the solvent mixture containing the specimen material—is atomized, and the difference ($e_1 - N$) is also recorded; the ratio between the two measurements is the result. In the presence of solvent alone or solvent with the sample, the light value at the detector is integrated for several cycles to improve the SNR, and the relevant median value is stored. In theory, it makes no difference if all corrections and normalizations are applied parallel to the data acquisition or afterwards. The value of sample transmission is based on Eq. (1.2) of *Fundamentals*[2], which in AAS is modified to

$$T = [(e_1 - N)/(e_0 - N)]. \tag{1.5}$$

Like "normal" absorption measurements, the logarithmic calculation leads to the AAS absorption equation:

$$A = -\log_{10}[(e_0 - N)/(e_1 - N)]. \tag{1.6}$$

As shown above, a synchronized detection system will sort and integrate the signals, taking into account the difference between the specific and nonspecific

signals, which requires an extended calculation. The absorption equation, valid for compensated AAS, becomes

$$A = -\log_{10}([(e_0 - N) - (BG - N)]/[(e_1 - N) - (BG - N)]). \quad (1.7)$$

In a 1-nm bandwidth, the atomic line may only cover 2 pm. Even if the element line were completely absorbed by the specific element, it would only make 2×10^{-3} of the broadband signal, which would be the maximum possible compensation error. It is advantageous to set the monochromator bandwidth as wide as possible, without creating line cross-talk, to keep the relation line/broadband small and simultaneously transfer a maximum of light for the best standard deviation (STD). In a dual-beam system, the e and BG values will need normalization before calculating absorption. Overall, the AAS method is not fast because it detects only one element per analysis; however, it is extremely element-specific. More compensation techniques are discussed in Section 1.3.1.4, and AAS with a nonspecific source is also described there.

1.3.1.2 Atomization

Flame atomization uses specially designed burners with slot-shaped nozzles 5–10 cm long. The light beam travels parallel above the nozzle. The distance depends on the flame temperature, flame speed, and element, and it will be adjusted case by case. Before the sample is run, it needs some preparation; in most cases, "cookbooks" offer guidance. To transfer the sample into the mixer chamber beneath the nozzle, the solution is sucked through a thin, flexible tube by a vacuum effect. In the chamber, the liquid is turbulently mixed with the gases for the burner, resulting in a homogeneous mixture of all components in the flame. For analysis electronics, the method is quasi-static. The data collection may take as long as required for a satisfactory SNR or until the sample supply is empty. The sample volume required is in the milliliter regime for an analysis.

The alternative atomization happens in an oven. The process is more complicated and comprises several steps. The oven consists of a small tube of special graphite that is loaded with a few microliters of sample volume by an injection syringe. The measurement light travels through the graphite tube, which is mounted onto an enclosure with quartz windows. The whole thing is purged with an inert safety gas to avoid damage. An analysis starts with drying the sample liquid by slowly heating the oven to the appropriate evaporation temperature and maintaining that temperature for a few seconds. The next step is the thermal preparation of the system. The temperature is slowly increased (again, for several seconds) to several hundred K, after which the system quickly heats to the element-specific atomization temperature and is held there for a short while ($\sim$3 s). During the fast heating and holding phase, the electronics obtain data. The transmission signal changes dynamically according the state of the atomic cloud in the beam, and thus the signal will be peak-shaped. The curve may show a flat top, depending on the

program, element, heating process, and chemistry. The data evaluation will either obtain the peak absorption during the atomization or perform area integration (the systems offer different approaches).

After the measurement is done, the temperature of the oven is further increased to the allowed maximum in order to remove residuals. The measurement also consists of the dark, background, and sample sequence; even if no background comes from the sample, the oven itself introduces a strong optical radiation that must be corrected. A graphite tube can usually be used many times and is easily replaced. There are several more atomization methods, such as glow discharge, hydride atomization, and vapor generation. However, because they are based on a chemical process rather than spectroscopic instrumentation, they are outside the scope of this book.

1.3.1.3 Applicable elements for AAS

Seventy elements can be analyzed by AAS,[3] but not noble gases, hydrogen, or the halogens. The nonmetal elements can be partially analyzed with some difficult sample preparation. In any case, the sample preparation and the flame parameters, with respect to the temperature program of the oven, have a strong impact on the applicability and success of the system. All instrument suppliers offer detailed cookbooks, and many modern instruments even have complete routines stored that can adjust and optimize themselves automatically.

1.3.1.4 Compensation techniques without broadband lamps

Zeeman background correction

In applications that use the graphite furnace, a strongly modulated electromagnet can envelop the atomizer. If an alternating magnetic field is applied, the atomic excitation line is split into three components.[4] The π component remains at the same position as the unpersuaded light signal, but it is attenuated. Two σ components are added within close proximity but outside the bandwidth of the π component. Thus, the σ components do not respond to the atomic absorption but rather to the nonspecific absorption near the measured wavelength. In order to reduce the nonspecific signal from the atomic absorption signal, two sets of measurements are required with and without sample in the oven: the specific analysis with the magnet turned off, and the other with the magnet turned on. To separate the data, two methods are available. If, during the nonspecific measurement, a polarizer after the atomizer deletes the π components, then only the nonspecific signal will remain. If the signals are totally separated, the reduction may also be performed by data processing. Zeeman compensation is not possible in flame systems because of the geometry of the flame and exhaust. It adds a lot of instrumentation to the spectrometer system and makes it much more expensive.

Smith–Hieftje background correction

If a HCL is driven by an extremely high cathode current, the linewidth will broaden by several orders. That effect is applied by the Smith–Hieftje compensation. A normal linewidth of less than 5 pm, for example, may increase to 50 or more pm in the overshot situation. Because a HCL will not stand that extra load in cw, the overshot process is realized with pulsed current. With standard current, the normal procedure is conducted, and the two measurements with and without the sample material are performed and stored. The excessive pulsed current is then applied for as short a time as possible. During that time, synchronized pulse acquisition with the help of boxcar data accumulation (see Section 4.2.1.3 of *Fundamentals*[2]) occurs, also for reference and sample. The dual difference of the data is calculated later. The maximum error may be larger than that of a real wideband lamp; the lamp lifetime will be substantially reduced, and more-complex electronics are required. On the chemical side, not all elements respond linearly to the different excitation modes. Therefore, whether the analysis works linearly with and without correction must be examined. If a D_2 lamp is used for compensation, the wavelength can be moved slightly such that the element line is outside the window and creates no impact.

Continuum source excitation

A rather new development is the continuum source technique (CS-AAS).[5] No HCL is used for excitation but rather a wideband source and a high-resolution spectrometer, which allows one to measure specific and nonspecific absorption in parallel. The light source may be a xenon or D_2 lamp. All kinds of atomization are compatible. The key element is a prism–grating Echelle double spectrometer, as described in Section 4.4.2 of *Fundamentals*.[2] It delivers a highly dispersed and order-free wavelength interval to an array detector of ~256 pixels in the wavelength axis. The typical dispersion depends on the wavelength, but it is less than 150 pm/mm in any case. In the most prominent range (around 300 nm), it is ~60 pm/mm. Because the detector receives a total of perhaps 200 pm, one channel represents roughly 0.7 pm. Thus, an atomic line will occupy 3–7 channels, which allows for measuring the specific and the nonspecific absorption simultaneously. Basically, no HCL is required, but any element-specific HCL can still be used for the reference measurement. In contrast to a standard AAS system, the CS-AAS depends on array detection. The reason is drift compensation. Even a thermally stabilized spectrometer may slightly move the exact spectral position in the output over time (see Section 2.7 of *Fundamentals*[2]). With an HCL source, that is no problem so long as all element-specific light reaches the detector, regardless if the output is a rather wide slit or a field.

In CS-AAS, the element-specific absorption line is created by the specific absorption itself. So, it may move slightly during an experimental series, which causes no trouble so long as recursive data reduction finds it within a predefined window and no obscure neighboring lines exist. The final result consists of a measurement of the whole experiment without the sample material and one with the specimen. Data processing is performed as before.

1.3.2 Polarized transmission: CD and ORD

Molecules in solution are usually arranged statistically. Thus, they show no dependence on the polarization of the measurement light, and they also do not modify the state of polarization. Solid state materials have a higher probability of polarization dependence or modification, especially in crystalline structures, which, for instance, are used in ellipsometry. However, apart from the effect of polarization modification of light in reflection, there are materials that vary the state of polarization also in transmission. Those materials are called "optically active" and can even be split into static and dynamic activity. Among the statically active substances are some containing C-, S-, P-, and other atoms. They create a change in the polarization angle that partially depends on the angle introduced. Absorption effects are normally overlaid.

Instruments for the analysis of the static change of angle are called polarimeters or ORD spectrometers. A different class of materials involves molecules that dynamically change absorption based on the circulation direction of the introduced polarized light. Absorption and optical activity are almost always combined. That effect is called circular dichroism (CD). Both effects—ORD and CD—show an increasing probability and strength toward higher photon energies (toward the UV); that is especially valid for CD, whose main application in biochemistry and biophysics involves samples with chiral structures. Consequently, CD spectrometers are optimized for the deep UV. Some CD setups are optionally able to directly detect ORD and, within certain limits, static absorption.[6]

1.3.2.1 The origin of circularly polarized light with alternating circulation

In Fig. 1.11, the blue curve marks the parallel vector **P** moving in the plane of the page. It is also called the horizontal plane H or real part r. The red curve, rising out of the plane of view, is the perpendicular vector **S**, also called the vertical plane H or imaginary part j. If no polarization exists in front of the polarizer, or if it is either +45 deg or −45 deg, then there is an ideal signal because P and S are perfectly in phase and show the same amplitude. From that scenario, a rotating polarizer would create perfectly rotating polarization behavior in the time domain t, which is called circular polarization (CP) and is used, i.e., in ellipsometry. Figure 1.11 shows the relations of a photoelastic modulator (PEM), a key component in a CD spectrometer system. Its heart is

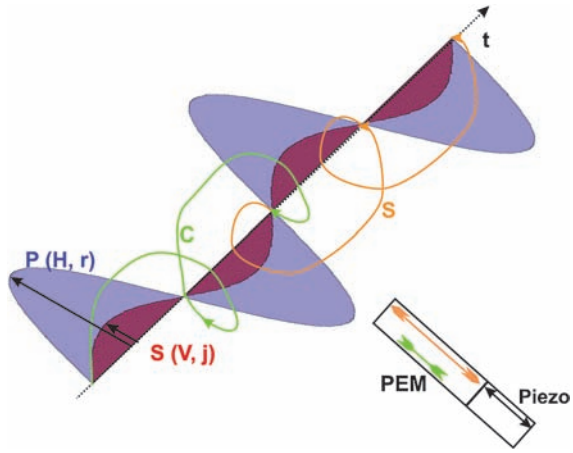

Figure 1.11 The behavior of polarized light after a photoelastic modulator is applied.

a birefringent crystal, vibrating in resonance. The resonance is supported by a piezoelectric element. The typical resonance frequency in CD instruments is 50 kHz. The crystal operates as a time-delay device. The entering light is collimated and polarized at 45 deg; thus, it contains both planes with the same phase and amplitude. In operation, the PEM transmits the **P** plane unattended but modulates the **S** plane with the resonance frequency. This behavior creates a rotating output polarization with an alternating direction of rotation. One complete sine-shaped sequence of the PEM contains a compression of the crystal followed by a stretch of the same magnitude. The compression (green arrow) creates a delay of the **S** plane as a direct function of the degree of compression. The result is a right-turning (**C** in green) full polarization vector.

At the zero crossing point, the crystal begins to stretch (orange arrow), and the **S** part accelerates, overtaking the **P** part. The resulting rotation is a full left-turning cycle (**S** in orange). The turning point is perfectly at zero, so an unbroken signal of polarized light is produced, providing a full-right- and a full-left-turning vector within 20 μs that is then sent through the sample and detected by a PMT. The electronics collect the signal via phase critical detection (lock-in principle, see Section 5.6.3.1 of *Fundamentals*[2]). Because a lock-in automatically records the difference between both the half waves as the measured result, the difference between the right-turning and left-turning waves (for the lock-in half-waves) present the difference in transmission between right- and left-turning intervals, which is the CD. For comparison, in a chopped system the difference is found by the integration of light with the chopper open minus the integration with the chopper blocked. From the value of both transmissions, the two absorbance values are easily calculated. Because a CD system is always a single-beam setup, a set of data consists of a scan with reacting material and one with everything but the reacting

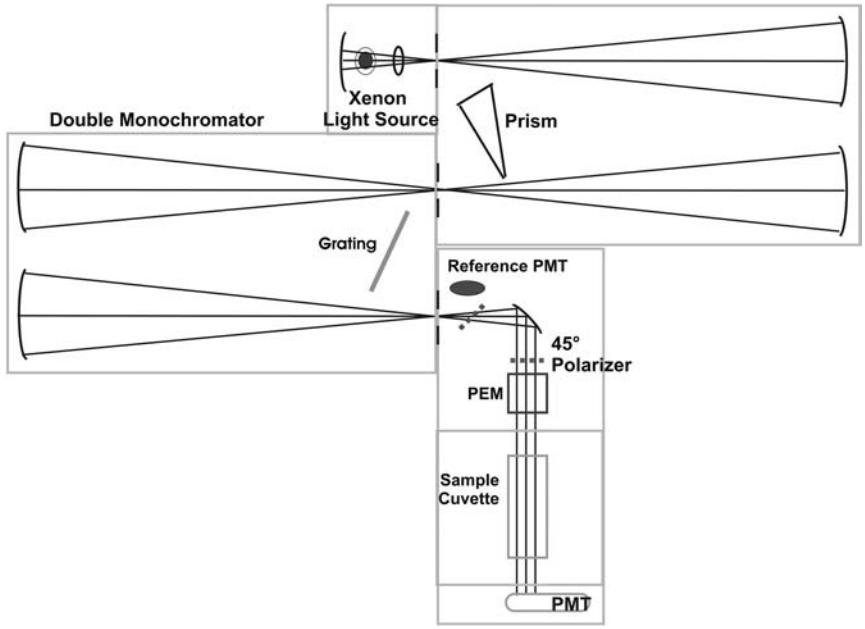

Figure 1.12 CD spectrometer components.

material (100 % T / 0 AU / reference) in the beam. A reference detector ensures the stability of the system.[7]

1.3.2.2 Set up and functionality of a CD spectrometer with ORD option

CD spectra are of special interest for biological samples in the range of 160–400 nm. A special class of samples are semiconductor materials in crystalline phase, which display CD in the range of 300–900 nm. Very often, the absorbance differences (the measured CD value) are tiny; typical values are in the range of 10^{-4} to 10^{-1} AU. In order to reach the required STD and detection limits, intense light is needed. Furthermore, the deeper the spectra reach into the UV, the closer the data grow together in the nanometer regime, which requires increasing dispersion toward shorter wavelengths. A common light source is a xenon high-pressure lamp combined with efficient collection optics and transfer. In front of the polarizer, ~10% of the monochromatic light is guided to a reference PMT that constantly records the monochromatic intensity for monitoring and normalization. The main part of the light is collimated by an ellipsoidal mirror sent through a stationary 45-deg polarizer and passed on to the PEM before it reaches the sample and finally the PMT. The PMT's output signal is collected by the lock-in technique. Regardless whether the final required output signal is the CD in the domain or the transmission of absorbance, it will reference the data of the reference scan and be stored as data 100% T, or 0 AU. Because it is not possible to find completely identical pairs of PEMs, double-beam technology makes no sense,

and a single PEM would require mirrors, which would change the polarization. These reasons are why CD systems are always single-beam instruments.

- **ORD**: Optical rotation dispersion. It describes the static modification of the angle of linearly polarized light in an optically active sample. An ORD spectrometer illuminates the sample with light of constant polarization and measures the polarization angle after the sample. The measurement is performed over a spectral range; the result is the optical rotation dispersion curve. The CD covers the static angular information, which is the ORD signal. According to an algorithm developed by Kramers and Krönig, it is possible to reduce the ORD from a measured CD spectrum if enough data points are provided. If the ORD will be analyzed by direct recording, an analyzer must be placed between the sample and the PMT, positioned at 90 deg in relation to the polarizer. If the sample does not turn the polarization angle, a zero signal will appear at angles where the PEM modulation crosses that angle. Otherwise, the rotation created by the sample is easily found by the PEM angle of minimum transfer.
- "**Unpolarized absorption**": Recording "normal" absorption spectra will only lead to approximate results because the CD setup is not built for that. If, on the other hand, the system is designed to replace the PEM with a chopper, a Pockels cell, or a similar modulation device, it would act as any other single-beam spectrophotometer.
- **MCD**: Magnetically induced circular dichroism. Materials with chiral structures or optically active crystal patterns often respond not only to polarized light but also to magnetic impact, which may enhance the CD effect (the effect can also be quenched or prevented entirely). Thus, a combination of CD and a programmed magnetic field increases the application range of the method. Special electromagnetic systems are on the market that fit the sample room and enclose the sample laterally without disturbing the light beam. The system program will combine the spectrometer and magnet. The user can create scans of the magnetic field versus the wavelength, or sequences of spectra with a stepped magnetic field.
- **Thermal variation**: It is obvious (especially for biological samples) that the CD effect may depend on temperature. Thermal-controlled sample holders or sample changers are therefore standard accessories, and stirring can help avoid sedimentation of the sample.
- **Stopped flow**: CD measurements during the dynamic mixing of two reagents is often performed by a stopped-flow apparatus (see Section 1.2.1.). There are units available that are small enough to fit the sample compartments of commercial CD spectrometers. For measurements below 190 nm, the optics of the accessory and the basic unit must fit each other, which must be kept in mind during purchase.

1.3.2.3 Instrumental considerations

The CD spectra of biological materials are of special interest in the wavelength range between 160 and 400 nm. CD systems are consequently designed so that the complete optical path can be purged by inert gas (the most popular is highly cleaned nitrogen). To achieve a good STD and detection limits (DLs), intense and dense light is required. The most-popular sources are 75-W xenon lamps, although 150 W is better and 450/500 W are best. All are available with a "W" bulb, transmitting light up from 150 nm (see Section 6.4.3 of *Fundamentals*[2]). A rear mirror and collecting lens provide maximum intensity to the following monochromator. The higher the lamp power is, the more important it becomes to provide cooling. Nitrogen is too expensive to realize that by convection, so water cooling is the solution for 150- or 450/500-W lamps. These lamps are available with a water-cooling jacket, and, in most cases, the cooling circulation also flows through the walls of the lamp house. The water itself will be cooled in a closed loop by an external thermostat. Sensors and program locks ensure that the lamp is on only while both water and nitrogen flow and that the temperature at several points is low enough to avoid any damage.

The entire optical system is equipped with components made from or coated with MgF_2 and/or CaF_2. The spectrometer must be a double monochromator because the stray light must be kept below 10^{-6} to provide errorless data in the CD range of 0.001 or even lower. The deeper the spectra reach into the UV, the closer the polarization features become, which also causes increasing dispersion toward the deep UV. Grating spectrometers do not behave that way. Thus, either double-prism monochromators or prism–Echellette–grating combinations are useful. MgF_2 prisms work from 122 nm throughout the IR, and Echelette gratings with a MgF_2 coating work efficiently in several spectral orders. A grating of 600 mm^{-1} (with a blaze of 8.5 deg) will produce a rather homogeneous transfer from 155–900 nm. In the range of 155–250 nm, it will be in the third order, acting like an 1800-mm^{-1} grating blazed to 166 nm. In the range of 200–600 nm, it is equivalent to a 1200-mm^{-1} grating blazed to 250 nm, whereas in the range of 400–900 nm it acts in the first order as an effective 600 mm^{-1} grating blazed to 500 nm. Assuming that both monochromator stages have a 300-mm focal length, they will provide a bandwidth of 1 nm at a slitwidth of 0.6 mm in the third order, thus transporting a high amount of light.

A small amount of the dispersed light is passed to a reference PMT, which must not be the same model as the sample PMT that will receive the majority of the light. The beam travels collimated through the polarizer and PEM. The sample compartment is prepared for different equipment, including compact magnets for MCD with 10-mm cells, and can also be furnished with sample changers, stopped flow, or magnetic equipment. All holders must be thermostat controlled and stirred. It is even better if long-path cells (5 or 10 cm) also fit the compartment. If the ORD data will be acquired directly, a motorized fixed-angle analyzer is required.

The final part of the chain is the PMT. It should have a rather large cathode to collect photons after slightly scattering samples; end-on types are suitable. The PMT housing must be shielded against magnetic impacts if a magnet is installed, and it needs thermal insulation. Sometimes, the PMT is easily accessible to allow replacing it with alternates optimized for different applications and wavelength ranges. PMT cooling is also a reasonable option. Sample cuvettes are an occasional source of problems. For CD (especially deep-UV CD), they must be free of birefringence. The leading cuvette manufacturers offer special cells for CD and ORD, which are also useful with thermal programs. The electronics and software are more or less standard; therefore, they do not appear in the block diagram.

1.3.3 Spectrometers for scattered transmission

Transmitting samples sometimes scatter light and need special measurement designs. Even if a sample appears clear in the visible range, it might be scattering in the UV. A sample may appear absorbent—even the light loss is only due to scattering. Following Rayleigh's laws, scattering effects at solid materials (such as floating particles or unsolved colloids) create scattering, which increases with the fourth power of photon energy, i.e., it increases rapidly toward shorter wavelengths. A spectrophotometer cannot determine whether the "lost" light was captured by the sample or scattered and left the beam. There is only one way to avoid errors: the scattered light must be collected.

1.3.3.1 Absorption spectrophotometer with an extra-large detector

As illustrated in Fig. 1.13, the front end of the absorption spectrophotometer, with the light sources, monochromator, and chopper system, is very similar to the

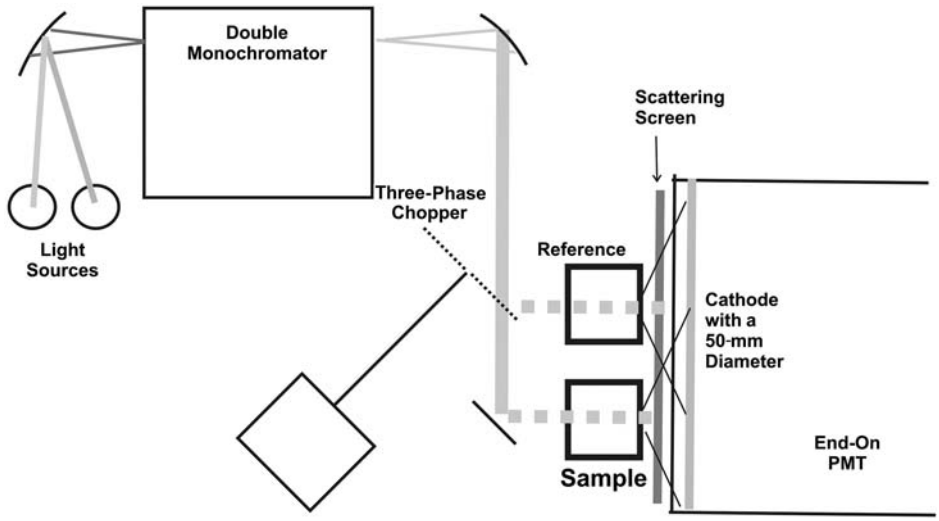

Figure 1.13 Example of a spectrophotometer for scattering samples.

classical spectrophotometer. The detection part, shown here with a PMT, differs in some regards: it is an end-on type with a very large cathode (typically with a 50-mm diameter). The sample and the reference cell are placed close to each other—20 mm from center to center is common, which is enough to accommodate thermostat holders. In addition, the cell holders are equipped with a stirring device to avoid sedimentation of samples during analysis. The length of the cells is limited to 10 mm. The light leaving the cells can be captured up to a cone angle of 130 deg. That angle, of course, is only valid for the end of the cell. Scattering from the early part of the cell is collected under smaller angles. Therefore, measurements are often done with shorter pathlengths, which, in turn, may lead to troubles with stirring. The distance from the cell holder to the PMT is only a few millimeters. In between them is a scattering screen that has two duties. It distributes the measurement light over a large area, even if the beam arrives collimated. That behavior avoids signal deviations from local variations of the cathode sensitivity. The screen also avoids local overload at the cathode in situations without a sample or a sample without any scatter because they can create durable local damage. A system with a PMT works from <200 nm to >800 nm with a high dynamic ratio. Following the same principle, UV silicon detectors with a diameter of up to 100 mm are also applied. Indeed, the detection limit and dynamic range, especially in the important UV, is remarkably limited in comparison to the PMT. Besides the larger area and the insensitivity to damage, it has the advantage of reaching up to 1100 nm, which is also the technical limit of the method. Toward longer wavelengths, no useful and affordable detectors of the required size are available for civilian use.

1.3.3.2 Dual-beam fiber optic spectrophotometer for kinetics and scattering

Other versions of spectrophotometers for scattering samples use either a set of optical fibers that collect the transmitted light after a wide collecting lenses or fiber optic tapers to collect the scattered light after the sample cell, and capture almost a 180-deg solid angle. There is often a compact system with parallel read-out that records the spectra on the spectrometer end. An advanced version combines efficient light collection with a CCD spectrometer and fast data acquisition, which is described here.

The system shown in Fig. 1.14 starts with a dual light source that combines the output of a D_2 and a tungsten-halogen (WH) lamp. Inside the housing are the collection optics and a fiber optic beam combiner. A shutter is mounted in the output ferrule of the housing and controlled by the system's PC. The red fiber cable splits the combined light into two identical forks that lead to the sample compartment. There, the light is collimated to a $\sim$3-mm diameter and travels through the reference (R) and the sample (S) cell, passing through a manual beam stop (BS) in each path. Both cells are standard 10-mm versions. The walls of the cell holders can be flushed by a thermally controlled liquid. If a stirring magnet is placed inside the cell, it can be driven by rotating magnets below the cell. Actuation and speed are controlled at the front of the

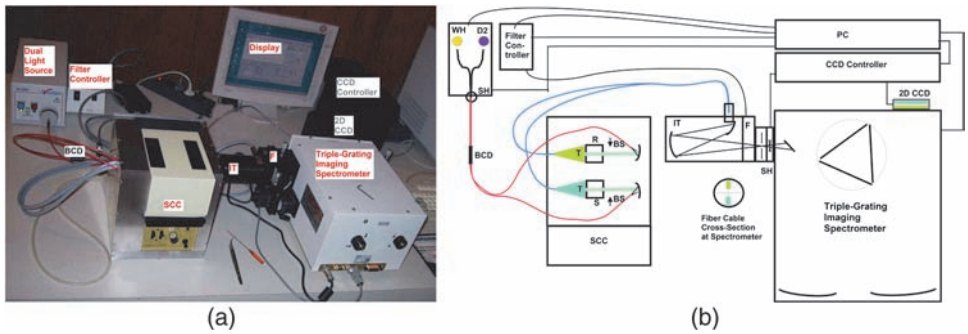

Figure 1.14 Dual-beam spectrometer for kinetics and scattered transmission: (a) image and (b) schematics.

sample control compartment (SCC). The two levers to the left of the SCC allow for independent vertical adjustment of the cells inside their holders while still being stirred. Thus, the required sample level can be minimized.

A pair of fiber optic tapers, shown as a green and a blue cone (T), are attached directly after the two cell holders. Both have an active diameter of 10 mm to collect the maximum amount of light. If no scattering took place inside the sample cell, the function of the tapers is not reduced. Each taper melts into a fiber cable with an active area of 2.2 mm^2. Both cable forks are combined to a single end at the spectrometer illumination box (IT). The end is shown extended, and it illuminates two areas with a 2.2-mm height, separated by another 2.2 mm. Therefore, the occupied height at the entrance slit is 6.6 mm. In between the two areas is an image transfer box with a 1:1 transfer ratio that has been adapted to the spectrometer requirements.

The spectrometer is equipped with an order-sorting filter wheel (F) and shutter (SH) (both of which are controlled by the PC), three gratings, and a 2D CCD. It incorporates thermoelectrical cooling and a chip of 1024 pixels × 256 pixels at 26.6 mm × 6.7 mm. The read-out speed (ADC) of the CCD can be set to either 10 μs or 1 μs per conversion. If no horizontal binning is programmed and both areas (dual beam) are converted, a time of either 5 ms (1-μs ADC) or 25 ms (10-μs ADC) is required. During that time, no light may reach the detector, or else the information of the two beams would merge. The CCD controller steers the shutter (SH) in the spectrograph entrance to avoid smearing and to control the exposure time. The maximal repetition rate of the shutter is four cycles per second. For kinetic experiments, it is therefore better to use only one beam and stop the other one with the help of the manual beam stop (BS) in the sample compartment. At this point, only one area of the CCD is defined for read out, and the read out is much faster. Most importantly, the shutter is no longer required. The read-out time is now the exposure time. A kinetic time resolution of 1 ms at full resolution, or even down to 100 μs (depending on pixel binning), can be performed this way. Section 5.8 of *Fundamentals*[2] describes all of the relations needed to justify the topic of timing.

The dispersion of the system varies with the grating. The CCD will cover 200–1030 nm with a grating of 100 mm^{-1}, an interval of 280 nm with 300 mm^{-1}, and a 140-nm interval with 600 mm^{-1}. The resolution with 1024 data channels will vary between 2.43 nm, 0.8 nm, and 0.4 nm, depending on the grating. If a high resolution is required over wide ranges, a step-and-combine technique with an automatic filter change will steer the acquisition, fit, and storage of data. This scenario also applies to single- and double-beam experiments, and data normalization.

1.3.3.3 Absorption spectrophotometer with an integrating sphere

General-purpose spectrophotometers utilize rather wide distances between the sample holders, and rather long pathlengths between the end of the cells and the detector. Large distances allow high flexibility, sample holders with a light path up to 10 cm, and accessories such as thermal control, a stirrer, reflection optics, etc. In order to run scattering samples, some manufacturers provide integrating-sphere accessories to replace or fit into the standard compartment, as shown in Fig. 1.15.

Both sample positions are placed at the equator, at the same distance from the absorption cells. The detector is at the north pole of the sphere. Cleverly constructed instruments allow the sample room with the detector compartment to be removed completely. A complete building block with sample holders and sphere can then be mounted instead. If the sample compartment is located inside the spectrometer housing, it will be cleared out and refurbished with the sphere accessory. This solution is less flexible and requires some cables to be reconnected; the sphere diameter is often smaller than the external version. In any case, the sample cells will either reach slightly into the sphere or be very close to it. Thermal control and stirring are also provided. Depending on the actual setup, the light rays leaving the cells can be collected

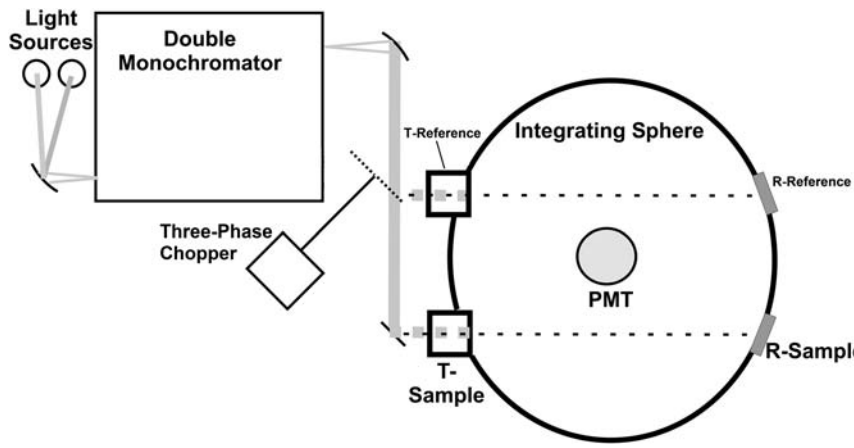

Figure 1.15 Principle of a "normal" dual-beam spectrophotometer with an integrating-sphere accessory installed.

up to almost 180 deg. In principle, the solution with an integrating sphere appears to be more efficient than the proximity solution discussed in Section 1.3.3.1. However, a remarkable amount of intensity is lost inside the sphere by the high number of reflections, which decreases the dynamic range. The size of the detector does not need to exceed the normal, making this solution also useful in the NIR–IR range. (General considerations for integrating spheres are discussed in Section 6.4.4 of *Fundamentals*.[2])

1.3.4 Photoacoustic (optoacoustic) spectroscopy

1.3.4.1 Basics

The photoacoustic effect was discovered by A.G. Bell during his work on telephone technology. The light absorbed by the sample material may have one of two effects: either it leads to luminescent radiation or it increases the thermal state of the sample. The latter is used for photoacoustic spectroscopy (PAS). The absorption slightly heats the sample; after the excitation is finished, the sample will return to its former thermal state by an *e*-function. In a small, tight sample compartment, the thermal changes create pressure changes that are linear to the heat changes of the sample. It is important that the measurement light is not required after the absorption. Whether or not the light is partially reflected, or scattered, or turned into luminescence has no impact on the result, with one exception: if some light is turned into NIR luminescence, it may also heat the sample.

Opaque samples are no problem for PAS. Theoretically, the PAS spectra are similar to absorption spectra; however, the depth to which the light penetrates into the sample at the wavelength of interest is important because it may produce saturation effects and affect how long it takes for the heat to return to the "ground state." Both parameters are a matter of optimization for good spectra. If the sample is thicker than the penetration depth of the light, then an exponential saturation effect appears. The thermal diffusion of the sample defines the time constant required for thermal equilibration and thus the time between excitations, which, in turn, is controlled by the modulation frequency. At first glance, PAS appears to be an optimal method for optically dense materials and strongly scattering samples, e.g., many solid state samples, colloids, and powders, as well as liquids that require intense sample preparation, such as blood, leaves, soot, carbon-like samples, paper, etc.

1.3.4.2 Parameters that affect the PAS signal

The pressure change requires modulated or pulsed light for measurement. Because the thermal change directly depends on the intensity of excitation, a high beam density is essential. The coefficient of absorption k is a key parameter, just like the relation of the sample volume to the cell volume. The density of the sample influences the time: the sample must emit the extra heat, along with the thermal coefficient, the thermal conductivity, and the thermal diffusion constant s. The parameters k and s are both *e*-functional.

The definition of penetration depth is the distance after which the intensity of light has dropped to 1/*e* (1/2.7183, or 0.368) of the arriving value, analogous to the constant of diffusion *s*. It is that distance between the origin of heat to the exterior where the heat difference has dropped to 1/*e*. Take, for example, two identical powders that comprise different grain sizes: they will have two different PAS signals that have the same peak wavelengths. If a sample with a short thermal constant *s* is excited with a slow modulation frequency, the measurement may become nonlinear. If, in turn, the frequency is too high, the sample may not return to equilibrium between the phases of illumination, and thus slowly heat up. The shape of the light modulation also plays a role. Sine-wave modulation and rectangular (chopped) light will produce different results.

The parameters that influence the PAS signal include the following:

- light density,
- light power,
- modulation frequency and curve shape,
- wavelength,
- absorption coefficient *k*,
- penetration depth,
- sample thickness,
- thermal coupling,
- thermal diffusion constant *s*,
- depth of thermal origin,
- consistency of the sample, and
- relative filling of the sample cell, among others.[8,9]

Based on those factors, the PAS method is well suited to evaluate the spectra of samples that are either not compatible with or create strong difficulties in transmission or reflection spectroscopy. Unfortunately, quantitative data reduction of PAS is nearly impossible. It is useful to at least use the modulation frequency to vary the penetration depth and depth of thermal origin to acquire spectra for different sample depths and reduce the results of layer profiles. Absorption curves can be recorded from samples not accessible for absorption measurement.

1.3.4.3 Setup of a PAS system

A broadband light source with a high light density is required for a PAS system; a 450/500-W xenon lamp with a small spot is suitable. Its light will be efficiently collected and lead into the monochromator. The best modulation method is to modulate the lamp itself. Between 1 Hz and 1 kHz, it delivers a stable sine-wave output, and the maximum amplitude can almost reach twice the median value compared to the DC signal required for a mechanical chopper. The typical frequencies are between 10 and 300 Hz. As shown in Fig. 1.16, the modulator (LM) is coupled to the power supply (LPS) and

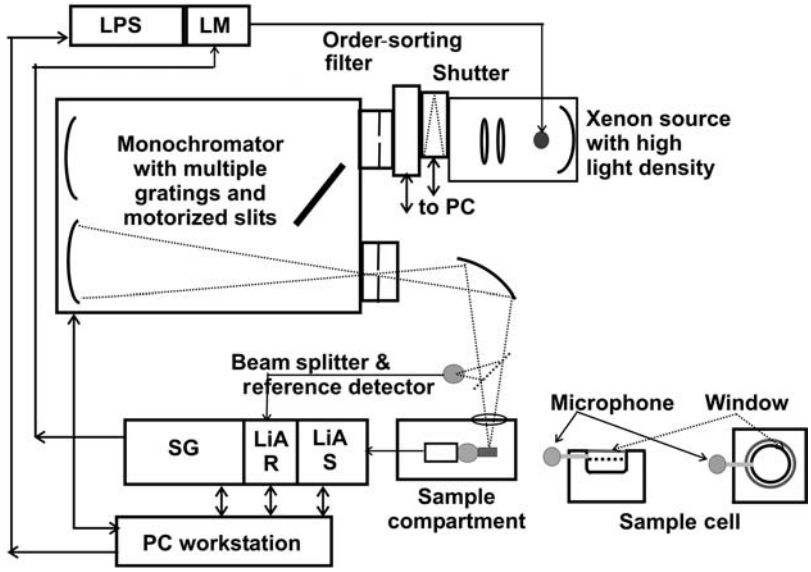

Figure 1.16 Photoacoustic spectrometer.

steered by the central unit (sine-wave generator, SG). If a chopper is used for modulation, it will be placed near the shutter, which is necessary to allow the measurement of the electronic and acoustic background, which is stored for subtraction. While the shutter is closed, the background frequency spectrum may be acquired and stored. This action allows for detecting disturbing frequencies and avoiding them during measurement. Another reason to use a shutter: because a modulated xenon lamp does not fully turn off, the background does not reach zero. Besides that, the beam travel is like that of other single-beam spectrophotometers. The monochromator will work efficiently and provide a contrast of >1000, which ensures that primarily the desired wavelengths excite the sample. A system with three gratings will transfer high light power between 190 nm and 2500 nm. Motorized slits help control the bandwidth and intensity simultaneously. The dispersed light hits the sample from the top. Along the way, a beamsplitter guides $\sim 10\%$ to the reference detector, which records the intensity for comparison and stabilization. Normalization to the reference is also an option for comparing different samples under identical parameters, but that comparison does not have the same function it has in transmission spectroscopy. The "sample compartment" building block comprises the sample cell itself, the enclosure, gaskets, microphone, and pressure channel. The microphone must respond linearly to small changes in pressure; electret or condenser microphones are suitable. The electrical signals of the reference detector and microphone are lead to separate lock-in amplifiers (marked LiA R and LiA S, see Section 5.6.3.1 of *Fundamentals*[2]). The output signals are delivered to the PC workstation for further signal processing, storage, and display.

The central part of the sample cell is shown extended in Fig. 1.16. The effective sample holder should be oriented horizontally to allow deposition of all kinds of samples. The trough where the sample is kept must be as least as large as the maximum beam. The graph does not show external optional beam masks, which may limit the illuminated area. On the other hand, the sample must fill the bottom of the trough, to avoid PAS signals from the cell itself. The cells are made from a robust material, such as stainless steel. Above the sample trough is a tight window (most often quartz). The window is rather thick because it must not respond to the pressure changes in order to not falsify the measured pressure and to avoid resonance. Just beneath the window, a tiny channel leads to one side wherein the microphone sits.

Several different sample cell systems are available for different applications. The entire cell system shall be portable and easily put in place. That enables sample preparation and the addition of safety gas under external environment. Moving a lever will close the window and also press the sample holder against a gasket, which isolates the entire thing. The filling volume of the holder is optimal if the trough is completely filled to a height slightly below the pressure channel without reaching it. Typical sample volumes are 3 mm $\times$ 3 mm $\times$ 3 mm, which require less than 30 μl of sample material.

1.3.4.4 Preferred PAS/OAS applications and referencing

Based on the large number of parameters, the spectra are only semiquantitative. The strengths of the method are apparent when standard absorption and reflection spectroscopy partially or completely fail, or when they require complicated sample preparation with a high probability of error. Opaque samples, or those with strong scattering effects, will still create useful spectra via PAS. Typical examples include solid state samples with layers; samples such as leaves, blood, wood, colloids, creams, plastics, grains, and soot; and many that are between liquid and solid states. To define the maximum possible PAS signal at a given instrumental set of parameters (slit width, wavelengths, frequency, sample cell/trough used), a total absorber is required. A pure, reproducible soot is preferred, i.e., carbon black.

Because the PAS method is extremely sensitive to pressure variations in the μbar range, it enables measurements of tiny samples in small volumes and gas, which would otherwise not provide useful results in transmission or reflection.[10] The variation of the modulation frequency provides for the analysis of layer structures, and the independence of the resulting signal (pressure) from the excitation (light) removes the need to take care of optical errors after excitation.

References

1. D. W. Ball, *The Basics of Spectroscopy*, SPIE Press, Bellingham, WA (2001) [doi: 10.1117/3.422981].

2. W. Neumann, *Fundamentals of Dispersive Optical Spectroscopy Systems*, SPIE Press, Bellingham, WA (2014) [doi: 10.1117/3.1002528].
3. B. Welz, *Atomic Absorption Spectroscopy*, Verlag Chemie, Weinheim, Germany (1976).
4. E. P. Lewis, M. Faraday, J. Kerr, and P. Zeeman, *The Effects of a Magnetic Field On Radiation: Memoirs by Faraday, Kerr, and Zeeman*, American Book Co., New York (1900).
5. B. Welz, H. Becker-Ross, S. Florek, and U. Heitmann, *High-Resolution Continuum Source AAS: The Better Way to Do Atomic Absorption Spectrometry*, Wiley-VCH, Weinheim, Germany (2005).
6. D. Clarke and J. F. Grainger, *Polarized Light and Optical Measurement*, Pergamon Press, Oxford, UK (1971).
7. A. Szilágyi, "Animations of electromagnetic waves," Software download available at http://www.enzim.hu/~szia/emanim/emanim.htm. Last revised 23 September 2011.
8. Y.-H. Pao, ed., *Optoacoustic Spectroscopy and Detection*, Academic Press, New York (1977).
9. A. Rosencwaig, *Photoacoustics and Photoacoustic Spectroscopy*, John Wiley & Sons, New York (1980).
10. P. Hess, ed., *Photoacoustic, Photothermal and Photochemical Processes in Gases*, Topics in Current Physics **46**, Springer-Verlag, Berlin (1989).

Chapter 2
Ellipsometry

2.0 Introduction

Ellipsometry makes use of the Fresnel features provided by polarized light and the modification to the state of polarization by the light's interaction with matter.[1] The name refers to the effect of turning a linearly polarized vector into an elliptical one. This method does not need the magnitude of intensity or the change of intensity to produce the required result; only the polarization behavior is relevant. The main applications are the recovery of optical constants and the analysis of thin layer systems. Single-wavelength ellipsometry creates a single set of data and is primarily applicable to product control, general surface definition, and single-layer calculations. Spectroscopic ellipsometry (SE) obtains data at many wavelengths, which enables the use of fit functions, multilayer data reduction, and the creation of reference data. Relevant literature exists in handbooks on optical constants,[2] and techniques, instrumentation, and data-reduction methods are also well documented.[3]

2.1 Elements of Spectroscopic Ellipsometers

Spectroscopic ellipsometry utilizes the laws applicable to linearly polarized light in reflection mode. If a sample is illuminated in the vicinity of the Brewster angle, the maximum sensitivity of polarized reflection conditions are given. The Brewster angle is identical to the angle calculated from the arctangent of the material's refractive index (RI). If $RI = 1.6$, then arctan = 58 deg. For an ideal sample of a single material with no roughness and no covering layers, at the Brewster angle, one polarization axis would be completely suppressed while the other polarization axis would be fully reflected. Real-world samples and layered substrates will show a different response at small changes of the illumination angle. Ellipsometry uses the Brewster effect because a sample will reflect the polarization planes differently for different linear polarized illumination and under different angles. Spectroscopic ellipsometry has the advantage that both parameters will be

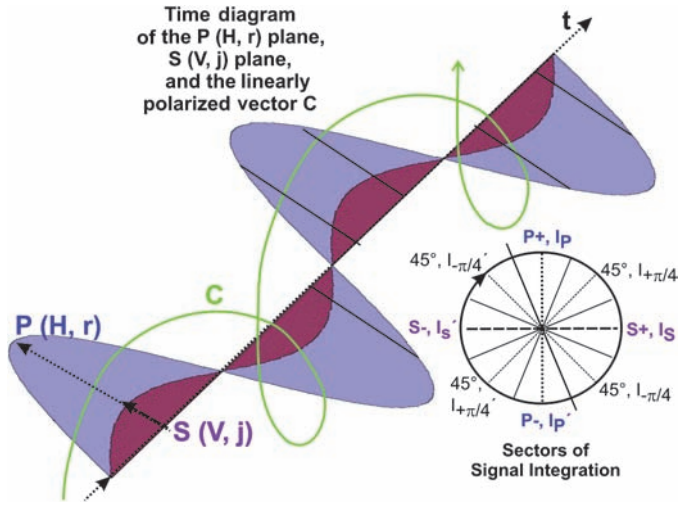

Figure 2.1 Behavior of a polarized light beam after the rotating polarizer, and an integration scheme.

different at different wavelengths. In other words, SE can apply a matrix of three independent parameters to recover the required result. In most literature, the illumination angle is marked Φ. Because the sample will respond differently to changes in the polarization angle of the impinging light, a rotating polarizer is one of the two possible sources of illumination polarization. For each wavelength λ and each illumination angle Φ, a set of four polarization data is stored, representing the four sectors I_1-I_4. After data acquisition, the ellipsometric parameters tanΨ and cosΔ and the Stokes parameters S_0–S_3 can be recovered. The interrelation of polarization and signal integration is shown in Fig. 2.1.

In the figure, the blue curve marks the parallel vector **P**, which is on the plane of the sheet and is also called the horizontal plane *H* or real part *r*. The red curve is the perpendicular counterpart, called vector **S**, vertical plane *V*, or imaginary part *j*. If the light in front of the polarizer is perfectly scrambled in polarization, then the signal after the polarizer will perfectly show the same amplitude at every output angle. So long as **P** and **S** are in phase, the rotation of the polarizer will produce perfectly linear polarized light **C** rotating in the axis of time *t*, illustrated by the green curve. The graph shows one full right-hand rotation of the clockwise-rotating polarizer. One full turn creates two full polarization circles. In a phase-locked detection system, the sign of the **P** and the **S** signals is not recognizable. Both create a positive integration so long as **P** and **S** are in phase. If a retarder (also called a compensator) is placed in front of or after the polarizer, it will cause a phase shift between **P** and **S**. This behavior allows for discrimination of the direction of rotation, i.e., positive and negative 180 deg, which allows one to control or monitor the sign of the vector.[4] This option is not required in ellipsometry, but it is helpful in polarized reflectometry and analysis of surface and layer roughness. The

Table 2.1 The Hadamard matrix required for ellipsometry. Note that data channels 2 and 4 will be identical if no phase shift is caused by a retarder. For ellipsometry, only I_s, I_p, and $I_{+\pi/4}$ or $I_{-\pi/4}$ are required.

	Data Channel 1	Data Channel 2	Data Channel 3	Data Channel 4
	I_s	$I_{+\pi/4}$	I_p	$I_{-\pi/4}$
Cycle 1	+	+	+	+
Cycle 2	+	+	−	−
Cycle 3	+	−	+	−
Cycle 4	+	−	−	+

sample response to the different planes of polarization is stored in four different places in the memory; each covers 45 deg.

The wheel in the figure represents the function of the detector signal integration. The position of the rotating polarizer steers the signal storage. In the figure, the polarization curve starts at the point marked by the arrow, which is 45 deg, $I_{+\pi/4}'$. The first signal integration would start 22.5 deg later (marked by the solid line reaching outside the wheel) for the next 45 deg, resulting in the integrated signal **P**, making up parameter I_p. At the end, the content of the integrator will only consist of **P** because the portions of the integrated **S** signal before and after 90 deg compensate for each other. All four sectors cover 45 deg, with the nominal angle in each center. After integration of the 45 deg, $I_{-\pi/4}$ sector, the cycle is completed (also marked by the extended marking line). The second half of the rotation will use the four integrators again.

Theoretically, all four integrations will have the same magnitude. The intrinsic behavior of the instrument, however, will show small residuals and asymmetries—they should be calibrated out at installation and occasionally checked (perhaps once a year). If, in a sample measurement, the **P**, **S**, and the 45-deg signals differ, it is a sample feature and thus a valid parameter for data reduction. If a retarder is present, there will be a remarkable phase shift that is also calibrated into the data reduction for later discrimination of data with and without retarder. Calibrations are described in Section 2.10. From the four sectors of signal integration, all data required for ellipsometric calculations are reduced by a Hadamard algorithm (see Section 9.4 of *Fundamentals*[5]). The Hadamard polarization matrix, according to Fig. 2.1, is presented in Table 2.1.

2.1.1 The Stokes parameters

The Stokes parameters are calculated from the four polarization values by

$$\begin{aligned} S_0 &= I_0 = I_p + I_s = I_{+\pi/4} + I_{-\pi/4} = I_l + I_r, \\ S_1 &= I_s - I_p, \\ S_2 &= I_{+\pi/4} - I_{-\pi/4}, \text{ and} \\ S_3 &= I_r - I_l, \end{aligned} \tag{2.1}$$

where S_0 through S_3 are the four Stokes parameters; I_0 is the sum of all measured combinations S_0 through S_3; I_p and I_s are the two planes of polarization; p, s, $+\pi/4$, and $-\pi/4$ are the four parameters of linear polarization; and I_l and I_r are the values of circular polarization. The Stokes parameters S_0–S_2 do not require a phase shift between **P** and **S**; parameters I_l, I_r, and S_3 require two sets of data with a compensator/retarder to define the direction of rotation.

2.1.2 Research-grade spectroscopic ellipsometers

2.1.2.1 Spectroscopic ellipsometer with a rotating polarizer

Figure 2.2 shows a standard SE setup with a rotating polarizer (RPSE). A light source delivers collimated broadband light to the polarizer, which illuminates the sample. The reflected light is collected and delivered to an analyzer, which may be a duplicate of the polarizer. From there, the light enters the spectrometer and, later, the detector. Control electronics steer the analyzer and polarizer and ensure that the required signals go to the appropriate memory. In the most advanced instruments, the illumination angle, sample position, and even a retarder can be software controlled.

In an RPSE system, the sample is illuminated by modulated light, which provides all of the advantages of lock-in technology, such as the suppression of light signals that have not passed through the polarizer. After the sample, the light will be lead through an analyzer, which is fixed during measurement. Before data acquisition, it will be rotated to an angle that provides signals from both planes, which is required to avoid zero signals during the cycle.

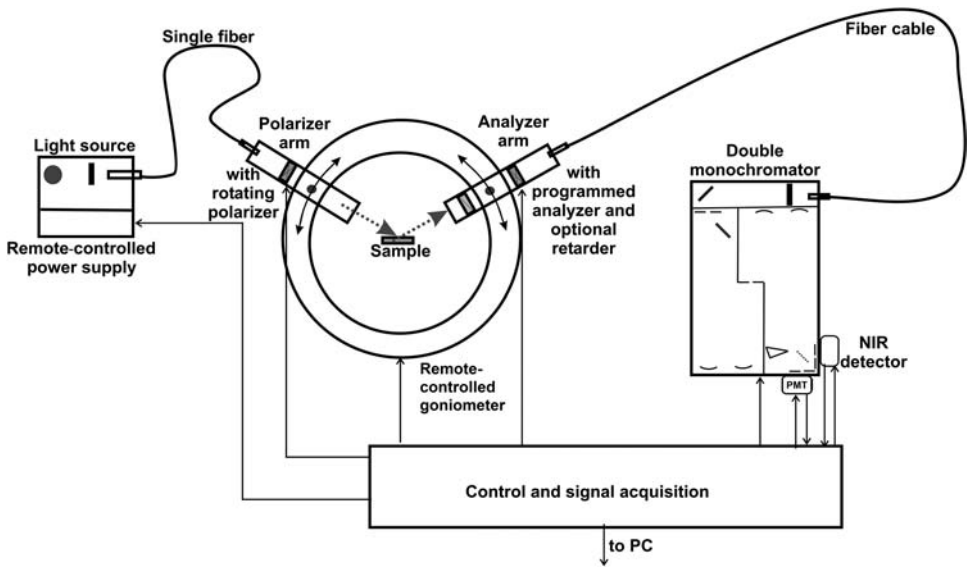

Figure 2.2 Schematic of a research-grade SE system.

The analyzer angle will be optimized at each wavelength, and its angular position is recorded as an additional parameter for further calculations. For the data reduction, that means that each set of data per wavelength must be correlated for the analyzer position, which is no problem for PC programs.

2.1.2.2 Spectroscopic ellipsometer with rotating analyzer

The setup for a spectroscopic ellipsometer with a rotating analyzer (RASE) is basically the same as a RPSE but with different control of the two polarizer elements. The polarizer is now fixed in position during data acquisition, and the analyzer rotates. This scenario raises two problems: (a) because the measurement light is no longer modulated, a reduction of the background light is only possible by an additional modulator, such as a chopper; and (b) double detection is required, which leads to complicated data discrimination and loss of light. In modern systems, the latter is performed by FFT data reduction. In summary, RPSE is more efficient and less complex. The following section will only address RPSE and the compatible data reduction equations.

2.2 Applications of Spectroscopic Ellipsometry

If the wavelength of the instrument, the angle of incidence, the polarization, and the collimation of the light are correct, an SE system needs no further calibration to measure the RI n and the absorption coefficient k correctly. Both are basic parameters to characterize materials. SE software can define the real structure when applied to the analysis of samples with an unknown layer thickness but based on a known structure system. That ability, in turn, needs the precise n and k values of the materials involved in the reduction and fit library. Theoretically, no calibration samples are required, but in practice, they are needed to check the above mentioned parameters and for day-to-day comparison. However, this fact does not diminish the utility of the method.

2.2.1 Building blocks of SE for research, material analysis, and product definition

An SE system consists of a set of components and building blocks[6] that work well together.

Light sources

The ideal light source would have a perfectly small and homogeneous origin; however, because that does not exist, the smallest wide-range sources on the market are used. A 75-W xenon lamp has a <1-mm-diameter spot, which can be easily collected and transferred. It is useful between <185 nm and 2600 nm. A D_2 lamp's origin has a <2-mm diameter, and its useful range is 120–600 nm. The spot of a thermal-filament lamp can be refocused to ~2 mm at the fiber and is useful from 400 nm to 2800 nm. (The different types are described in Section 6.4 of *Fundamentals*.[5]) The most-popular light source is the xenon lamp

because it provides high-light-density, wide-range light. The strong peaks within the spectrum will not cause any disturbance so long as they create no detector overload. Some programs allow for the choice of "forbidden wavelengths" to avoid measurements at the peaks.

Light transfer is typically done by a single fiber; even systems with one or two lamps in the illumination arm are also available. The source installed in the arm delivers the highest efficiency but also thermal problems, and it increases the size and weight of the arm. It either requires a set of mirrors or lenses to deliver well-collimated light to the polarizer. This version still suffers due to the shape and distribution of the sole source. Regardless of whether the light source is in an external device or in the arm, it requires a specific supply and a software-controlled shutter to ensure that the sample is only illuminated when required. Typical systems, based on fiber optics or not, work fine between 230 nm and 1100 nm.

Fiber coupling between the lamp and goniometer

The coupling between an external light source and the arm (achieved by fiber optics) is flexible at low weights. Because light source and arm are separated, there are no thermal problems, and the fiber homogenizes the intensity distribution within the field. If dual lamps are used, a special device combines the light into a single fiber, e.g., a single 500–1500-μm-diameter fiber. Its image is reproduced at the sample surface. The changes in efficiency when the arm is moved have no impact on the result. The wideband fiber transfer benefits from both the homogenization of intensity and polarization; the only disadvantage is the light loss. Depending on the application, a standard quartz fiber material is good for a range of 230–1100 nm. Extension to 190 nm or above 1100 nm may require special materials that have other drawbacks. Because changing the fiber cables is done quickly, optimization of the wavelength is done rather quickly, and calibration curves with different fibers may be recalled from memory. A set of two fiber systems can cover the 190–2600-nm range.

Polarizer arm

The illumination arm incorporates a rotating polarizer. Because the light beam has a diameter of <3 mm, a Rochon-type device is typically mounted inside the hollow axis of the motor. Standard quartz models work from <190 nm to >2600 nm, whereas an MgF_2 prism extends to 115 nm. Thus, the polarizer is not the limiting element in the chain. The rotation is typically 10–20 full turns per second and controlled by a DC motor, which delivers 40–80 polarization cycles and avoids technical frequencies (e.g., 50 or 60 Hz). An encoder disc is mounted at the axis of the motor that provides the control triggers for data storage. An additional retarder may be provided and moved into position, as required. The arm can

be moved between 0 deg (transmission position) and ~85 deg (specular reflectance). Whether the movement is done manually or by motor depends on the required automatic functions.

Sample holder

The typical sample holder is a flat table with a vacuum pump connected to hold the sample in a safe position. If the arms are vertical, the sample is in a horizontal position, which is safest. If the arms are motorized, they will probably be too heavy for motorized positioning, and the sample will be placed vertically. The sample holder must be capable of precise adjustments for rotation, "vertical" movement, and both tilt angles. Whether the adjustments are done manually or by software-controlled stepper motors is a matter of requirements and price.

Adjustment monitor

A viewing system is provided to place the sample in the perfect position. It includes a laser and a microscope. The output may be an objective lens or a small CCD camera. The system incorporates a crosshair and works in full back reflection. As soon as the illumination and reflection crosshair are perfectly superimposed and sharp, the sample is perfectly positioned with respect to both height and angles. The monitor system needs calibration only once (at installation).

Analyzer arm

The analyzer arm is a copy of the polarizer arm. A retarder is only required in one of the arms, if required at all. The analyzer is placed in the hollow axis of a stepper motor. The light collection may be optimized for a lager type of fiber cross-section, which will tolerate some beam widening by the sample. The fiber material will be identical to that of the illumination side.

Fiber guide to the spectrometer

The collimated light after the analyzer has a diameter of <3 mm, which is less than 7 mm^2. A lens or mirror will focus it under an optimized angle into a fiber system. The best solution to fit the other end to the spectrometer is a cable of several 100–250-μm-diameter fibers. A probable solution is a rosace of 39 fibers, each with a 200-μm active diameter at a 220-μm distance at the arm. On the side of the spectrometer, the fibers will be arranged in a line shape, covering 8.6 $\times$ 0.2 mm; the required illumination angle is reached by an adapted optical system between the fiber cable and spectrometer entrance.

The spectrometer

At first glance, the fidelity of the spectrometer does not seem to be crucial; however, it plays a key role. The entrant signal will contain the full

spectrum, and wavelengths in a close neighborhood may carry rather different polarization information (as shown in Fig. 2.5). Even little cross-talk may lead to errors in data reduction. If a data accuracy of 10^{-4} is the target, the spectrometer must be better than 10^{-6} in cross-talk (stray light), which requires a double-spectrometer setup. The data reduction schemes are designed to work with constant intervals and bandwidths in the eV domain. In order to capture the data with a constant bandwidth in the eV domain while using a double-grating spectrometer, the slitwidth must be varied many times during a scan. In the UV, the slitwidth would be four times smaller compared to the red end; however, the lamps and the transfer are weaker in the UV, and the samples reflect less. Requirements like that are compatible with the behavior of a combination of an Echelle or Echelette grating and a prism, as illustrated in Fig. 2.2 (see also Sections 4.1.8 and 4.4.1 of *Fundamentals*[5]). Advantages include no need for order selection, a grating that works in several orders, and increased dispersion toward the UV when physically necessary. Stepper motors control the grating, prism, and slits.

The monochromator consists of two stages with at least a 300-mm focal length. It features two exits: one for a PMT, and the other for an InGaAs detector. At that focal length and with an Echelette grating of 300 mm^{-1}, blazed to 1300 nm (11 deg), it will provide the following typical data:

- First order: a working range between 1.0–2.6 μm, and a RD of 10 nm/mm;
- Second order: a working range between 500–1300 nm, and a RD of ~5 nm/mm;
- Third order: a working range of 300–700 nm, and a RD of ~3.3 nm/mm; and
- Fourth order: a working range of 190–450 nm, and a RD of ~2.5 nm/mm.

The second stage, equipped with a 20-deg quartz prism, is compatible with those dispersion values and adds ~30% extra dispersion. Most of the SE applications perform best if the spectral bandwidth is in the range of 0.3 nm in the UV up to 3 nm in the NIR. Those values can be reached with slitwidths between 0.5 mm and 3 mm overall, which, in turn, fits the fiber cross-section nicely. The stray light level will be in the range of 10^{-7} or less and within a distance of five bandwidths from the center, thus fulfilling all needs. The unit is equipped with a motorized entrance and exit slit, while the intermediate slit can be set to 3 mm for most applications.

Detectors

Single-point detectors are typically a PMT, for 190–850 nm (6.526–1.46 eV), and InGaAs, for 700 nm (1.77 eV) upward. The upper limit

of the NIR detector can be selected from 1650 nm (0.75 eV), 2100 nm (0.56 eV), and 2600 nm (0.47 eV), keeping the compromise in SNR and linear range in mind (see also Sections 5.2 and 5.6 of *Fundamentals*[5]). To reproduce data in the 10^{-4} range safely, the detectors must deliver a linear range of 10^5, which requires TE cooling for the NIR detector (a PMT can do this at the ambient temperature). Because all data gathering is done in a modulated mode, the background signals of the detector will be automatically suppressed.

Goniometer and electronics

All electronic functions for control and acquisition are collected in a central unit that connects to the system PC. If the sample's substrate material does not change often, a manual goniometer may be sufficient; it saves money and permits vertical operation, which, in turn, utilizes horizontal sample placement. The goniometer should have 180 deg between the arms for calibration and for transmission measurement.

2.3 Basic Equations of RPSE Parameters Presented by Software and in Literature

SE data are based on the Fresnel equations:

$$\frac{r_p}{r_s} = \frac{|r_p|\exp(j\delta_p)}{|r_s|\exp(j\delta_s)} = \frac{|r_p|}{|r_s|}\exp(j\Delta) = \rho, \tag{2.2}$$

where r_p and r_s are the absolute parallel and vertical polarization values, respectively; δ is the actual phase shift; and ρ is the complex result, which itself leads to $\tan\Psi$ and $\cos\Delta$, the parameters used by data reduction programs and in most papers. The illumination angle at the sample is marked by Φ.
Equation (2.2) is also represented as

$$\rho = \tan\Psi\exp(j\Delta). \tag{2.3}$$

The complex value of ρ in a system with a polarizer–sample–compensator/retarder–analyzer arrangement is created by

$$\rho = \frac{-\tan A(\tan C - \tan(P - C))}{(1 + j\tan C\tan(P - C))}, \tag{2.4}$$

where A, C, and P are the angles of the polarizer, compensator, and analyzer, respectively. For all standard SE measurements, it is sufficient to recover only the real part, which needs no algebraic sign and can be done without a compensator.

In a SE system with a rotating polarizer and a programmed analyzer but no compensator, the measured data are created by

$$I = I_0(\alpha\cos 2P + \beta\sin 2P + 1), \quad |\alpha| \le 1, \quad |\beta| \le 1, \tag{2.5}$$

where the coefficients α and β are also recovered by Hadamard reduction. The result produces tanΨ and cosΔ:

$$\tan\Psi = \tan A\sqrt{\frac{1+\alpha}{1-\alpha}} \text{ and } \cos\Delta = \frac{\beta}{\sqrt{1-\alpha^2}}. \tag{2.6}$$

Data acquired by optimal working instruments and from well-suited samples can be reduced to an absolute thicknesses of 0.1 nm and an accuracy of ±0.0005 in n and k.

2.4 Comparison between SE and Single-Wavelength Ellipsometry

The light source used in single-wavelength ellipsometry (SWE) is typically a laser in the visible area that can illuminate a smaller area and provide a higher intensity for a better SNR than a lamp. Because more light at a single wavelength reaches the detector, the source can be an optimized silicon diode. To limit the wavelength range to only the portion that is used, a narrowband filter will be placed in front of the detector. The source and detector may be placed directly in the arms, which reduces the total footprint and makes the application easier. SWE is well suited for single-layer systems; it is also useful for double-layer samples if the illumination angle is variable. Thus, the advantages of SE are immense because SWE only works correctly if the structure is known. If modeling is required, if more than two layers are involved, or if the layers have a gradient, SWE can no longer perform the analysis. SWE cannot be used to characterize materials because one wavelength is not sufficient for safe n and k measurements. In short, SWE is fine for product and production control but not for research tasks.

2.5 Production-Oriented SE

2.5.1 SE with parallel detection

Like many other measurement systems, SE balances time versus precision. In process environments or quality control (QC), time is an important factor. One way to speed up data acquisition is the parallel detection of all wavelengths of interest. A diode array or CCD detector with 512 or more data points in the wavelength axis can recover ~250–1050 nm within a few milliseconds. The detector, without an additional averaging process, will provide a signal resolution in the 10^{-4} regime. Due to the large number of data points, the data reduction (including curve fit functions) will be suitable for the tasks mentioned earlier; however, they will not be sufficient for research or for product characterization. Because the data will not deliver the ultimate accuracy, a single-stage spectrograph will be fine— a single-stage prism spectrometer that provides 10^{-3} stray light at all wavelengths and an almost linear dispersion in the eV domain will probably fit. The fact that the analyzer will not be optimized for

each wavelength but rather set to a median angle will also be fine for the target applications. For QC applications, a standard goniometer with robotic sample handling will be fine. For production control, the key components must fit the process environment and the other equipment.

The context between the spectral performance and time differs from that of single-wavelength SE. Two methods—static and dynamic—are applied. The static method controls the polarizer with a stepper motor; it has the advantage of keeping the polarizer at the perfect angular position during detector illumination, which can be variable and is controlled by the camera shutter. During read-out, the camera shutter is closed, and the polarizer moves. The method's disadvantages are that the experimental background is not automatically subtracted and the camera shutter will, at best, allow four data to be acquired per second. The camera and experimental background, with the light source shut, will be acquired before measurement and subtracted from each shot. The other method benefits from the lock-in principles. The polarizer will turn constantly, and the signal integration and read-out occur while the polarizer rotates. If, for example, the detector read-out time is 10 ms, and one turn requires 100 ms, then the polarizer will turn 36 deg during read-out, which is 80% of one 45-deg sector. Thus, as soon as the trigger from the encoder arrives, the detector will clean the signal and wait for 4.5 ms, until the read-out starts. During read-out, the polarizer moves ahead; therefore, the polarization for each pixel (wavelength) is slightly different. This scenario is not a problem because the calibration is done with the same procedures, and the differences are reduced. The camera and experimental background are recorded once with the light source shut and subtracted from each data set. The camera shutter stays open during measurement, making the process much faster. The only disadvantage is that the integration and read-out timing are fixed. Some parameters will influence the signal magnitude. One is the spectrograph slit, and another is the applied grouping/binning of the detector and the speed of rotation of the polarizer; both are combined to vary the detector integration time. All of these parameters require a new calibration after being modified.

2.5.2 *in situ* SE

The components to apply SE to vacuum chambers and other process equipment are basically the same as those described earlier. The optical approach to a product in an enclosure, such as a plasma or ion etch chamber, requires a special beam path. The arms must be coupled to windows, which necessitates a perpendicular orientation that will avoid affecting the polarization of the measurement light. Two windows under the required angle to the sample surface and at the right position are required. A small range of angular variation between the arm and sample will ensure *in situ* adjustment. Removing the arms and the windows for test and calibration should be provided by the setup. Parallel detection is the most suitable

method. Special software may access and use the real-time tanΨ and cosΔ data of the system for process control.

2.5.3 SE with a reduced spot size

The original spot available after the polarizer will have a diameter between 1 mm and 3 mm. Due to the illumination angle, the size will increase in one dimension by a factor of $\sim$2. For some samples, that size is too large. Two solutions will limit the spot size: either a variable iris aperture or a set of fixed apertures. These options reduce the light flux drastically but preserve the collimation. Alternatively, a set of lenses, similar to a microscope objective, can be placed at the end of the illumination arm; this allows spot sizes down to $\sim$100 μm at the expense of collimation. An angle of $<$1 deg would be required if the distance to the sample is 100 mm and the size is reduced from 3 mm to 0.1 mm. This situation will slightly reduce the accuracy and increase the spread of data. Typically, the impact on the data is on the same order as an imperfect surface or a technical roughness of the sample. In other words, the extra optics are insufficient for the acquisition of reference data but fine for the reduction of multilayer systems. Both arms of the goniometer require the same optics to capture the angled light and collimate it.

2.6 Data Origin and Reduction

Many sources of SE reference data are available for data import. Regardless, the best suggestion is to create references with one's own samples; this ensures full tracing of all parameters. Data reduction methods compatible with SE can be found in the literature and sources for the different kinds of material structures.

2.7 Limits of the SE Method

The detection limits of SE are 10^{-3} in the range of tanΨ and cosΔ, which is equivalent to changes in the n and k material values of $\sim 10^{-4}$. The data reduction modes include fit functions over wide wavelength intervals, which improve the precision to better than 10^{-4}. The sample itself is very important: roughness, homogeneity, and other practical aspects may limit the method more than the SE system. The best practical detection limits in a 0.1-nm layer thickness range produce an uncertainty of 1%. A research system, as described, may perform more applications besides SE if the rotating analyzer is driven by a stepper motor that can be stopped at any angle, allowing stationary reflection/transmission/scattering measurements under any polarization condition. The optimal use of all possible methods requires the acquisition of all Stokes parameters, including the algebraic sign of angular functions; that, in turn, requires a retarder.

2.7.1 Measurement of *P*, the degree of polarization

If all four Stokes parameters are available, then parameter P (the degree of polarization of the light after the sample) can be calculated. It defines the

ultimate detection limit and is also important for the analysis of sample roughness:

$$P = \sqrt{\frac{S_1^2 + S_2^2 + S_3^2}{S_0^2}}. \tag{2.7}$$

2.8 SE Examples

The wafer measured in Fig. 2.3 carries a thin layer of native oxide (SiO_2) that is reduced to be 1.38 nm thick. The solid curve is the data acquired, and the dotted line is the fit curve of the reduced data.

Certified samples are used to justify the fidelity of the data delivered by a spectroscopic ellipsometer. In Fig. 2.4, the reference sample consists of a silicon wafer (crystalline silicon) with a 151-nm-thick layer of SiO_2. Again, the solid curve shows the acquired data, and the dotted one is the fit curve. The perfect fit proves that the system is in the best shape.

The sample used in Fig. 2.5 consists of a silicon wafer with a known layer of SiO_2; the thickness of the layer is 2.517 μm. The peaks of the fit curve appear higher because the rather thick layer has lower reflection, which it theoretically should have. However, that fact has no impact on the reduced result. Because the interferences get very close, the measurement is near the upper thickness limit of the method in the UV–Vis range.

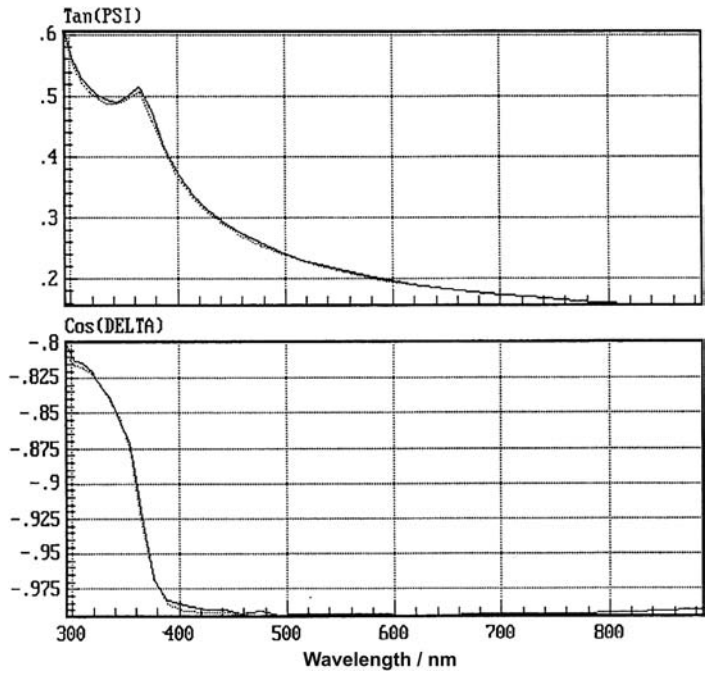

Figure 2.3 Ellipsometric data of a bare silicon wafer (crystalline silicon).

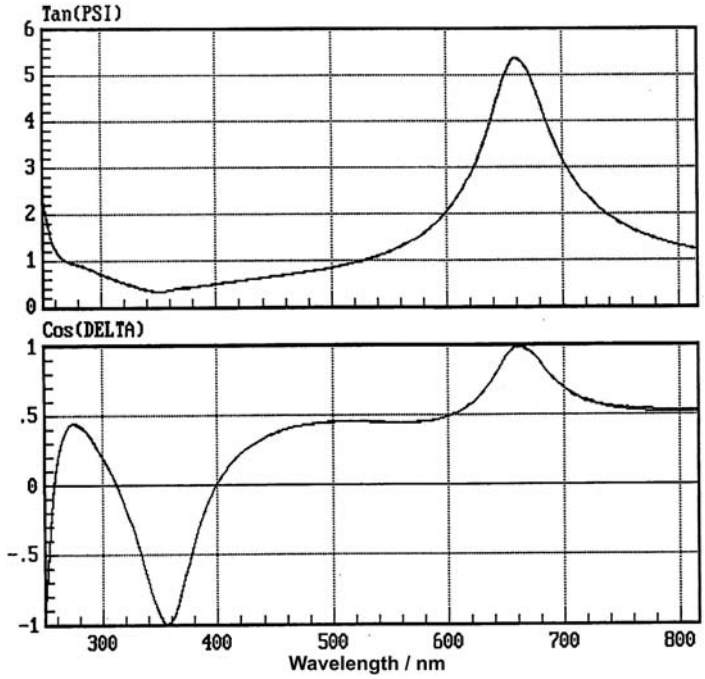

Figure 2.4 Ellipsometric data of a calibration sample.

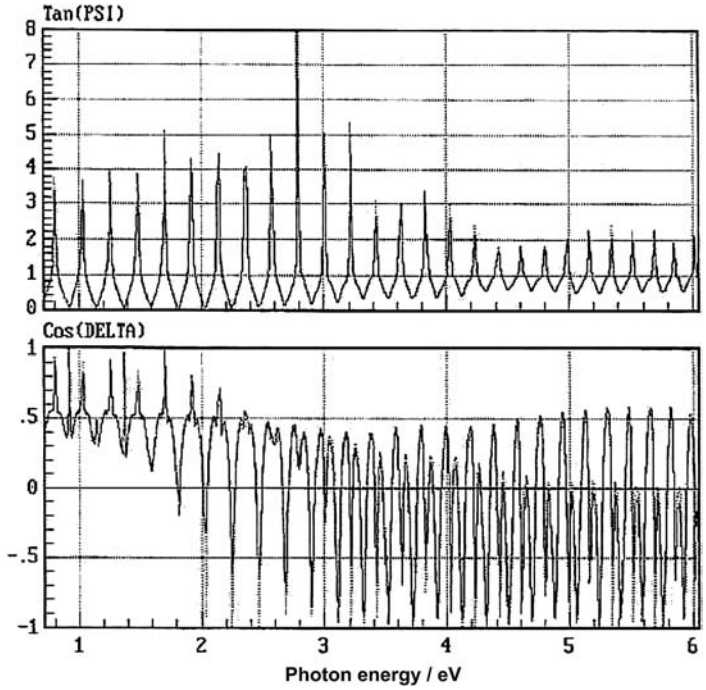

Figure 2.5 Ellipsometric data of a thick layer calibration sample.

2.9 Extensions of the Instrumentation for Spectroscopic Ellipsometry

The SE method only works at wavelengths that have reasonable transmission of all layers involved. If the substrate is opaque or transparent, it plays no role, but its precise n and k data are required for reference. If the substrate is transparent, it must be thick enough to avoid so that the reflected signal from its back side is within the acceptance aperture of the analyzer arm. Otherwise, data subtraction methods for correction after measurement and before data fit procedures must be applied.

In short, the SE measurement must happen in wavelength intervals with at least some regions of transparency. Materials and layer systems are often opaque in the UV and/or visible range but appear transparent in the NIR or IR. A second reason to apply longer wavelengths is the upper limit of the detectable layer thickness. As Fig. 2.5 shows, the frequency of interferences increases with the photon energy, equal to the decreasing wavelengths. This effect is beneficial when analyzing very thin layers, whereas relatively thick layers are better measured at low photon energies. A third reason is based on the need to measure optical components, such as mirrors, lenses, etc., at the wavelengths of their designated use. Thus, the SE system must be able to acquire data within those wavelength ranges.

A typical standard unit with fiber optic transfer works between ~230 nm and 900 nm (5.4–1.37 eV). With little effort, the unit can be modified ~190 nm (6.53 eV), 1650 nm (0.75 eV), or even >2000 nm. No standard fiber material is available below 190 nm. An IR fiber material, however, does not transmit below ~1500 nm; thus, other concepts are used.

2.9.1 SE system for the deep UV

In order to measure thin layers and characterize materials and products to be used in the deep-UV range, the SE system must work at that range. The setup (Fig. 2.6) is similar to the standard one but without fiber optics. If the wavelength needs to reach below 185 nm (>6.7 eV), the air must be eliminated from the beam travel via nitrogen purging or evacuation. All of the optical components and the sample are placed inside a chamber. Mounting the light source into the polarizer arm is no problem. The collimated beam is created by several (probably movable) lenses combined with pinholes. The polarizers will probably be MgF_2 Rochons. The light source will either be a xenon lamp (>155 nm) with a very small spot or a D_2 lamp (120–600 nm, equal to 10.4–2.07 eV). The heat created by the lamp must be removed, which is automatically done by purging with nitrogen. Under vacuum conditions, there are special lamp designs with an integrated cooling jacket and water circulation. It is difficult to move the combination analyzer arm/spectrometer/detector around the goniometer; therefore, that part becomes the fixed part of the goniometric setup, which works best in a horizontal position. The sample holder then needs to rotate and hold the sample, even in an evacuated environment. Intelligent sample fixtures and sample-handling attachments that avoid ventilation of the vacuum chamber are very helpful in vacuum systems.

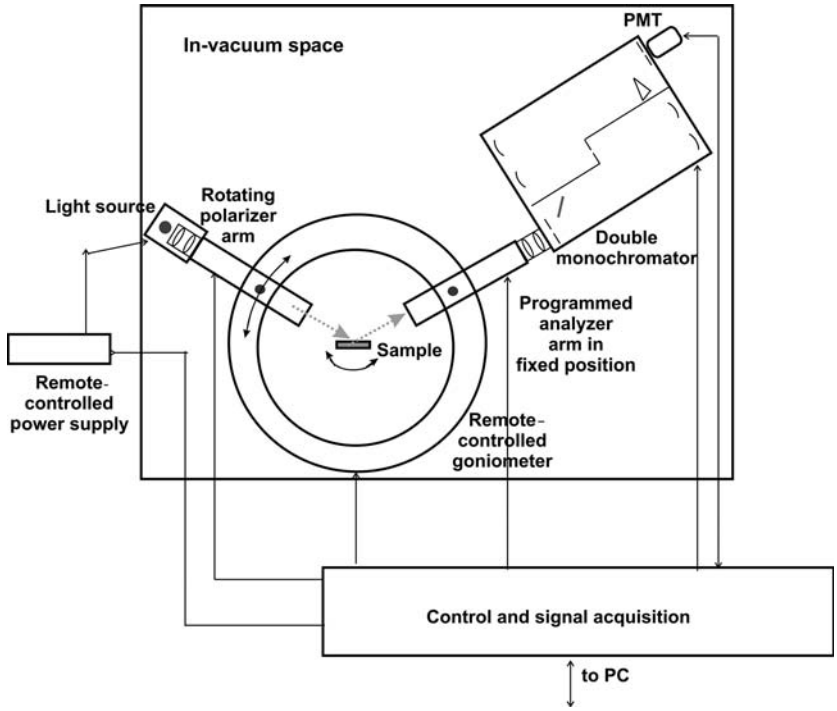

Figure 2.6 Vacuum–UV SE system.

2.9.2 SE system for the IR range

In order to analyze relatively thick layers and to characterize materials and products in the IR range, the SE system must work at that range. Two setups can solve that:

- The setup may look similar to that of a UV system because that enables the use of a complete FT–IR spectrometer (Fig. 2.7) without massive modification. The key unit is an industrial FT–IR instrument that has a light source with interference modulation. The beam will be collimated by lenses, which can optionally be moved, and pinholes. The spot of a UV–Vis system may be in the range of a millimeter, but due to its source dimensions in the IR, the spot will increase to several millimeters in diameter. Although the reference detector stays inside the FT–IR instrument, the final experimental detector is removed from the FT–IR part and mounted to the analyzer arm. The typical wavelength range is 500–7000 cm^{-1} (1.6–20 μm, or 0.775–0.062 eV). The polarizer and analyzer are realized in most instruments by mechanical crossed-wire constructions that also rotate to achieve the different polarization states. The combination of a spectrometer and polarizer arm is too heavy to be moved; thus, it is the fixed part of the goniometric system and is best placed horizontally. The sample holder must rotate around the pivoting point. In most cases, the sample will be fixed

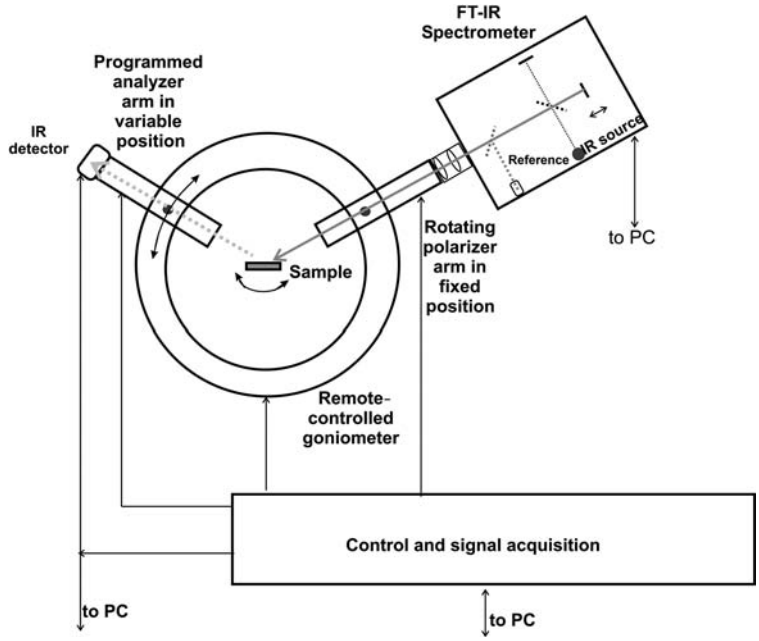

Figure 2.7 FT–IR SE system.

with a vacuum pump, but automatic holders and sample changers are also available. Although the upper limit of layer thickness in the UV–Vis is perhaps 3 μm, a FT–IR–SE can reduce thicknesses up to ~30 μm. It is of even more importance that many materials that are opaque in the UV and/or the visible range are transparent in the IR. The system requires special data acquisition software to create the data for the Stokes sectors. Thus, the functionality between the goniometer, arms, FT–IR spectrometer, and data storage requires special programs to achieve the fit.

- Because polycrystalline IR (PIR) fibers are available for the range between ~2.5 μm and 20 μm (see Fig. 6.22 of *Fundamentals*[5]), a dispersive setup can also solve the application. The system will then look like the one shown in Fig. 2.2. The components of the arms, sample holder, etc., will be the same as those in the FT solution, but the goniometer may stand vertically, and the sample may lay flat. Due to the low light power and light density provided by the available wide-range sources, the spot will not be smaller, as in the FT–IR. Data acquisition and data reduction will be the same as for a dispersive UV–Vis SE system. The SNR of the scanning system will be remarkably worse than the FT–IR, even if much more time is invested.

2.10 Calibration of SE Systems

Data reduction and equations assume that the parameters I_p, I_s, and both 45-deg positions are identical in magnitude at all wavelengths. If a retarder is

used, it is also necessary to know the phase shift versus the wavelength. All information needed to provide the correction parameters can be obtained by the apparatus itself without extra tools. Setting the arms to the transmission position and the analyzer (assuming a RPSE setup) to the *P*, *S*, and both 45-deg positions allows one to scan the wavelength range four times. The captured data will be stored as references and used to create a polarization correction curve. After that, the baseline of the system will provide flat behavior for the ellipsometric parameters. The supplier software incorporates all required steps and functions. After that, the retarder can be put in place. Its function versus the wavelength will also be recorded and stored for reference; it contains the phase shift versus the spectral position. To check the calibration, the samples described earlier are very useful (completed by a substrate with known surface roughness) when checking parameter *P*.

2.11 Photometric Applications by SE Systems

The sample illumination and collection for SE is performed in reflection mode. Variable angles and programmed polarization are provided; thus, reflectance anisotropy spectroscopy (RAS) is a natural extension. However, RAS requires different (not more) data-storage schemes and special data processing software to present reflection spectra instead of ellipsometric data. If they are provided, general reflectance and RAS are available without any hardware modification. A modified means of data storage and reduction is also necessary for transmission/absorption measurements, even if no polarization specific data are the goal. It first needs a free 180-deg beam, just like the calibration. Most likely, it also requires special adapters to hold the solid sample or transmission cell. If all of those items are available, a spectroscopic ellipsometer performs well as a single-beam spectrophotometer.

References

1. D. Clarke and J. F. Grainger, *Polarized Light and Optical Measurement*, PergamonPress, Oxford (1971).
2. E. D. Palik, ed., *Handbook of Optical Constants* and *Handbook of Optical Constants II*, Academic Press, Orlando, FL (1985) and Boston (1991).
3. A. C. Boccara, C. Pickering, R. Rivory, eds., *Spectroscopic Ellipsometry*, Proc. 1st Intl. Conf. on SE, Elsevier Science Publishers (1993).
4. A. Szilágyi, "Animations of electromagnetic waves," www.enzim.hu/~szia/emanim/emanim.htm.
5. W. Neumann, *Fundamentals of Dispersive Optical Spectroscopy Systems*, SPIE Press, Bellingham, WA (2014) [doi: 10.1117/3.1002528].
6. J. Gardavsky and W. Neumann, "Spektroskopische Ellipsometrie – Grundlagen, Stand der Technik und Anwendungen," *Jahrbuch für Optik und Feinmechanik*, p. 51–86, Verlag Schiele & Schön, Berlin (1995).

Chapter 3
Emission Spectroscopy

3.0 Introduction

Every measurement of a radiating object is naturally an emission measurement. However, it makes sense to use the term "emission spectroscopy" for applications that target excited molecules, plasmas, or atoms. The spectrum often undergoes changes over time or follows a pulsed excitation, both of which require synchronization and/or time resolution. This chapter discusses the following emission applications:

- Atomic emission spectroscopy (AES),
- Cathodo luminescence (CL),
- Inductively coupled plasma (ICP) spectroscopy,
- Spark optical emission spectroscopy (Spark-OES),
- Laser ablation (LA),
- Laser-induced breakdown spectroscopy (LIBS),
- Laser-induced plasma spectroscopy (LIPS),
- Laser-induced plasma deposition (LD),
- Plasma etch (PE) spectroscopy,
- Solar and stellar emission, and
- Combustion emission (spectroscopy of flames and explosions).

As stated in the Preface, the physics, chemistry, and biology of applications are not the topic of this book. Many applications require a spectral light source to work, such as absorption or luminescence applications. Primary sources like that are directly linked to the final result, making them the sole part of the issues discussed. In the emission applications described here, that direct relation is not the case; therefore, the excitation origin of the emitted signals are only mentioned as far as necessary to produce the signal collection and spectral processing.

3.0.1 Instrumental technology for the acquisition of emission spectra

Even though the previously mentioned methods apply to a variety of applications with different excitation, the acquisition of the emitted spectra is

very similar. In all cases, a high number of spectral lines may occur that are partially in a very close neighborhood and spread over wide intervals at the same time. In addition, the signals are often either short-term or depend on time.

The best-suited system for many applications is a 2D Echelle spectrometer that is equipped with a CCD (comprising a large number of pixels) and an optional gateable MCP image intensifier. Capturing the elusive light signals of "true emission applications" is almost always realized with nearby collection optics and fiber optic transfer into the spectrometer.

3.0.2 Typical emission spectra

Plasmas, as well as atoms in the excited state, emit local, exactly defined spectral lines that have bandwidths clearly below 1 nm. The more different molecules make up the sample, the more lines are to be expected.

The spectral range shown in Fig. 3.1 is 225–800 nm. The height of the lines does not represent any amplitude—it is an arbitrary tool to visually discriminate the spectral positions of the involved elements. Lines of the same height represent the same molecule, and thus the vertical numbering is a "line marker." In Fig. 3.2, the overview is improved by limiting the wavelength range to 225–295 nm. Only 25 of the 55 radiation sources are involved.

The lines appear extremely close to each other at some spectral places, requiring subpicometer spectral bandwidths to be resolved. Thus, it is very

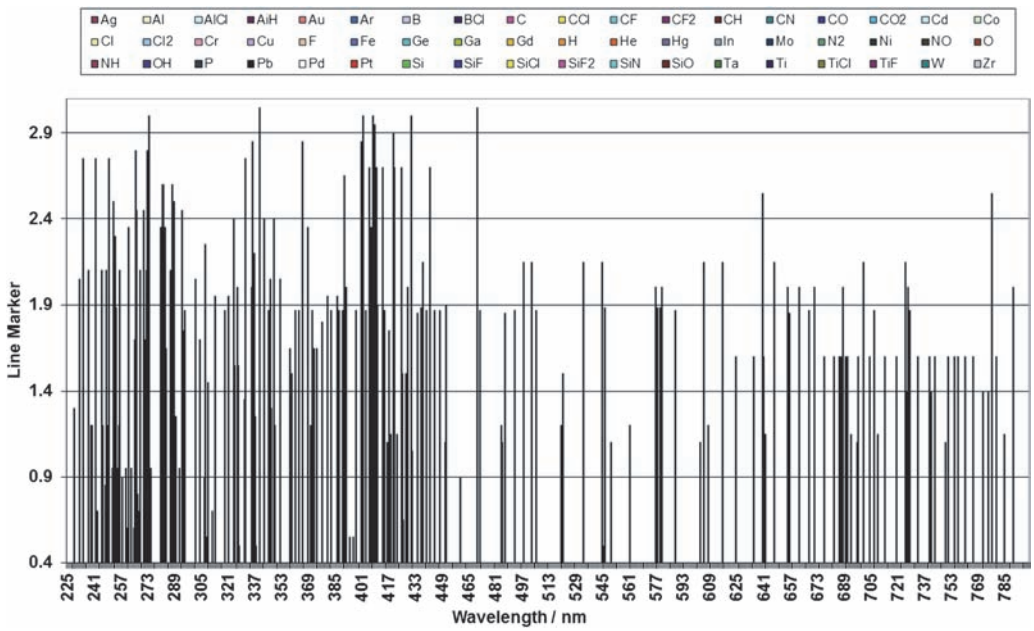

Figure 3.1 The most prominent lines of 55 different molecules in semiconductor technology, presented by plasma emission spectroscopy.

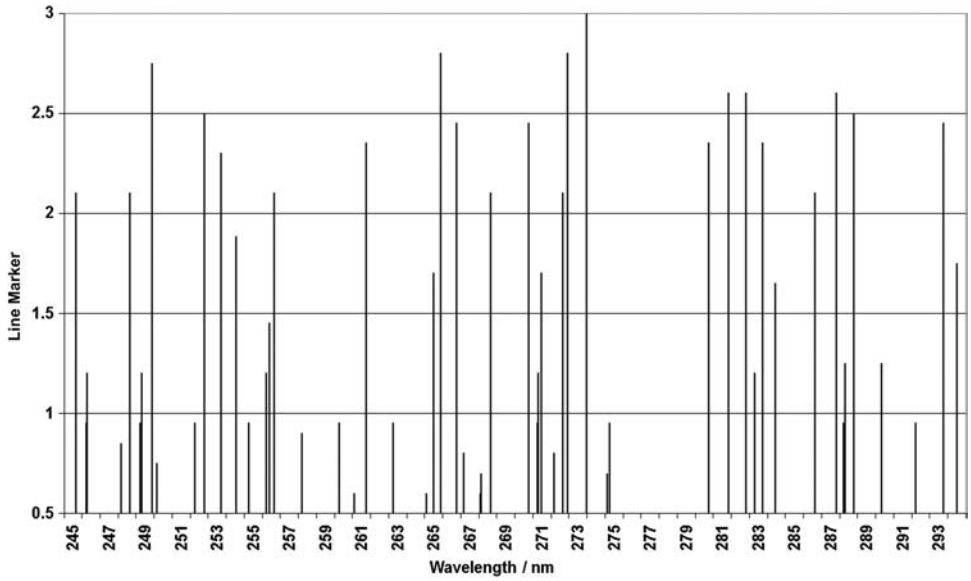

Figure 3.2 The same plasma emission lines shown in Fig. 3.1, reduced to an interval of 50 nm.

helpful that most of the elements offer a reasonable number of lines. With the help of correlation techniques, the elements involved can be detected. The numerous signals also allow for the selection of a rather free-standing line even though it might not be the strongest. This mechanic can avoid confusion or even overlap at the detector.

3.0.3 Setup based on 2D Echelle spectrometers

3.0.3.1 Stationary 2D Echelle spectrometer

The calculations of key parameters of a 2D Echelle spectrometer (Table 3.1) are based on a CCD with an active surface of 26.6 mm × 26.6 mm, comprising 2048 pixels × 2048 pixels, and on Sections 4.4 and 5.8 in *Fundamentals*.[1] The size of each pixel is 13 μm × 13 μm, which ensures that the Rayleigh limit is overcome at all detected wavelengths. In the vertical plane, the spectrometer covers 215 spectral orders (the 52^{nd} through the 267^{th}), which appear in superposed horizontal stripes. It performs bandwidth/resolution (B/R) specifications between 1.76 pm / 5 pm near 200 nm and 8.7 pm / 26 pm at 950 nm. Reading the 215 stripes with full spectroscopic (horizontal) resolution, running at an ADC rate of 1 μs (1 MHz), will theoretically take 438 ms. Because some vertical shift times are added, it will realistically take ~500 ms. In total, the system may reach a rep rate of ~1 s if an illumination time of roughly 500 ms is sufficient, which, in turn, would produce a duty ratio of 0.5. These are good numbers for an electromechanical

Table 3.1 Key parameters of Echelle CCD systems.

Wavelength [nm]	Grating order	Covered interval [nm]	Vertical position at CCD [mm]	Overlapping pixels per order	Horizontal title angle [deg]	Bandwidth per pixel [pm]	Position [deg]
1000	52	18.4	−12.4	—	—	—	—
950	55	17.7	−12.2	6	−0.5	8.64	−2.5
900	58	16.5	−11.9	5	−0.6	8.06	−2.4
850	61	15.7	−11.7	5	−0.6	7.67	−2.4
800	65	14.7	−11.5	3	−0.6	7.18	−2.4
750	70	13.8	−11.3	3	−0.7	6.74	−2.3
700	74	12.9	−11.1	3	−0.7	6.30	−2.3
650	80	12.0	−10.9	4	−0.8	5.86	−2.2
600	87	11.0	−10.5	4	−0.9	5.37	−2.2
550	95	10.1	−10.2	4	−0.9	4.93	−2.1
500	104	9.2	−9.6	5	−1.0	4.49	−2.0
460	113	8.5	−9.1	4	−1.2	4.15	−1.8
420	124	7.7	−8.5	6	−1.3	3.76	−1.7
380	137	7.0	−7.3	7	−1.5	3.42	−1.5
340	153	6.3	−5.9	7	−1.8	3.08	−1.2
315	166	5.8	−4.5	7	−2.0	2.83	−1.0
290	180	5.3	−3.3	8	−2.3	2.59	−0.7
265	197	4.9	−1.2	10	−2.9	2.39	−0.1
240	217	4.4	1.7	13	−3.4	2.15	0.4
215	243	4.0	6.7	17	−4.4	1.95	1.4
195	267	3.6	12.8	21	−5.9	1.76	2.9
192	271	3.5	14.3	25	−6.5	1.72	3.5

shutter in continuous operation. If the experiment requires shorter illumination times, the use of a gated MCP image intensifier is advised.

A 2D Echelle needs rather-high light levels for a reasonable SNR. The reasons are found in the method itself: in most cases, the entrance slit is a pinhole (the example here has a diameter of 26 μm) because along with the horizontal (wavelength) resolution, the vertical (order) resolution must also lie within a range of a few pixels. Because of the limitation of luminosity due to the small entrance aperture, each wavelength only illuminates a very small detector area of ∼20 pixels, or 0.0034 mm^2. It is not difficult to calculate the luminosity and compare it with classical monochromator or spectrograph concepts.

In short, many applications will produce relatively long exposure times, or, if pulsed experiments are performed, several repetitions may be required before the CCD is read out. Another critical parameter is the mechanical and thermal system stability. Even if the 2D Echelle instrument is kept stationary in the lab, it needs to be robust because even the smallest change will have remarkable effects in terms of light transfer and calibration. This effect is much more critical compared to "normal" CCD spectrometers. Many of the following applications may introduce external temperature variations of more than 2 °C. If that is the case, the measurement system must be thermally protected and stabilized to ensure functionality.

3.0.3.2 2D Echelle spectrometer with a small detector surface

If the ultimate performance in terms of dispersion/resolution and stray light are not required, then smaller spectrographs with less useful *xy* output areas can be used. They typically have focal lengths of 0.25–0.33 m and expose detectors with up to 13 mm per side, covering 1024 pixels × 1024 pixels. The resolution and contrast losses are partially compensated by better luminosity. These concepts are of special interest in cases where an MCP image intensifier is part of the chain.

3.0.3.3 MCP–2D-Echelle spectrometer

Experiments wherein one of the following parameters is valid are better performed with a gateable MCP in front of the CCD:

- The flux of photons is not enough to create a reasonable SNR during the available exposure time (the intensification function of the MCP is used).
- Time resolution is required, which is out of the range of mechanical shutters (an MCP reaches into the nanosecond range and performs in the kilohertz repetition range for long periods).
- Pulsed excitation must be separated from rather-high background signals (the gating capability of the MCP is used).
- Synchronization of excitation pulses with rep rates of >1 Hz, including the read out (the gating capability of the MCP is used).
- Summation of a predefined number of excitation pulses before one CCD read out occurs (the gating capability of the MCP is used).

The basic functions and application of gateable image intensifiers are described in Section 5.4 of *Fundamentals*[1]. For a CCD area of 26 × 26 mm^2, a 40-mm-diameter MCP is required. These are available only from a few suppliers, and several versions are limited to the military. In general, the 40-mm versions feature less variety of cathodes, and the gating times do not reach below 10 ns.

For CCD areas up to 13 × 13 mm^2, an MCP with an 18-mm diameter is perfect. These are available from more vendors and are offered for general use, with the exception of a few special cathodes. Thus, they are offered in a large variety of spectral behavior, and gating speeds reach down to <2 ns (some reach 0.3 ns).

3.0.4 Scanning (Echelle) spectrometers

Experiments wherein one of the following parameters is valid are better done with a monochromator system in favor of a 2D spectrometer:

- Only one spectral line is of interest.
- One spectral line will be recorded with very high time resolution.
- For research purposes, a quasi-static experiment will be measured with the highest spectral resolution and negligible stray light.

Table 3.2 Typical monochromator resolution parameters with different gratings, at a slitwidth of 20 μm for standard gratings in first order, compared to a 63-deg version.

	Standard grating			Echelle grating	
Wavelength [nm]	3600 mm^{-1} [pm]	2400 mm^{-1} [pm]	1800 mm^{-1} [pm]	316 mm^{-1} [pm]	Order no. [pm]
170	2.5	4.0	5.5	0.4	33
190	2.5	2.9	5.3	0.4	30
220	2.5	3.9	5.3	0.4	26
250	2.4	3.8	5.2	0.5	23
300	2.2	3.8	5.2	0.6	19
350	2.0	3.6	5.1	0.8	16
400	1.8	3.5	5.0	0.9	14
500	—	3.2	4.8	1.2	11
600	—	2.7	4.5	1.6	9
700	—	—	4.1	1.6	8
800	—	—	3.6	1.8	7

For those tasks, a single-stage monochromator with a focal length of 1 m or more offers much-better dispersion/resolution than a 2D Echelle at lower orders of stray-light levels. Double monochromators and scanning Echelle spectrometers perform even better. (Sections 4.3 and 4.4 of *Fundamentals*[1] offer all information on that topic.) The luminosity of scanning systems with large detectors exceeds that of 2D Echelles also by several orders. If only up to 50 pre-defined spectral lines must be monitored, and if they can be found at the Rowland circle (Fig. 3.4 of *Fundamentals*[1]), a multiline spectrograph will also beat the 2D Echelle in all parameters except flexibility.

3.1 Atomic Emission Spectroscopy

Atomic emission spectroscopy (AES) is the inversion of atomic absorption spectroscopy (AAS, see Chapter 1.3.1). The sample introduction and atomization is similar. The dissolution and excitation of the liquid sample occurs in flames or electrically heated ovens. The process is almost always performed in the normal atmosphere. One of its features is that not only one pre-defined element is detected but rather a selected spectral range is recorded. The data acquisition techniques depend on the process used. Depending on the atomization and the sample material, AES may produce a large number of spectral lines. In a flame, for example, the lines of the burning gas components will appear. If that is the case, powerful software for data reduction is required, which is why parallel-detecting AES grew quickly after affordable computers became available by the end of the 1970s. The collection optics are focused on an adjustable area above the burner slot (as in AAS) and collect part of the emission. The best efficiency is reached by mirror optics, consisting

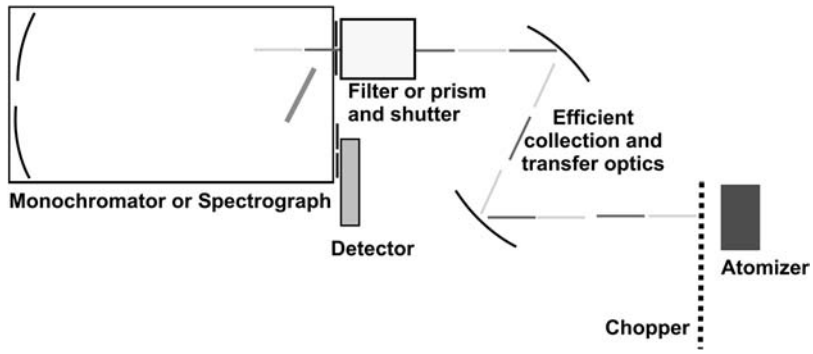

Figure 3.3 An atomic emission spectrometer.

of a wide collection cone, while illuminating the spectrometer according to its acceptance cone.

3.1.1 Scanning AES

If single-wavelength systems are used (like that shown in Fig. 3.3), a chopper modulates the signal, and thus it will present very stable results. A single-stage monochromator with the required dispersion/resolution will be sufficient. Stray light is a minor problem, and spectral order overlay is blocked by filtering or a prism pre-disperser. The detector is almost always a PMT. The data acquisition per line will be fast, typically milliseconds, which also enables the method for dynamic atomization methods. Very efficient signal collection is provided by utilizing rather wide slits, high luminosity, and high-sensitivity detectors. The scanning AES method was a competitor of AAS for many years.

3.1.2 Parallel-detecting AES

Parallel-detecting systems are much faster than scanning systems. Before useful semiconductor line detectors became available in the 1980s, multi-wavelength detection was based on the Rowland spectrograph. Even with the typical 1024 channels of diode line arrays, only a limited improvement was possible. Due to the high amount of dispersion required, only a rather short wavelength interval is detected in a parallel manner. This arrangement is sufficient for certain applications and families of elements or molecules that send out spectral lines in a close vicinity. Compared to single-channel detection, this method has the advantage of allowing little drift or misalignment (so long as the line is fully at the detector), as well as simultaneous detection of the line and background. If the method is applied, the detector typically rides on a slider that moves at the Rowland circle.

The dispersed wavelengths, in a classical spectrometer with spherical mirrors and plane grating, will land at a radius and present the best foci there. This feature is utilized in the "Rowland" or "Paschen–Runge" spectrograph

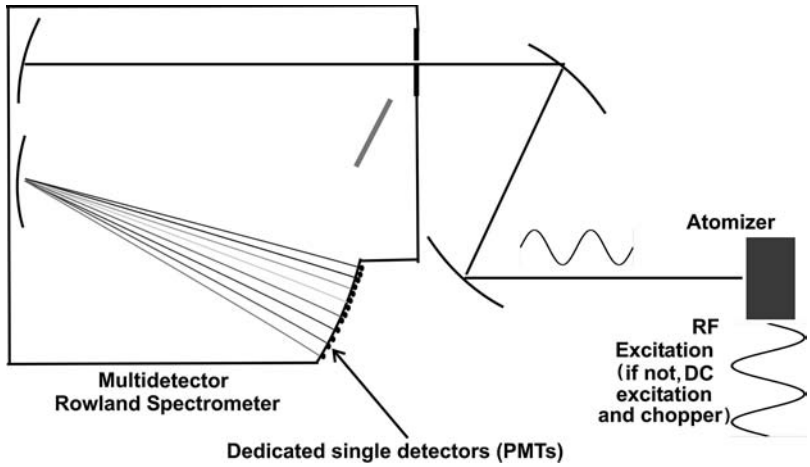

Figure 3.4 Emission spectrograph in Rowland configuration.

(see Section 2.5 of *Fundamentals*[1]) by a number of separate detectors placed at dedicated wavelengths of pre-defined elements. Overlay of spectral orders is not a problem because each wavelength can be individually filtered. Very small end-on PMTs allow high density in the arrangement. Compared to a 2D Echelle, the luminosity is very high because the beam height will be in the millimeter range and the slit may have a rather large geometry.

The setup needs discrete electronics for each channel (HV, pre-amp, etc.), which allows different amplification and integration parameters for each single wavelength; however, it is rather expensive and likely to require frequent maintenance and service. For that reason, 2D Echelles are primarily used for general applications today, although the diode array is still used for short wavelength ranges. A 1-m Rowland spectrograph, for example, featuring a useful exit angle of 30 deg, provides a field length of 58 cm. If a grating of 1800 mm^{-1} is used under 15 deg, it delivers the range between 170 and 470 nm to the installed detectors. If each detector surface is 1 mm wide, the bandwidth has a median of 0.5 nm. Because filters can be individually placed in front of each detector, crosstalk can be avoided. Such a system would work between perhaps 150 nm and 1000 nm, depending on the grating frequency and angle, but the position of the detectors requires complete re-alignment after each variation of the grating.

Thermal background

In addition to the reaction partner's emission lines, flames introduce a continuous background signal: Planck radiation. The element lines will "ride" at the background. Because the lines are very sharp and the background is homogeneous, it is not a problem for modern data processing to separate one from the other. The background radiation may even be used to check the flame temperature. (More on the topic

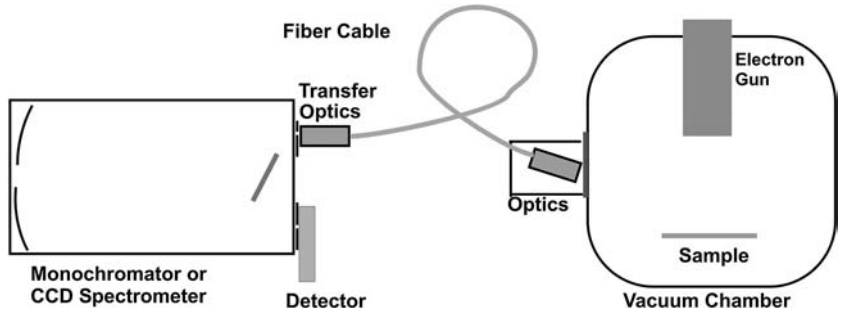

Figure 3.5 A cathodo luminescence spectrometer.

of thermal radiation is found in Section 5.6.9 and in Fig. 3.15 of *Fundamentals*.[1]) In the case of individual detector elements, the background subtraction can be made easy with the help of a chopper (as in Fig. 3.3). If the atomization is not created by flame but electricity (i.e., inductive-like ICP applications, see Section 3.3), signal modulation may be preferable because the signal can be sine-wave modulated, and phase critical detection may be applied. If a rather-short array detector is used, shuttered or synchronized detection will also be applied.

3.2 Cathodo luminescence spectroscopy

If a ray of electrons hits a solid material, it will pump excessive energy into the molecular/atomic structure. The sample atoms will then be lifted to excited states and emit specific line spectra at relaxation. This process is called cathodo luminescence. Vacuum is required to allow the electron beam travel between the gun and sample. A typical application is the cathode ray tube in televisions.

In a vacuum chamber, an electronic beam excites a solid sample, which in turn emits a specific line spectrum. The light spreads in a (half) spherical shape. An objective looks at the sample surface through a window to collect an optimum amount of light and lead it to the spectrometer via fiber optic cable. Depending on the goal of the measurement, the spectrometer will be a monochromator, a parallel spectrograph, or a CCD spectrograph. The application is often solved with 2D Echelle systems. The electron gun may create a rather-wide beam that excites a relatively large sample area; however, there are also systems on the market that create a very fine beam that is scanned over the sample surface in *xy* mode. At each pre-defined *xy* position, an emission spectrum or a single spectral line is recorded and stored. This method is called scanning electron microscopy (SEM). With respect to the collection of light, the coarse or fine method makes no general difference because the intensity emitted in SEM is much smaller. A system like the one shown in Fig. 3.5 will work between 190 and 1000 nm.

3.3 Spectroscopy at Inductively Coupled Plasma

Atomic emission spectroscopy dissolves and excites the sample in flames or electrically heated ovens. The process is almost always performed in the normal atmosphere. For inductively coupled plasma (ICP) and laser ICP spectroscopy, sample chambers are also used, which has the advantage of processing under an inert safety gas, thus avoiding interference and possibly allowing measurements below 190 nm. It also permits sucking out the plasma products. The liquid sample material will be introduced to the sample burner by the carrier gas (mostly argon) or the plasma will "burn" in vacuum. The plasma zone is the area close above the inductor (plasma generator), which runs at high frequency (most systems use 10–40 MHz). There, the sample is transferred into the plasma phase, similar to the plasma in a high-pressure xenon lamp. The collection optics will recover a substantial part of the emission. The best efficiency is reached if the spectrometer is fixed to the window of the chamber or sample environment. If the chamber and spectrometer are purged by a noble gas or are evacuated, the measured spectrum may reach far below 190 nm. For solid samples, the plasma may be replaced by a spark (Section 3.4), or a laser pulse (Section 3.5). A complementary method involves ICP with a mass spectrometer (ICP-MS). The plasma products are sucked into the vacuum chamber of a mass spectrometer for elemental analysis.

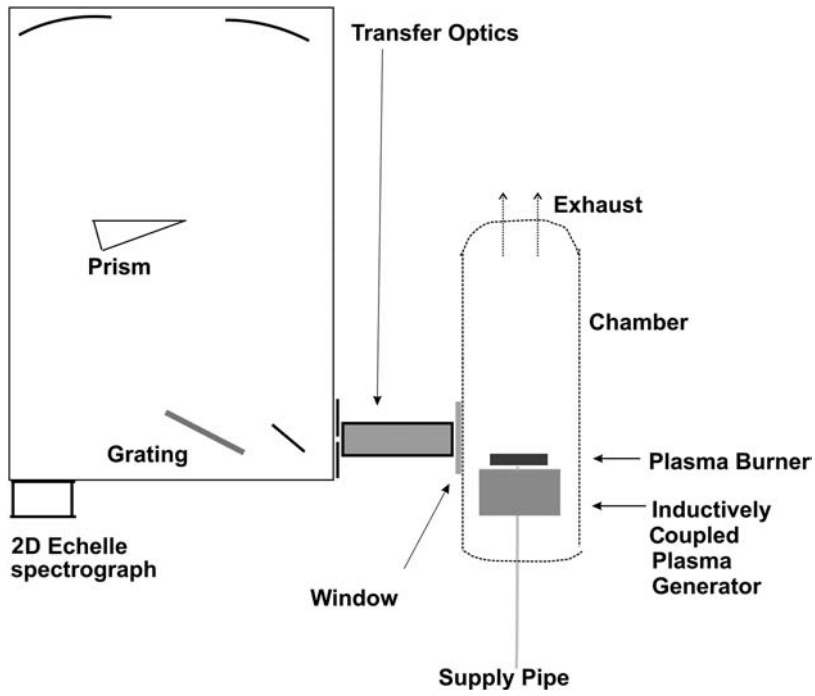

Figure 3.6 One of many ICP spectrometer versions available.

In the diagram shown in Fig. 3.6, the plasma generator is positioned beneath the plasma torch. It provides the high energy necessary to convert the liquid sample into the plasma state via high frequency. The atomized material exits at the torch and immediately emits the atomic lines. The entire process happens in a chamber. The light is collected by efficient wide-range optics and transferred into a high-resolution, nitrogen-purged 2D Echelle spectrograph. If a vacuum chamber is used, the entire optical system can be designed for the VUV. The chamber and spectrograph may be filled with a different gas, or one or both may be evacuated. The working range is typically <170–1000 nm. If the detector is a CCD, it will be coated with a VUV scintillator, which allows detection (practically without disadvantage) down to the wavelength limit of the window (see Section 5.8.11 of *Fundamentals*[1]). Likewise, image-intensified detectors may also be coated with a scintillator (see Section 5.2.5 of *Fundamentals*[1]). In addition to the atomic lines, the ICP spectrum also carries the lines of the solvent and carrier gas. In a so-called "empty" measurement, those data are stored for reduction from the sample spectrum, similar to AAS. ICP is a proven quantitative method, and powerful data-reduction software is required for the final result. If, for example, organic liquids are analyzed for their qualitative content of O, P, S, and other contents, numerous C lines will occur in the range between 160 and 220 nm. The application of ICP requires very high reproducibility of wavelength, along with online wavelength calibration and correlation techniques, e.g., some of the C lines can be used for that.

3.3.1 ICP examples

The element uranium (U) provides several hundred spectral emission lines, creating an Echellogram like that shown in Fig. 3.7. The many hundred emission lines are distributed over the range between 166 through 800 nm. In the image, the shorter wavelengths appear at the lower end, and the longer ones are toward the upper end. Within one order, the shorter wavelengths are on the left, and the longer ones are on the right. The brightness of the spots marks the intensity. In addition to the spectral points, it is easy to monitor the slightly tilted orientation of the lines within one order. The horizontal structures are called stripes.

Less complicated is the Echellogram of the rare-earth ytterbium (Yb), shown in Fig. 3.8. The roughly 100 emission lines cover the range of 211.67 nm through 555.65 nm, equaling 245 spectral orders in the Echellogram. Each piece of spectral information is easily viewed and well resolved. The main lines are listed in the table, descending from strong to weak. The strongest line, at 328.95 nm, is marked red; it appears in two neighboring orders. The second-strongest signal, at 369.42 nm, is marked yellow. Here, also, the short-wavelength information is located at the bottom, and the long wavelengths are at the top. Inside one order, the wavelength increases from left to right.

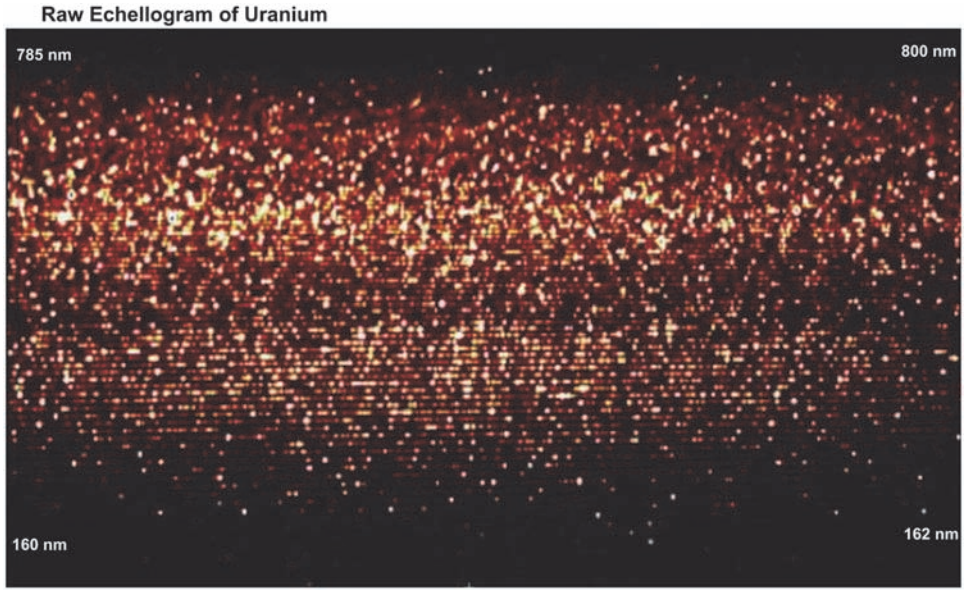

Figure 3.7 3D Echellogram of uranium (figure courtesy of Thermo Fisher Scientific GmbH).

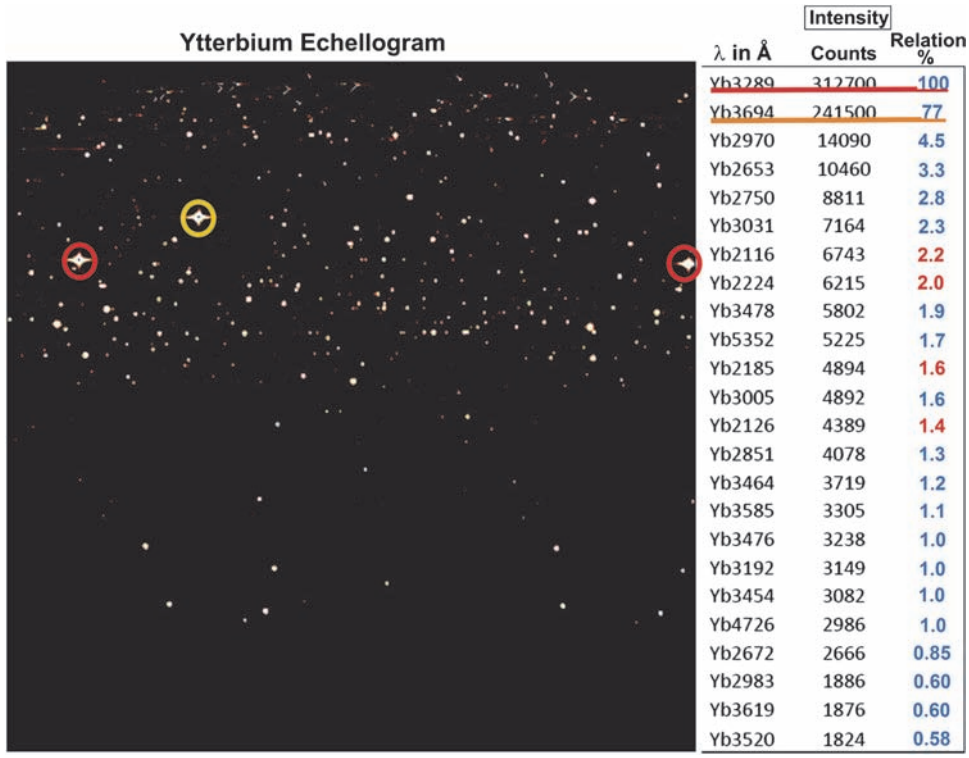

λ in Å	Intensity Counts	Relation %
Yb3289	312700	100
Yb3694	241500	77
Yb2970	14090	4.5
Yb2653	10460	3.3
Yb2750	8811	2.8
Yb3031	7164	2.3
Yb2116	6743	2.2
Yb2224	6215	2.0
Yb3478	5802	1.9
Yb5352	5225	1.7
Yb2185	4894	1.6
Yb3005	4892	1.6
Yb2126	4389	1.4
Yb2851	4078	1.3
Yb3464	3719	1.2
Yb3585	3305	1.1
Yb3476	3238	1.0
Yb3192	3149	1.0
Yb3454	3082	1.0
Yb4726	2986	1.0
Yb2672	2666	0.85
Yb2983	1886	0.60
Yb3619	1876	0.60
Yb3520	1824	0.58

Figure 3.8 3D Echellogram of ytterbium (figure courtesy of Thermo Fisher Scientific GmbH).

3.4 Spark Optical Emission Spectroscopy

Spark optical emission spectroscopy (Spark-OES) is a frequently applied method in metallurgy. It is used to define the material mix in metallic alloys. The sample must be electrically conductive. Similar to ICP, this method can be applied in the open atmosphere or in a chamber with inert gas. The sample is fixed to the table, which also makes up the cathode. Above that, the tip of the spark gap, which is the anode, is adjusted close above the point of analysis. The high-voltage power supply generates a short spark that atomizes the sample material out of the surface. The measurement works as described earlier: by a monochromator, a Rowland spectrograph, or a 2D Echelle spectrograph. Handheld portable systems are also often used.

The spark emission spectrometer is very similar to the ICP setup; the optical system may even be the same. A metallic sample table and an adjustable spark tip are placed inside the experimental chamber. Again, the wavelength range of interest is ~170–1000 nm. The data acquisition is synchronized with the high-voltage unit, which does not mean that a gateable detector is required—it only means that the read-out happens after a certain number of sparks. Immediately after one or more sparks, the spark generator is blocked, and the CCD is read. In addition to the atomic lines, a rather-strong "white" background signal is involved, created by the spark itself. The lines and continuum are separated by applying a curve fit and elemental peak search software. Spark-OES is a fully quantitative method; the right part of Fig. 3.9 illustrates a mobile version. The contact with the sample, which is also the cathode, is realized by an extension from the holder and can be ring-shaped. It also defines the length of the spark gap. The spark is supplied by cables from the central unit. The emitted light is collected and refocused to a fiber optic cable that leads to the spectrometer.

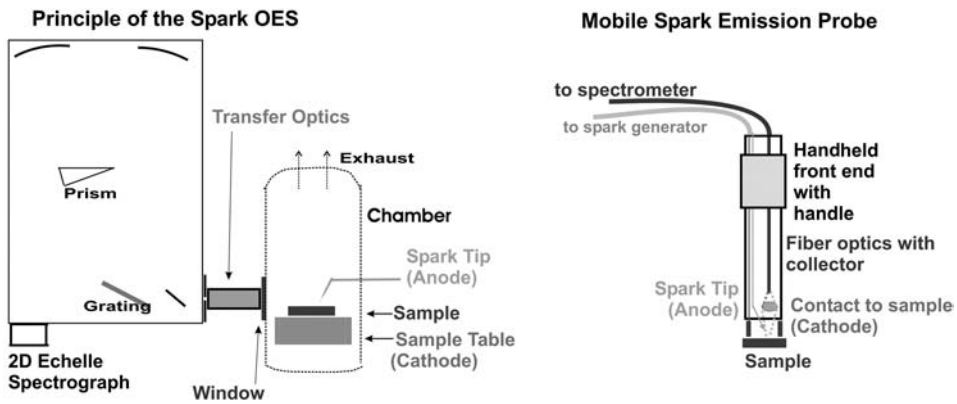

Figure 3.9 The spark emission spectrometer.

3.5 Laser Ablation

The methods of laser ablation (LA), laser-induced breakdown spectroscopy (LIBS), laser-induced plasma spectroscopy (LIPS), and laser deposition (LD) are all used for very different technical purposes, although the opto-spectroscopic part is similar for all four. Laser ablation is used for the analysis and modification of solid state materials; it is the only one of the applications that is useful for analysis, material processing, and deposition. With LIBS and LIPS, the system may be operated in the open atmosphere, except in cases that require signal collection below 190 nm. In the case of deposition, a vacuum chamber is required. A strong laser (such as an Nd-YAG at 1064 nm or an excimer in the UV) supplies a pulse nanoseconds long. The geometrical size of the light beam often is variable. Its power density is so strong that all molecular and atomic links in the upper micrometers of the sample break down (thus the name "breakdown"), and all molecules and elements are transferred into the plasma state. Like in the other methods, the cloud emits light in a spherical shape. Part of the radiation is lead to the spectrometer and the detector. A small crater is left at the sample after ablation. Automatic ablation systems are available that enable the sample to be *xy* positioned. Those systems can ablate layers from the sample and modify the structure. After each shot, the emission can be detected, and the spectrum can be compared to the reference. Therefore, the status of the process can be monitored after each single shot of the laser. If that is sufficient, the sample is moved to the next position, and the process starts again. Thus far, no vacuum or electrical contact is required. If the experiment is done inside a vacuum chamber, and a sample intended for deposition is placed near the ablated sample, the material can be transferred. Both partners must be conductors: one works as an anode, the other as a cathode. This process is called laser-induced deposition.

As shown in Fig. 3.10, laser ablation is similar to the ICP system. After a strong laser pulse, a small plasma volume is created above the ablated sample. The laser is normally fixed in position, and the sample is moved, if required by the application program. Therefore, the optical position of the light out of the cloud is stationary. The electric connection (electrodes) is optional; it assures that the ablation product does not return to the specimen. The material collected at the anode may be used for further evaluation, and the collected light is refocused into the entrance slit of the spectrometer. Depending on the application, with known elements, it is usually not necessary to apply a very-high-resolution spectrometer. The ratio between the predefined lines must be calculated and traced in time. A 1D spectrograph with a line array or standard CCD may often fulfill the requirements. In comparison to a 2D Echelle system, it provides faster repetitions, fewer calculations, and improved luminosity. Thus, pulse rep rates of milliseconds can be reached. In preparative ablation or deposition processes, the target sample may be measured in parallel by a second spectrometer in reflection mode (not shown in the figure), enabling an additive process control.

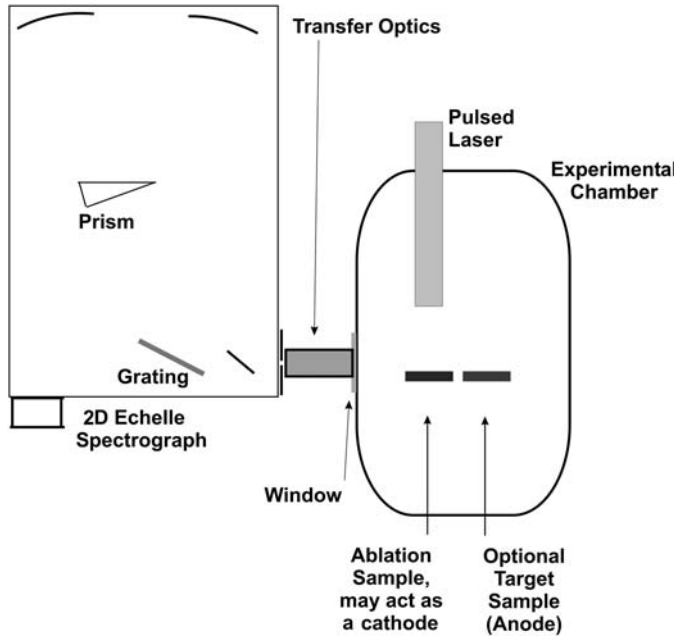

Figure 3.10 A laser-ablation system.

3.6 Plasma Etching

Plasma etching (PE) is a method that runs parallel to a production process and controls it. It is routinely applied in semiconductor manufacturing. The method is based on the structures of semiconductor wafers, which consist of several layers of different materials that are subject to reduction by aggressive plasma. The sample areas that are not to be etched are covered by a mask that does not respond to the plasma. The exposed areas are slowly etched off. The plasma may be created by different techniques, e.g., a current of argon with the addition of fluorine, in a high-frequency plasma generator, a microwave-induced plasma, or a glow discharge. Even chemical process applications are applied. In PE systems, the spectrometer is aimed to monitor the process and stop it at the right time. Because only a few spectral lines need to be detected, it is sufficient to use a line array after a rather-simple spectrograph.

As shown in Fig. 3.11, the sample is placed in a vacuum chamber and irradiated by a beam of plasma; an example of an etch sample is shown on the right of the figure. The substrate is assumed to be aluminum, layer 1 is crystalline silicon, layer 2 is silicon dioxide, and the cap is photoresist. The measurement system will gather as much light as possible immediately above the sample surface. The window is interchangeable and vacuum-tight. Because it gets deposited by the etch products, it must be occasionally replaced and cleaned. Typically, only a few elements or materials are involved, and an interference-free line can be selected for each one. A spectral

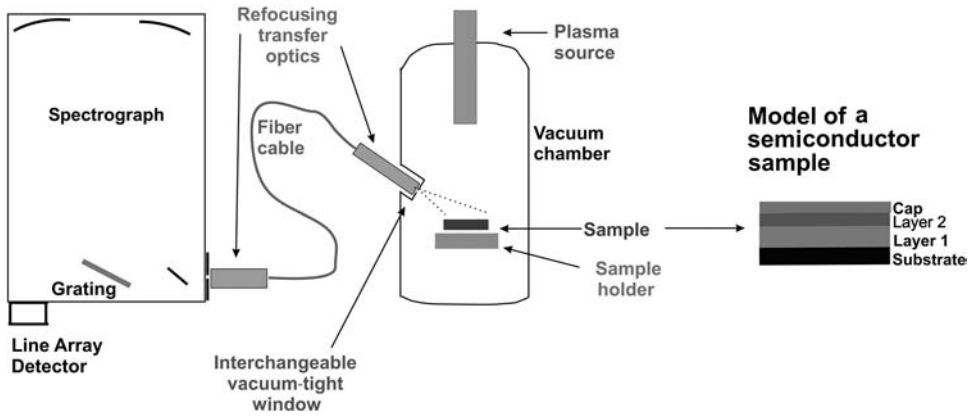

Figure 3.11 Plasma-etching equipment.

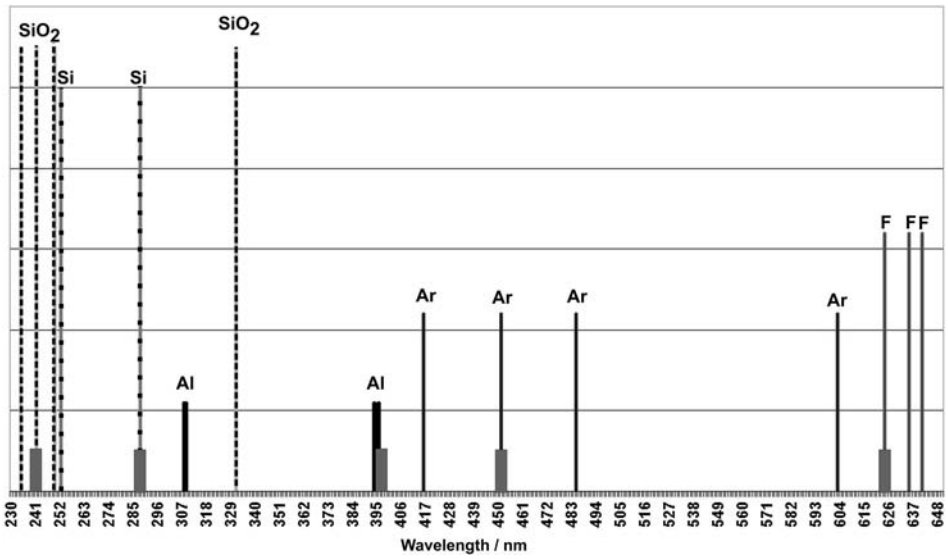

Figure 3.12 Prominent spectral lines of a semiconductor plasma-etch process.

resolution in the range of 1 nm fits well. Thus, a rather-short spectrograph with a line array that recovers an interval of ~500 nm will fit.

The lines in Fig. 3.12 represent the main lines of four elements plus silicon oxide (SiO_2). The vertical scale does not show the line intensity—lines of the same height belong to the same molecule. Four SiO_2 lines are marked with dashes, whereas two Si lines are dotted. The two places with Al lines carry two lines each and are separated by >1 nm. The extended feet mark the normally best-suited spectral line for each of the reaction species. Note that the aluminum signal at 395 nm is made of two lines: one at 394.4 nm, and the other at 396.15 nm. The latter is the one selected for analysis.

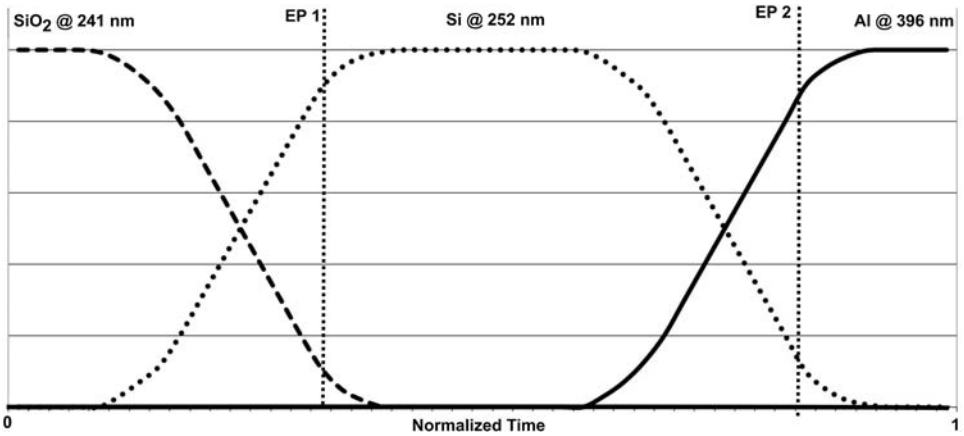

Figure 3.13 Simulation of a plasma-etch process.

The example illustrated by Fig. 3.13 considers the presence of Ar, F, Si, SiO_2, and Al. The spectral data of Ar and F are only used to monitor their mixture; they are not relevant for the endpoint detection. The etch process is monitored by detection of the wavelengths 241 nm (SiO_2), 252 nm (Si), and 396 nm (Al). Note that the lines are not always distributed so nicely. It often happens that an interval of 600 nm must be monitored. In this case, that would be true if the concentration of F were required for analysis. The figure displays the time behavior of the etch process. After the start, the silicon oxide is removed first and monitored by the 241-nm plasma line (dashed). As soon as the first perforations occur, the silicon line (dotted) at 252 nm rises, and the intensity of the 241-nm SiO_2 line decreases. By definition, an endpoint is reached as soon as the process reaches 95% or the intensity of the line has decreased to 5% of the start value. The sequence then runs again until the Si layer is etched and only the Al substrate at 396 nm (solid line) responds. The total process is then finished, and the monitor stops the machine. At each endpoint, the chemical mixture of the plasma may be modified to better process the next material.

A typical endpoint detector consists of the collection optics, the fiber optic transfer, the entrance coupling into the spectrometer (which may have a focal length of 0.25 m), the array detector, and special software. The spectrograph–array combination will present spectra of ~200–900 nm in a parallel fashion. An array or CCD with roughly 1000 pixels on the wavelength axis will result in a resolution of 3 nm. For most processes, that level is sufficient because all considered materials provide several lines for detection, which helps avoid interferences. Even order-sorting filtering is only required in the set-up and process-definition phase. At that point, the best-suited lines in the first order will be selected and programmed.

Online data reduction plays an important role: it quickly works to convert the spectra into time functions between two read-outs. A typical endpoint

detector allows for the definition of up to 20 signal legs. The legs can be monitored independently or calculated by different algorithms, just like differences or ratios. An endpoint may result from rather complex relations. The measurement sequence typically has a repetition on the order of 0.1–1.0 s. Within that time, all algorithms must be processed. Each endpoint may actuate a different switch or set a pre-defined bit pattern for process steering.

3.7 Solar and Stellar Emission

The research of solar phenomena is of special interest: not only because all life on earth depends on solar radiation but also from a research standpoint to investigate the origin of the universe. The requirements are extremely high. The measurement of solar spectra combines wideband analysis (temperature) with that of plasma lines (elements), e.g., in protuberances. This means that the researcher wants to simultaneously see a very wide interval and lines in the picometer regime. In addition, extremely dynamic signal differences must be detected linearly. The earth's atmosphere absorbs all wavelengths <300 nm and modifies the spectrum at the bands of the associated atmospheric gases strongly (with massive variations over time). However, the arriving power of the radiation may be substantial, leading to rather-short exposure times. Many solar observatories run several spectrometer systems in parallel after common collection optics to provide real parallel-beam treatment. The broadband 2D Echelle spectrograph is often the reference for detection within the 300–1100-nm range because it is fast-working and highly resolved. Unfortunately, the intensely wideband and dynamic nature of the radiation will create stray light problems that cannot be resolved. To work around this, the Echelle may be combined with a short-interval spectrograph equipped with bandfilters to reduce the spectrum and the stray light level.

Systems installed in satellites and space ships are much more complicated because the full electromagnetic spectrum is present, as well as all sources of disturbance and background. Even worse, size, weight, and power consumption play key roles and compete with the spectroscopic requirements.

At first glance, stellar spectroscopy appears to be very similar, but in reality the opposite is true. It is necessary to collect weak spectra of low signal with a good dynamic ratio, but in the presence of a bright background. Again, we find the requirement to analyze wide intervals with a high spectral resolution. Because the level of light is very low, the observatory or the satellite cannot deviate the small number of photons to several detection systems. However, the exposure time will not be short (hours are standard), which calls for a precise and smooth positioning system to track the source. Modern tracking systems provide that perfectly and also follow during the illumination time of the detector. One of the main interests of astrophysicists is the exact position and bandwidth of atomic lines. Through the Doppler effect and the bandwidth broadening, the relative movement and temperature

of the examined star are calculated. Because the spectral position of the atomic lines (without the Doppler shift) provides information about the elements in the star, the entire available spectrum is of strong interest.

In short, the highest requirements involve the accurate spectral position and physical bandwidth of the lines. Therefore, the calibration of the spectroscopy systems is constantly checked, and it receives the best thermal stabilization. The detectors are often cooled by LN, enabling them to integrate signals over days and deliver the best linearity, dynamic range, and reproducibility for the highest SNR.

3.8 Emission Measurements at Explosions and Flames

Combustion measurements are always time-critical. In the case of an explosion, one wants to know what kind of spectrum appears at what geometrical point and at what time during the blast. With flames, the researcher wants to know, for example, how uniform it is, what the turbulences are, how the temperature is distributed, and other parameters. Thus, the difference in both applications is time. Explosions always require short exposures for imaging and spectroscopy. A spectroscopy system may look like that shown in Fig. 3.14.

The experiment is indicated by the star, and the light is transferred by fiber optics. Explosions almost always need time resolution, which is performed by the gateable MCP between the spectrograph and 2D-CCD. The equipment

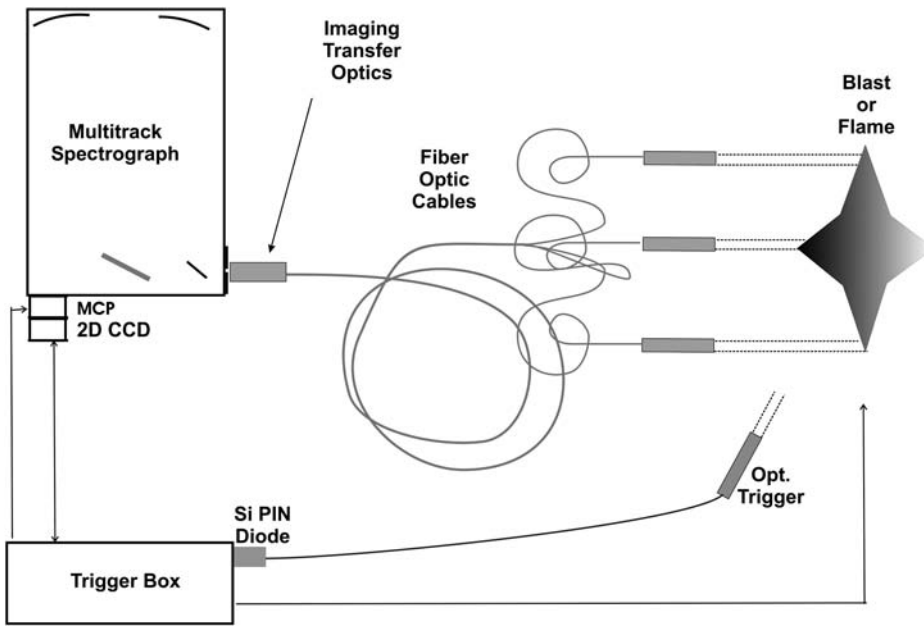

Figure 3.14 A spectroscopy system used to measure combustion.

may be designed as a 2D Echelle, which would allow one to detect elemental lines with a high spectral resolution. In cases of routine measurements, the standard system will not be an Echelle: the vertical plane of the spectrograph will be used to recover multiple spectral tracks of the same wavelength interval. An 18-mm-diameter image intensifier can be gated at 2 ns or even faster. It will also completely illuminate a 12.6 × 12.6 mm CCD. If that area represents 512 × 512 pixels, it facilitates the separate read out and storage of up to 25 spectra on top of each other (indicated in the figure by the three transfer optics near the light source). The objectives may look in different directions or look from different angles at the explosion. A large number of variations have been realized.

A very critical parameter is the synchronization of the experiment, MCP gate, and CCD read-out. Explosions are generally subject to variations in time, which requires that the MCP be started by the real event and not the trigger, which starts the blast. This problem can be solved with optical time-delay tailoring. A fast detector, such as a Si PIN diode with a picosecond response time, will detect the rising edge of the explosion and start the trigger electronics. With a delay of ∼50 ns and a jitter of 100 ps, the trigger electronics will send a start signal to the MCP electronics, which may add another 50 ns before the MCP opens. That process adds up to a ∼100-ns delay with extremely good reproducibility. Depending on the experimental setup and safety requirements, the distance from the experiment to the spectrometer may be 30 m, which adds another 100-ns delay due to the electric and fiber optic cables of the optical trigger system. There are then some delay times in the electric connectors and cables, perhaps another 30 ns. The total delay in the trigger system may be 130–150 ns, with a jitter of 0.2 ns. If the multileg fiber optic cable, which transfers the light of interest from the experiment to the spectrograph, is 50 m long and the light path in the spectrometer is 1.5 m, then the nominal time for the light to reach the detector is between 160 and 170 ns with almost no jitter. This scenario leaves enough time to measure the place of the explosion before the combustion starts. It is naturally of extreme importance that nothing is substantially moved between measurements and that all legs of the multiple optical fibers are of identical length. After each explosion, the CCD will usually be read out completely and stored in up to 25 memories. This process may take between one and ten seconds before the experiment can be repeated.

For flames, which make up more static processes from the perspective of the spectroscopy system, the same equipment can be used with a much-easier triggering concept. Gating the MCP will control the exposure time and ensure that the CCD is kept dark during the read-out. Because combustions expose high temperatures, Planck's algorithms for the calculation of temperatures are applied to the detected place and time.

Planck's radiation rules apply to all kind of combustions and create a spectral background. The line spectrum created by the associated molecules

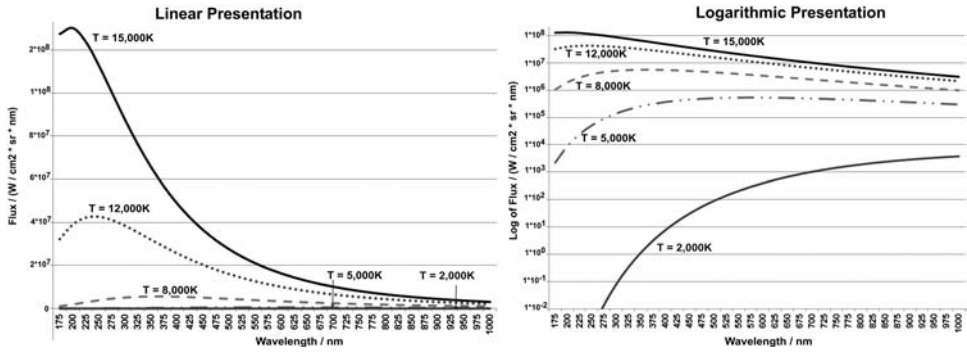

Figure 3.15 The impact of temperature on the measured spectrum.

and elements "rides" on the thermal background. Separation of the two is not a problem with modern software because the thermal signals are homogeneous. The atomic and plasma lines in the opposite are very small and ride on the thermal information. Thus, the two sets of data are divided before being processed separately. The graphs in Fig. 3.15 show Planck's radiation between 2,000 K and 15,000 K in the wavelength range well processed by image intensifiers (200–900 nm). The left part of the graph is linear in the scale of intensity, whereas the right part is logarithmic. In total, up to 50 spectroscopic independent parameters can be reduced from a single combustion measurement if the system contains a 25-leg fiber cable with separate collection optics.

Reference

1. W. Neumann, *Fundamentals of Dispersive Optical Spectroscopy Systems*, SPIE Press, Bellingham, WA (2014) [doi: 10.1117/3.1002528].

Chapter 4
Luminescence

4.0 Introduction

The interaction between light and matter may lead to the following effects:

1. Transmission without interaction,
2. Reflection without absorption effects,
3. Transmission/reflection where the light changes the energetic state of the sample, and
4. Transmission/reflection with light-scattering effects at the sample.

The law of conservation of energy states that the light transmitted through any sample, plus the sum of reflections by the sample, results in a factor of 1 of the introduced energy:

$$T + R = 1.$$

The law does not regard the fact that transmitted light may be refracted, diffracted, or scattered by the sample. It also does not take into account that absorbed energies may appear in the beam as luminescent signals.

Luminescence is the collective description for the emission of electromagnetic energies by an atomic or molecular sample, which may be caused by different reasons, such as chemical reactions, mechanical pressure, or the excitation by external electromagnetic radiation. The latter is the topic of this chapter. The energy that is absorbed by the sample is briefly stored in the electron's orbits and re-emitted to a lower level of energy. Thus, a previous excitation by light with a shorter wavelength than that of the emission must have taken place. The optically excited luminescence is called photoluminescence.

After excitation, regardless if the signal is constant or short-term, the intensity of emission will drop in an *e*-function. The time constant of the decay is $k = 1/\tau$ (rounded to 37% of the starting value, see Section 1.7.1 in *Fundamentals*[1]). The time constant is also called the lifetime. Luminescence phenomena are defined by their wavelength, intensity (efficiency, quantum yield), and the time constant of their decay. If the excitation constantly

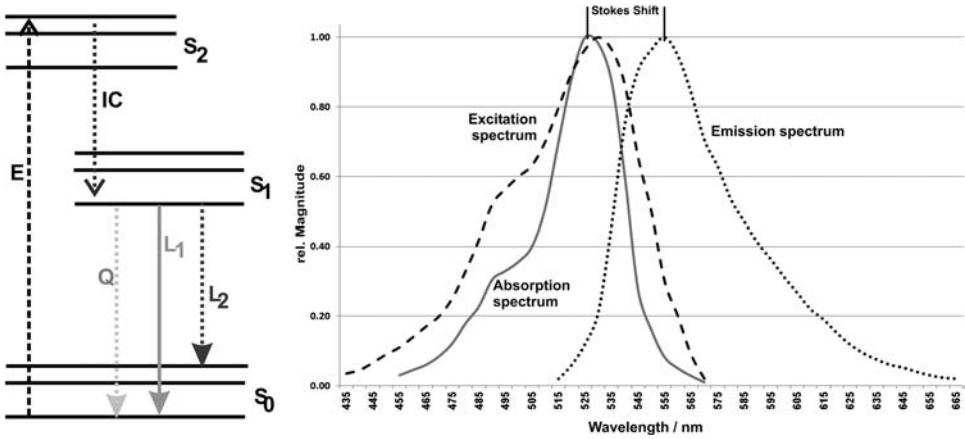

Figure 4.1 The Jablonski diagram and a typical fluorescence spectrum, demonstrated with Rhodamin-6G.

provides fresh energy, the multiple decays will add up and create a quasi-constant emission signal. If the time constant k is shorter than 30 ms, it is called fluorescence; if longer, it is called phosphorescence. The name is based on the decay of phosphorus, which can be seen by the human eye.

The physical basics of luminescence have been defined by Stokes (Stokes shift) and Jablonski (Jablonski diagram) and are very well documented in the literature.[2] In Figure 4.1, the diagram on the left represents the general electronic levels involved. The black dashed arrow indicates the excitation E from the ground state S_0 into the excited state S_2. Internal conversions (ICs), which include the warm-up of the sample, typically first reduce the energetic state to S_1 (dotted black arrow). The ICs are spontaneous and occur within femtoseconds to picoseconds. After a dwell time at state S_1 (the luminescence lifetime), the system returns to the basic state S_0, indicated by the L_1 and L_2 arrows. The number of processes involved defines the complexity of the excitation and emission spectra. The emission intensity may be minimized by chemical interactions, called quenching Q, shown in dotted light grey. If the final relaxation happens after a short dwell time, typically in the nanosecond time regime, the process is called fluorescence. Delayed relaxations may take hours or days to return to the ground state (phosphorescence).

The right part of Fig. 4.1 represents the typical spectra involved in luminescence, represented by the dye Rhodamin-6G. The solid grey curve shows the normalized absorption spectrum. The dashed curve is the excitation spectrum, which was measured at the maximum of emission (ca. 555 nm). The dotted spectrum is the normalized emission spectrum created at the maximum of excitation (ca. 530 nm).

The energetic difference between the maximum of absorption (ca. 525 nm) and the maximum of emission is the Stokes shift. The smaller the share of ICs in the Jablonski scheme is, the narrower the Stokes shift. The shape of the

excitation and the emission spectra often (but not always) is symmetrical. This is best seen with fluorophores that have multiple conversions. The shape and position of both spectra are independent from each other, which means that the shape and position of the measured spectrum (e.g., emission) will not change if the set position of the other (e.g., excitation wavelength) is changed so long as the parameter is kept within the other curve. However, the magnitude of the recorded curve will change, as will the excitation and absorption curves. The differences in shape and position are just a part of the reason why the absorbed energies do not only serve luminescence but also other processes. In the example shown, it is easy to confirm from the shoulder at 490 nm that this energy contributes more strongly to luminescence than to the total energy scheme of the sample.

4.0.1 Parameters of luminescence measurements

The emission distributed by the sample and the measured signal depends on many parameters. Apart from the wavelength of excitation, the beam density in the sample volume ($\mu W/mm^3$) is very important, followed by the number of exposed atoms or molecules in the volume count (n/mm^3), as well as their probability of response q (quantum yield). All three parameters are proportional and linear in principle (true for gas, liquids, and solids), but in all cases the penetration depth or absorption length in the volume plays a role. The light is emitted in a ball shape from each point of the sample. At high absorption coefficients and/or high sample concentrations, the intensity of excitation is not homogeneous inside the sample volume, which may create problems with collection. If excitation and emission wavelengths overlay, which is the case for Rhodamin, self-excitation and self-absorption by the sample are possible. The final goal is to collect as much emitted light as possible and then transfer and disperse it efficiently.

4.0.2 Requirements of luminescence measurements

The optical excitation of a fluorescent sample happens at photon energies (wavelength), which also absorb. The higher the light density in the beam is, the higher the fluorescence intensity. The relation is linear until the sample reaches saturation, which is the case if all available transitions are set. Such a scenario is rare if a lamp is the primary source, but it happens often if lasers[3] are used. The following list includes the requirements for luminescence measurements:

1. The excitation light in the sample volume should be well focused to provide a high density. Strong light sources are welcome. Many fluorescent dyes (fluorophores) respond to a range of excitation wavelengths and show an excitation spectrum. The response to the different wavelengths differs. If more than one fluorophore is present, spectral overlay may happen and eventually influence the measured result.

2. The excitation light should be monochromatic to ensure that only the target transition is excited. The fluorescent light emits in a ball shape.
3. As much emitted light as possible should be collected from the ball-shaped emission and brought to the detector. Comparing the axis of excitation polarization, fluorophores prefer the parallel polarization plane. The asymmetry on the polarization is called anisotropy. Compared to the excitation plane, the emission light may incorporate an angular change in polarization. That, in turn, provides information on the dynamics of the fluorescence.
4. In both channels—excitation and emission—a programmable polarizer is advantageous.
5. In order to allow normalization, a (calibrated, if possible) reference detection is required in the excitation arm. In order to allow emission normalization, the spectrometer system should be capable of radiometric calibration. The intensity of excitation and the efficiency of emission have strong variations over the working wavelength range. Thus, normalization of both channels is necessary to compare samples and publications.

4.1 Setup of a Static Luminescence Spectrophotometer

The optics of a high-performance system can be based on either mirrors or lenses. Mirrors offer the advantage of keeping the focal behavior constant at all wavelengths. For a limited wavelength interval (about 1 octave), very high reflection efficiencies can be realized with special coatings. The disadvantage is the more-complicated beam deflections, which may require more components and produce more loss. Lens systems provide the advantage of "straight-through" beam travel, special coatings are also available for very high total efficiency, and simpler setups are produced. The disadvantage is that the focus travels over the wavelength, which will also create focal variations in the sample volume. If 25-mm-wide quartz lenses at a focal length of 100 mm (*fl*4) are used, the focus travels 7 mm (at 800 nm, $f = 100$ mm; at 220 nm, $f = 93$ mm). It helps that a focal spot is not required (more of an area or a cylindrical volume) because the monochromator output slit is re-imaged in the sample volume, which significantly minimizes the disadvantage (see also Section 4.1.3.4 of *Fundamentals*[1]). With regard to the five requirements listed earlier, the high-performance setup illustrated in Fig. 4.2 is a possible solution.

4.1.1 Instrumental considerations

According to requirement 1, a strong light source with high light density is used. Because many fluorophores require excitation between 250 and 500 nm, a xenon lamp is the first choice (75–500 W are available), and a rear mirror (RM) enhances the collection efficiency. It illuminates a double monochromator with *fl* 4 ($\Omega = 0.05$), comprising slits up to 3 mm wide at a 3–5-mm height, and a 250–300-mm focal length. The dispersion will be ~3 nm/mm. At a bandwidth of 5 nm,

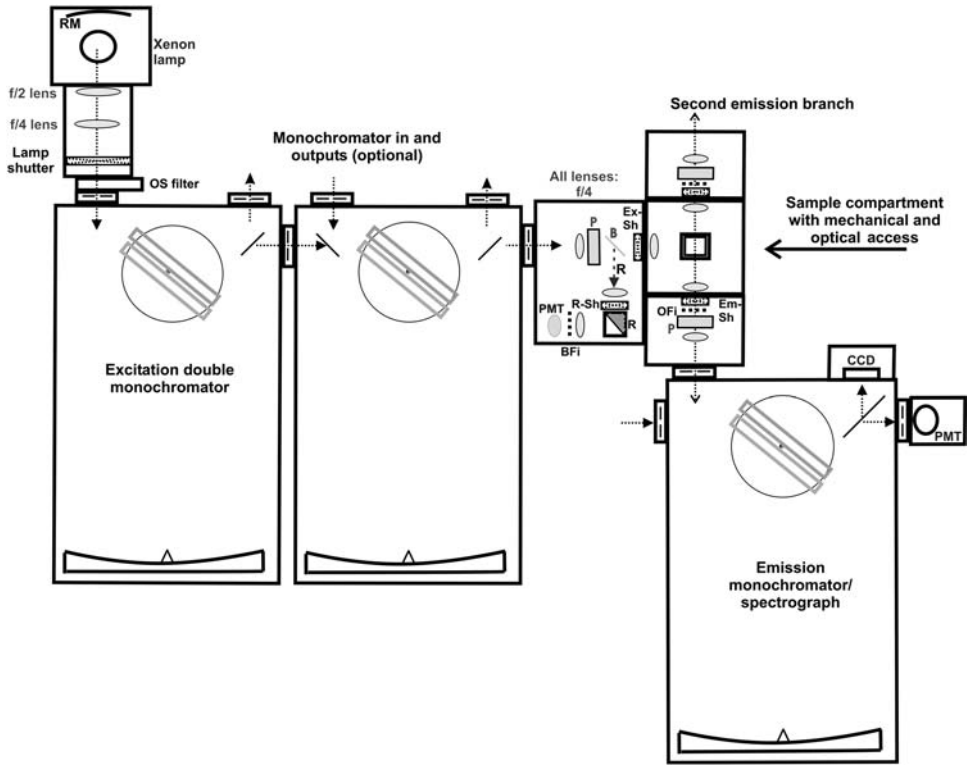

Figure 4.2 A lens-coupled, high-performance luminescence system setup.

the following power output can be expected: between >10 and <1000 μW for a 75-W xenon lamp, whereas the excitation power will be in the lower milliwatt range for a 450-W Xe lamp.

A double monochromator is used to illuminate the sample with spectrally clean light (requirement 2). It is helpful to have two gratings installed, both of which are 600 mm^{-1} for rather-high efficiency between 200 and 2000 nm. This arrangement makes the system compatible with NIR applications. The image of the lamp spark will be transported through the spectrometer and well reproduced in the sample place to represent high light density. Requirement 5 is realized by a beamsplitter B and a reference detection system R. Before and after the sample, a polarizer (P, requirement 4) is available that is motor controlled for actuation and positioning per program. The most-qualified options are Glan–Taylor and Glan–Thompson quartz polarizers, covering 220–2500 nm. In the T-optics configuration shown in Fig. 4.2, there are several collimated beam areas that allow the best performance of polarizers, filters, and other optical components (such as depolarizers). Finally, the spectrometer angles are well matched, and the luminescence is collected efficiently (requirement 3). The best angle between the excitation and emission light path to suppress excitation scatter and reflection into the emission channel as much as possible is 90 deg.

In most cases, a single-stage emission spectrometer will be sufficient. It is recommended to select a model with two exits to allow the use of NIR or area detectors in addition to the PMT. It is also good to have the spectrometer equipped with multiple gratings to better optimize the wavelength efficiency and probably to fit the dispersion/interval of a CCD. If samples with strong scattering or weak emission in the UV are measured, a double-stage spectrometer should be considered (it is necessary for sensitive polarization detection). A T-optics design comprises two equal emission exits. In the figure, only one is allocated; the second exit can be equipped with a spectrometer at any time, which may be optimized differently or used with a filter/detector combination. The proposed sample compartment is accessible from the front, top, and bottom, which makes it suitable for sample changers, solid state sample holders, titrators, etc. The sample can be laser-excited through the front wall. The proposed spectrometers provide extra entrances and exits that allow the optional use of fiber optics for remote spectroscopy or other applications. At each critical position in the setup, an electromagnetic shutter is placed to protect the samples and detectors from excessive illumination. The shutters are part of the acquisition program but can be manually actuated at any time.

4.1.2 Light path and spectral disturbance

The light path incorporates many optical components: windows, lenses, mirrors, sample cells, eventually fiber optics, and others. Incorrect materials and coatings may be sources of spectral interference, e.g., superposed fluorescence, created in glass, fiber optics, or mirror coating. When constructing a system, it is therefore important to discuss those possible impacts with suppliers in order to avoid them. During operation, all of the components need protection from dirt and dust; otherwise, in addition to loss of efficiency, they may cause fluorescence problems and scatter. Many of the materials create (by their nature) Raman and/or Brillouin signals. They cannot be completely suppressed, but the user can be aware of them and their position relative to the excitation beam. That knowledge enables the user to account for possible disturbances and probably data reduction. Clever selection of materials is always helpful. (More on the topic is found in Chapter 6 of this book and Chapter 8 of *Fundamentals*.[1])

4.1.3 Details of a static photoluminescence spectrophotometer

4.1.3.1 The excitation arm

The ideal light source would provide a strong and homogeneous spectrum between ~200 and 2000 nm. The primary source would be a tiny arc. Lasers are ideal, but they do not (yet) emit continuously, and programmatically, over wide spectral ranges. Due to the rapid development of semiconductor lasers, this source covers an increasing number of applications, including steady state and time-resolved (see Section 4.1.4.8). If pulsed lasers are applied, side effects

within the pulse must be considered and eventually reduced to avoid problems in the luminescence signal.[3] The xenon high-pressure arc source (see Section 6.4.3 of *Fundamentals*[1]) is the top choice because it offers the highest light density among the sources considered. At first glance, the additional xenon gas lines seem to disturb strongly; however, most of them are narrowband and are integrated out within bandwidths of 3–7 nm (ranges typically used in luminescence work). Furthermore, the steep ascent of power below 300 nm can be compensated by proper selection of gratings. Thus, the excitation monochromator must have at least two gratings to provide high efficiency over the range of interest. A typical example of the excitation of the fluorophore Rhodamin-B, a substance often used as a quantum counter, is shown in Fig. 4.3.

All of the curves in the figure are shown normalized. The pink curve represents the original emission of an ozone-free 75-W xenon lamp, measured with a 1-nm bandwidth (BW). The lamp illuminates an additive 0.3-m double monochromator equipped with gratings of 600 mm^{-1} and optimized to 300 nm. The dispersion is roughly 2.4 nm/mm, allowing bandwidths of up to 7.5 nm at a slitwidth of 3 mm. 1.67-mm-wide slits result in a 4-nm BW, which offers high light transfer. The spectrum marked blue will appear at the exit of the monochromator. The sharp xenon structures are almost averaged out, and the residing structures are reproducible and reliably quantified.

The green curve represents the excitation response behavior of Rhodamin-B. That function is convolved with the power of the excitation light—the final result is the real excitation curve, colored yellow. The convolved curve is remarkably different than the original response curve of the dye stuff, which is used, and recorded, to normalize the excitation reference spectrum. A basic rule

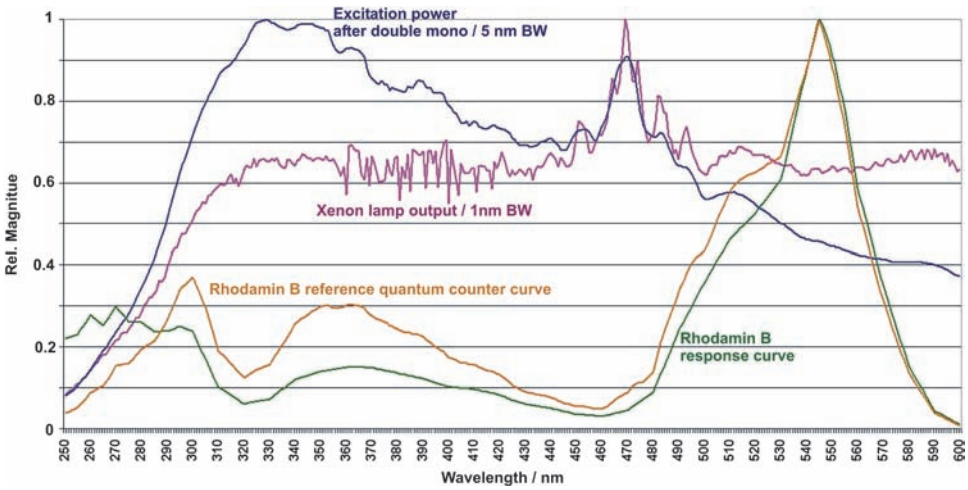

Figure 4.3 The most-important spectra in the excitation arm, demonstrated by Rhodamin-B.

for the quality of excitation should be kept in mind: all errors and problems in the excitation will reappear in the emission signal.

4.1.3.2 Creation of the reference signal

The excitation beam for the reference signal is realized by a beamsplitter, marked B in Fig. 4.2. It is placed in front of the sample chamber and directs ~8% of the light to the reference. It is located behind the polarizer P and represents the actual status of excitation. The reference beam R illuminates (a) a calibrated detector, (b) a quantum counter, or (c) a scattering device.

a. Calibrated UV silicon detectors are often used for reference measurement. They guarantee high reproducibility over long time. The output signal is calibrated in watts; by accounting for the beamsplitter function, the power introduced to the sample can be calculated for each wavelength. Their disadvantages are the rather strong variation in response over the wavelength and ambient temperature, and a poor SNR at low light levels.
b. The combination of a fluorophore and PMT is called a quantum counter (shown in Fig. 4.2). The reference solution is placed in the (grey) triangular cell, which reveals a neat trick. Different dye stuffs are available that are all prepared in rather high concentrations because the reference ought to reach saturation. In addition to Rhodamin-B, other substances—such as quinine sulfate and fluorescein—are useful for reference purposes. The triangular cell comprises all pathlengths between 0 and 10 mm, which "automatically" fits the pathlength. The emitted fluorescent light will represent the optical power at the reference, which is part of the power at the sample. It depends on the wavelength, lamp power, efficiencies, and slitwidths. Each dye material useful for reference has a different optimal wavelength range. For a very wide range, more than one dye may eventually be required. For each one, a special bandfilter (BFi) should be placed between the reference cell and the PMT to eliminate unwanted signals.
c. The same arrangement may be used for the direct collection of the excitation signal. In this case, a scattering sample is used instead of the reference cell. Suitable examples include PTFE surfaces or barium sulfate layers, which work well between 200 and 1000 nm. Because no reflected rays will reach the detector, the scattering surface should not be placed under the angle of 45 deg, the optimal angle for a triangular cell containing a fluorophore. Scattering is better done under 30 or 60 deg, or in a standard cell.

An important note for all three methods: as soon as the optical power is precisely measured with a calibrated detector at the reference position and the sample place, and all measurement conditions and parameters have been recorded and stored, the recorded reference data are valid for radiometric reduction at a later time.

4.1.3.3 Justification of a double monochromator in the excitation branch

Rhodamin-B demonstrates how false light modifies the excitation and, consequently, the emission spectrum. Assume that the excitation monochromator is set to the rather small 270-nm peak and that the Rhodamin emission spectrum for that dedicated excitation is recorded. Figure 4.3 shows that the system efficiency is 0.3 of the maximum, whereas the sample efficiency is ~0.25 of its maximum. Thus, the expected measured value will be 0.075, and the normalized value will appear to be 0.15 of the maximum. If a double monochromator with stray light of $<10^{-5}$ is used, those values will also be the measured result.

Now consider a single-stage excitation monochromator. Below 300 nm, it will carry a stray light level between 0.3% and 3% (1% estimated). The false light will come from the upper wavelengths, including 500–600 nm. For those wavelengths, the excitation efficiency of Rhodamin-B is higher by a factor of 3. The lamp power is stronger by another factor of 3, adding to a rounded total factor of 10. The result is that the contribution shown for 270 nm will not be 1% but 10%; in other words, the emission will be recorded much higher than it really is. The stronger the dynamic variation in the excitation efficiency of the sample is, the worse the falsification resulting. Note that an additive double monochromator at the same bandwidth will provide roughly the same optical power because the lower transfer efficiency is at least compensated by the doubled slitwidth. All of the errors and issues of the excitation signal will reappear in the emission spectrum, which is why a clean excitation is more important than its power.

4.1.3.4 Illumination of the sample

After the excitation monochromator, the light will be collimated, possibly filtered, and/or polarized, and perhaps 8% is used for the reference beam. The main part is refocused to provide high light density in the sample position (S). In Fig. 4.2, the aperture (besides the collection system at the lamp) is $f/4$ ($\Omega = 0.05$) throughout. A typical case is a monochromator slit size of 3×3 mm, which will be re-imaged in the sample volume. If so, the excited volume will be in the range of 100 μl.

The image of the monochromator's exit slit appears inside the sample volume like a tunnel. Standard cells have a 10 mm × 10 mm cross-section, and the beam shows a waist-type shape within. The proposed lens optics will have the disadvantage of a focal spot that will travel a maximum of 2.5 mm back and forth as the wavelength changes. If standard cells are used, that scenario will not be a problem because the tunnel's total cross-section will not change (it just travels slightly). In Fig. 4.4 that is valid for illumination cases 1, 4, and 5. The situation changes when microcells are applied (case 2), typically exposing a volume of $3 \times 3 \times 3$ mm (27 μl). The focal travel may then affect the result; the same may apply to front surface applications (case 3). The effects can be compensated with the help of an additional correction lens,

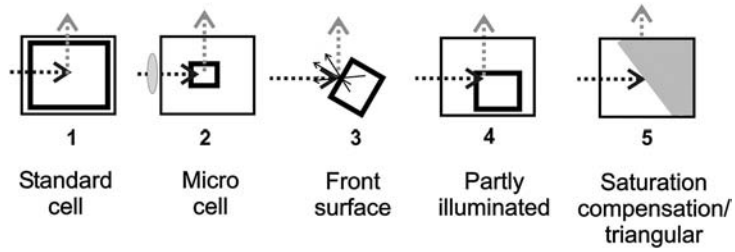

Figure 4.4 The most-popular sample geometries and illumination modes.

which is mounted in an adjustable holder just in front of the sample, or a moveable focusing lens. Both options will effect a sharp focus over a limited wavelength interval. An additional option involves a small slit, e.g., 1 × 1 mm. This slit limits the excited sample volume to 1–5 μl with extremely high beam densities inside.

An important construction decision is the orientation of the excitation beam. If the output slit of the excitation monochromator is perpendicular to the orientation of the sample cell, a minimum of volume is required (see Fig. 4.5). Naturally, the orientation of the emission-monochromator entrance slit should always be identical.

Inside the sample volume, the beam is reproduced like a waist-shaped rectangular block. The left part of the figure shows an almost-square beam with an aperture of *f*/4 ($\Omega = 0.05$). The image also illustrates that a short travel of the waist will not create critical impact. If the spectrometer slit has the "normal" vertical orientation, the beam illuminates a sample volume that is taller than its width (light grey). If the slit orientation is horizontal, the beam will travel in a "lying" fashion (dark grey). Much less height is required inside the sample cell, which reduces the filling volume. Several commercially available luminescence spectrophotometers have been designed with that advantage. If the slit is a maximum 6 mm high and opens up to 3 mm, it is sufficient to adjust the beam center to ~5 mm above the cell bottom and fill it to 8 mm, which results in a volume of 80 μl. If the orientation is vertical and the slit is the same, almost double the volume is required. In both cases, a magnetic stirrer up to 2 mm thick can be applied without interfering with the beam.

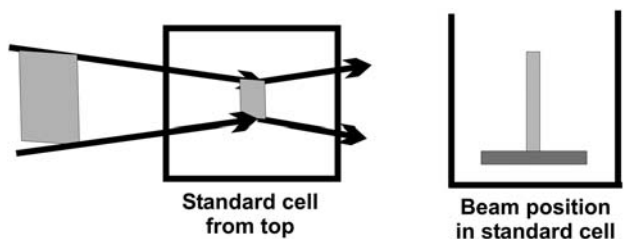

Figure 4.5 Beam orientation: vertical versus horizontal.

Two more effects should be considered. A luminescent sample is excited upon absorption, which reduces the excitation intensity while traveling through the sample. For example, if the absorbance is 1 AU over the length of beam travel (typically 1 cm), the specimen (molecules) near the front wall will be exposed to 9 times as much excitation intensity compared to those at the end of the beam travel in the volume. That effect is called the "inner lens effect" and leads to linearity problems. With an increasing concentration of the absorbing specimen, the resulting integral of luminescence, emitted from the illuminated volume, will increase slower than the concentration increases. The inner lens effect can be partially (but not fully) compensated by correction algorithms that calculate the loss of intensity over the volume or by geometric modifications. In Fig. 4.4, cases 3–5 show a possible option. All three collect only luminescence light from a rather short part of the volume. In cases 3 and 5, the 45-deg angle should be avoided because it reflects part of the excitation into the emission channel.

4.1.3.5 The emission light pass

Although a best-possible, spectrally clean excitation with a high light density is important, the purpose of the emission arm is to capture and process as many emitted photons as possible. Theoretically, an *f*/2 optics design ($\Omega = 0.25$) would collect 2% of the ball-shaped luminescence emission, which initially seems like the perfect solution and could even be achieved with an additional close-up lens; however, it deserves a closer look.

Figure 4.6 shows the real angles in the emission collection arm with apertures of $f/4$ (left), $f/2$ (center), and $f/4$ optimized for microcells. The excitation light arrives from the left. As illustrated, the $f/4$ version only illuminates a slender volume. The $f/2$ version (center) needs a substantially larger sample volume. It provides a less-concentrated light density—even the total light flux is about five times as much. The rightmost figure shows the $f/4$ solution with a far-better image within solid angles of 15 deg. The $f/2$ version, on the other hand, uses a solid angle of 26 deg. The center image demonstrates that not all emission rays (traveling downward) that reach the first lens also reach the second, and they will fail to enter the emission monochromator under the required angles. Neither effect appears in the $f/4$ version, but both effects together will mean that $f/2$ optics, whether lenses or mirrors, will not produce a reasonable increase in total efficiency but rather more imaging problems. However, $f/2$ optics are well suited to collect light from small sample volumes or small luminescent surfaces, which is why areas of up to 3×3 mm (the grey square in the right image) are predestined for $f/2$ collection. A pre-collection lens near the sample is the proper solution. Some commercial systems are prepared for the pre-lens solution, which may also be applied in mirror optics systems.

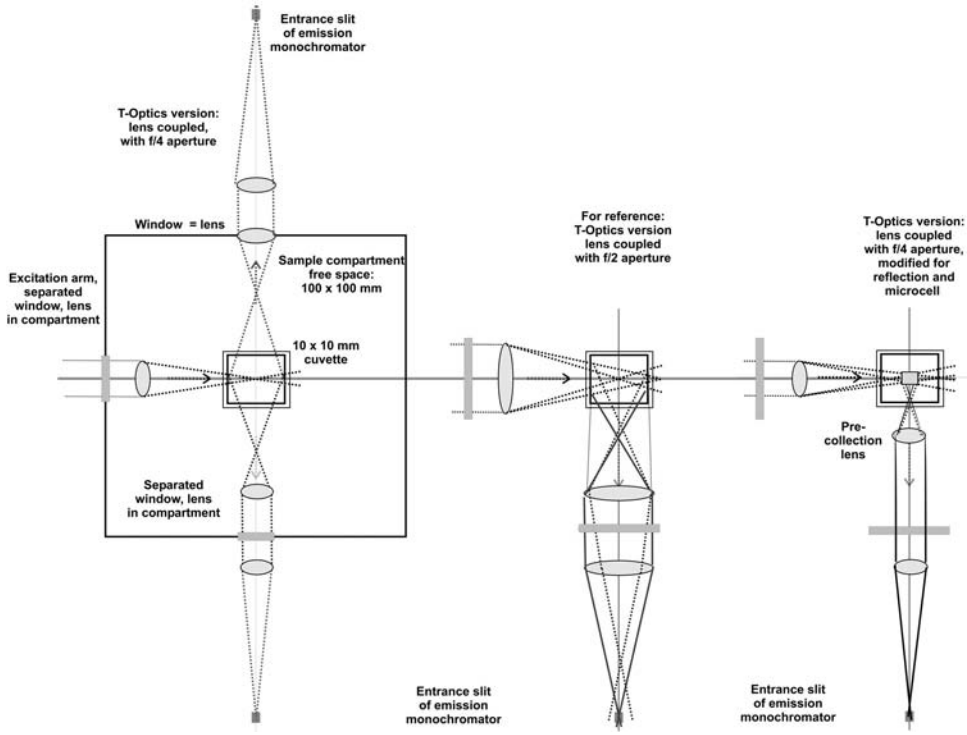

Figure 4.6 Comparison of collection systems with an *f*/2 and an *f*/4 aperture.

4.1.3.6 Spectral dispersion and processing of the luminescent light

Assuming that the entrance slit of the emission spectrometer is well illuminated, the light will be efficiently processed by optimized gratings and transferred to detectors with high sensitivity. Although stray light in the excitation arm may be fatal, a single-stage unit in the emission arm with a focal length of 0.20–0.35 m is often sufficient. The following scenarios require double monochromators in the emission arm:

1. the excitation and emission spectrally overlap closely (e.g., Rhodamin-B),
2. intense scattering effects are evident,
3. the polarization must be precisely measured, and
4. a combination of wide wavelength ranges and large variations in signal flux are expected.

Suitable detectors in the UV–Vis range are PMTs—the best are those that work in both analog and photon-counting mode. The second output may optionally be equipped with a high-efficiency CCD. For wavelengths above ~850 nm, APDs are very useful; they are available for Si and InGaAs detection (see Section 5.7.3 of *Fundamentals*[1]). For most applications, a resolution of 1–2 nm will fulfill the requirements with a typical dispersion of 2–4 nm/mm.

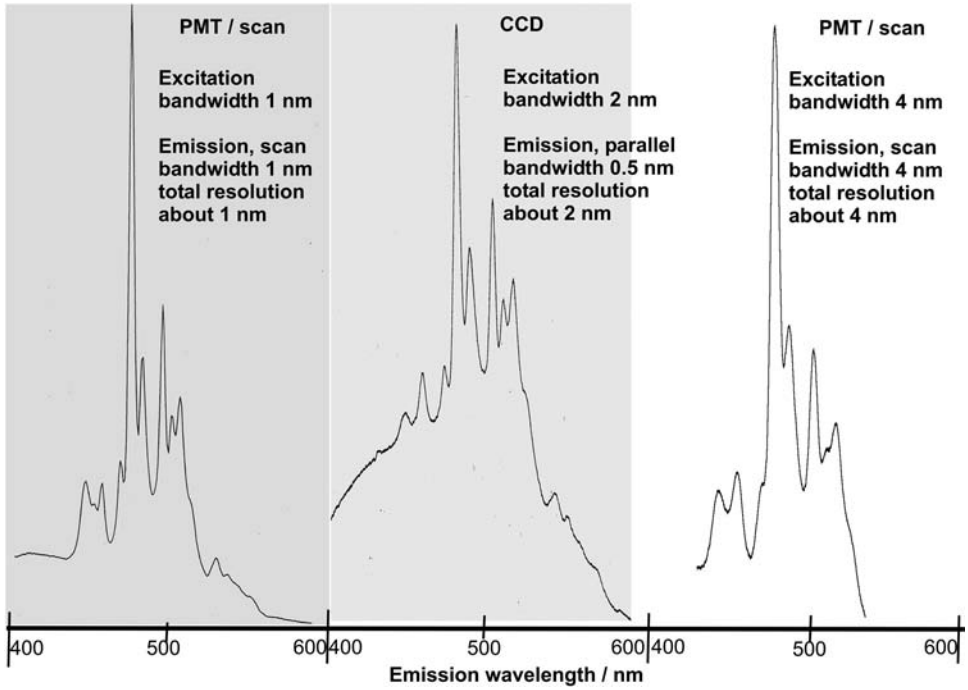

Figure 4.7 Impact of the system bandwidth, and the difference between scan and parallel detection.

Ovalene is a polycylcic, aromatic hydrocarbon that can be bound in solid samples, such as PMMA. It makes for a suitable luminescence reference sample because it has a rather complex absorption/excitation spectrum with a maximum at 350 nm. The three emission measurements shown in Fig. 4.7 have been made with the same instrument and the same PMMA block; excitation is always 350 nm. The emission spectrum consists of sharp peaks riding on remarkable wideband fluorescence. The left diagram shows excitation/emission bandwidths of 1 nm, and the right graph was taken with a 4-nm bandwidth. In the center is a measurement with CCD detection at a 2-nm excitation bandwidth and a 0.5-nm emission bandwidth (400 pixels at a 200-nm interval). The resulting CCD resolution of 1.5 nm fits a scanning resolution with a 2-nm bandwidth. All important spectral features are observed. At a 4-nm bandwidth, some information is already lost.

The example proves that a high resolution not only shows small features but also reduces the impact of broadband signals. This fact is true because the optical power of broadband signals drops in a squared function, whereas the specific peaks drop in a linear function. Effects like that are more troublesome for multichannel detection than for scanning and single-channel mode. For that reason, the center CCD detection presents a reduced ratio between specific and nonspecific fluorescence signals.

4.1.4 Measurement methods of static luminescence spectroscopy

4.1.4.1 Emission scan

The emission scan is the most-executed routine. It is conducted by setting the excitation to a fixed wavelength and scanning the emission spectrum. If the scan includes the upper spectral orders of the excitation, they will either appear as scattered signals or need to be blocked by filters in the emission arm. The primary use of the reference signal is to monitor the excitation stability and intensity.

4.1.4.2 Excitation scan

The excitation scan is the inversion of the emission scan: the emission wavelength is fixed while the excitation is scanned. The upper spectral orders are treated the same. Recording the reference signal allows normalization processes. The measured intensity will often be recalculated with the existing radiometric calibration curve and produce radiometric excitation data.

4.1.4.3 Fluorescence polarization

A photon-excited fluorophore addresses different states of polarization in the excitation. Theoretically, the fluorescence has the same polarization as the excitation, but several parameters may vary that basic rule. The most-important depolarizing impact is diffusion coming from the molecular rotation. Scattering effects and internal excitation may also cause depolarization. Measuring the degree of polarization of the emission, and its anisotropy, requires the excitation to be single-plane. The sample polarization (the degree of polarization) is

$$P = [(I_p - I_s)/(I_p + I_s)], \tag{4.1}$$

and the anisotropy is

$$r = [(I_p - I_s)/(I_p + 2I_s)], \tag{4.2}$$

where I_p is the parallel plane of polarization, and I_s is the vertically oriented plane.

With perfectly polarized excitation light at the sample (I_p), we find that $I_s = 0$, resulting in $P = r = 1$. If the excitation $I_s = 1$, the inverse is true. Perfectly nonpolarized excitation ($I_p = I_s$) leads to $P = r = 0$. All intermediate states of excitation polarization result in P and $r > 0$ but < 1.

It is important for all types of polarized applications to excite with spectrally clean and linearly polarized light at the sample. This, in turn, does not allow the state of polarization to change after the polarizer (see Fig. 4.2). If the optics are based on lenses and travel straight through, that scenario is guaranteed. Mirrors would require reflection angles within 15 deg to maintain the polarization, which is not easy to achieve at *f*/4. Polarization errors are often accepted to facilitate a less-complex system, and a more-complicated calibration process will correct the error. The beam of mirror-based systems

does not usually have a collimated sector (for the polarizer and filters); therefore, the polarizer will be illuminated with diverging or focused light, and imperfect polarization follows. In any case, the state of polarization and the transfer efficiency in the excitation arm will change over the wavelength. It is necessary to record both polarization situations for the parallel and the perpendicular plane, in addition to the "nonpolarized" (scrambled) light. Also note that no perfectly scrambled light will leave a grating monochromator, as shown in Chapter 3 of *Fundamentals*.[1] If well-scrambled light is the ultimate goal, a depolarizer (scambler) should be put in place of the polarizer (Lyot or Hanle scramblers are suitable).

In the emission arm, the state of polarization of the emitted light should not experience changes before it reaches the analyzing polarizer. Otherwise, the calibration becomes difficult because it requires several runs. The analytical polarization measurement is intended to quantify the change of the state of polarization between the excitation and emission light, which requires at least two measurements with a 90-deg change in the analyzer angle between them. A better choice would be T-optics with both arms equipped with analyzers under a 90-deg difference. Because the emission light may carry different polarization information for different wavelengths, stray light in the emission system will bastardize the polarization data obtained. Consequently, it is better to use a double-emission monochromator. Valid information is found in the emission anisotropy: the decay time (lifetime) of the different polarization components may be different, which means that the polarization is a very valuable parameter in lifetime measurements.

The calibration of the polarizers is possible by several means. To create a perfect P or S polarization in the excitation, a calibrated analysis polarizer may be put directly in front of a detector sitting in place of the sample. At the wavelengths of interest, the angular position of the excitation polarizer is adjusted for perfect P or S, and the corrected angle is put in a look-up or working table. The table will be used during data acquisition to ensure correct settings. With the correct excitation angles, the emission is calibrated by setting the excitation to P or S and then illuminating an aqueous glycogen solution (a strongly scattering sample without any fluorescence). Thus, the emitted light will have the same polarization as the excitation. The combined methods provide complete calibration of both arms over the available wavelength range.

4.1.4.4 Acquisition of the total fluorescence

The term "total fluorescence" refers to a 3D diagram that combines the emission spectra with an interval of excitation wavelengths. To acquire it, the excitation is changed in spectral steps close to the bandwidth, and an emission spectrum is taken at each step, including steps near the bandwidth value. The data are presented in 3D graphs, and a menu offers different views and colors. Many industrial luminescence spectrometers include the required hardware

and software. Recovering data over long wavelength ranges may require changing additional parameters within the scans, such as the order-sorting filters. If the basic software does not provide that ability, the program should be able to run macros that enable users to write their own sequences.

In most cases, the total acquisition time of a scanning system will be relatively long. Take, for example, a 5-nm bandwidth in excitation and emission: the excitation range is 250–600 nm, requiring 71 steps, and an order-sorting filter change below 500 nm would be useful. The emission range would be 300–800 nm (101 steps), and a filter change between 500 and 600 nm would be good. If the emission scan speed is 0.2 s/step, equal to a scan time of 25 nm/s, one spectrum takes ~20 s plus the monochromator reset time and the change of excitation wavelength. All actions may require 25 s/spectrum. Acquiring 71 spectra will take 26 min for the total fluorescence acquisition. If the application is required often, the time advantage of a system with parallel detection will save precious time. An array of at least 400 pixels in the wavelength axis is necessary for comparable data quality. If more pixels are available, binning will produce the desired bandwidth. The illumination time depends on the emission intensity, e.g., 5 s per emission spectrum, plus 2 s to set the next excitation, makes 7 s/spectrum. The total fluorescence will be captured within 8.3 minutes. The full power of an automated parallel detection system appears if more options, such as a sample changer, circulation pump, titrator, and other periphery, are added and the system runs in a pre-programmed fashion.

Figure 4.8 shows 40 emission spectra taken with 2-nm steps. The upper-left graph shows the data "from the front;" the strongest emission spectrum is the last one and appears in the rear of the set. The upper-right graph is the reverse, displaying the emission "from the rear," where the strongest spectrum is again the last one. Both maxima represent an excitation of 330 nm; from that perspective, the traversing excitation peak dominates. Both views

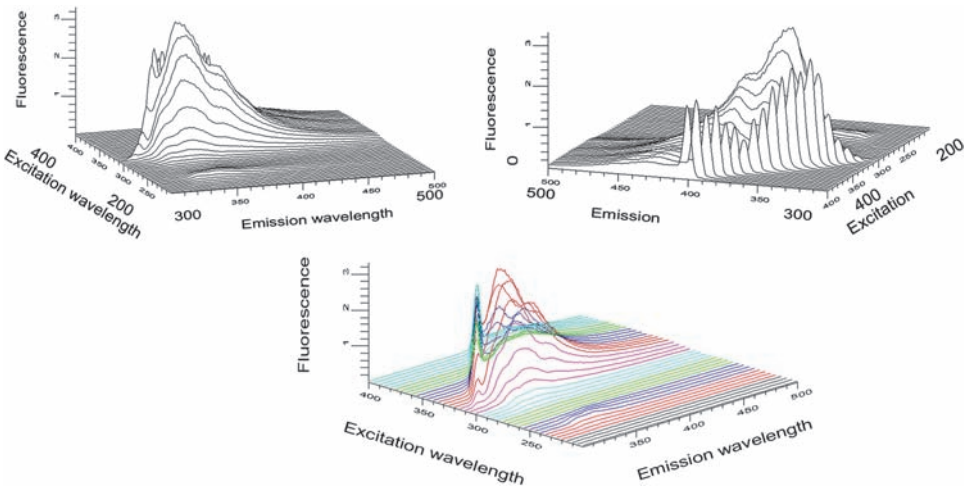

Figure 4.8 The total luminescence displayed in 3D mode.

suppress the "hidden" data to avoid confusion. The lower graph includes the "hidden" data, making the graph more complicated, but colors improve the picture. The lower curve is shown in "equal angle mode" between excitation and emission. Therefore, the sharp excitation peaks are under 45 deg and seem to stand in a row.

4.1.4.5 Fluorescence resonance energy transfer (FRET), also called the Förster energy transfer

If two optically active molecules are in a close neighborhood, it is possible in certain circumstances that one molecule (the donor, short for "donator") absorbs the excitation energy and transfers the energy radiation-free to the other molecule (the acceptor). The latter will then emit luminescent light. The basic requirement for the mechanics is that the absorption band of the acceptor and the emission band of the donor strongly overlap. Furthermore, the molecules must be very close to each other, typically within a 10-nm geometrical distance. The closer they are, the better the transfer efficiency.

The left part of Fig. 4.9 shows a simulated situation for the Förster transfer with a strong overlap of the donor emission spectrum and the acceptor excitation band. The right part is the general efficiency curve of the geometrical distance. Fluorescence resonance energy transfer (FRET) is, for example, the basis for the natural process of photosynthesis. The effect is also utilized in laser technology when one band is excited but another emits. A typical example in biochemistry is the interaction between tyrosine (donor) and tryptophan (acceptor), working at the FRET wavelength of 278 nm.

The instrumental requirements for FRET are

1. the precise measurement of both absorption spectra to locate the transfer energies;
2. variable and precisely defined excitation and emission bandwidths to perfectly hit the spectral overlap; and
3. a minimum of stray light in the excitation to ensure that, apart from the FRET wavelength, no other states are excited.

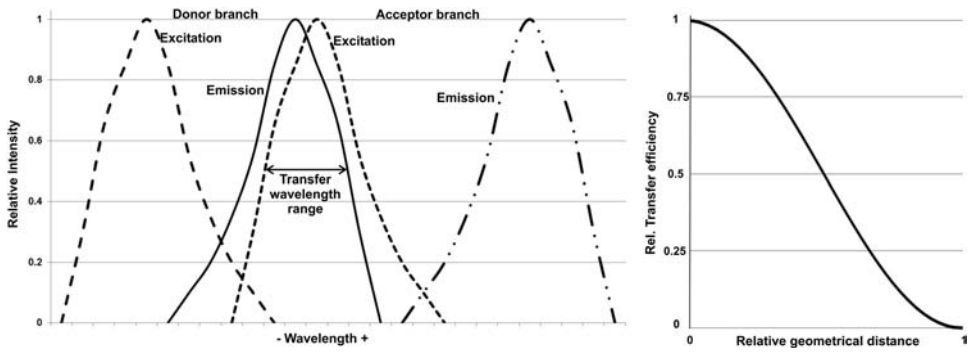

Figure 4.9 Spectral requirements for FRET and the coupling efficiency.

In other words, the performance of a double monochromator is required. If no high-class absorption spectrophotometer is available, the excitation arm can be used to acquire the reference spectra. A detector may then be placed behind the sample cell (e.g., a silicon element), and the transmission data are obtained according to the rules of single-beam photometry. FRET experiments are performed in both environments, macroscopic (in cuvettes) and microscopic. The analysis of FRET phenomena uses all three fluorescence methods: static, lifetime, and polarization anisotropy. Both the biological or chemical process and the spectroscopic measurement are specific for each FRET application. Other literature provide further insight into the specific task.[2]

4.1.4.6 Two-photon excitation/upward luminescence

Some molecules require more energy to become excited than a single photon can provide. To shift them into a higher energy state for later relaxation through photon emission, either two photons of the same or different wavelength (energy) must be absorbed in a quasi-parallel (within a picosecond) manner to procure excitation. The resulting emission wavelength may be between the two excitation wavelengths or below both. It may also appear above both excitation wavelengths if they are very close together or identical, and only negligible energy is lost by internal conversions.

As shown in Fig. 4.10, one photon (E_1) lifts the molecule to a virtual intermediate level (S_{virt}), and the other photon (E_2) brings the molecule to the excited level S_2. From there, a "normal" relaxation occurs. The excitation in

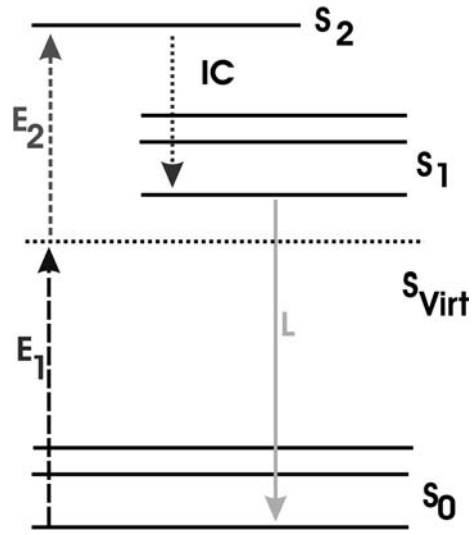

Figure 4.10 The Jablonski model for two-photon absorption/luminescence.

the figure is created by two different energies ($E_1 > E_2$), and the luminescent energy L is larger than either of them. This is a case of upward conversion because the luminescence emission wavelength is shorter (and the photon energy is higher) than the two excitation wavelengths.

Two different excitation wavelengths are required to create a case like this. Because two-photon excitation is statistically rare, it will only seldom happen with lamp/monochromator excitation. Most cases require one or two lasers. The system setup will look closer to a Raman measurement system than a classical luminescence spectrophotometer, and it will appear again in the Raman application (see Section 6.6.7). Due to the low excitation efficiency, the emission signal is expected to be orders smaller than in classical luminescence cases. A double or even a triple spectrometer is required to remove the strong stray light expected in the emission arm; this is especially important if the emission happens between the two excitation wavelengths.

4.1.4.7 Modulated excitation for NIR/IR, and phosphorescence

Sections 5.6.2 and 5.6.3 of *Fundamentals*[1] demonstrate how detectors with working ranges above ~800 nm suffer from a thermal background signal and how modulation can suppress the background. Because the efficiency of PMTs drops toward the NIR, other detector technology is necessary for emission measurements above the PMT limit, and the background must be reduced. The first choice is light modulation along with detection by a lock-in amplifier. Several options are available to produce the modulation; for example, a mechanical chopper can be placed between the emission source (luminescent sample) and the emission monochromator. This setup will cost 50% of the signal emission, and the thermal background signal from the sample is not discriminated because the sample is constantly excited. If the chopper sits in the excitation arm, then the thermal signal will be suppressed, but 50% of the excitation light will be lost. If long-glowing luminescent samples (phosphorescence) are processed, it is possible that the decay will not be finished when the next illumination begins, and overlap will occur. That problem can be solved by variation of the chopper frequency within certain limits (~10–800 Hz). The third choice is to modulate the light source itself, which has multiple advantages given the following parameters:

1. A xenon lamp must not extinguish during the modulation or else it will become unstable. If the minimum current is set to 5–10% of the nominal value, a clean sine wave can be produced between <1 Hz and >1 kHz. A modulation depth of <100% is no problem because only the modulated signal part is processed by the lock-in.
2. The modulation amplitude can be increased to the value stated in the data sheet of the lamp because the median power of the lamp is only about half the maximum of DC mode. Thus, the peak number of excitation photons may exceed that of DC operation, and a good SNR will be produced.

4.1.4.8 Laser excitation

Besides gas lasers, semiconductor laser diodes experience a rapid development toward blue or UV wavelengths. Their use in luminescence applications has increased because solid state lasers are substantially cheaper and much easier to handle than gas lasers. Adding an excitation laser to the system or completely removing the lamp greatly reduces the requirements in the excitation arm. The emission characteristics of the laser determine whether a monochromator is required at all. Gas lasers require wavelength selection to block the unwanted lines, which is often provided by the laser system itself. If not, a single-stage excitation monochromator will select one line out of several. The risk of stray light is far less than with wideband sources. In the case of pulsed lasers, the original spectral bandwidth might be wider than required for the luminescence measurement. Again, a single-stage monochromator will efficiently limit the bandwidth to the required specification. In steady state applications, a pulsed laser is useful. If its repetition rate provides a large number of pulses within one integration cycle, no synchronization may be required. Solid state lasers provide energies in the upper microvolt or millivolt range. Because the majority of lasers are used in lifetime systems, they are discussed further in Section 4.2.1.2. In any case, utilizing a laser might require several modifications to the excitation beam, which will reduce the spread of applications and variability. However, due to the substantially higher light density, it may provide shorter measurement times and an improved SNR. [See Section 6.5.1 (Raman excitation) for a table of lasers useful for luminescence excitation.]

4.1.4.9 Luminescence microscopy

Because luminescence methods are generally applied to life science, very small sample volumes are of primary interest, e.g., analysis of single cells or extremely small sample volumes. Thus, applications in combination with a microscope and probably special dyestuffs started in the mid-1980s. A typical case involves the calcium-carrying sample response on Fura or Indo dyestuffs.

- Fura-2 is used to measure intracellular calcium concentration. The fluorescence emission signal at 510 nm is rapidly recorded while the excitation switches between 340 and 380 nm multiple times. The ratio of the two excitations leads to the Ca concentration. The measurement, either spectral or spatial, requires a constant emission wavelength and quickly switching excitation.
- Indo-1 is also used to measure intracellular calcium concentration. The fluorescence excitation is kept at 340 nm, but the emission signal switches between 405 and 485 nm. The ratio of the two emissions reveals the Ca concentration. The measurement, either spectral or spatial, requires a constant excitation wavelength and quickly switching emission or parallel detection.

For microscopic imaging applications, it is generally easier to switch the excitation wavelength and spot the image through a constant filter than the other way around. Fiber optic illumination systems with switching filters are standard accessories today. In order to keep the excitation wavelength constant and switch the emission, different filter changers and even special cameras have been developed.

For spectroscopy, it makes almost no difference whether or not the excitation or the emission monochromator switches. It is a matter of design and electronics how fast, reliable, and efficient the switching is. Luminescence microscopy is almost always done in epi mode, which means that the emission travels through the same objective as the excitation. Therefore, it does not matter if the substrate holding the sample is transparent or not, and it allows the setup of confocal systems. The disadvantage is that the excitation signal will reflect or scatter parallel to the emission system without geometric suppression. If reduction through filters is possible, that is fine; if not, the emission spectrometer must provide reasonable contrast.

4.1.4.10 Confocal microscopy and fluorescence correlation spectroscopy

In order to analyze the luminescence of a very small area or volume with extreme sharpness and concentration on the evaluated area, a confocal technique is applied. The confocal effect reduces the influence of light outside the wanted area twice. A precise transfer of the illumination light via pinholes (Fig. 4.11) ensures the reproduction of the pinhole at the sample surface. The diameter is typically a few microns. The light source of choice is a laser because it provides the best refocusing and the required light density. The signal emitted by the sample is transferred along the same path until it reaches the beamsplitter. After that is passed, it hits the output pinhole before it enters a fiber line to the spectrograph. Between the beamsplitter and refocusing objective is an optional notch filter to remove the excitation line from the measured spectrum. Both pinholes are perfectly aligned to the identical optical axis and have the same size. This design provides extremely sharp geometric filtering at the sample surface. Scanning over the surface of the sample is done by a stepper-motor-driven mirror, deflecting the beam in both axes. Naturally, only a rather small area can be addressed, defined by the optical performance of the objective systems (typically 100×100 times the illuminated area); however, that area already serves 10^4 single measurements. Each may provide a different luminescence spectrum, but if not, the system only looks for one or a few spectral lines. This setup is also useful for other confocal applications, such as Raman, which only requires some different components.

4.1.4.11 Remote luminescence

Besides microscopes, remote luminescence monitoring almost always utilizes fiber optics and the epi mode. This means that the excitation and illumination

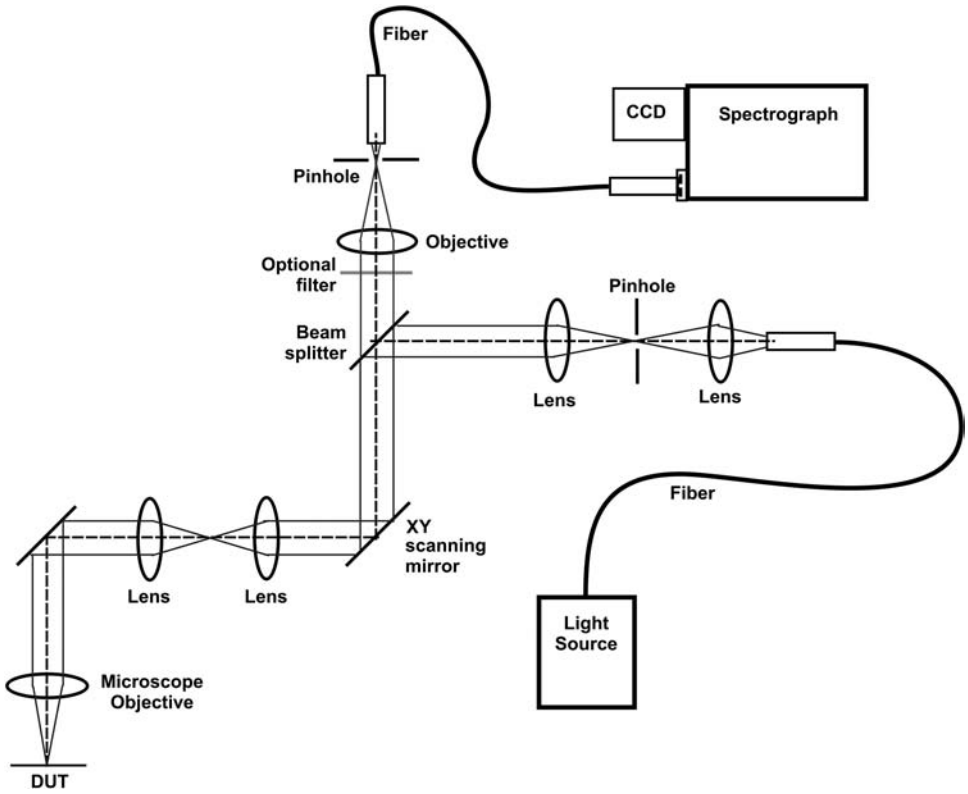

Figure 4.11 A confocal scanning microscopy luminescence spectrometer.

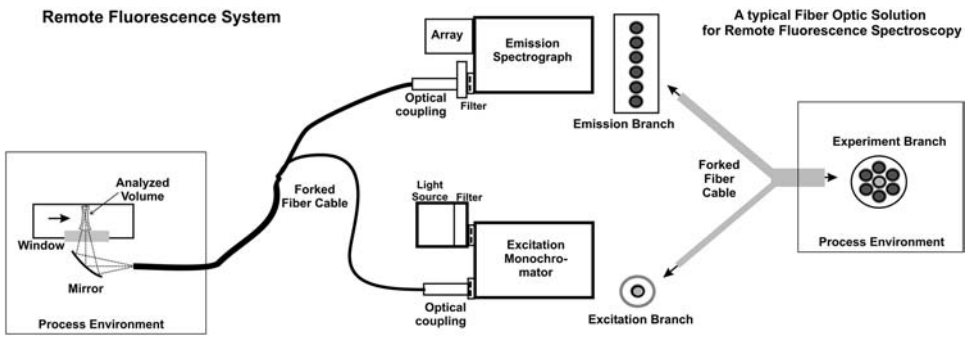

Figure 4.12 Example of a production control luminescence system.

path are more or less the same, as is the case in the microscopes shown earlier. Process control is often the goal, as shown in Fig. 4.12.

Real-time process control or fast quality-control luminescence systems can be derived based on the data created by a laboratory system (Fig. 4.12). The light source and excitation spectrometer are reduced to the required wavelengths. A single line is often fine, such as that provided by a solid

state laser or LED, or a combination of a lamp and bandpass filter. The DUT (on a robotic carrier) or the moving volume may be separated by a window to protect the analytical part from hazards. In the figure, a moving liquid is shown, and the analyzed volume is defined by the size of the excitation beam (it is waist-shaped in the example). The excitation and emission signals travel in epi mode, and separation happens in the forked fiber cable. Depending on the excitation source, the cable design may follow one of the versions shown in Section 6.7.5.1, Fig. 6.23 of *Fundamentals*.[1] One of the most efficient fiber cable versions is shown in Fig. 4.12 here. The excitation is a single fiber that creates a small excitation spot, which would also work with laser or LED sources. The emission branch consists of several fibers, allowing efficient collection of light from the experiment's emission; the spectrometer side is adapted for illumination of the slit.

The emission light will typically be recorded by an array spectrometer, allowing for rep rates as fast as a millisecond for the selected spectral interval. The useful speed depends on the emission signal level and the required precision of data. The absolute accuracy of the luminescence data may not be important—the repeatability and comparison with pre-defined reference data is typically more important, as provided by compact spectrometers. Online reduction programs can create digital process steering signals (or good/bad decisions) within the integration of the next spectrum and store the important parameters.

4.1.5 Summary of the requirements for a static luminescence spectrophotometer

- The light source should cover the requested wavelength range as homogeneously as possible and provide high light density in a small spot (if possible, smaller than the slit of the excitation monochromator). It should emit high optical power to ensure that reasonable power is also transferred if large slits are used.
- The excitation monochromator should cover the required wavelength range efficiently, the grating selection should compensate for variations in the lamp spectrum, and both planes of polarization should be transferred as similarly as possible. The dispersion should allow bandwidths of up to 10 nm, the slitwidth used most often should recover the lamp spot completely, and the contrast should at least be sufficient for the samples planned. If the system is used for general applications, the contrast ratio should be at least 10^5.
- The sample illumination and the sample positioning should illuminate the sample with concentrated, dense light. It should be compatible with different geometries (including microcells). The focus should either not move over the wavelength range or be adjustable. Efficient polarizers and order-sorting filters are optional, and T-optics are the first choice.

Automatic sample positioning and variable sample handling are desirable.

- The collection of the emitted light should be efficient, conserve the state of polarization, and provide optimal transfer to the emission monochromator.
- The emission monochromator should process the luminescent light efficiently over the entire working range. It should at least offer the contrast that the measurement methods require; instruments for general use (including polarization analysis) should provide a contrast of 10^5. Depending on the application, the system should be prepared to serve two detectors, probably working as a spectrograph. It should provide a reproducible variation of output bandwidth between ~0.1 and 10 nm. Filtering for spectral orders should be provided.
- The detector should have the highest available efficiency along with the optimal SNR in the requested emission range. A PMT is the most useful in the visible range, with the choice of working in photon-counting and analog mode; provisional cooling improves performance. In the NIR, Si and InGaAs avalanche diodes should be considered. If parallel detection is applied, rear-side-illuminated CCDs with efficient cooling are the most suitable.

4.1.6 Calibration, comparison of systems, and stray light tests

4.1.6.1 Calibration

The calibration of the wavelength, like all other spectrometer applications, is performed with line sources that provide safe spectral lines in the required spectral range. (The principles are discussed further in Chapter 7 of *Fundamentals*.[1]) The calibration of intensity is described in Section 4.1.3.2.

4.1.6.2 Comparison of luminescence systems and performance test

The best way to compare the performance of luminescence spectrophotometers may be to run one or more of one's own samples considered critical and difficult because the only internationally accepted test may not be compatible with the actual application. This test is a measurement of the SNR of the Raman signal in distilled water. With excitation at 350 nm, the Raman maximum will appear at 397 nm (3383 cm^{-1}). The bandwidth in both the excitation and emission will be set to 4 nm, the time constant to 1 s, and the scan speed to 1 nm/s. Whether or not the scan includes the primary scattering signal at 350 nm is not relevant. The scan should reach up to 440 nm for baseline analysis. After the 360–440-nm scan, the Raman amplitude is determined, whereas the baseline signal is reduced to find the net value. The test is still valid if the water or the cell is not perfectly clean and a little fluorescence is created. The background noise must then be appointed; there are two ways to calculate the noise in the background:

1. the last 10 nm of the recorded spectrum (430–440 nm) are used to find the STD of the background, or
2. a time scan of 10 s (10 data points) at a freely selected wavelength between 430 and 440 nm is taken, and its STD is calculated.

Finally, the ratio of [(net Raman maximum)/(background STD)] will be calculated. The result is the SNR value, which is presented in many data sheets. A depiction of the Raman SNR measurement is shown in Fig. 4.13.

The upper left of the figure shows an overview with the primary scattering peak at 350 nm; it has no means in the calculation but represents the system bandwidth (BE). The excitation and the Raman peak are marked with arrows, while the range for background calculation is marked by a thick grey line. In the top right is only the Raman peak and the baseline to be subtracted; the net height of the peak is used for further calculations. The bandwidth of the Raman peak (BR) will be twice the BE if both monochromators are set to the same value. The lower left presents the expanded background noise (BGN) between 430 and 439 nm: the minimum and maximum values are included, as are the STD and the ratio of the signal to the background noise [Signal / BGN] (e.g., 1675/1). In the center is the noise curve of a 10-s time scan at 440 nm, also with the minimum and maximum values, STD, and SNR (1791/1), which would produce a result 7% better than the SNR from the spectral background measurement. In the lower right is one more measurement that is sensible but not commonly applied. The noise of the Raman peak maximum is obtained in a 100-s time scan and used for the SNR calculation; it would lead to a much lower number, e.g., 352/1.

4.1.6.3 Weakness of the Raman-on-water method

Fluorescence systems often use monochromators with fixed slits, which provides the best reproducibility in bandwidth. However, not every vendor

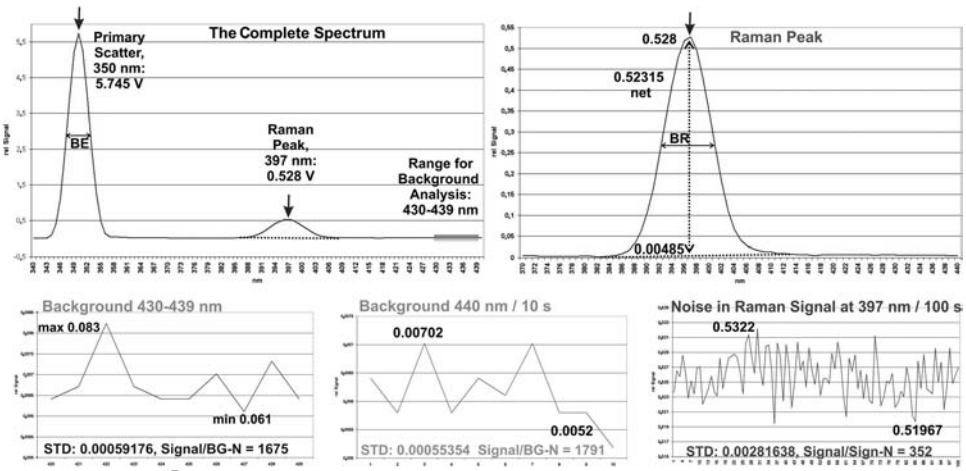

Figure 4.13 Signals required to calculate the Raman SNR measurement in water.

offers a nominal 4 nm; 5 nm are often selectable, which produces a light flux of factor 2.45 compared to a 4-nm bandwidth (the signal increase is the same). The used bandwidth can be checked in the Raman peak. In the example shown in Fig. 4.13, the bandwidth is 4 nm in both the excitation and emission, leading to 8 nm in total. The slit height used for the test is not defined in the rules, nor is it documented, but it naturally has a strong impact on the signal. Furthermore, some vendors specify the resolution but not the bandwidth. Sections 2.6.4–2.6.6 of *Fundamentals*[1] describe why the resolution of a monochromator requires a numerically wider bandwidth. An instrument specified in resolution numbers will have wider slits than one defined in bandwidth. Another issue lies in the integration time or the time constant, as discussed in Section 1.7 of *Fundamentals*.[1] If a photometer works purely analogously and the time constant is set to 1 s, the true signal value will be reached after 5 s. If it works digitally, it is possible (depending on the algorithms) that the true value will be reached after 1 s. Therefore, a digital system like that would be better compared with an analog version set to a 0.2-s time constant. Next, and very important, is the detector itself, most likely a PMT. If it has an S25 cathode (reaching up to almost 900 nm), it will have a noise floor at 25 °C, which is ∼3–4 times higher than that of a PMT with an S20 cathode (working to ∼750 nm). Cooled to –20 °C, the S25 will drop to ∼1/10–1/20 of the noise value at ambient temperature, whereas the S20 model improves less. Finally, xenon lamps are available for different nominal powers, with increased light density for fewer working hours, compared to the standard models. Again, a better SNR is produced. It is thus imperative that all parameters of the test procedures be kept under control to accurately compare competing systems. Make sure that the configuration being considered for purchase is the system being tested and not a different one.

The common method discussed thus far takes into consideration the noise of the detector system but not the noise of the light source. The stability of the power supply and lamp affect the short-term stability of the excitation. It would be better if the noise value of the SNR algorithm were not taken from the background (as is standard) but from the Raman signal maximum. This scenario is shown in the lower-right curve of Fig. 4.13. The SNR will, of course, be worse, and it will depend on the photon statistics, e.g., 352/1. However, it presents a much better rating than the general method. When purchasing a luminescence system, consider whether the majority of applications require excitation between 320 and 400 nm. Outside that range, the quality of the test results may widely vary. Note that the "world-wide accepted method" is a number that is only useful if all of the parameters are actually comparable, documented, and in the spectral vicinity of the intended applications. Systems with an SNR test result of 2000 in the real experiment may be worse than one that presented an SNR of 1000. Again, one's own samples at the required wavelength combinations will probably create a more-useful picture.

In short, the common method is correct and useful, but comparisons are only helpful if all parameters are documented. It may also be necessary to comment on the interpretation of the data and values; spectra and numbers alone are not sufficient.

4.1.6.3.1 Proposal to extend the Raman test

Because the 4-nm bandwidth is not available in all commercial systems using fixed slits, 5 nm will eventually be the next choice—keep in mind that the signal will grow by a factor of ~2.5. The Raman of water measurement should be obtained at a 350-nm excitation and emission scan from 370–440 nm. The peak maximum is determined as described previously. Next, a time scan at 440 nm over 100 s is taken, and the STD is calculated. The measurement at the Raman peak max (397 nm) is then taken for 100 s, and its STD is also calculated. Thus, two SNR results are available, which creates a rather-good performance characterization of the system in the near-UV range. In order to justify the performance over the entire working range, other tests are proposed: many fluorophores are excited between 270 and 320 nm, and they behave differently compared with 350 nm. Thus, water excitation at 280 nm and emission between 290 and 350 nm is a good choice. The Raman line will then appear at 309 nm, and the background time scan will be done at 350 nm. That gives increased understanding of the whole UV performance. For the visible range, a third test is proposed. To avoid the strong xenon lines, 540 nm will be a good excitation wavelength, the Raman line will appear at 660 nm, the scan range will be 600–700 nm, and the background time scan will be taken at 700 nm. For all three tests, three data acquisitions are required, and two results are produced, providing a good measure of the system performance.

If the data reduction program does not allow calculating the STD, a good estimation is reached by subtracting the minimum noise value from the maximum. The difference divided by 3 will be close to the STD. The Raman signal grows with the fourth power of photon energy. If the excitation/emission pair 350 nm/397 nm is taken as a reference, the excitation at 280 nm will lead to a Raman signal with a factor of 2.4, while the excitation at 540 nm will be attenuated to a factor of 0.18. Table 4.1 shows the spectroscopic interrelations.

Table 4.1 Interrelations of Raman signals.

Excitation WL [nm]	Excitation WL [cm^{-1}]	Scattering factor	Slit size for a 4-nm BW [mm]	4-nm linear signal factor	Slit size for a 5-nm BW [mm]	5-nm linear signal factor
280	35,714	2.4	4.9	12.0	6.1	15.0
350	28,571	1.0	5.0	5.0	6.2	6.2
540	18,519	0.2	5.1	0.9	6.4	1.1

The leftmost column is the excitation wavelength, and the following column is the corresponding wavenumber. As scattering increases with the fourth power of photon energy, the scattering factors result. The four columns on the right show the relative excitation power at the sample depending on bandwidth (BW). A sample 0.3-m monochromator with a 1200-mm^{-1} grating is used for excitation; the geometrical slitwidths are listed in the column "slit size for a *x*-nm BW," while the "*x*-nm linear signal factor" compares the relative amount of scattering signal created by the sample. The table shows that the change of bandwidth will produce a 30% difference in the SNR specification and also that design decisions determine at what wavelength and how the Raman test is performed. More about the specifics of Raman measurements are presented in Chapter 6.

4.1.6.4 Stray light test of the excitation arm

The excitation error can be well defined with the help of wideband fluorophores, such as Rhodamin-B. Scattering tests in glycogen are also useful. Stray light originates mainly from the spectral range of the strongest source emission, which mostly affects the deep-UV range. The following methods detect stray light in the excitation. First, an emission spectrum, e.g., Rhodamin-B excited at 270 nm, is obtained. A short-pass filter with an edge wavelength of 290–310 nm is then put in the excitation beam. The filter will block all longer wavelengths above the edge, and thus only the true deep-UV light is left through. A second emission scan is taken; if it is lower in amplitude than the first one, stray light in the excitation is the reason. The ratio shows the total impact. Unfortunately, it is not evident from which wavelengths above the filter's edge the errors come, although the second method may help with this. If the scattered signal of a strong scattering sample, such as glycogen in water, is measured, then the emission spectrum will only contain two signals: the primary scatter at the excitation line and the water Raman signal. All other signals are created by stray light. Absolutely clean sample components and a perfectly clean cell are necessary or else luminescent signals will appear. Long-pass filters may be required to avoid order overlay. To detect likely problems, all excitation wavelengths of the future samples must be tested, and the full emission spectra must be recorded with high sensitivity. The method will detect all troublesome wavelengths and wideband disturbance. If no scattering sample is available, a mirror may be placed in the sample position instead of the glycogen to reflect the excitation light directly into the emission arm.

4.1.6.5 Stray light test of the emission arm

A false light test in the emission arm requires clean light from the excitation or from a different source (laser), and a mirror is used instead of a sample. The mirror is adjusted so that it reflects directly into the emission arm. The critical emission wavelength is then chosen, and an emission spectrum is recorded,

probably starting just above the source. It will quickly be seen whether unwanted signals appear and at what spectral position. Because an emission spectrometer responds differently to different input wavelengths, a total-fluorescence-like measurement is required for the full picture. Even at this point, not all problems may emerge because only the light of a small band is used for illumination, and cross-talk effects may not appear. Quantification is not possible; that would require standard stray light tests with special filter sets and a white light source.

4.2 Dynamic Luminescence/Lifetime Measurements

Photoluminescence phenomena are pump (excitation) and relaxation (emission) processes. All of the excited states will return to the original, unexcited state, more or less quickly. So-called static luminescence is the equilibration between the two scenarios. While the excitation light constantly pumps some electrons up to a higher state of energy, some others return to the ground state and emit light. The time span between the excitation and the end of the emission has a spread that is defined by the chemical structure, the chemical environment, and thermal situation of the sample. The emission starts quickly after excitation, but the delay is never zero. Not all electrons return from the excited state at the same time—they follow an exponential relaxation function (*e*-function). The time between any point of the decay curve (such as the end of the excitation) and an emission level of 1/*e* (or 36.8%) of the reference point is called the lifetime. It may reach from the upper picosecond range to hours or even days. The general behavior of luminescence decays is explained by

$$[dN_{(t)}/d_t] = -(\gamma + k) \times N_{(t)}, \tag{4.3}$$

where $N_{(t)}$ is the number of excited molecules at the time t of excitation, γ is the emissive rate (the luminescence efficiency), and k is the nonradiative decay, like the thermal equilibration;

$$N_{(t)} = N_0 \times e^{-t/\tau}; \tag{4.4}$$

and

$$\tau = (\gamma + k)^{-1}, \tag{4.5}$$

where N_0 is the start of the measurement at referenced time zero $N_{(t)} = N_0$, and τ is the lifetime of the excited state. The decay is depicted in Fig. 4.14.

After 1 time constant τ, the luminescence intensity drops to 0.368 of the starting value. This behavior is true at any place in the curve if no additional excitation occurs. Therefore, the lifetime τ can be calculated from any interval within the decay curve. Both edges (rise and fall) of the excitation strongly affect the decay curve. The ideal excitation would be a perfect rectangular pulse (dashed column) with a width far less than the lifetime but enough peak power to saturate the sample. Both requirements are not fulfilled at the same time by any kind of source. Pulsed lasers may offer enough power for

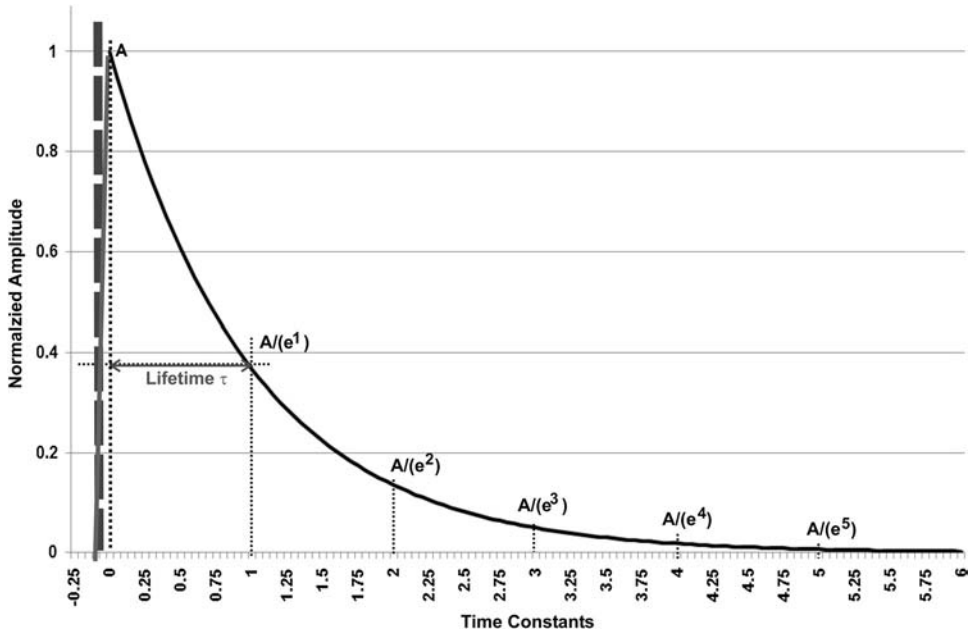

Figure 4.14 Normalized decay of every kind of luminescence.

saturation and may offer FWHMs in the picosecond range, but they do not provide perfect rise and fall. A synchrotron can fulfill all of the requirements, but it is not generally available. The curve also shows that the emission signal may still increase while the excitation intensity drops. This behavior is due to the internal conversions processed in the electronic structure of the sample material. The combination of all effects produces an overlay of emission curves; Fig. 4.15 shows a theoretically constructed example.

All curves are presented in normalized mode. Due to the nonideal rise and fall of the excitation, the emission may start before the excitation has reached its maximum. The figure demonstrates a selection of emission curves resulting from different excitations in front of the maximum. The grey curve is the one excited at maximum excitation, and thus it represents the true lifetime. The orange curve represents the measured signal. It may rise with a certain delay upon excitation, and it contains all time-dependent information. In the simulated case, no excitation would happen from the trailing edge of the excitation pulse. This scenario assumes that the sample was saturated before the excitation pulse extinguished. In real cases, there will be an infinite number of curves overlaying each other, excited from the excitation maximum and both edges. Thus, all lifetime systems need time calibration, which is done best with a pure scattering sample, to find the system's answer, if the sample provides zero lifetime. A second sample with a known lifetime similar to the expected unknown (and with similar saturation behavior) would improve the probability of correct results.

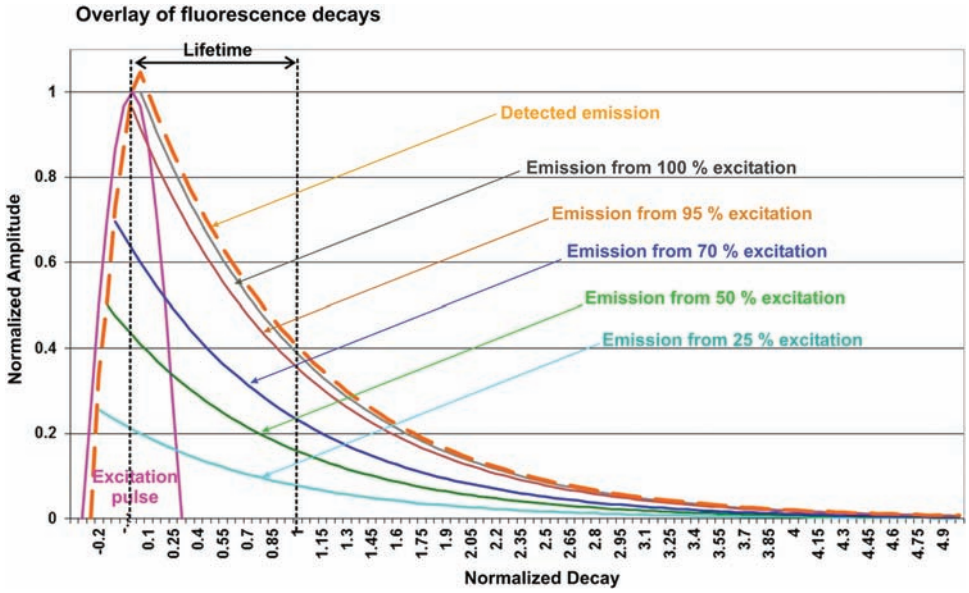

Figure 4.15 A selection of several emission curves, and the measured output.

To make it even more complicated, samples might not only contain a single lifetime—they might present more than one relaxation process. Technically, this means that the overlay of more than one *e*-functional decay creates the output signal. Furthermore, the lifetime may change with the sample's environment (temperature, pH, other species in the sample, etc.). A positive effect lies in the spectral structure: the maxima of excitation and emission for the different lifetime species are often also at different wavelengths. Using spectrometers in both arms can help select a single decay curve out of several. This, in turn, may detract from efficiency and add to the total measurement time at a reduced SNR. All of these factors must be monitored when lifetime measurements are performed.

In Fig. 4.16, the 1-ns FWHM excitation pulse (pink) is close to Gaussian, but it rises faster than it extinguishes. It excites two independent lifetimes of 1 ns (blue-dashed) and 2 ns (green-dotted). The theoretical convolution of

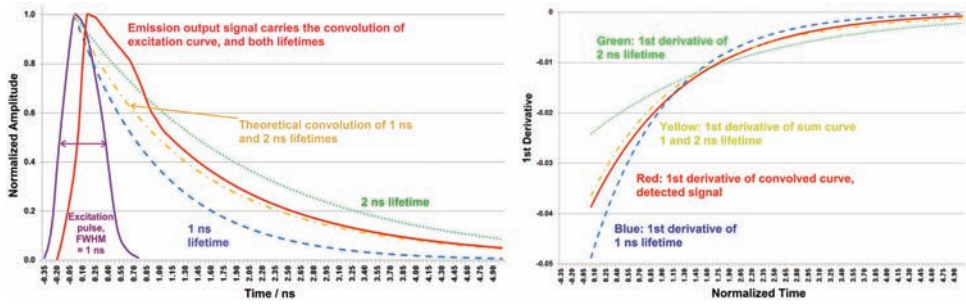

Figure 4.16 Simulated example of two lifetimes excited by a pulse.

both would be the yellow dotted-line curve. The detected emission (red) is the convolution of all functions, as described above. Curve deconvolution and differentiation are required to find the result. A simulated, idealized result of the derivation is shown on the right. In reality, because rather small intensities per time unit are involved, the output signal will not be as clear as the simulated curves in the graphs; the (red) signal will be noisy. Thus, averaging and fit algorithms are also required, calling for rather-complex programs.

4.2.1 Available instrumentation

There are two basic methods available on the market: pulsed and modulated systems. Both methods can be combined with polarization analysis and parallel wavelength detection.

4.2.1.1 Analysis of the change in the state of polarization

The relation of the state of polarization between excitation and emission changes with the lifetime. The longer the lifetime, the stronger the degree of depolarization of the light emitted. When exciting with linearly polarized light, the measure of depolarization provides a conclusion of the lifetime. Even more, the measurement of the change in polarization can be combined to all the methods described hereafter. The measurement of polarization itself is described in Section 4.1.4.3.

4.2.1.2 Pulsed methods

Pulsed methods depend on an excitation light source that provides small, steep, intensive, and repeatable light pulses. Five types of sources are available:

- **Synchrotron:** A synchrotron is the ultimate pulsed light source because it provides all spectral energies at high, uniform intensity levels, and the excitation can be gated to narrow, steep pulses. Saturation of all possible states of the sample is not a problem. However, a synchrotron is large and very expensive, and the running costs are immense. Thus, it is only used in reference labs and at laboratories where the device can be applied to many different purposes.
- **Pulsed lasers:** All lasers provide one or more discrete spectral line(s) or interval(s). The user can select the best-suited laser from a large selection (if available) for the required excitation wavelengths. In laboratories that require a wide range of excitation wavelengths, that may become very expensive and not viable. Very different parameters are found: the pulses may be steep and narrow but also relatively wide with remarkable rise and fall times. The spectral bandwidth may also reach from a picometer to tens of nanometers. Lasers often need an additional monochromator to select the working wavelength or cut the bandwidth. Most lasers offer that as a built-in option. One major advantage is true for all lasers: they can be triggered reliably and at rates up to the megahertz range. Careful selection of pulsed lasers is required because

eventual side effects within the pulse, such as oscillations, will be convolved into the fluorescence signal and complicate the deconvolution of the lifetime signal. This fact should be kept in mind if a pulsed laser is used for cw luminescence excitation.[3]

- **LEDs and laser diodes:** As the range of available products increases constantly, LEDs and laser diodes become more and more popular. Currently, laser diodes cover the wavelength range between 300 and 1600 nm. Again, different parameters are selectable. The choice involves the pulsewidth and steepness, pulse frequency, and pulse power. The spectral position and bandwidth are parameters of selection. At this time, laser diodes and LEDs are not yet available for the UV range below 300 nm, where many of the fluorophores are best excited. Because solid state sources generally only emit at one spectral position, no excitation spectrometer is needed except to narrow the excitation bandwidth. Diodes perform repetition rates up to the megahertz range or even more; the pulsewidth is typically in the lower nanosecond or even the picosecond range. The availability of lasers providing even shorter wavelengths is just a matter of time.
- **Continuous wave lasers:** Continuous wave (cw) lasers emit the minimum spectral bandwidth available for laboratory excitation. If a cw laser is used for lifetime detection, then modulation or gating of the beam is required. That function is typically performed by Kerr or Pockels cells, performing pulsewidths in the picosecond range, and repetition rates of megahertz or even gigahertz. Disadvantages include the footprint, price, and handling. If gas lasers are chosen, argon ion or krypton are the most popular for fluorescence analyis, offering many lines between 248 and 700 nm at power levels from milliwatts to watts. If the application requires a defined excitation wavelength not provided by the laser, a tunable dye option can be used to vary the excitation wavelength.

  Note that all lasers emit strongly polarized light. If the plane of polarization does not fit the experiment, scramblers or polarization optics, such as half-wave plates or similar, must be added between source and sample.
- **Flash lamps:** Flash lamps provide wide spectral ranges but cannot be pulsed as fast and steep as the sources described earlier. High-pressure xenon lamps reach from ~220 to 2000 nm, which is sufficient for the vast majority of fluorophores. Special fillings, such as N_2 or Hg, add lines in the UV to increase the spectral power at discrete wavelengths. A monochromator or a bandpass filter is always required to sort out the desired spectral energy from the wide spectral range. The intensity at the sample will rarely be sufficient to saturate the sample. The major drawbacks are the achieved pulsewidth, the steepness of the pulses, and the pulse frequency. The pulsewidths for standard lamps are in the range of 10 ns FWHM or more. Special coaxial types provide FWHMs down

to ~1 ns (as shown in Figs. 4.14 and 4.15) at the expense of peak power. All pulse shapes are near to Gaussian, which means that the footwidth is twice or more the FWHM. The repetition rates of flash lamps span a very wide range. The more power a pulse has and the wider the FWHM is, the slower the rep rate. Lamps with kW per pulse and μs width perform between 30 and 300 Hz, whereas coaxial models can repeat up to 50 kHz, depending on the size and power of the arc. The rep rate will ultimately define the total experiment time if the lifetime, detector, and data acquisition electronics allow faster processes. The emitted light contains all states of polarization; selecting a specific plane thus reduces the optical power.

4.2.1.3 Synchronized integration, also called boxcar integration or pulse/sample analysis

In Fig. 4.17, t_0 marks the beginning of the time to be analyzed with regard to the trigger. The trigger, in turn, is locked to the excitation pulse and typically arrives at the start of the pulse. After time t_1, a window opens and allows the signal from the detector to run into an integrator until the window closes at time t_2. The collected integral is digitized and stored, and then the timing generator shifts both t_1 and t_2 by a pre-defined amount of time [typically the window time (marked grey)] and waits for the next trigger. The loop will be repeated until t_3 is reached and the full curve is stored. A graphical display will show the data already gathered at any point of time. The operator can decide if the curve is good and if the SNR is sufficient. If not, the operator does not stop the system, and it will integrate and add another curve. Some system

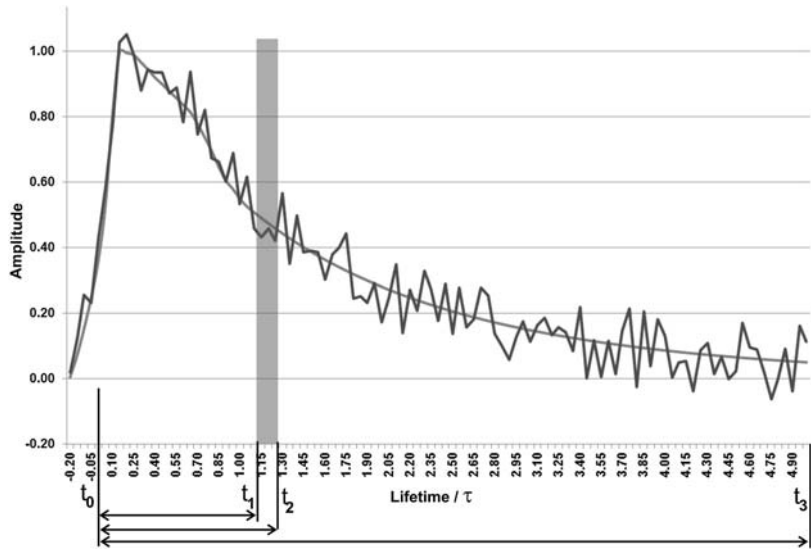

Figure 4.17 Signal timing in boxcar mode.

software can calculate the SNR on the fly and stop as soon as the pre-defined ratio is reached. An alternative mode lets the integrating time window sit at a point of time for a given number of triggers before it goes to the next point of the curve. This alternative has no direct impact on the total time, but it may allow the software to stay for a different time at the different points of the curve and produce the same SNR throughout. Another mode offers the ability to change the width of the integration window between t_0 and t_3, which allows fine time resolution in the sections of rapid change and wide windows in areas with little change. The result may not require extra noise suppression, but deconvolution is still required after the resulting curve, marked by the continuous line.

4.2.1.3.1 How a boxcar system works

In Fig. 4.18, the master trigger and delay generator provides several precise trigger signals. The first one starts the flash lamp, which may have a delay of several microseconds. Taking that delay into account, the master starts the boxcar system, which comprises two signal channels and has a minimum delay of ~40 ns. The input I2 integrates the signal from the reference detector R for normalization. Channel I1 collects the analysis signal from the lifetime detector LD and works as described earlier. The boxcar may present the two data separated, or it may normalize each time-resolved I1 signal to the parallel, integrated I2 signal. The precise time delay between the trigger and effective lamp pulse, captured by the lamp trigger sensor LTS, may be fed to the PC data, if required. The system reset, which releases the next cycle, may be free running or come from the boxcar or even from the system PC. Both detectors—the emission detector LD and the reference detector R—must be fast and linear to allow sufficient integration. Limiting parameters are typically the "gate" or "sample" time of the boxcar integrators, the system jitter, and the rep rate. Gate/sample times reach between <100 ps into

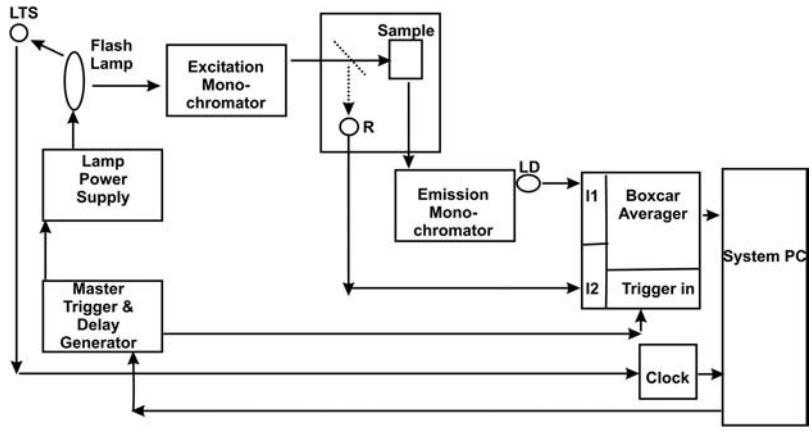

Figure 4.18 A typical boxcar setup.

the millisecond range, making the method useful for all lifetimes >1 ns. The jitter of each unit involved should be kept <20 ps, and the total system jitter <50 ps. Due to the different sample/hold electronics and resets, the maximum repetition rate is in the range of 10 kHz, which cannot be reached by pulsed lamps but by LEDs and lasers. The process to recover the single or multiple decay (lifetime) requires deconvolution and data fitting. Both are provided by instrument manufacturers, research societies, and institutes.

4.2.1.4 Single photon counting: TCSPC

The theory behind single photon counting is statistical. After the flash of the excitation source, only a single photon (or none) emitted by the sample is detected and stored in a multichannel analyzer (MCA). In the timing diagram in Fig. 4.17, only the start (t_0) is defined; the end (t_3) is given by the electronics. At t_0, the MCA discriminator electronics are armed and record the arrival of the first sample photon detected. That event is correlated in time to the excitation pulse. Therefore, the full name of the method is time-correlated single photon counting (TCSPC). After many excitation pulses, the convolved decay curve will become visible and grow out of the statistical noise.

In Fig. 4.19, the master generator starts the excitation source and "arms" the MCA, taking into account the different delays. The MCA now waits for two trigger signals: the first, T1, comes from the reference R and starts the internal timing generator; the second, T2, comes from the sample and stops the time counter. This procedure requires normalized trigger signals from the reference and lifetime detector (LD) that are created by amplifier/discriminator (A/D) electronics. As soon as the detector discriminator level is exceeded, the A/D emits one trigger. This happens whenever a detected photon arrives. Each of the two channels records only the first signal from its detector. The sample photon cannot be faster than the reference. If that occurs, it is

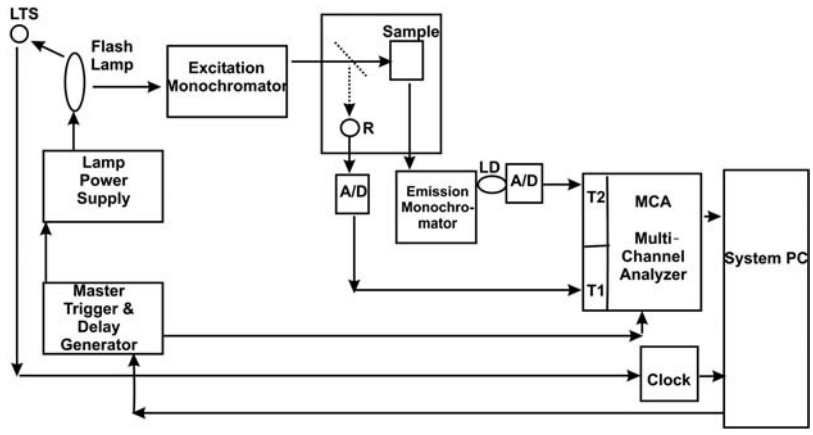

Figure 4.19 Schematic of a TCSPC system.

cancelled, and no data storage happens. By starting and stopping an internal clock in the MCA, the delay time between the reference and sample is measured (correlated), and both can be referenced to the excitation source. The correlated time (a single event) is turned into a digital number, which is equivalent to the channel number of the MCA. One count is added to that channel. After the cycle time is over, the next pulse is started. The probability of a photon to be detected is linear to the intensity at that specific point of the experimental lifetime. Thus, the decay curve is reconstructed after a lot of cycles.

The detectors do not need to work linearly with intensity—they need to be fast and have a reliable response to single photons for discrimination. Because the probability of a "false" signal (not created by experimental photons) increases with the square of time, the TCSPC method is only useful for rather fast lifetimes, up to a typical value of 100 ns. The master generator needs to take several time differences into account, such as the intrinsic travel times, plus the intrinsic electronic delays. Limiting parameters are response times and jitters of the detectors, the system jitter, and the rep rate. Suitable PMTs provide rise time jitters between 5 and 10 ps; thus, it makes little sense to try a time resolution below that. The maximum time is defined in the MCA setup. If the MCA has 1000 channels and is set to a 20-ns end time, the resolution will be 20 ps. The jitter of each unit involved will be kept <20 ps, and the total system jitter <50 ps. The different jitters, except the detector rise time, will be partially averaged out, statistically. A TCSPC system works very quickly; the maximum repetition rate can even reach above 100 kHz, which is beyond the time frame of pulsed lamps but fine for LEDs and lasers. Because the data occur statistically, the display will show the growing curve. This allows the user to stop the process at any time or just let it end at the preset time. The process of lifetime recovery requires deconvolution and data fitting. Both are provided by instrument manufacturers and also by research societies and institutes.

4.2.2 Continuous methods

4.2.2.1 Phase/modulation analysis

In electrotechnical engineering, it is common to define the frequency-to-time behavior of a system by the transfer function of a continuous, externally introduced electric signal, which is perfectly known in frequency, amplitude, and phase. The response of the sample under test to the introduced signal is recorded and correlated with the original signal. The result is the damping and the phase shift of the sample, tested at a certain frequency. A map of frequencies and the corresponding sample response provides the frequency behavior of the system in the frequency (time) range of interest. The method is called frequency response analysis (FRA). Because the frequency and time are physically the same, FRA is also used for lifetime experiments. The method is called phase/modulation analysis. Either the excitation source itself is sine-

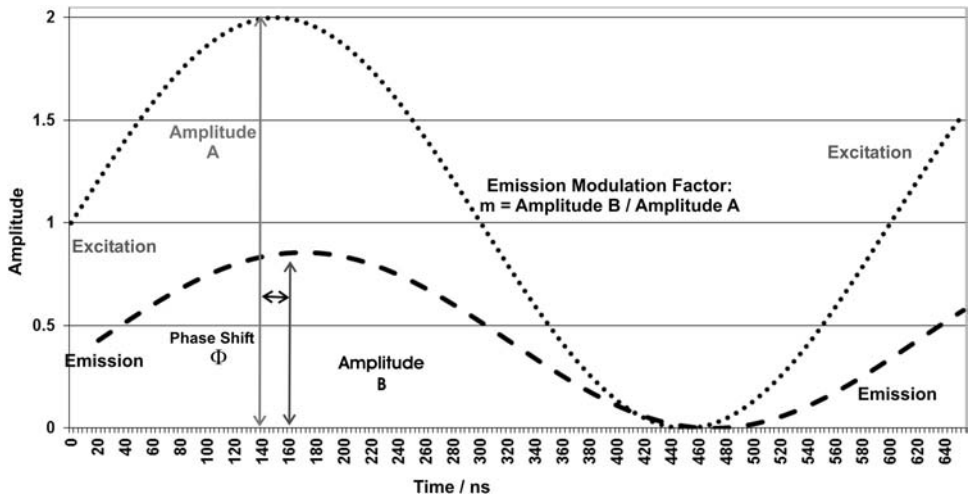

Figure 4.20 Parameters to recalculate the lifetime from a modulated excitation/emission scheme.

wave modulated or the DC light of the source is modulated. The most used optical modulator is the Pockels cell, which works from <1 Hz to >1 GHz. A fluorescent sample will provide two answers to the modulated excitation: a shift in phase (the direct time information), which has a linear behavior in relation to the lifetime, and the damping (the modulation factor), which works exponentially (as does the fluorescence decay). Both parameters are correlated and will produce the same result, which is double-checked, as shown in Fig. 4.20.

Note that the excitation light at no time begins completely turned off. The average intensity is half the maximum, which, in turn, creates a certain "steady state population" of excited electrons. The electrons with extra charge "flow around" the steady state. The modulated emission curve follows the excitation with a delay resulting from the modulation frequency and lifetime. The time of the x axis is representative for the sine-wave modulation but not for the lifetime, which must be calculated. The attenuation of the emission also depends on the frequency and lifetime. The higher the frequency is, the fewer electrons participate from the modulation. Therefore, the emission amplitude decreases while the frequency increases. The modulation factor m carries linear information about the frequency and exponential information about the lifetime. The time scale in Fig. 4.20 represents a frequency of 3 MHz.

The general equation to calculate the phase angle for lifetime spectroscopy by phase/modulation analysis is

$$\tan \Phi = \Omega \times \tau_p, \tag{4.6}$$

and the equation for the modulation factor is

$$m = [1 + \Omega^2 \times \tau^2{}_m]^{-1/2}, \tag{4.7}$$

where Φ is the resulting phase angle, Ω is the circular frequency of modulation, τ is the lifetime, and m is the resulting modulation factor. The frequency behavior of the two parameters is shown in Fig. 4.21 for an 11-ns lifetime.

The simulation was performed for a lifetime of 11 ns and measurements at 1, 3, 10, and 30 MHz (Fig. 4.21). Although the factor at 1 MHz is high ($m = 0.815$), the phase shift is only $\Phi = 4$ deg, which provides a low error potential for m, but high for Φ. Better data is attained at 3 MHz: $\Phi = 12$ deg and $m = 0.43$. At 10 MHz, $\Phi = 35$ deg and $m = 0.14$, which are also good for reliable data. Finally, at 30 MHz, the results are $\Phi = 65$ deg and $m = 0.048$; the small m value will not be good for reliable lifetime calculations.

From the example, the exciting advantage of the method appears: the result is not created from a single parameter, as in pulsed methods, but rather it is based on three parameters that are all accessible: frequency, phase, and modulation. By collecting data over a range of frequencies, a map of results is created, leading to safe results. Commercially available instruments work mainly in the range of 1 to 400 MHz, making them most suitable for lifetimes between 0.4 and 160 ns, which covers the vast majority of fluorophores. Special versions even reach up to 1 GHz (good for lifetimes down to 150 ps), whereas low-frequency systems start to work from 1 kHz (good for a 1.6-ms lifetime). If the phosphorescence decay is even slower, either lock-in technology or a system-internal DC intensity recording can be used. The latter may be recorded by the ADC alone at a rate of 1–10 ms. For very-slowly-relaxing samples, the internal shutter can be incorporated, which

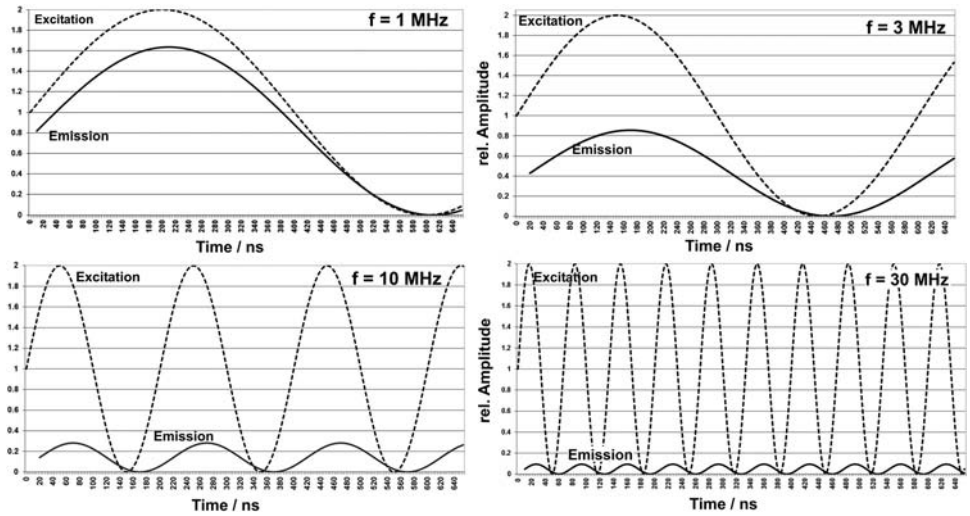

Figure 4.21 The change in phase shift Φ and the modulation factor m versus frequency.

allows small emission data to be safely recovered. Because the light source is DC anyway, all of these modes are provided.

4.2.2.2 Setup of a phase/modulation system

In Fig. 4.22, the solid lines represent the light path, the dashed lines represent the detector supply and electrical interconnections, and the dotted lines represent the signal travel. The system works in heterodyning mode: The Pockels cell receives a complex heterofrequency signal and modulates the excitation light accordingly. The Pockels cell is a perfect polarizer, and the modulated output light is polarized horizontally, which is also the preferred axis of most samples. The output axis of polarization can be varied by optional polarizers or retarders (Pol). For steady state experiments, the modulator can be moved out of the beam, and a reflecting mirror can take its place (marked by the dashed double arrow), turning the system into a

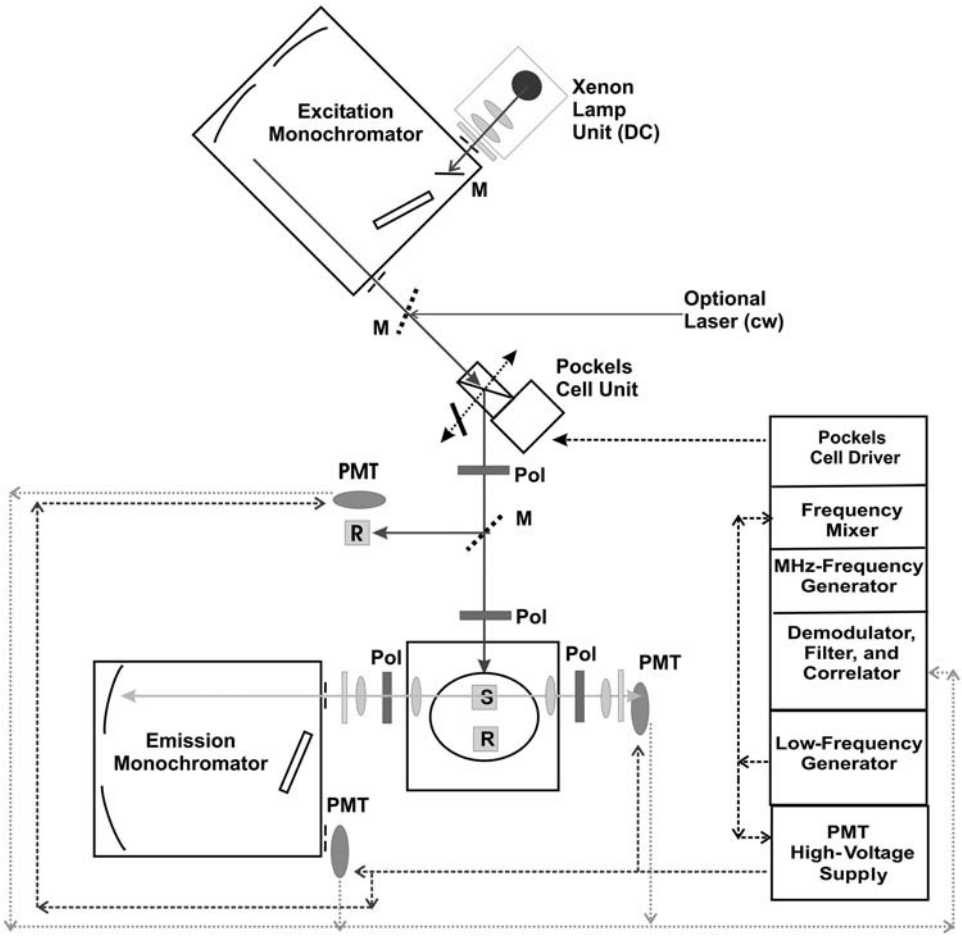

Figure 4.22 Components of a phase/modulation system.

standard steady state instrument. The standard light source is a normal DC xenon lamp, illuminating a standard excitation (double) monochromator. Between the light source and the modulator is a movable mirror that can guide other sources into the beam, such as lasers. If the laser emits at several wavelengths, it may also be routed through the monochromator, probably with a second entrance slit. The modulated excitation light is split (dashed M) ~10/90 to serve a reference system (R/PMT), as in a steady state version, which might use a scattering sample. It will take care of the internal-reference zero time. The pathlength between the beamsplitter and sample cell is the same as that to the reference cell. Then there is the sample compartment, holding two (or more) cells, sample and reference. The emitted light travels to the left and the right. Both may be equipped with emission monochromators, or there will be filters for higher collection efficiency. Both are often equipped, as shown in the figure. The main application of dual emission channels is to use two polarizers of perpendicular polarization planes, which enables collecting the polarization modification at each modulation frequency. The "demodulator, filter, and correlator" unit can read up to three detectors, usually PMTs. A PC (not shown) will steer the entire system and collect the data for further treatment.

The system works in heterodyning mode because, in the MHz–GHz range, any small change in cabling or optics would produce different phase/modulation signals. In heterodyning, as in radios or TVs, the MHz generator does not deliver its signal directly to the Pockels cell driver. In between is a "frequency mixer" unit that adds the signals of the MHz generator with a fixed low frequency, perhaps 70 Hz. The resulting signal drives the light modulator and also synchronizes the demodulator electronics. Because the detector's (PMT) high voltages are also modulated and phase-locked by the low frequency (LF, i.e., 70 Hz), the entire system is in lock-in mode; only signals correlated to the LF are valid.

Signals of the system

The modulated excitation light carries the MHz frequency, which is superimposed by the LF. The reference and sample emission signals correlate the excitation modulation with that of the PMT high voltage, and they are also guided to the demodulator unit. It filters out the high frequency and looks only for the heterodyned LF, which is then superimposed by the information in phase and amplitude; the sample was added. The correlator processes a phase-sensitive analysis of the PMT signals, and the result is the DC signals of phase Φ and modulation m coming from the emission channels. The data are averaged over either a preset time or until the PC program is satisfied with the SNR of the data, and then it goes to the next MHz test frequency. The data gathered so far are not final phase and modulation values—they need normalization. At each frequency, the response of the amplifiers, drivers, modulators, and finally the detectors is different. This means that the

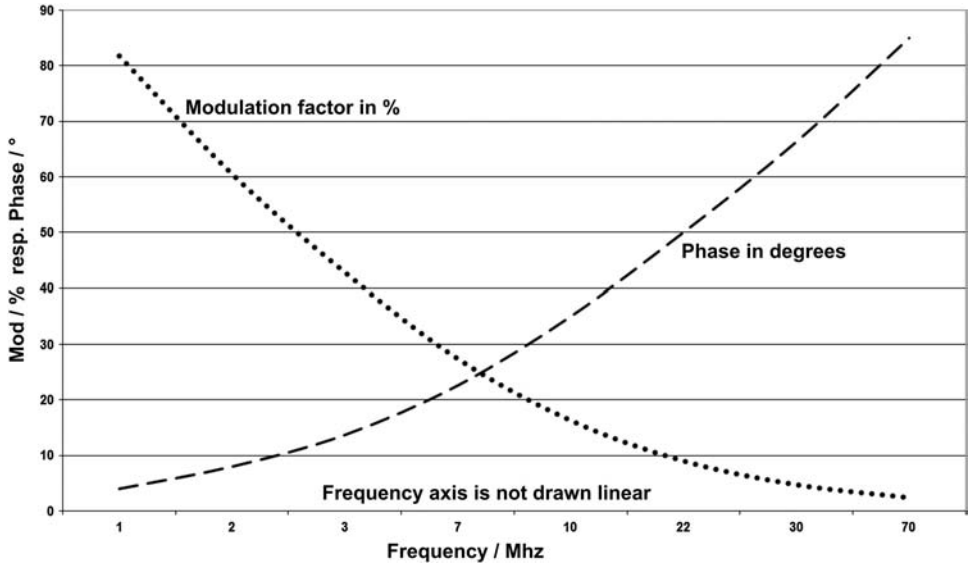

Figure 4.23 Reproduction of the phase/modulation data at a lifetime of 11 ns.

system needs time (frequency) calibration at each step of the experiment. To achieve that, a second reference is placed at a rotating table in the sample compartment. The reference material normally scatters, e.g., a glycogen solution. The system knows that the data collected at this point are zero phase and normalized modulation. After having taken that, the table rotates, and the sample is measured against the reference, and the (difference) data are finally stored. In total, the upper standard reference channel R is not absolutely required, but it increases data safety. The data may be presented in a dual curve, as shown in Fig. 4.23.

Timing

An analysis will probably take five data points per decade, in a 1-2-4-7-10 fashion. If the system works from 1 to 400 MHz, that will add up to 11 test frequencies, or 22 measurements. One measurement may take 30 s; the sample rotation may add 10 s, and thus the total will be 15 min, which is a typical value. Such a time is no longer (and probably faster) than a typical boxcar or TCSPC measurement, and the data provide a higher degree of correlation and safety. The process to recover single or multiple decay (lifetimes) requires data fitting but no deconvolution. Programs are provided by instrument manufacturers, research societies, and institutes.

4.2.2.3 Multiharmonic Fourier transform systems

The phase/modulation method was developed further and produced the multiharmonic Fourier transform (MFT) analysis. The setup and the signals

are almost the same as in single-frequency systems; the differences are in the modulation itself. The high-frequency generator produces an assembly of parallel frequencies, all of which are multiples (harmonics) of the base frequency. For example, if the frequency is 4 MHz, the others may (but not necessarily) be 8, 16, 32, 64, 128, and 256 MHz. Their sum produces a signal pulse that contains all of the frequencies. The assembly, as shown in Fig. 4.24, is superimposed on the basic LF, which now is applied to the modulator, PMTs, and electronics in a pulse-like shape. The on-time and the rep rate of the pulse is variable. Naturally, the share of each frequency is small, and the total time is very short; however, the sample will respond to all incorporated frequencies.

The data captured from a number of repeated pulse trains can be summed and averaged before data reduction. That analysis is performed by a fast Fourier process, which essentially produces the same results as the standard phase/modulation data. The clear advantage is time. If a good SNR is provided, the experiment and result can be obtained within seconds. Due to the low optical work in a pulse train and analysis, very high optical excitation power is required. A xenon lamp, followed by a monochromator, will not satisfy the needs. Strong cw lasers are required for excitation, and the emission monochromator is often dropped in favor of wideband filtering. Compared to Fig. 4.22, the system must use the laser entrance for excitation and will most likely not guide the fluorescence emission light through a monochromator. The modulation/demodulation and data reduction is more complicated than in a model that uses discrete single frequencies. Regardless, if the system will be used for steady state luminescence measurements, the excitation and emission monochromators can be incorporated.

As depicted in Fig. 4.24, the seven superposed frequencies are created in binary order (1st to 64th). The resulting conglomerate results in a cycle time of

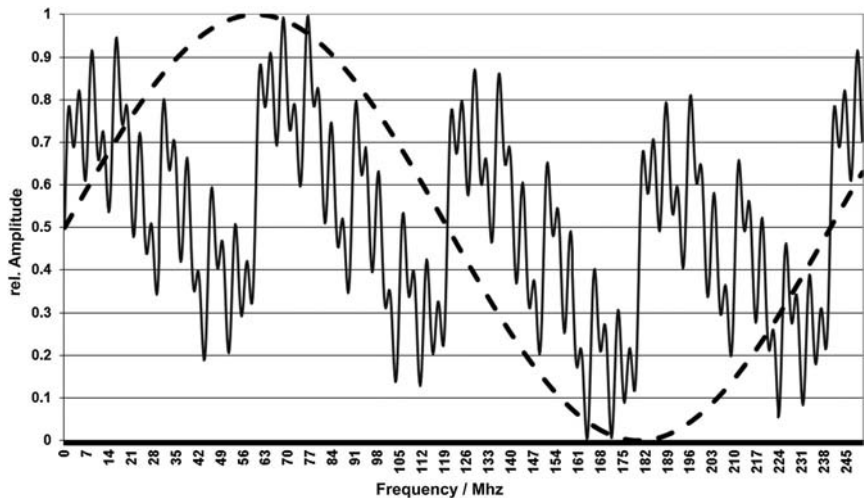

Figure 4.24 Basic 4-MHz sine wave and the summing curve of seven harmonics.

250 ns; not shown is the LF on which it rides. A single-excitation pulse train consists at least of one LF cycle (e.g., 70 Hz, or 14.3 ms). Theoretically, a complete lifetime analysis would require less than 20 ms. Realistically, a predefined number of those cycles will be applied for an improved SNR.

4.2.3 Methods using parallel wavelength detection

4.2.3.1 Synchronized CCD gating

The application of a gated MCP with an array or CCD enables the combination of boxcar signal integration mode with parallel wavelength detection. (The hardware principles are presented in Sections 5.4 and 5.8 of *Fundamentals*.[1]) The entire timing is very similar to that of a boxcar system (Figs. 4.17 and 4.18) with one exception: the measured lifetime cannot be correlated to the arrival of the reference R emission. The reference intensity (maximum or integral) can still be fed into either an input of the system PC or a reference channel of the CCD controller to allow data normalization.

As shown in Fig. 4.25, the master trigger and delay generator provides several precise trigger signals. The first starts the lamp pulse, which may have a delay of 1 μs. Taking that delay into account, the master starts the MCP-CCD system, which has a minimum delay of ~40 ns. The signal from the reference detector R can be fed either into an extra channel of the CCD controller or directly into the PC. The pre-set gate and read parameters respond to the trigger from the master generator. The MCP may have its own control unit or be part of the CCD controller. After one shot is acquired by the MCP-CCD combination, the data are directly transferred to the PC and displayed. They can be normalized to the reference. The precise time delay

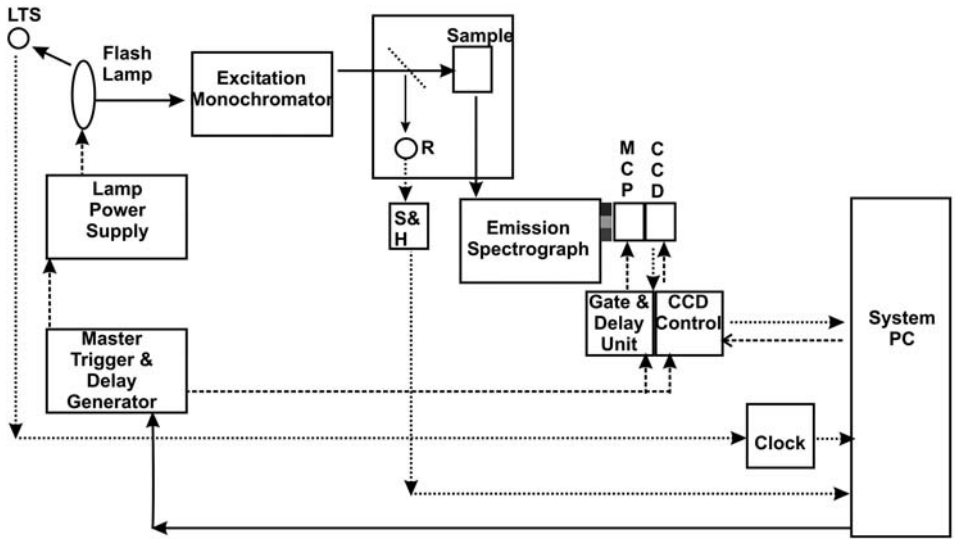

Figure 4.25 Gated, synchronized MCP-CCD lifetime system.

between the trigger and effective lamp pulse, captured by the lamp trigger sensor LTS, may also be read by the PC data, allowing for accurate time-delay calculation of each data set.

After all of that is done, the PC will either order the next flash, or (probably better) the lamp may be in free-run mode. If free-run mode is chosen, the rep rate must be calculated such that all procedures are done before the next flash starts. As in a boxcar setup, the timing can be programmed such that the measurement window is shifted after each pulse, and a full 3D curve is presented after the appropriate number of pulses. A realistic rep rate for that mode is <100 Hz, leading to rather-long acquisition times. Therefore, the pulse integration mode might be better. It has the ability to accumulate signals at the CCD before read-out. A pre-set number of gated signals is then added at the CCD and later read at once, which will allow pulse bursts of up to 10 kHz before one readout takes place. To keep the light source in a quasi-static mode, the flashes will occur even during read-out, but the MCP gate is suppressed to avoid the addition of obscure signals. In this mode, the full curve will only appear toward the end of the experiment. The decay time of the MCP phosphor is also critical because the afterglow must have disappeared before the MCP opens for the next exposure.

The limiting parameters are the MCP gatewidth, the system jitter, the rep rate, and the phosphor decay. Currently available standard gating technology allows variable gating from <2 ns up to milliseconds, which is obviously not fast enough for short lifetimes. Therefore, gate techniques have been developed that allow one more fixed gatewidth of typically 300 ps, whereas the variable range above 2 ns is still available. Converted to lifetime, a gated MCP-CCD is useful for 3 ns and longer. The jitter of each unit involved should be kept <50 ps and the total system jitter <100 ps. Due to the gating electronics, the maximum repetition rate in burst mode is 1–10 kHz, which may not be reached by pulsed lamps but by LEDs and lasers. Channel grouping and pre-defined regions of interest (ROIs) in the detector read-out pattern may increase the SNR and quicken the rep rate. In data reduction, each of the data channels needs "personal" data reduction. In summary, a gated MCP-CCD spectrometer will be slower than a single-channel system (boxcar, TCSPC), but it collects many wavelengths in parallel.

4.2.3.2 Modulated MCP/CCD analysis

Combining phase/modulation technology with parallel detection adds another dimension. A commercially modulated MCP-CCD detection system is available at the time of this book's publication, but (to the knowledge of the author) there is no complete fluorescence lifetime system that utilizes this particular technique. However, the required technology is available, and several researchers use it. The phase/mod-MCP-CCD detection combines the application of heterodyned excitation and synchronized detection, as described earlier. Imagine a multiwavelength detector instead of the PMT,

incorporating a low-frequency modulated MCP. The low-frequency modulation is much less critical than fast gating because the gate control voltage is not switched but modulated by the LF. During an LF cycle it is never turned off—signals linear to the light intensity can always pass. The most-critical points are the array or CCD read-out and the decay time of the MCP phosphor. In order to detect fine phase shifts, the read-out time must be <1% of the low frequency. If the LF is 10 Hz (100 ms), the read-out must be 1 ms or even faster to reconstruct the full curve. A detector with 512 pixels in the wavelength axis and a 1-MHz read-out frequency (0.512 ms/read) is compatible with that requirement. In reality, it would be even faster because it is not normal to read each channel separately. Predefined ROIs and channel grouping are standard, speeding up the read-out and improving the SNR. An MCP with a fast decay phosphor (at the expense of efficiency) will decay within 100 μs. The system will scan the readout time over the 100 ms of a single cycle because each wavelength (or pixel group) may present different phase and modulation information. The result is a beat frequency that can be reduced to phase. For each spectral channel, a maximum signal at optimum phase Φ, which represents the modulation *m*, will be attained. This behavior is very interesting because the MCP gate does not need to be able to resolve the lifetime—it must be able to resolve small differences, which is not a practical problem. At high test frequencies (e.g., 100 MHz), the number of excited photons is rather small. Not many MCPs with fast decay can provide the SNR and linearity required for the small changes that occur during a single cycle of the beat frequency. The dynamic linearity of the MCP is important, as is the phosphor decay. One complete analysis at one single-modulation frequency may produce 360 spectra. If the system takes 100 averages per test frequency, it may require 36 seconds for one of the pre-programmed frequencies. The reference and sample each require a collection, so the total time is not shorter than that of the single-wavelength data collection, but it presents the complete emission spectrum. This method is very useful in cases where the luminescence produces complex lifetime results over time and wavelength. It goes without saying that the required data crunching is enormous: one frequency may produce more than 10,000 data points, and several of those packets are required to find the different lifetimes.

4.2.4 Pulsed excitation and streak camera detection

A streak/framing camera (see Section 5.9.3 of *Fundamentals*[1]) is probably the fastest detector for lifetime analysis. Such a system may look like that shown in Fig. 4.26.

4.2.4.1 Description of a streak camera lifetime system

A laser, probably a semiconductor, emits a single pulse. The optical signal is split into a main beam and refocused into a fiber optic cable, while a small

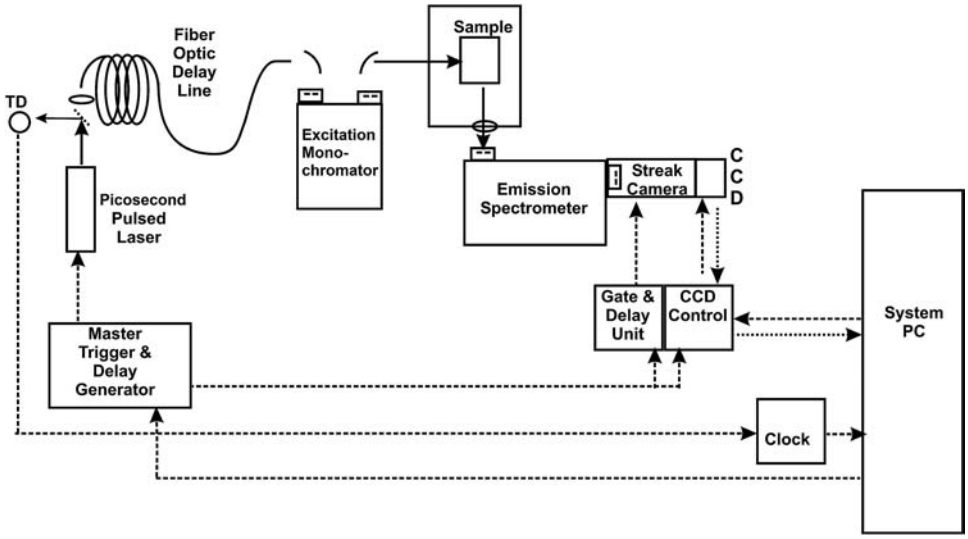

Figure 4.26 Block diagram of a streak-camera luminescence lifetime spectrometer.

portion hits a nearby fast trigger diode (TD). The TD signal will travel as short a distance as possible to start the streak camera/CCD controller and leave a time stamp in the system PC. The time between the optical emission of the laser and the beginning sweep of the camera may be on the order of 50 ns. A jitter similar to the resolution of the streak camera, or even shorter, is very important. In air, light will travel ~15 m in 50 ns. The travel time of the main part of excitation light through fiber optics, the optional excitation monochromator to the sample, plus the delay created by the sample and the travel time of emission light to the cathode of the streak camera, will require a slightly longer interval than the trigger signal, which is required for programmed delay times. Assuming two 0.3-m spectrometers and an additional 50 cm around the chamber, the light path may result in 5 m in air, or roughly 16 ns. If the refractive index of the fiber cable is 1.5, a length of 8 m will add 40 ns, resulting in a total of 56 ns before any experimental light can reach the streak camera. That assumption is valid if a direct reflector is in the sample position, which is a reasonable basis for starting the evaluation of the system. If the emission spectrometer is a monochromator, the camera will record the intensity at one wavelength over time.

However, according to Fig. 4.27, if a spectrograph is used, the "vertical" axis of the camera will represent a spread of wavelengths, depending on the dispersion of the spectrograph and the illuminated height of the cathode, while the "horizontal" axis provides the time, and the saturation ratio represents the fluorescence intensity over wavelengths (vertical) and time (horizontal). Because the fastest streak cameras can resolve <1 ps, the system is not only extremely fast, it is also 2D. Because the spread of laser pulses is often >1 ps, deconvolution may be required, which, in turn, calls for a

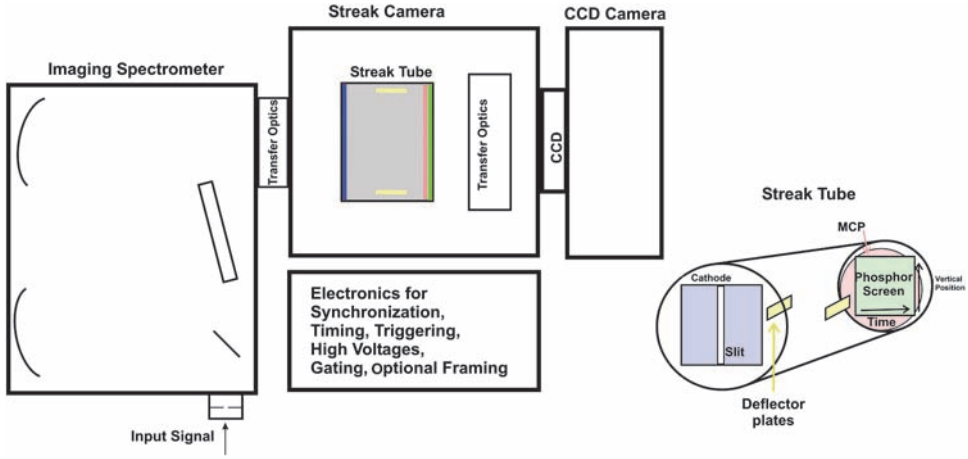

Figure 4.27 A spectroscopic streak and framing camera.

precisely repeatable shape of the laser pulse, recorded with the help of a mirror and stored for later data reduction. Femtosecond-wide laser pulses with a very narrow spectral bandwidth are produced by cw lasers, followed by a Kerr or Pockels cell, which can "open" for extremely short periods of time. The single pulse is necessary because the CCD or CMOS camera, reading out the streak system in 2D mode, will need at least a few milliseconds after each excitation. That calls for a streak instead of a framing camera. The resolution of a streak camera is typically 1% of the sweep time, which can be programmed from ~100 ps to 1 μs. That range fits well the lifetime of the analyzed fluorophores. Some streak camera providers offer interchangeable time base electronics, which allow sweep times into the millisecond range (bridging the gap to phosphorescence measurements) and the switch from streak to framing applications.

References

1. W. Neumann, *Fundamentals of Dispersive Optical Spectroscopy Systems*, SPIE Press, Bellingham, WA (2014) [doi: 10.1117/3.1002528].
2. J. R. Lakowicz, *Principles of Fluorescence Spectroscopy*, Plenum Press, New York (1983).
3. P. Milonni and J. Eberly, *Lasers*, John Wiley and Sons, New York (1988).

Chapter 5
Radiometry

5.0 Introduction

Spectroscopic radiometry is divided into two groups:

- the spectral and quantitative measurement (analysis) of light sources, which can be further divided into two principles:
  - the measurement of rays in all directions and under all angles, and
  - the measurement of rays traveling into a defined direction and under defined angles;
- and the illumination of a sample by light of a known wavelength, known bandwidth, and known intensity (also called light flux), and the detection of the sample's response.

In principle, the radiometric methods are very closely connected to the illumination techniques described in Section 6.2 of *Fundamentals*.[1] The definitions directly applied in radiometric applications are summarized in Section 5.1 of this book. Other books offer an online introduction[2] and a substantial educational reference[3] on radiometry.

The only optical unit in the SI system is the light power (light flux) at one selected wavelength. The unit is the candela (Cd), its symbol is j_V, and its dimension is J:

$$1\,\mathrm{Cd} = 1.464\,[10^{-3}\,\mathrm{W/sr}]\,\mathrm{at}\,540\,\times 10^{12}\,\mathrm{Hz}. \tag{5.1}$$

One Cd is the light power traveling from a source in a certain direction with a monochromatic frequency of 540×10^{12} Hz (which is almost exactly 555 nm) and a directed light power of 1/683 W (1.464 mW) per steradian. Unfortunately, it is the only unit and dimension available for spectroscopy because all other units in the (extended) SI system are photometric values and dimensions that have weighting factors implemented to fit the human eye. Because the bandwidth at the reference frequency is not specified, it is hard to use the SI unit in spectroscopic applications.

The data taken by a spectroscopy system, with all of the different variables and parameters, require lots of calculations if introduced in reliable,

convertible, and spectral radiometric units. The experiments require a high degree of care, reproducibility, reliability, and accuracy. They further call for statistics, comparisons, and frequent calibrations to provide "correct" values. If the radiance at 555 nm from a light source is known, only a single data point is available for reference. A spectral light source for wideband applications must be specified at many pairs of wavelength and light power to control and interpolate radiometric measurements. By old standards, the spectral data are provided with a bandwidth of 5 nm and steps of 5 nm. Actual standards call for 1 nm in both parameters. It is also necessary to define the accuracy and reproducibility of the data measured, which will allow one to check the SNR and variance at any data point.

5.1 Radiometric Parameters

The spectral radiant energy is the optical energy (work) of a source (Fig. 5.1). The symbol is $Q_{(\delta\lambda)}$ or $Q_{e(\delta\lambda)}$, and the unit is J/nm, equal to Ws/nm. If the time parameter is reduced from the optical energy, the optical power remains, leaving one to deal with the (spectral) radiant power (also called radiant flux), which has the symbol $\Phi_{(\delta\lambda)}$ or $\Phi_{e(\delta\lambda)}$ [W/nm]. Both parameters define a source without accounting for the area of origin. If the power (flux) is related to the area of its origin, it is called radiant exitance or radiant emittance:

$$M_{e(\delta\lambda)} = \Phi_{e(\delta\lambda)}/(\mathrm{m}^2 \times \mathrm{nm})[\mathrm{W}/(\mathrm{m}^2 \times \mathrm{nm})]. \tag{5.2}$$

The inversion is the relation of radiant power to the illuminated area, which is a passive, illuminated area; it is called the spectral irradiance, and the equations are basically the same:

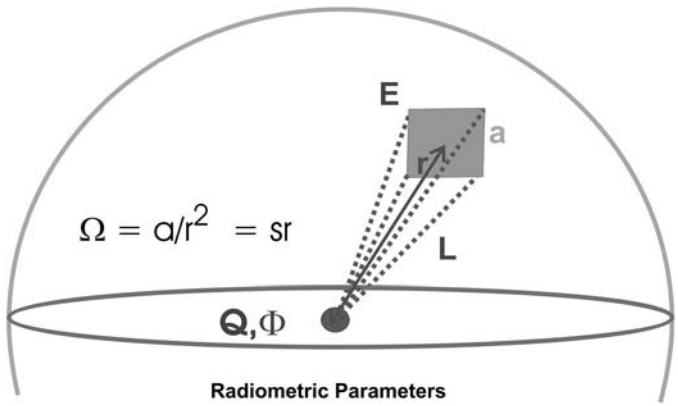

Figure 5.1 Radiometric nomenclature and parameters.

$$E_{e(\lambda)} = \Phi_{e(\delta\lambda)}/(\mathrm{m}^2 \times \mathrm{nm})\,[\mathrm{W}/(\mathrm{m}^2 \times \mathrm{nm})]. \tag{5.3}$$

The SI system does not cover angles in degrees or angular functions. The normalized angle Ω is entered to include the angle of emission from the source. Note that the effective aperture of spectrometers (see Section 2.6.2 in *Fundamentals*[1]) is the counterpart. Ω is equally valid for reception and transfer as for the emission in a spherical shape. Ω accounts for the fact that that the density of light diminishes by the square of the distance to the source:

$$\Omega = a/r^2. \tag{5.4}$$

Ω is often called in the literature the "light guiding factor," and the calculations are identical to its counterpart on the spectrometer side $\Omega = A_g/f^2$ [Eq. (2.15) in Section 2.6.2 of *Fundamentals*[1]].

The expression steradian (sr) combines space and radiation. If a geometric area a of 1 m^2 is illuminated from a spot source at a 1-m distance r, the result is 1 sr. An entire sphere consists of the wall area of $4\pi r^2$. At a 1-m radius or 2-m diameter, the area is 12.567 m^2, which also represents 12.567 sr. With a light source with homogenous spatial radiation in a sphere, the radiation will be equally distributed everywhere in space, but it only becomes apparent at the wall. If the radius increases by two, the wall area will increase by four, leading to a light density of 1/4 per area unit. Thus, Ω is an excellent tool for normalized calculations. The normalized (spectral) light density is called radiance, expressed by

$$L_{e(\delta\lambda)} = \Phi_{e(\delta\lambda)}/(\mathrm{sr} \times \mathrm{nm})[\mathrm{W}/\mathrm{nm}]. \tag{5.5}$$

The density or radiance of radiation traveling fan-shaped into space is constant if Ω is constant.

Parameters, including W/m^2, are not very handy for spectroscopy; smaller dimensions are more useful. The reduction of dimensions to $\mu\mathrm{W}/\mathrm{mm}^2$ will produce the same numbers but can be better applied. The $\mathrm{mW}/\mathrm{cm}^2$ version used here and in the literature uses numbers of a factor of 1/10. The radiance or spectral density is given by

$$L = (\Phi \times \Omega)/(A \times \delta\lambda)[\mu\mathrm{W}/(\mathrm{sr} \times \mathrm{mm}^2 \times \mathrm{nm})], \tag{5.6}$$

where L is the spectral density of light or radiance, Φ is the light flux or radiant power of the source (in W, mW, or μW), Ω is the normalized light guiding factor of the radiator, A is the illuminated or emitting area (in m^2, cm^2, or mm^2), and $\delta\lambda$ is the wavelength interval involved (in nm).

5.1.1 Definition and measurement of the spectral radiant power

The terms "spectral radiant power" and "radiant flux" both describe the total power released by a source at a defined wavelength interval in terms of either energy or power. The optical energy (radiant energy) has the symbol $Q_{(\lambda)}$ or $Q_{e(\lambda)}$, and the unit is J/nm = Ws/nm. The spectral radiant power (radiant flux) has the symbol $\Phi_{(\lambda)}$ or $\Phi_{e(\lambda)}$, and the unit is W/nm.

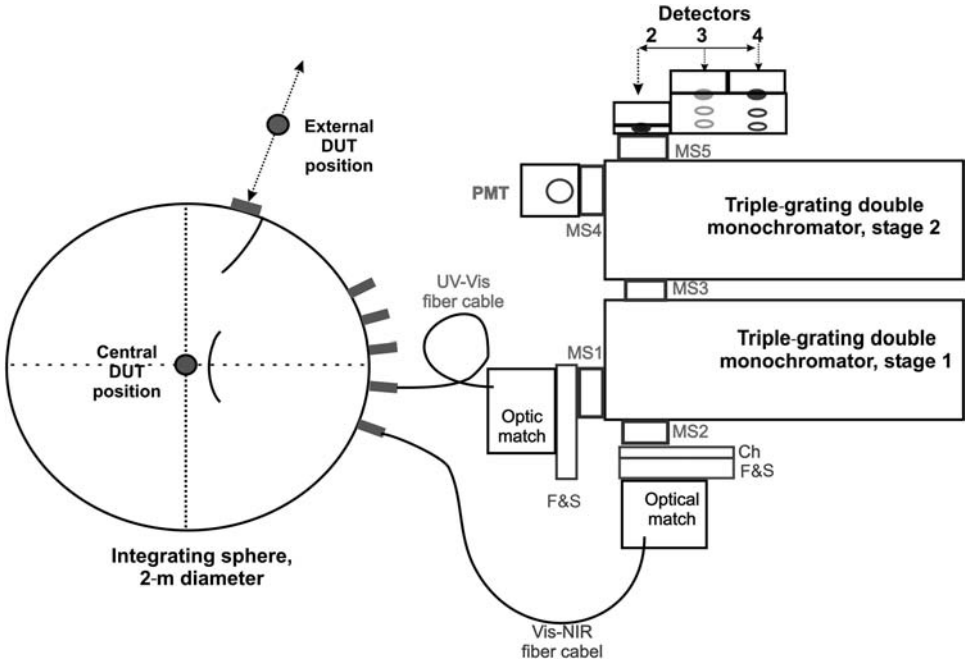

Figure 5.2 Reference system for the measurement of the spectral radiant flux. The sphere is shown from the top. SD: solid state detector; MS: motorized slit; PMT: photomultiplier; F&S: filter and shutter; and Ch: chopper.

To collect the total radiation from ball-shaped sources, it is essential to collect and integrate all radiation in the space around the origin. To ensure that all directions and angles are treated identically, the space must be spherical. The size of the sphere will be found by the relations described in Section 5.1.1.1. To collect white light from sources of up to 2 kW, the sphere will have >1 m Ø. A 2-m sphere, which is here considered to be the reference, typically works with lamps between 0.1 and 2 kW radiant power. It is advantageous if the sphere can analyze the radiance. The reference system in Fig. 5.2 is extended by the option to measure the irradiance and the radiance in addition to the spectral radiant power.

5.1.1.1 The sphere

The specifics of integrating spheres are discussed in Section 6.4 of *Fundamentals*.[1] The considered sphere features a diameter of 2 m, which has an inner surface of 12.567 m^2. The light source is placed in the center of the sphere. The sphere itself is best fixed when hanging from a ceiling or carriage. The sphere consists of two half balls, one of which can be moved horizontally. The test object is mounted to a pipe (vertical dotted line) that also contains the supply cables. On the fixed side is an optical shield that prohibits the direct illumination of the receiver positions (five grey joints). All access avenues are detachable. If the modes of irradiance and radiance are to

be added to the flux measurement, a special aperture (on the periphery) can be added. All avenues are placed at the equator rather close together to keep the shield small. Because the complete characterization and monitoring of a radiant object needs several sensors, five joints are prepared, plus one for irradiance and radiance measurements. The typical diameter of the joints is 25 mm. All access avenues are equipped with 28-mm threads to allow mounting of different components. Unused apertures are tightened by threaded caps, which are coated by the same material as the sphere itself. Each access has an area of 8.8 cm^2; together they sum to 44 cm^2. If the aperture for radiance measurement is 50 cm Ø, then 1963 cm^2 are added, which is also capped if not used. In total, the theoretical maximum deprivation of the reflective area will be 2006 cm^2, or 1.6×10^{-2} (1.6%). The collision plate (curved near the external entrance) is only mounted if the sphere is externally illuminated. It ensures that more than one reflection is required to reach a sensor, it will be removed when internal sources are used, and it is coated with the sphere´s material. In "normal" flux applications, the area losses will only be 7×10^{-4}. Because a strong source will introduce some heat to the sphere, an exhaust for the warm air and probably ozone should be provided by a laminar flow through the ball. Near the poles, a hole and fans will serve that purpose. Coated caps will be placed near the holes and will have almost no impact on the functions of the sphere (not shown in the figure).

With an integrating sphere like that, all kinds of radiators can be analyzed, including blackbodies. The coating of the inner wall is selected for the planned wavelength ranges. If the measurement of strong lasers is also planned, an additional collision plate may be required, one specially adapted to the beam shape and intensity of the measured lasers.

5.1.1.2 Spectrometer

The spectrometer used should be a double monochromator with a 500-mm focal length, an aperture of *f*/6–*f*/8, and three gratings installed. In the following examples, a grating surface of 70^2 mm^2 is used, leading to $\Omega = 0.0196$ (rounded to 0.02 in further calculations). All slits are motorized and set per program. They have an accuracy of 1 μm or better and open up to 5 mm. The used slit height is primarily defined by the detector connected and can reach up to 10 mm. One entrance is used for each of the two fiber cables; two exits serve the detectors. The dispersion will allow at least a 5-nm bandwidth. An additive 500-mm double monochromator with gratings of 600^{-1} will perform a dispersion of ~1.6 nm/mm at 200 nm, 1.55 nm/mm at 600 nm, 1.5 nm/mm at 1200 nm, 1.25 nm/mm at 2000 nm; and 0.95 nm/mm at 2600 nm. The resolution (for the measurement of spectral features) will be found between 30 and 50 pm. The geometric width for a bandwidth of 1 nm will be between 625 μm in the UV and 1.05 at the upper end, providing a reproducibility and accuracy better than 1%. It is a limiting factor that above

2500 nm, where the dispersion is 1 nm/mm, a 5-nm bandwidth will not be possible. If required, a linear calculation can replace the true measurement.

A typical PMT will provide an active area that is larger than the exit slit. The Si detector will be 10 mm Ø, but InGaAs elements are hardly available larger than 5 mm Ø. All in all, the slit height will be 10 mm. The monochromator will produce a vertical distortion (stretch) of ~2 mm. Thus, the Si detector will be slightly over-illuminated, whereas for the two InGaAs detectors, an intermediate optical fit by transfer lenses is proposed. The fiber cables have an emitting area of 5 mm × 10 mm on the spectrometer side. The exit of the fiber cables will be reproduced in the plane of the slit with the correct angle for the spectrometer. In alignment with the detectors, the UV grating will be blazed to 250 nm in the first order, the one for the Vis range will have a first-order blaze at 600 nm, and the NIR grating is selected with a blaze of 1600 nm. The switching points will be best at 450 and 1200 nm. At first glance, the choice may not seem the best, but after locking up the detector efficiency curves and correlating them with the gratings, it appears that at no point will the range of the total system signal vary more than a factor of 2.5. Further calculations will be done with a slit size of 10 mm × 0.7 mm.

5.1.1.3 Detectors

Detectors and the number of spectrometer exits depend on the wavelength span. Because it is planned to start at 190 nm, a PMT (mounted to MS4) seems best. To acquire data between 750 nm and 1650 nm, an InGaAs-1700 is the first choice. Above that, and up to 2600 nm, a second InGaAs is suggested because InGaAs-1700 is available with 5 mm Ø, but InGaAs-2600 is limited to 3 mm Ø, which results in an area factor of 2.7. Over a wide range, the InGaAs-2600 only has ~30% of the InGaAs-1700 detectivity, which already makes a factor of 5–10. Furthermore, the InGaAs-1700 has a far better D* than the InGaAs-2600 (see Section 5.6 of *Fundamentals*[1]). To protect the PMT from damage and spread the spectral range, a UV–Si detector is also suggested to run applications with a strong signal emission. Because monochromators with three or four exit slits are not standard, the three solid state detectors are placed in a housing that is light, tight, and mobile (mounted to MS5). The detectors sit on a rail that is positioned by a stepper motor and program. All three are Peltier cooled to −70 °C, while the PMT Peltier will cool to −25 °C. Cooling all detectors is doubly advantageous: it provides improved reproducibility in addition to the reduced background.

5.1.1.4 Coupling

Coupling between the sphere and spectrometer is caused by fiber optic cables for two reasons. For direct, optical coupling, the entire spectrometer system must follow the motions of the sphere, and access to the sphere's avenues would be very limited. Two types of fiber guides are used: the quartz type transmits between 190 and 1100 nm, and the glass type between 400 and

2600 nm. The fiber cables are installed and fixed in a way that avoids more motion than absolutely required. In the sense of optical benches, the fibers will be treated like any other component (Section 6.7.4 of *Fundamentals*[1]) to enable stable transfer. In the plane of the spectrometer slit, they will be re-imaged in an effective area of 5 mm × 10 mm. Due to the magnification of the transfer optics, the end of the fiber cables will be smaller. Because of the optical gain of a factor of 2 by the entrance optics, the geometrical size will be 3 mm × 6 mm. That area of 18 mm^2 is converted into a disk shape of 4.8 mm Ø at the sphere end of the fiber cables. Both fiber guide materials provide an acceptance and emission angle of 30 deg. With that angle, the fibers recover light from a spherical wall segment of 1.07 m Ø, or 0.9 m^2, which represents $\Omega = 0.225$. The UV cable covers the full working ranges of both the PMT and Si detector. A set of mirrors (optical match) transfers the light to the entrance slit (MS1) through a filter wheel, incorporating two order-sorting filters (F&S, Fi1 = 320 nm, Fi2 = 570 nm). The wheel also has a beam stop for background measurements. The Vis–NIR fiber cable is used between 700 and 2600 nm, and is re-imaged through a gold-coated optical set (optic match at MS2). There is also a filter wheel (F&S) with three filters (Fi3 = 620 nm, Fi4 = 1100 nm, Fi5 = 1800 nm) and a beam stop. An additional optical chopper is placed in that path. The light modulation will separate the thermal and spectral signals and greatly improve the dynamic ratio and stability of the NIR measurement. When the chopper is out of operation, it stops in an open position to enable measurements without modulation. All solid state detectors are able to work in DC or AC mode through a lock-in amplifier. The photocurrent of the PMT will only be detected in DC mode; it will not be affected by thermal signals. The total transmission of the transfer and coupling system is assumed to be 60%.

The intensities in Fig. 5.3(a) are drawn in a logarithmic fashion. The dotted line shows the radiant flux Φ of a 1-kW quartz-tungsten-halogen (QTH) lamp in mW/nm. The lamp operates in the center of a 2-m sphere, and the coating is PTFE-S [from Fig. 5.3(b)]. The sphere has four exits, each with a 25-mm diameter. The dashed curve is the irradiance E in the exits in $\mu W/(cm^2 \times nm)$. The efficiency of the most-popular coating materials are shown in Fig. 5.3(b). In the sample calculations, the PTFE "S" and Gold are applied.

Figure 5.4 adds the parameters within and after the sphere, also in a logarithmic fashion. The black dashed curve is the radiant flux Φ after the spectrometer entrance slit, in μW/nm. The transfer efficiency between the sphere and spectrometer entrance is simplified to constantly be 0.6. The solid grey curve represents the efficiency of the spectrometer, which is found to be between 0.1 and 0.35. All gratings will be 600 mm^{-1} and provide a dispersion of ~1.4 nm/mm, which leads to the assumption of a constant slitwidth of 0.7 mm to achieve a bandwidth of 1 nm. The gratings are changed at 500 and 1200 nm. The dashed-dotted grey curve illustrates the

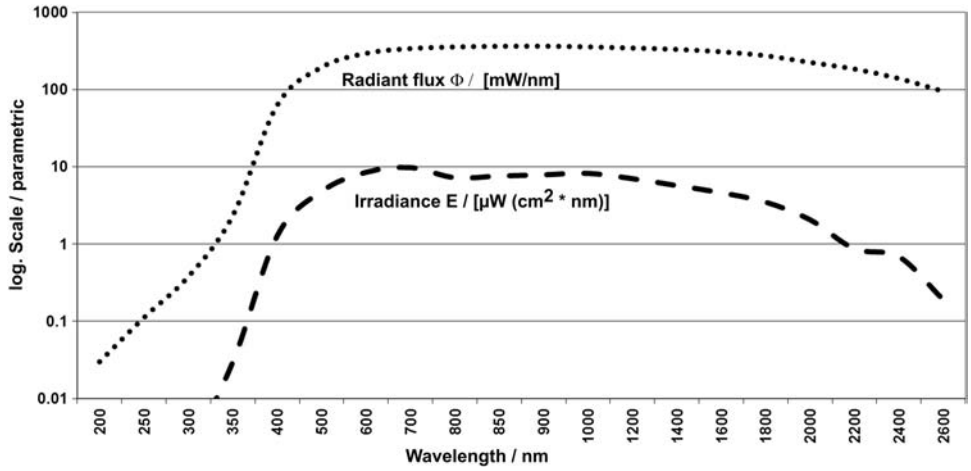

Figure 5.3(a) Radiant intensities in the sphere.

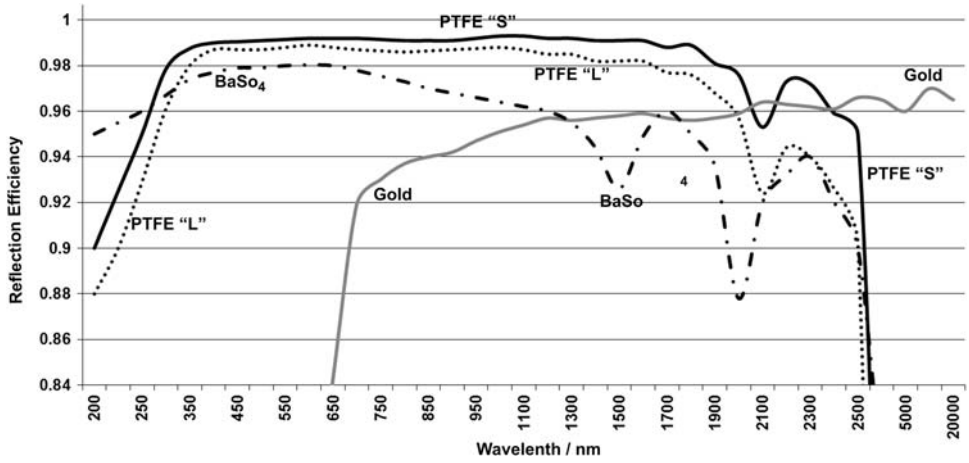

Figure 5.3(b) Typical efficiency behavior of sphere-coating materials.

radiant power Φ (flux) reaching the detector, now in nW/nm. To avoid more-complex curves and calculations, only two of the four detectors are used in the sample calculations: the PMT up to 800 nm, and the InGaAs-2600 for all the range above 800 nm. The change-over between the two creates the sharp drop in the two remaining curves. The output current of the detectors is the dotted back curve, presented in nA/nm. In addition to the efficiency, the curve takes care of the smaller size of the NIR detector element, which is only 3 mm high, while the PMT recovers the full height of 10 mm. Finally, the solid black curve represents the final SNR of the system. The estimated SNR values are found by multiplying the numbers of the scale by a factor of 10^6. Thus, the SNR can be expected to vary between 10^2 and 10^7.

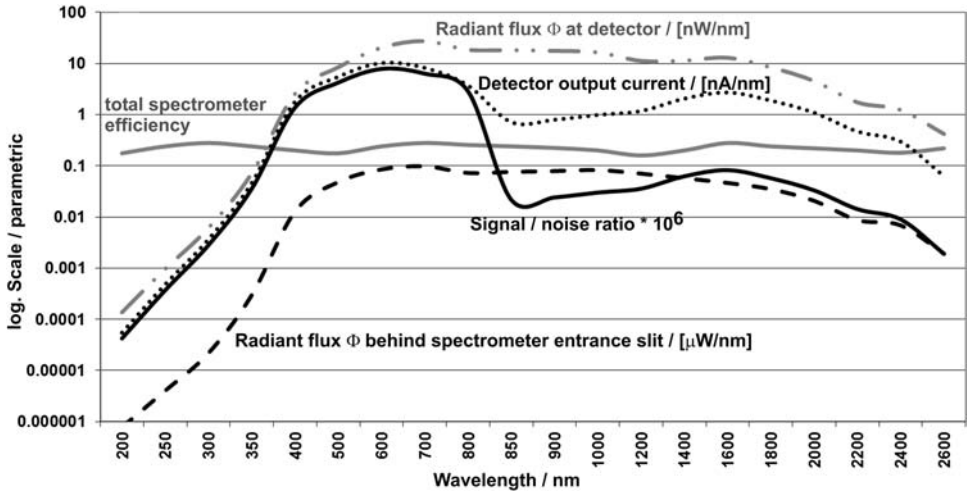

Figure 5.4 Spectrometer and detector signals.

5.1.1.5 Data collection, interpretation, and processing, exemplary for a radiant flux measurement

All functions of the spectrometer system, the filters, and detection should be attachable via program and automated. The data acquisition program will take care of all relevant parameters to ensure the best possible reproducibility. The acquired data will be in open ASCII; the real-time acquisition of other parameters and measurement data is essential for online control and monitoring of radiometric experiments. If the test object is placed inside the sphere, the obtained data represent the spectral radiant flux Φ, also called the spectral radiant power; in the provided example, it is 468 mW/nm at 700 nm. The data collected on the measured source are stored as the "system response" SR. The final data are the product of many parameters, whereas the radiant flux of the device under test only involves one. In the sample calculation, the sphere has 2 m $\varnothing$, and the entrance of the fiber cable has 3 mm $\varnothing$ (7 mm^2). This is the effective area and includes the correction factor for the transfer optics and used slit area. With the help of Eqs. (5.3)–(5.5), the irradiance at the fiber cable entrance is found to be $\Phi \times 2.06 \times 10^{-6}$ W/mm^2, providing an E of up to 0.96 μW/(mm^2 $\times$ nm). Because the light-guiding factor of the cable is $\omega = 0.225$ and the area of the cable is 18 mm^2, the light flux $E = \Phi \times 2.06 \times 10^{-6} \times 7 \times 0.225 = 3.9$ μW per nm, traveling into the fiber cables. The transfer efficiency between the sphere and spectrometer is simplified to be 0.6. The light-guiding factor at the spectrometer entrance is Ω = 0.02. Thus, behind the entrance slit (which also has 7 mm^2), there is 1.518 μW/nm $\times$ 0.0266 / 0.225 = 0.179 μW/nm. The total efficiency from the sphere to the spectrometer is in the range of (nW $\times$ nm) / (W $\times$ nm). With the efficiencies of the spectrometer and detector, a measured value of 11.33 nA/nm is created at 700 nm. If the bandwidth were increased, for example,

from 1 nm to 5 nm, the output signal would increase by a factor of 25. The background and noise will be in the femtowatt range. At 700 nm, the SNR is expected to be $\sim 8.7 \times 10^6$. The system limitation would become evident if weak light sources, such as 10-W lamps or small LEDs, do not provide enough photons/bandwidth for reasonable results. The scenario where the source is placed outside the sphere, which brings substantially weaker flux into the sphere, will be considered next.

It is a general rule in spectral radiometry to fix all system settings between measurements or to have failsafe algorithms for further calculations. The bandwidth of a spectrometer changes over wavelength if the slitwidth is kept constant. To get normalized bandwidths, a program may perform an online manipulation of slitwidths, in which case the slit changes should not be left to an online program that runs during data acquisition because small variations between scans may develop. In terms of reproducibility, it will be better to use a look-up table. In most cases, it will be easiest and most satisfying to run each grating with fixed values. The flux can be calculated later by normalizing the bandwidth. The look-up table method is also suggested for any other parameter, such as integration time, PMT-HV, etc., that is subject to change during acquisition.

Now that reliable data are assured, what is required to resume "correct" data? The first requirement is to introduce and store the physically correct Φ values of a reference lamp in the data system. Each calibrated lamp is delivered with a table carrying the 1-nm step values of the radiant flux $\Phi_{e(\delta\lambda)}$ in W/nm. These data are called the "original data" (OD). The OD are entered into a spectrum that is fully compatible with the measured data. The measurement of the calibrated source is then acquired and stored as the SR, and the provided OD are divided by the SR, resulting in the "calibration data" (CD):

$$\mathrm{CD}(\Phi_{e(\delta\lambda)}\,\mathrm{in\,W/nm}) = \mathrm{OD}(\Phi_{e(\delta\lambda)}\,\mathrm{in\,W/nm})/\mathrm{SR}.$$

All of the following measurement data, called "measured data" (MD), obtained under the same parameters can be easily converted into "light source data" (LSD):

$$\mathrm{LSD}(\Phi_{e(\delta\lambda)}\,\mathrm{in\,W/nm}) = \mathrm{MD} \times \mathrm{CD}(\Phi_{e(\delta\lambda)}\,\mathrm{in\,W/nm}).$$

It is useful at this point to add an estimate of the SNR to the result, plus the reliability, variation, and error bandwidth numbers. All of these values can be collected by statistics programs, but all measurements must be run repeatedly and stored separately.

5.1.1.6 System limits

The SNR curve in Fig. 5.4 shows that the detection with a PMT produces the best results: the SNR is ~100 times better compared to the InGaAs-2600 if all data are taken with a 1-s integration time. It assumes that the PMT is read directly, but the InGaAs is read via lock-in. To ensure a standard deviation

better than 1% in the result, the SNR must always exceed 1000. In the case of the 1-kW filament lamp, that is the case above 250 nm. The SNR of the InGaAs can be improved by varying the lock-in parameters. With declining signals, it is possible to improve the gain of the PMT, whereas the lock-in offers variation of the integration time. If the curves of the source are very uniform over the wavelength, there is one more option: the bandwidth can be increased, and the data recalculated after acquisition. In the UV–Vis, the useful limits of a system as described, with the source placed inside the sphere, will require Φ values on the order of at least 0.1 mW per measured bandwidth. In the NIR (with a 1-s integration time) the Φ must be on the order of 50 mW per measured bandwidth. For comparison, consider the parameters with a weak source in the sphere. Figure 5.5 illustrates a simulation based on the data of a 20-W halogen lamp inside a 2-m sphere. Even the scale numbers are similar to Fig. 5.4: the numbers are typically weaker by a factor of 1000, resulting in an SNR in the range of 10^3–10^5.

At the same filament temperature, the average spectral output of a 20-W lamp (grey solid curve, <10 mW/nm) is 1/50 of the 1-kW lamp. Thus, only a flux of 2% arrives at the detector (dashed-dotted grey curve, displayed in nW/nm), creating a detector current in the pA range (dotted black curve). The SNR (solid black curve) now only exceeds the value of 10^3 between 300 and 800 nm, running at a bandwidth of 1 nm. 10^3 is a safe minimum SNR in radiometric applications, but the regions outside that will probably not be stable enough.

Now the radiant flux Φ in the sphere required for safe results can be estimated. In the UV range <350 nm, it will be ~200 μW per measured bandwidth; in the visible range, ~100 μW. In the range around 1200 nm, ~10 mW are required, and above 2000 nm, a Φ of at least 50 mW/bandwidth

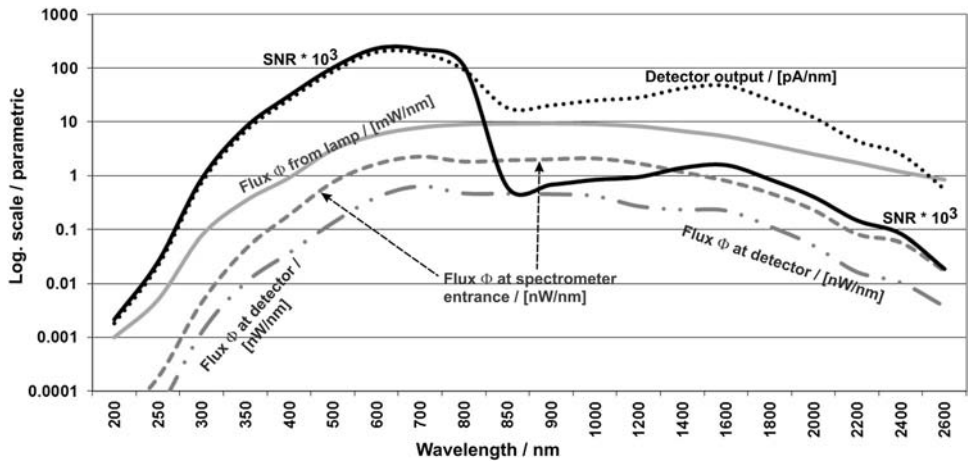

Figure 5.5(a) Functions of the reference system with a 20-W halogen lamp inside the sphere.

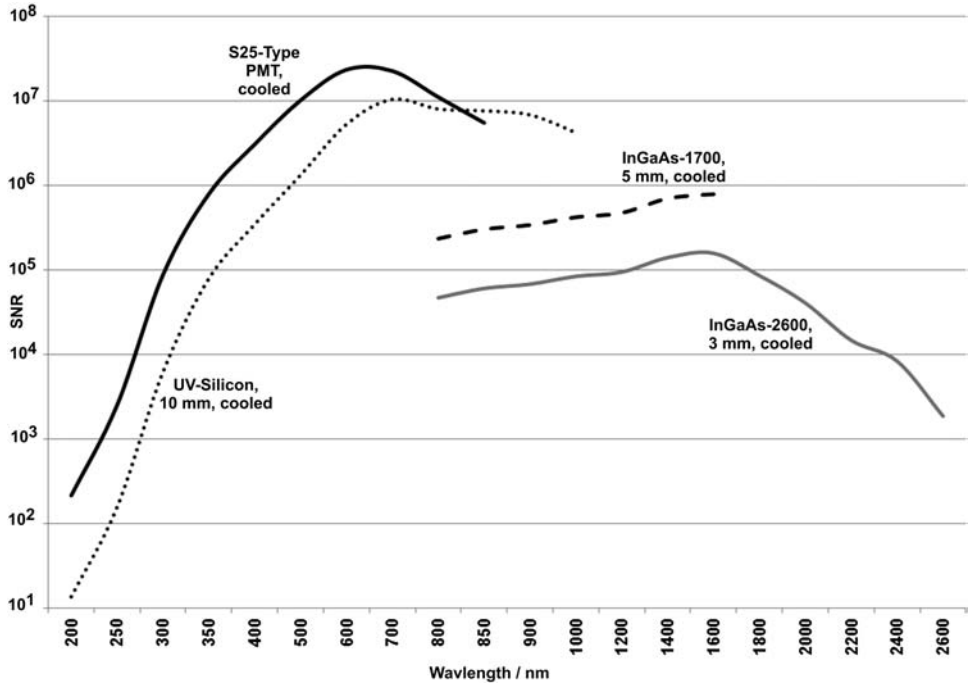

Figure 5.5(b) General comparison curves of the SNR for four detector models.

will create an SNR of at least 1000. All data presented so far are based on an integration time of 1 s. Variation of the lock-in parameters, the PMT high voltage, and the integration time will improve the SNR 300–2600 nm. Note that only two of the four detectors are considered, which means that the reality will be better than the estimation. A general comparison of the four projected detectors is presented in Fig. 5.5(b).

In the simulations of Figs. 5.4 and 5.5, only the behavior of a PMT and an InGaAs-2600 are considered. To understand the full picture, all four detectors described in the project should be justified for their typical SNR curves if detecting the radiation of a tungsten-halogen lamp. The simulation indicates that the two additional detectors improve the spectral signal reasonably above those shown earlier. The two kinds of detectors left out of the figures have been neglected in favor of keeping the figures convenient, whereas in a real system, they might be the most-used ones for the range between 300 and 1500 nm.

5.1.2 Measurement of the spectral irradiance *E* and the radiance *L*

The total spectral radiant flux, emitted by a ball-shaped source, can only be captured for spectroscopic needs by an integrating sphere; otherwise, only a segment of the radiation is seen and recovered. For that reason, the parameters $E_{(\lambda)}$ and $L_{(\lambda)}$ are very important. In both cases, the directed optical

energy or power is meant. To address the irradiation E [W/(m^2 × nm)], it is collected at a defined distance in a defined area. Thus, the irradiation of the source under test creates the resulting radiance L [W/(sr × nm)], which is measured. Both expressions are linked by the equations used and the light guiding factor Ω.

Unfortunately, the industry data sheets do not present stringent data. Besides the definition of the radiance L, there may also be the specification of the irradiance E, completed with the specification for area a and distance r, which lead to Ω. The exchange of values is given by the steradian sr. To make it a bit more complicated, the area varies from 1 mm^2, via 1 cm^2 up to 1 m^2, while the distance varies between 10, 50, 70, and 100 cm. If a sphere is designed especially for the measurement of E and L, one deciding parameter is the entrance area a, which leads to the required inner surface and diameter. Let us consider $\Omega = 1$, created by $a = 1$ m^2 at a 1-m distance; it requires either an entrance aperture of 1 m × 1 m (1.128 m ∅), which leads to a sphere with at least a 30-m^2 inner surface, or 3.5 m ∅. In the large standardization laboratories (PTB, NIST, and others), even spheres with a diameter of 5 m are in use. The sphere discussed here offers the use of a 50-cm aperture. If $\Omega = 1$ is achieved at a diameter of 0.5 m ($a = 0.1963$ m^2) Ω, the distance will need to be 20 cm, which is not a common specification. Thus, the parameters $a = 0.2$ m^2, $r = 0.5$ m, and $\Omega = 0.8$ are used. The 1-kW lamp in this example emits ~550 mW/nm within 12.567 sr at 555 nm. According to Eq. 5.6, $L = (\Phi \times \Omega) / (a \times \delta\lambda)$ in the dimension [mW/(sr × m^2 × nm)], a maximum of 35 mW/nm will enter the sphere, which is sufficient for good measurements. Now consider more-interesting dimensions $a = 1$ cm^2, $r = 50$ cm, and $\Omega = 4 \times 10^{-4}$. The entrance aperture now has 1.128 cm ∅. The 1-kW lamp will only send up to 227 μW/nm (at 850 nm) into the sphere, which is tight for good results with a bandwidth of 1 nm. Last, there is the design to measure E and L with an entrance of up to 50 mm ∅. The rest of the equipment will stay the same as before with one exception: in order to reduce transfer losses, and because the sphere will be much smaller and lighter, the sphere will be directly mounted onto the spectrometer entrance slit.

Defining the irradiance E with the dimensions $a = 1$ cm^2 and $r = 50$ cm has the advantage of using the sphere for other radiators that do not emit in a ball shape, such as diodes or fibers. Furthermore, it can be used to illuminate filter/detector combinations without a spectrometer. It should be kept in mind that fixed systems like that require constant geometric settings throughout a series of calibrations and measurements. An integrating sphere will cause a perfectly homogeneous diffuse light to exit. Conversion calculations to find the flux at different areas will not produce errors.

5.1.2.1 Fixed mounting of a sphere and spectrometer

The spectral configuration in Fig. 5.6 may be similar to Fig. 5.2. The distance between the sphere and slit must be adjusted so that the illumination cone

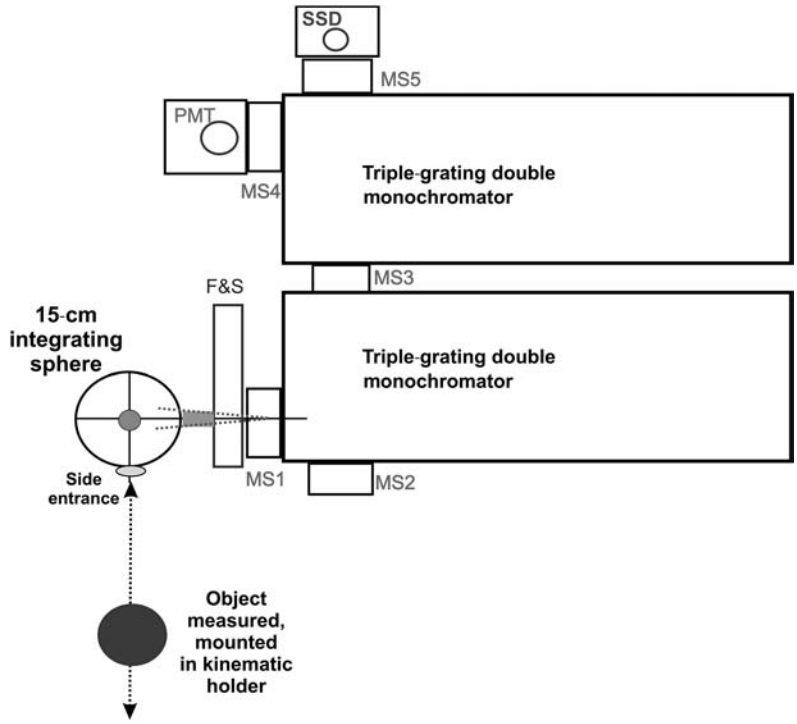

Figure 5.6 Spectrometer with the sphere directly connected. SD: solid state detector, MS: motorized slit, PMT: photomultiplier tube, and F&S: filter and shutter.

agrees with Ω of the spectrometer. The grey tube shown in the graph takes care of the correct Ω. If a chopper is required, it may be combined with the tube. The sample position (dark grey) is movable. It is useful to move the source in all directions and rotate it in order to investigate all kinds of emission patterns. The sphere's entrance should be equipped with a thread to fix different apertures with various shape and area. If required, additional apertures, filters, etc., can be placed between the test device and sphere. At the north pole of the sphere, an exit is provided to allow the measurement of the integrated radiation.

5.1.2.2 Definition of a sphere to work with a pre-defined Ω or steradian

The sphere in Fig. 5.6, described for irradiance and radiance (besides the variable 50 mm Ø aperture), has at least two more connectors with 10 mm Ø—one connects to the spectrometer, and the other to a reference detector—to monitor the integral signal. In the given example, the sum of all apertures is 21.2 cm^2. To keep that parameter within 3% of the total, the inner surface must be 700 cm^2, which results in 15 cm Ø. Geometrically, that number fits the spectrometer well. The entrance aperture's inner surface, or the caps, will carry the appropriate coating. For the application described here, it will have 11.28 mm Ø, or 1 cm^2.

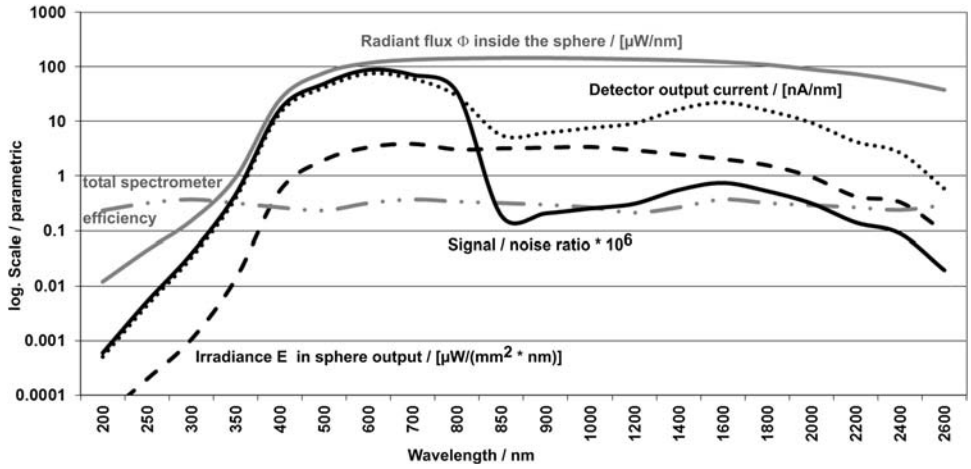

Figure 5.7 Signals introduced by an external 1-kW QTH lamp.

Thus, the sum of open apertures will only be 2.57 cm^2, which is <1% of the inner surface. In the example based on a 1-kW lamp, a maximum of 227 µW/nm will enter the sphere and lead to the data shown in Fig. 5.7.

Simulation of the relations of the system introduced in Fig. 5.6 are based on a 15-cm sphere to acquire the E and L data, calculated for $\Omega = 0.0004$ illumination. The detectors are again a PMT and InGaAs-2600.

5.1.2.3 Interpretation

A maximum light flux of 227 µW/nm enters the sphere (solid grey curve). In the output of the sphere, the irradiation E (dashed black curve) of a maximum 5 µW/(mm^2 × nm) is evident. With a slit area of 7 mm^2 and spectrometer efficiency (grey dashed-dotted curve) between 0.2 and 0.35, the detectors generate a current of up to 85 nA/nm (dotted curve). The SNR (solid black curve) exceeds the value of 1000 at all wavelengths above 250 nm.

5.1.2.4 Acquisition of radiation from pulsed sources

Comparing the radiation from a pulsed source with the cw calibration of a radiometric spectrometer is not a simple problem. Assuming that the integration time is long enough to collect a known large number of pulses into one data point, and if a number of averages allows for the calculation of the STD of the pulses, the detection channel response must be fast enough to collect the photons emitted by the DUT. No resonance, echo, or ringing effects must take place in the entire analytical channel. The pulses must not damage or bleach any surface in the analytical setup. So long as these precautions are obeyed, and the light power is in the right magnitude, nothing prevents comparing the pulsed light signal to the cw calibration.

5.1.3 Radiometry with parallel-detecting spectrographs

Systems with parallel detection (CCD, array) are very useful in quality and production control if it is agreed that the "physically true" emission of a source is not the goal of the measurement and that the result is used only for internal good/bad analysis. Furthermore, measurements within limited spectral ranges are well suited for parallel detection so long as the data come from a single spectral order and stray light errors stay within tolerable limits. The behavior of parallel-detecting systems must fit the task and is subject to verification by a reference system.

5.2 Radiometric Sample Illumination

The answer of a material or detector to light of a defined wavelength and known irradiation E is called the "spectral response" or "spectral efficiency." The necessity to define it is given for all kinds of materials processed by light or intended for use in optical detection. In most cases, the area under test must be illuminated with homogeneous light of a known wavelength and intensity. Thus, this section addresses the inversion of radiometric analysis.

The key element in this kind of measurement is a calibrated detector whose electric response is exactly known for the wavelengths and intensities (or irradiation) of interest. Because the external temperature influences the signal and noise, the detector element should be cooled. The pre-amplifier will incorporate different gain and filter functions to adjust the detector to the best working parameters. With the exception of zero suppression, there shall be no analog adjustments to ensure best reproducibility. If photomultiplier detectors are used, a high-voltage supply providing stability and reproducibility of 10^{-5} or better is necessary to achieve the full dynamic range of that kind of detector. In almost all cases, photon counters are not a good choice. If less than 10^5 photons/s are detected and counted, the natural SNR does not allow reasonable radiometric data. Above $10^5\ s^{-1}$, a cooled analog PMT works equally well or better than the counter. An active area that collects all light leaving the spectrometer is valid for all kinds of detectors. If that is not possible, which is not unusual for IR detectors, two solutions exist: an optical image reduction can be applied, or a calculation corrects the area. Both options are considered here. Calibrated detectors can often be purchased from the manufacturer directly. If not, a suitable model can be given to a facility that performs calibration services.

5.2.1 General requirements, independent from the application

Several parameters are valid for all kinds of radiometric illumination. The most important are reviewed now.

5.2.1.1 Bandwidth: the spectral bandwidth

The bandwidth (see Sections 1.7.3 and 2.6.4 of *Fundamentals*[1]) results from the dispersion and the geometrical slitwidth. The required bandwidth is given

by the demands of the spectral response of the sample tested. Atomic transfers demand bandwidths of <1 nm, luminescence experiments want excitation within ~1 nm, and detector response tests are often fine with 10-nm steps and bandwidths.

Possible solution

The spectral bandwidth results from the focal length of the spectrometer, the grating's line density, the spectral order, and the slitwidth. To achieve a wide variety of available bandwidths, multiple gratings are a good solution. It is always advisable to work with rather large slit sizes in order to transfer large amounts of light. It is almost always easy to attenuate precisely, and tolerances in slit size are relatively small at large widths.

5.2.1.2 Bandwidth: the uniformity of the wavelength over the slitwidth

A single-stage spectrometer always creates a variation in the wavelength over the slitwidth (see Sections 2.6.4, 4.1, and 4.3.2 of *Fundamentals*[1]), produced by spectral dispersion. Fully subtractive double monochromators provide zero dispersion in the output (Section 4.3.3.2 of *Fundamentals*[1]). If the sample responds critically to wavelength variations over the surface, either a subtractive illumination monochromator or an additional homogenizing device is required.

Possible solution

Homogenized wavelengths in the output are produced by a subtractive double monochromator automatically. If one is not available, an additional device, such as a fiber optic homogenizer or an integrating sphere, can be chosen.

5.2.1.3 Wavelength (wavenumber, photon energy, frequency): accuracy of the wavelength

The wavelength calibration of a monochromator must be checked from time to time. It depends on the stability/reproducibility of the spectrometer and the thermal state of the environment (Section 2.7 of *Fundamentals*[1]). Typical expectations for a system in a stable environment (constantly within 2 °C): for an instrument with a 2400-mm^{1} grating, within 0.05 nm reproducibility; with a 1200-mm^{1} grating, within 0.1 nm; with a 600-mm^{1} grating, within 0.25 nm; with a 300-mm^{1} grating, within 0.5 nm; and with a 150-mm^{1} grating, within 1 nm. These rules of thumb are reached with stable mechanics and drives. When using strong light sources, especially thermal lamps, near the entrance, thermal stability will be difficult to achieve.

Possible solution

Under thermally unstable conditions and with the requirement of high reproducibility of wavelength, a thermally isolated and stabilized extra housing will keep the heat away and the spectrometer stable. If that cannot be achieved, a calibration lamp should always be available for quick control of the wavelength accuracy. The switch between the two sources should be automated.

5.2.1.4 Wavelength range: the useful range

The applicable wavelength range is dominated by the light source, the transfer optics, and the spectrometer components. Four ranges can be roughly defined: deuterium lamps for 120–400 nm, xenon for 150–2600 nm (note that the continuum is disturbed by strong lines, see Section 6.4.3 of *Fundamentals*[1]), tungsten-halogen for 300–3200 nm, and IR sources are useful above 1500 nm. Below 190 nm, nitrogen purging or evacuation of the entire system is advised. Above 1 μm, nitrogen purging is also advantageous; otherwise, the oxygen and water in air will cause disturbance. Because the concentration and humidity may change, correction of the disturbance is difficult.

5.2.1.5 Illuminated area: size and shape

The useful height of the slit of a monochromator is typically between 5 and 20 mm. Depending on the source type, the maximum intensity may be concentrated on a limited height (see 6.4.3.4 of *Fundamentals*[1]). The slitwidth needs to be set for the required bandwidth; more than 5 mm will not often be used. Even at that width, homogenous illumination does not come automatically. A primary source image 5 mm high and 1 mm wide is often found, which can be transferred well through the slit. On the other hand, if a square-shaped or circular sample area waits for homogenous illumination, the conversion and homogenization of the light may be required.

Possible solution

Fit of the shapes of exit slit and sample area may be achieved by classical optics (mirror, lens, probably with cylindrical function). Fiber optic solutions are also well suited, as is the use of an integrating sphere.

5.2.1.6 Irradiance *E* at the illuminated surface

The imaging capabilities of illumination monochromators differ strongly between models. The irradiation, distributed vertically at the entrance slit, will

be roughly represented in the output slit. The horizontal spread in the exit will be the spectral distribution of the wavelength interval presented. The radiant flux in the exit can, in the best case, be the theoretically transferred bandwidth, reduced by the losses of the monochromator. The calculations are identical to those applied for irradiance E and radiance L earlier. If the slit size exceeds the size of the experiment, image reduction is suggested via optics or fiber optics. The limiting element in the chain, at the end, is always the flux and the emission density of the primary source.

5.2.1.7 Uniformity of irradiance *E* over the illuminated area

As soon as the slit area in the exit exceeds $\sim 1 \times 1$ mm, a homogeneous distribution of irradiation should not be expected anymore. The primary source will not be homogeneous over larger surfaces (see Section 6.4 of *Fundamentals*[1]): the larger the source area is, the larger the variation (blackbody radiators and the exits of integrating spheres are exceptions). Assuming a perfect homogeneous illumination of the entrance slit, the result in the exit would be a vertical cosine distribution. At the rims, the light density would be ~20% less compared to the center. In the horizontal, the distribution is a convolution of the spectral intensity, the spectrometer efficiency (i.e., grating efficiency versus wavelength), and the triangular or cosine-shaped behavior of the transfer (Section 2.6.4 in *Fundamentals*[1]).

Possible solution

If the experiment requires very small variations over the area, homogenization is needed. Again, dedicated fiber optics or integrating spheres may be the answer.

5.2.1.8 Stray light/false light, tolerated by the experiment

For response and efficiency tests that require wide wavelength ranges, the stray light is a decisive parameter (see Chapter 8 of *Fundamentals*[1]). This fact can be demonstrated by an example: consider a detector material with an efficiency of 1% at 200 nm but an efficiency of 80% at 800 nm. The experiment records the exact response curve, and the illumination system will carry 1% stray light. To make it easy, the stray light might be originating from 800-nm radiation. The device under test (DUT) will add the sum of the "true" light (0.01) and the "false" light (0.008) at 200 nm. The total is 0.018, which means that 44% of the signal generated by the DUT is due to incorrect wavelengths. For applications like this, the maximum part of the false output signal will be 10^{-3} s, which will allow the maximum of the false light to be $<10^{-5}$.

Possible solution

Whenever large dynamic ranges are expected from the sample response, a double spectrometer is strongly advised (see Section 4.3.2 in *Fundamentals*[1]). If one is not available, a set of short-pass filters will help; they suppress false light from longer wavelengths. Of course, this is only a temporary fix because continuous scans will not be possible.

5.2.1.9 Polarization

Every grating spectrometer modifies the state of polarization of the incoming light (see Sections 3.2 and 3.6.1 of *Fundamentals*[1]) with two exceptions: specially designed gratings for lasers and standard grating applications with linearly polarized illumination light. If a certain plane of polarization is required at the output, it might be best to place a polarizer directly in front of the sample or in the collimated part of the beam between the exit slit and sample. On the other hand, if unpolarized light is really required, a depolarizer (scrambler) is essential. If an integrating sphere is used to illuminate the sample (Fig. 5.8), depolarization is automatically provided. Wide-range standard fiber optics also scramble the polarization; lengths above 1 m can be considered to be perfect depolarizers.

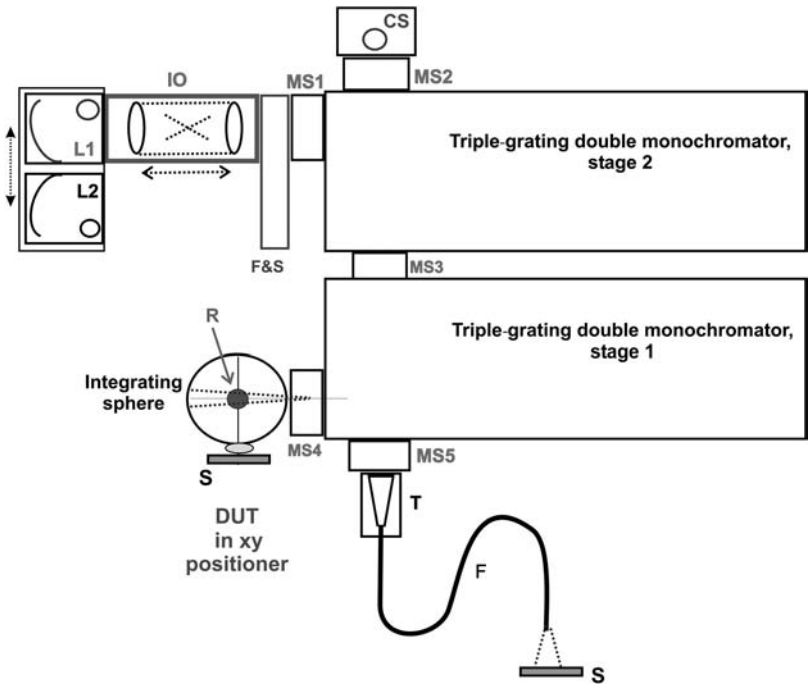

Figure 5.8 Radiometric illumination system for wide wavelength ranges, with two methods of homogenizing, and reference channel.

A double monochromator with multiple gratings is illuminated by three sources. The side entrance MS2 receives light from a calibration source, such as a mercury line lamp CS. The power sources are mounted at the front entrance MS1; they consist of a deuterium (or xenon) lamp L1 and a halogen lamp L2. Collection and refocusing is done by lens optics IO. In front of the slit is a combination filter wheel and shutter F&S. All slits of the monochromator are program-controlled by stepper motors. The exit will direct the light either into an integrating sphere MS4 or a fiber optic cable MS5; both will illuminate the sample S. The fiber optic system F may modify the cross-section of illumination, and it is connected through refocusing optics T. It will deliver an optimum of flux to the sample. Further optics between the fiber output and sample are optional. The integrating sphere, on the other side, will deliver even better homogenized light and incorporates a reference detector that monitors the integral of light in real time. Sample S delivers electric signals to the analysis channel (not shown).

5.2.1.10 Spectral illumination with a reference channel for calibrated flux of radiation

A multiple-grating double monochromator, assumed to work additively, is equipped with a calibration lamp CS, which allows one to check the wavelength calibration at any time. The experiment light comes from a deuterium (or xenon) lamp L1 and a halogen lamp L2. The refocusing system IO collects an optimum of light and guides it to the spectrometer entrance slit MS1; it fits the spectrometer's Ω. In order to keep the focus versus wavelength constant, the two lenses are independently positioned by stepper motors and a program (dotted arrow). If the lenses are made of cultured quartz, the system will work between 180 nm and 2600 nm. The crossed dotted lines inside IO mark a mechanic attenuator made of metallic lamellas, again controlled by a stepper motor.

The variation range of the attenuator is 0 to $>90\%$ of the incoming light, which allows programmatic control of the homogeneous light flux in the monochromator and thus to the experiment.

Next comes a package with an order-sorting filter set and shutter F&S. All slits and beam-steering mirrors of the monochromator are motor-driven. The calibration source CS is not filtered, so the calibration is possible in many spectral orders. The dispersed light after the monochromator is either directed into a sphere with a calibrated detector (R, mounted to the north pole of the sphere) or into a homogenizing fiber guide system to enable different types of sample illumination. Illumination experiments are rarely optimized to narrow spectral bandwidths. In most cases, a minimum bandwidth of 0.1 nm will offer sufficient flexibility and reserve. Thus, the focal length and gratings can be optimized for luminosity and stray light. A contrast ratio of 10^5 or better is already provided by a double monochromator with a 250–300-mm focal length and *f*/4, or $\Omega = 0.0625$. If the UV source is an XBO-75 xenon lamp

(see Section 6.4.3.3 of *Fundamentals*[1]), an average $M = 100$ W/(sr $\times$ cm^2 $\times$ nm) is emitted in a ball shape. The system will transfer an average $E = 3$ mW/(mm^2 $\times$ nm) into the monochromator. If the monochromator has an average transfer efficiency of 0.33 and the slits sizes are 5 mm $\times$ 0.2 mm, an average of 1 mW/(mm^2 $\times$ nm) will leave the output slit. If the sample is directly connected to the output slit, there is no further loss. If the beam must be homogenized, that will happen at the expense of flux. In any case, before the final mounting of the sphere and fiber cable, the reference detector will be placed alternatively to both outputs MS4 and MS5. Measurements with both lamps at many wavelengths and at least two slitwidths are required to investigate and store the maximum intensities leaving the two outputs. It is then possible to define the maximum light flux available and the ratio of outputs when switching between them.

5.2.1.10.1 Fiber optic homogenizer

The fiber optic system consists of a fixed taper T that collects the light up to the maximum slit area of 5 $\times$ 5 mm and transfers it into a solid fiber with a 3-mm diameter (F, not a cable). The solid fiber is "S"-shaped vertically and horizontally in order to force a certain number of internal reflections in both planes. At its output, after a 1-m length, the output area is spectrally and spatially uniform and depolarized. The fiber optic system will have an efficiency of 20–50%, delivering an average maximum of 0.35 mW/(mm^2 $\times$ nm). Unfortunately, the fiber system has a limited range: either from 210 nm to 1100 nm (quartz) or from 400 nm to 2100 nm (glass). Independent of the actual exit slit size, the signal at the fiber optic exit will be commonly distributed over the full area of 7 mm^2. If 1 mW/(mm^2 $\times$ nm) is sent to 1 mm^2 at the taper, and the efficiency is 0.5, only 71.4 μW/(mm^2 $\times$ nm) will leave. The larger the exit slit of the spectrometer is, the higher the light density at the fiber exit with constant flux. The sample S will finally be illuminated directly or through further optics.

5.2.1.10.2 Integrating sphere homogenizer

The sphere is more flexible but delivers less irradiance and radiant flux to the sample S. In the case reviewed here, the sphere illuminates samples of up to 20 mm Ø. The exit slit is up to 5 $\times$ 5 mm^2 (7-mm Ø aperture at the sphere). The sum of all apertures of the sphere is 3.6 cm^2, which requires an inner surface of at least 120 cm^2, or at least 6.2 cm Ø. Better is 8 cm Ø, consisting of an inner area of 201 cm^2. As opposed to the fiber guide, the irradiance in the sphere exit does not depend on the size of the spectrometer slit illuminating the sphere; only the flux available in the sphere matters. According to Eq. (5.6), the average irradiance in the exit ports can be calculated. With a sample area of 1 mm^2 and $\Phi = 1$ mW/nm inside the sphere, one can expect, depending on wavelength and coating, an E of 0.1–0.6 μW/(mm^2 $\times$ nm). Thus, the "efficiency" of the entire system is much weaker compared to the fiber optic solution, but it works over the full range, and it has the advantage

of enabling real-time reference measurements through the reference detector R while running samples.

5.3. Analysis of Spectral and Power Spatial Distribution Provided by the System

5.3.1 Reference analysis by a single point detector

Most response applications require knowledge of irradiance E [Eq. (5.3)] and radiance L [Eqs. (5.5) and (5.6)] delivered to the DUT. The safest way to reference that is to illuminate a calibrated detector in the same fashion as the DUT, in both intensity/wavelength and size. After replacing the reference detector with the DUT, the measurement is repeated by the same parameters, which can calculate the response directly. The reference should not be smaller than the DUT or else extreme homogeneity over the field must be provided. Running the reference detector at more than one output of the monochromator enables one to detect and store the differences in transfer for further calculations. Having taken all steps and learned the tolerances, secondary standards can be created if more than one system must be monitored.

5.3.2 Analysis of spectral and power distribution over the illuminated field

There are response measurements wherein the homogeneity of the wavelength and intensity over the xy position of the field is not of importance. Surface response analysis, on the other hand, depends on very narrow specifications and low tolerances. A system can be designed to detect both parameters. In the xy plane of the illuminated field, a small positioning system holds a single optical fiber. The fiber size can be selected based on the planned geometrical resolution of the future DUT. Assuming an area of 10 mm $\times$ 10 mm and a 1% geometrical resolution, a 100-μm fiber might be perfect, moved by steps of the same size in both directions. This scenario will lead to 10,000 points being measured, but the measurement is rarely required, and the number of xy points acquired may be strongly reduced by programming special patterns. Normally, systems like that will not suffer from remarkable variations in the output field. The fiber may move the light into a small, compact parallel spectrograph for point-to-point analysis. The spectral bandwidth of the spectrograph will be one-fifth or smaller than the bandwidth of the light analyzed. The reproducibility of the system will be at least 5 times better than the required homogeneity over the analyzed surface. A system like that even offers the choice to adapt to curved illuminated fields by adding a third axis of motion. Requirements to realize such a device are rather high. No other light, apart from the analyzed light, will reach the tested area; the analysis system requires extra tools and programs; and the fiber cable should be held in such a way that the changes between data points are negligible to avoid internal errors. The proposed system will also reveal stray light and other troubles.

5.4 Calibration of Radiometric Spectral Data

To perform calibrated measurements of light sources, it is necessary to have a calibrated reference source that covers at least the wavelength range of interest and emits light on a comparable order of intensity. To perform calibrated sample illumination, it is necessary to have a calibrated detector that covers at least the wavelength range of interest. Both are available from suppliers in the field of radiometry. In practice, some lamp and detector companies offer certain products suited for calibrated work and deliver them with certification sheets and warranties. A second option is to deliver one's own reference product (which can perform to the requirements and can be kept under controlled parameters) to an institution or company for calibration and certification.

5.4.1 Description of a realized system and its calibration with a certified source, enabling calibrated source analysis

The following procedure follows the steps described in Chapter 7 of *Fundamentals*[1] on radiometric calibration. A monochromator system for the radiometric analysis of light sources was installed. The light-collection algorithm fits irradiance E in favor of emittance/exitance Φ, while conversion is provided anyway.

The system shown in Fig. 5.9 is applied to spectral irradiance analysis. It contains a 0.5-m additive double Czerny–Turner equipped with an automatic order-sorting filter, shutter, triple grating, and two detectors: a PMT for 180–850 nm and a Si–InGaAs sandwich SD for 750–1650 nm. The front end of the system is a fiber optic cable, fixed in position to avoid reproducibility

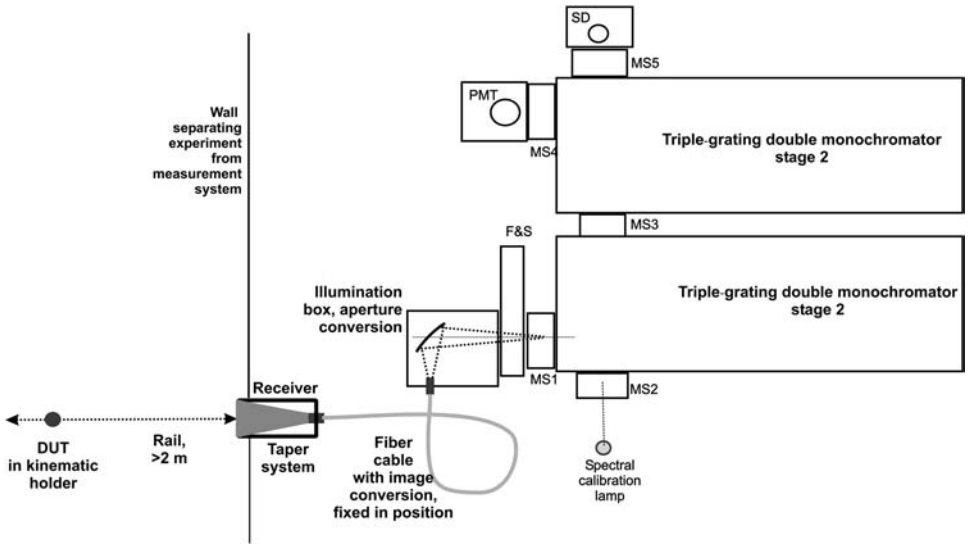

Figure 5.9 Example of a fiber-optics-based radiometric system.

problems. The receiver (entrance) of the fiber cable has an active diameter of 1 cm × 1 cm. Due to its acceptance cone angle of 25 deg, it can be illuminated by very close sources. In the experiment described here, the source was a calibrated tungsten-halogen HLX-100 lamp, operated according to manufacturer specifications, at a distance of 70 cm from the receiver. That distance/receiver ratio provides $\Omega = 0.0002041$, which is the weakest in the whole system and thus the limiting parameter. At the spectrometer end of the cable, the exit shape is converted to match the spectrometer slit. To collect the fiber's emission angle of 25 deg and fit the spectrometer's acceptance angle of 8 deg, a single ellipsoidal 90-deg mirror is used. Its focal length is 46 mm toward the fiber cable and 150 mm toward the spectrometer slit. That ratio creates an image magnification of a factor of 3.26 at the plane of the slit. The maximum slit size is 10 mm high and 5 mm wide. Due to the magnification, the fiber exit's shape is 3 mm × 1.5 mm. This size, in turn, requires a reduction between the receiver and illumination box of active fiber area from 100 mm^2 to 4.5 mm^2. This reduction was achieved by putting a fiber optic taper to the receiver end, which reduces the cross-section accordingly. The cable itself creates the image conversion from squared to rectangular. A total of 150 fibers, each with a 200-μm cross-section, ensures homogeneous slit illumination. The light-guiding factors at the spectrometer side are $\Omega_{fiber} = 0.45$ and $\Omega_{spectro} = 0.043$, respectively. The following test was performed with a 300-mm^{-1} grating, blazed to 300 nm, delivering a dispersion of ~1.5 nm/mm. To get an average bandwidth of 1 nm, the slits were set to 660 μm. The sandwich detector has TE cooling and a pre-amplifier; the output was read by a 20-bit ADC system.

5.4.1.1 Experimental considerations

In comparison to an integrating sphere, the system offers the advantage of varying the Ω by moving the emitter closer to or farther from the receiver. Cone transmitters, such as LEDs, can probably be collected completely. In total, the efficiency will be better for most experiments. However, it will not be possible to collect the whole radiation emitted into 4π, equal to $\Omega = 12.56$, if ball-shaped sources are involved.

5.4.1.2 Experimental operations

Five spectra of the HLX-100 lamp were obtained and averaged to create the calibration curve shown in Fig. 5.10. The STDs between all five single curves had to be less than 0.1%, which was true.

The graphical conversion of the table shows a typical thermal light source. Both the bandwidth and stepwidth are 1 nm, covering 250–1200 nm.

Because the lamp emission takes off at 350 nm, only data above that wavelength are recorded. The curve in Fig. 5.11 proves that it was a good decision to use a short-wavelength blazed grating. The dip between 800 and 900 nm and the small humps come from grating anomalies. They are repeatable and are calibrated out. The detector output range is 10 V, and the

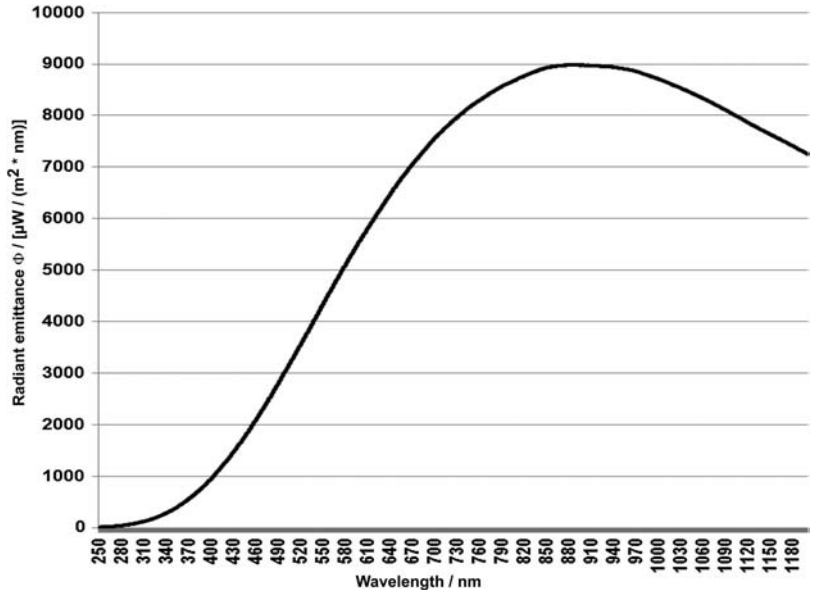

Figure 5.10 Original source data as a table with calibrated HLX-100 lamps.

Figure 5.11 Averaged curve produced by the monochromator system with a calibrated HLX-100 source.

measurement occupies ~10% of the linear range. High-precision measurements are possible between <0.1 and 10 V. Thus, thermal sources at a 70-cm distance are well analyzed between 10 W and 1 kW DC.

The division [detector output/original source data] produces the system response curve (Fig. 5.12). The vertical scale is the factor of multiplication,

Figure 5.12 System response curve required to recalculate source characteristics.

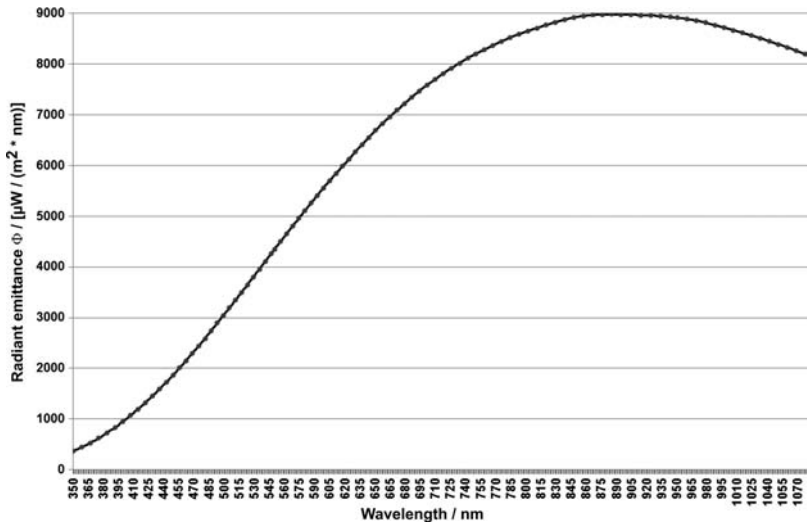

Figure 5.13 Original source data overlaid with the recalculated data after the second measurement.

applied to the measured data, that results in the DUT's optical power. So long as the source is placed in the calibration position (70 cm in front of the receiver) and the slits are not changed, no further corrections are required.

After all calculations, curve creations, and examinations were sufficient, the lamp was turned off and removed. The next day, it was brought back into position and run again according to specification. The result proves a perfect match. The system is then ready for more unknown emitters. The solid line in

Fig. 5.13 represents the original lamp data, whereas the overlaid dots are measured and recalculated data points.

It might be a good idea to not publish the results as radiant emittance Φ but as irradiance E, which is the radiation actually hitting the receiver. That would have the advantage that all kinds of sources can be processed, not only ball-shaped emitters at a 70-cm distance, so long as the light fills the surface of the receiver.

5.4.2 Calibration facilities

The institutions and companies for calibration service are often also the suppliers for sources and detectors, or even complete systems. In the USA, NIST is the leading institute; in Germany, the PTP and the DKD; and a notable European association is EURAMET. Other facilities are available all over the world. For every country, a reference lab is available. Unfortunately, the standards provided by the different authorities are not the same. The certificate provided for a calibrated detector and/or a calibrated light source will at least include the calibrated parameter values versus wavelength, the applied variation in bandwidth and stepwidth, and the validity of the calibration (running hours and maximum date). Some companies will also accept complete spectroscopic radiometry systems for calibration.

References

1. W. Neumann, *Fundamentals of Dispersive Optical Spectroscopy Systems*, SPIE Press, Bellingham, WA (2014) [doi: 10.1117/3.1002528].
2. J. Palmer and B. Grant, *The Art of Radiometry*, SPIE Press, Bellingham, WA (2009) [doi: 10.1117/3.798237].
3. W. L. Wolfe, *Introduction to Radiometry*, SPIE Press, Bellingham, WA (1998) [doi: 10.1117/3.287476].

Chapter 6
Raman and Brillouin Spectroscopy

6.0 Introduction to Scattering Spectroscopy

The interactive effects of light scattering at molecules can be separated into two main groups: inelastic and elastic scattering. Rayleigh scattering is elastic because the energy of the scattered photons remains unchanged, whereas the direction of travel is modified. In inelastic (Raman) scattering processes, the photon energy/frequency/wavelength of the light after interaction with the sample is different, and the distribution is spherical. Thus, it is possible to measure only the intensity and 3D angular distribution of the elastic scattering at the original wavelength (Rayleigh, excitation). The Raman photons, on the other hand, will carry a slightly different energy/frequency/wavelength after interaction. Raman spectra appear on both sides of the excitation energy. The side with lower energies (longer wavelengths) is called the Stokes side; the range of higher energies is called the anti-Stokes side. This behavior is due to the fact that the interacting molecule may absorb and transfer a certain amount into its rotational structure and vary the vibrational state (stretch), which is measured on the Raman Stokes side of the spectrum. Conversely, the molecule will add some energy from its own rotation, resulting in spectral features on the Raman anti-Stokes side.

The Stokes spectrum is usually stronger than the anti-Stokes part and is used for analysis more often. The effect was proposed for solid state structures by Adolf Smekal in 1923. C. V. Raman added the theoretical base to liquids. In 1928, the effect was first proven by Raman and K. S. Krishnan. Raman received the Nobel Prize in 1930 for his work, and his name is popularly attached to the phenomenon. The name "Raman–Smekal effect" is also used. If inelastic scattering occurs in the range of optical phonons, it is called Brillouin scattering, and the spectrum appears largely symmetric. This effect was predicted by Leon Brillouin in 1922, based on Schrödinger's equations for inelastic vibration scattering. The sense of both effects is different but complementary: the spectra may overlap, and they require basically the same

equipment. Both effects—Raman–Smekal and Brillouin—are very weak; typically only 10^{-14} to 10^{-10} of the photons present in the sample volume are converted, and they are spectrally and spatially distributed evenly. The spectral distribution covers 0 to ± 4500 cm^{-1}, or 0 to ± 0.6 eV.

In contrast to absorption/reflection, luminescence, emission, and polarization spectroscopy, the scattering features appear in absolute difference of energy/wavenumbers, always with the same spectral difference. This behavior is independent from the wavelength of excitation, but note that all scattering effects depend on the excitation photon energy in the fourth power. The relative bandwidth and dispersion of grating spectrometers are inverse to that in principle. The distribution of the photons, scattered by the Raman or Brillouin effect, is spherical and statistical, whereas elastic scattering carries information in the direction of the scattered photons. The bandwidth of Raman signals can appear rather narrow, typically on the order of 10 cm^{-1}, or 0.001 eV. The Brillouin lines are even narrower, mainly in the range of <1 cm^{-1}, or 10^{-4} eV, and they appear rather close to the excitation. Raman and Brillouin are quantitative methods, and both are complementary to IR absorption/reflection spectroscopy, which senses the rotation of the molecules. There are samples that do not absorb in the IR but produce Raman/Brillouin signals, and vice versa.

Justification or calculation of Raman experiments may lead to the amusing situation that the Raman signals are specified in cm^{-1}, but the excitation laser[1] is defined in nm (its bandwidth may be given in GHz). Thus, it is convenient to use conversion equations (1.4)–(1.10) in Section 1.3 of *Fundamentals*.[2]

6.1 The Principle of Raman Spectroscopy Measurements

A laser with a very narrow bandwidth and high beam density illuminates the sample. A single or a group of polarizers is placed in between to optimize the plane of polarization. Additional optics for beam shaping is also sometimes placed there; lenses are the most popular because in many cases only one excitation wavelength is used. For quantitative work, a beamsplitter will sit in front of the sample to divert a small part of the excitation light to the reference detector. The Raman signal will leave the sample in a spherical shape. Naturally, depending on the consistency of the sample (gas, liquid, or solid state) and the absorption behavior at excitation wavelength, several parameters must be considered. The collection optics will view under 90 deg versus the excitation because a minimum of Rayleigh scattering is expected there. The decision of whether lenses, mirrors, or a combination of both are used to collect as much light as possible is up to the system designer. A second optical arrangement must fit the acceptance angle of the spectrometer for efficient transfer of the collected light. The spectrometer itself, and the detector, may be one of several suitable variations.

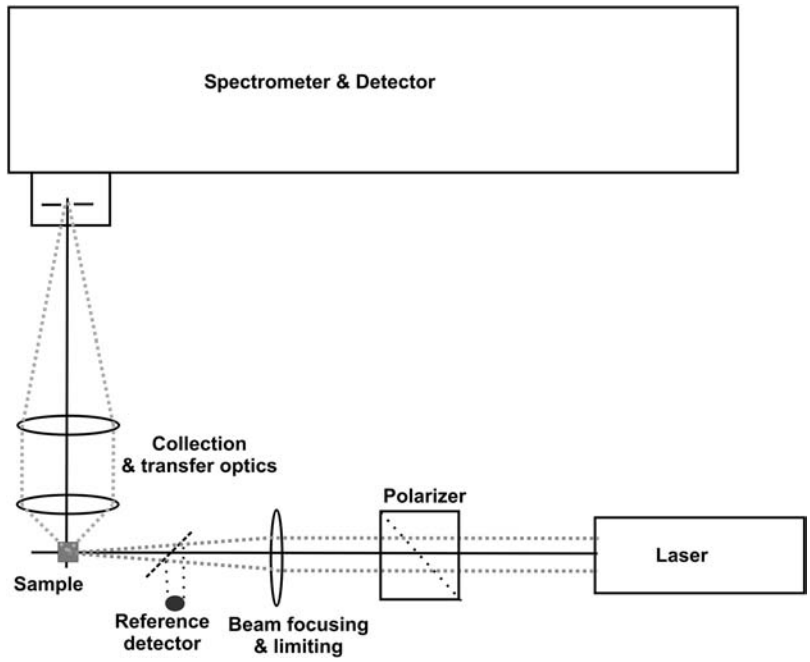

Figure 6.1 System for Raman and Brillouin spectroscopy.

6.2 Requirements for a Raman Spectrometer

Based on the definitions given earlier, it is not difficult to see the requirements:

- The excitation source should provide very high intensity and light density at the minimum spectral distribution (the optimum is a laser with a narrow bandwidth, i.e., a single-mode laser).
- The sample should tolerate the high density of energy without degrading or changing its characteristics or structure; otherwise, the excitation intensity must be reduced.
- Because the information of interest leaves the sample in a spherical shape, an efficient collection system is advantageous. It should take into account that elastic scattered light is expected to be minimal under an angle of 90 deg with respect to the incoming beam.
- The Rayleigh scattering may, even at transparent samples, still be more intense than the signal of interest by several orders; thus, the excitation wavelength must be efficiently suppressed.
- The transfer of light between the sample and detector should be as efficient as possible to protect the viewed photons from loss and to keep the time-dependent background and noise low for a good SNR.
- High-dispersion spectrometers are beneficial to resolve the rather small signal bandwidths often provided by the sample.

- If, besides the qualitative data acquisition, quantization is also possible and required, the method is complementary to IR absorption spectroscopy. The excitation intensity at a constant cross-section must then be measured in parallel.

6.2.1 Spectrometer options

The shift of Raman signals is constant in the axis of energy (cm^{-1} or eV). Therefore, the scale of wavenumbers ($\tilde{\nu}$) is almost always used, whereas the excitation is presented in nanometers (λ). Converting Raman data into the nanometer domain may produce strong variations. The following figures and calculations represent a popular combination for Raman, consisting of an additive double-spectrometer system with a 500-mm focal length (FL) and 1800-mm^{-1} gratings. The dispersion behaves like that of a 1-m single-stage spectrometer.

In Fig. 6.2, the solid curve represents the intensity of scattered signals, which at 200 nm are a factor of 625 stronger compared to 1000 nm. It seems reasonable, at first glance, to work in the UV range, especially because the Raman signals are qualitatively independent from the wavelength of excitation. Thus, a comparison of the bandwidth in wavenumbers or eV ($\tilde{\nu}$ or ν) and in nanometers (λ) is provided. The dotted curve shows the bandwidth in wavenumbers for a slitwidth of 1 mm, whereas the dashed curve indicates the bandwidth in the nanometer domain. Both present a smaller bandwidth, and thus a better resolution, toward longer wavelengths, but the nanometer curve varies much less. Conversely, for a

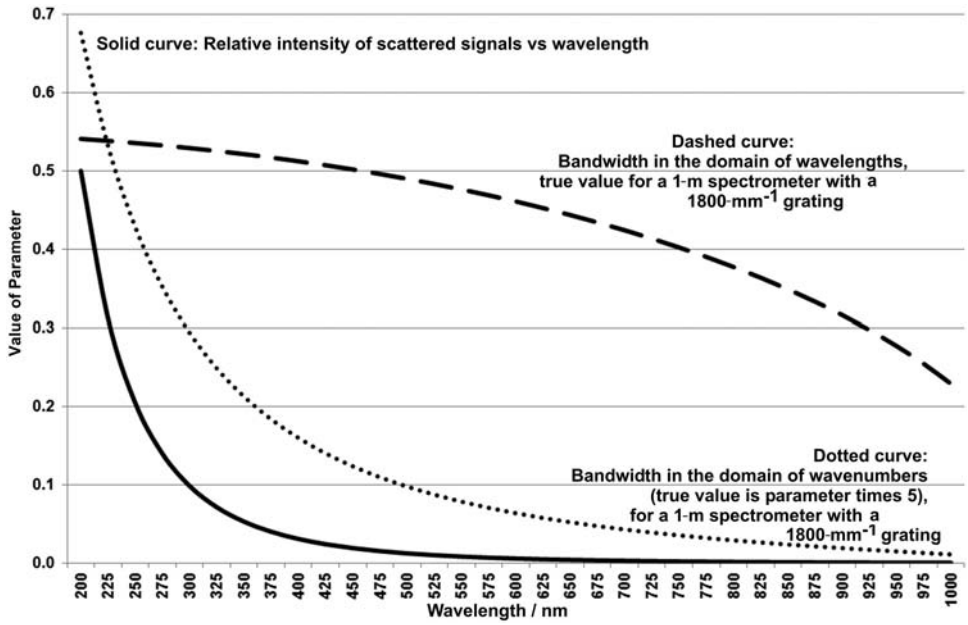

Figure 6.2 Behavior of the magnitude of scatter over λ, and the relation of the bandwidth in the domains λ versus $\tilde{\nu}$, in the 200–1000-nm range.

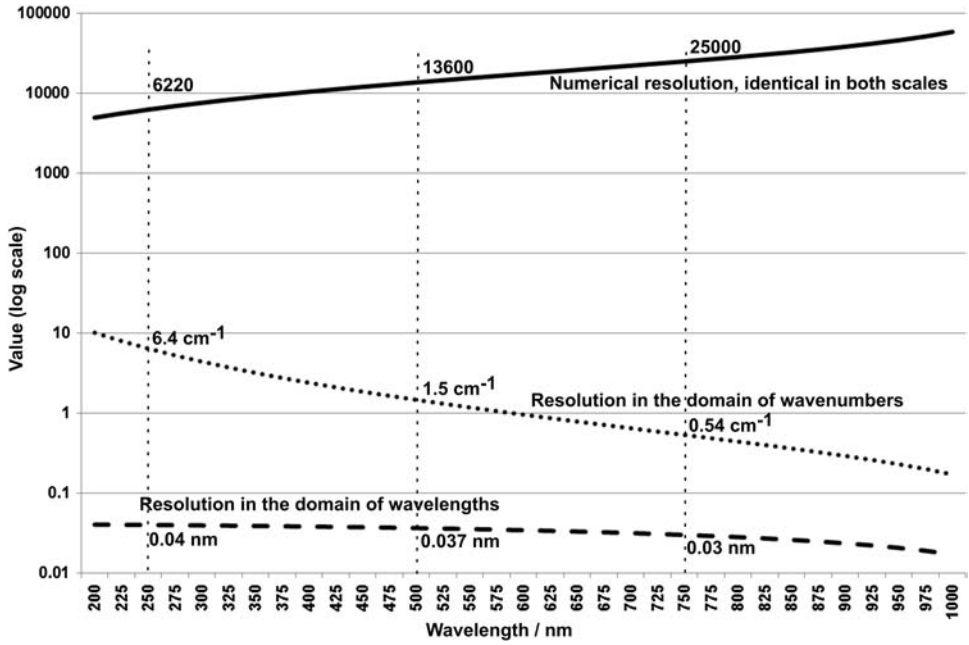

Figure 6.3 Practical resolution of a 500-mm additive double spectrometer.

constant resolution, the slits in the wavenumber scaling must close much more toward the UV to keep that parameter constant. Figure 6.3 addresses typical resolution numbers of the reviewed system, proposing a CCD with 25-μm pixels or a monochromator with 50-μm-wide slits.

In Fig. 6.3, the numerical resolution is given by $R = \lambda/\Delta\lambda = \tilde{\nu}/\Delta\tilde{\nu}$. It is represented in the solid top curve and is identical in both domains. The spectral numbers differ as the domains differ. The numbers of the three parameters for three frequently used wavelength regions are provided. Although the spectral resolution in the wavelength regime only changes by 30%, it varies by a factor of ~10 in the wavenumber regime and by a factor of 4 in the numerical ratio. This scenario leads to very different wavelength intervals in the wavelength domain after variation of the excitation wavelength.

Raman signals appear between roughly 10 cm^{-1} and 4500 cm^{-1}, symmetric to both sides of the excitation. In Fig. 6.4, the distance conversion is drawn in nanometers for the two extremes. The working range covers the range between the curves. The shorter the excitation wavelength is, the closer the signals move together in the nanometer scale. Note that the figure uses dual vertical scales: 0–1 nm in the lower part for nearby Raman signals, and 0–410 nm for more-distant Raman signals.

6.2.2 Summary of wavelength dependence

Raman signals grow in the fourth order with increasing energy of the excitation photons. Unfortunately, all other scattered phenomena do the

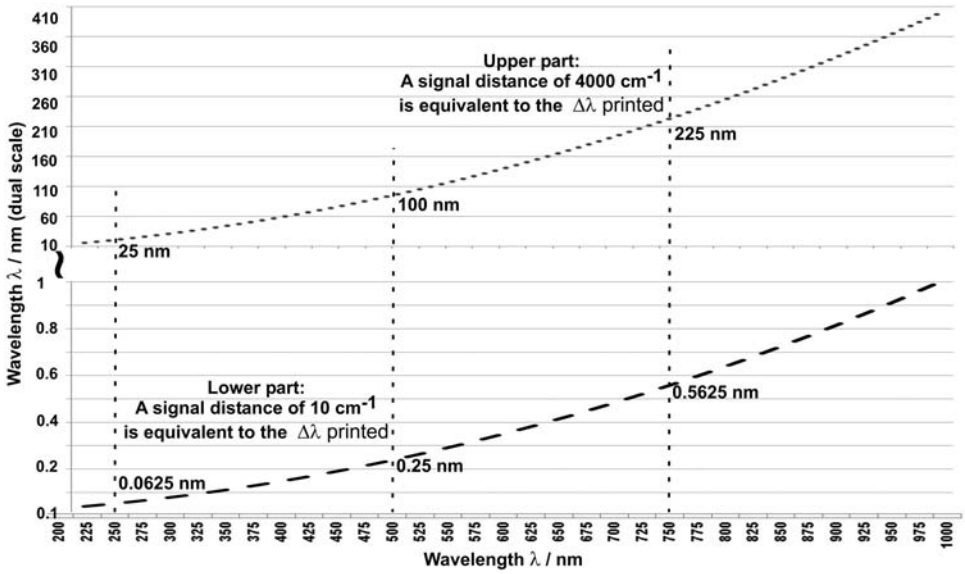

Figure 6.4 Relation between the distance of Raman signals from 10−4000 cm^{-1} as the laser wavelength changes.

same, more or less, so the SNR may stay rather constant. For a constant bandwidth and resolution in the domain of $\tilde{\nu}$, the slitwidth must shrink toward a shorter λ, which has a dramatic impact on the luminosity (see Section 2.6.2 of *Fundamentals*[2]). Compensating for that, at least partially, requires the use of gratings with a high line density and probably an increased focal length, which, in turn, may attenuate the luminosity again. For almost all types of solid state detectors, the efficiency drops toward the UV; their maximum is usually in the red or NIR. PMTs and MCPs behave in the opposite fashion: they work better in the UV compared to the red range. Finally, narrowband lasers with small focal spots are also easier to handle and lower priced in the visible range. Beside HeCd (325 and 420 nm), special versions of Ar ion and Kr lasers offer many UV wavelengths, but they are weaker than those in the visible range. Another drawback is that UV light is not visible to the human eye, which creates more hazards. The visible range is a good balance between efficiency, resolution, and flexibility. Excellent lasers and detectors are available, making blue-to-green the preferred excitation range. Adjustments can be performed to view the original wavelength, and vagabond laser rays can be easily monitored. If the detector is a CCD, NIR excitation up to 750 nm is useful if the decreasing Raman efficiency is acceptable. Above excitation wavelengths of 800 nm, the upper limit of Raman detection on the Stokes side will be shortened because of the vanishing CCD efficiency beyond 1000 nm. The following sections discuss further advantages and disadvantages for the different wavelength ranges.

6.3 Beam Travel and Spectral Interferences

The light path contains many optical components that interact with the light: windows, lenses, mirrors, sample cells or other holders, eventually fiber guides, etc. If optimal materials and coatings are not chosen, spectral interference may occur, such as troubles with fluorescence, which may be excited in glass, in components (e.g., fiber optics), or in mirror coatings. When designing Raman systems, it is useful to discuss possible disturbances with the components suppliers to avoid future problems. During use, pollution of the components must be prevented because, besides loss of efficiency, fluorescence may appear. Many materials create (by their nature) Raman and/or Brillouin signals; they cannot be completely avoided, but they should be acknowledged and kept under consideration. It may be important that they vary at different wavelengths. Clever selection of materials can avoid problems, and especially in a Raman or Brillouin spectrometer, it is important to know the relative spectral position and probably also the signal magnitude of existing interferences to prepare for their reduction, if required. (See also Chapter 4 in this book and Chapter 8 in *Fundamentals*.)

6.4 Exemplary Raman and Brillouin Spectra

Many samples are solved in aqueous solutions, and thus the Raman spectrum of water is of interest. The same applies to the spectra of materials used in typical equipment that may become a source of interference.

In Figs. 6.5 and 6.6, the materials have been excited by a 514.5-nm argon ion laser, and the spectra have been measured by a 0.5-m single-stage Raman spectrograph equipped with a notch filter. The setup provides useful data between 120 and 4500 cm^{-1}. The turquoise curve represents water. The yellow curve represents glass, and the blue represents quartz. The vertical shift is true because the sharp features ride on continuous signals. The pink calcium fluoride and the red sapphire curves carry almost no background. However, both have been shifted by 20,000 and 40,000 units, respectively, for better separation.

Figure 6.6 demonstrates the analytical power of Raman spectroscopy. The spectra have been collected from several systems and reconstructed in a common table. The solid black spike represents a natural diamond, which makes for an (expensive) calibration standard because it consists of a single, narrow peak at 1332 cm^{-1}. The blue curve represents industrial-packed graphite, which adds a major signal at 1580 cm^{-1} and some minor peaks that may be used as a product marker. As soon as the material is compressed, the 1580-cm^{-1} peak disappears, and the curve becomes closer to that of natural diamond. However, it will never be identical—it will always be wider and shifted. The maximum of the compression process is reached by "diamond-like carbon," indicated by the grey curve. Raman spectroscopy is the accepted method to discriminate between natural and artificial diamond, and the

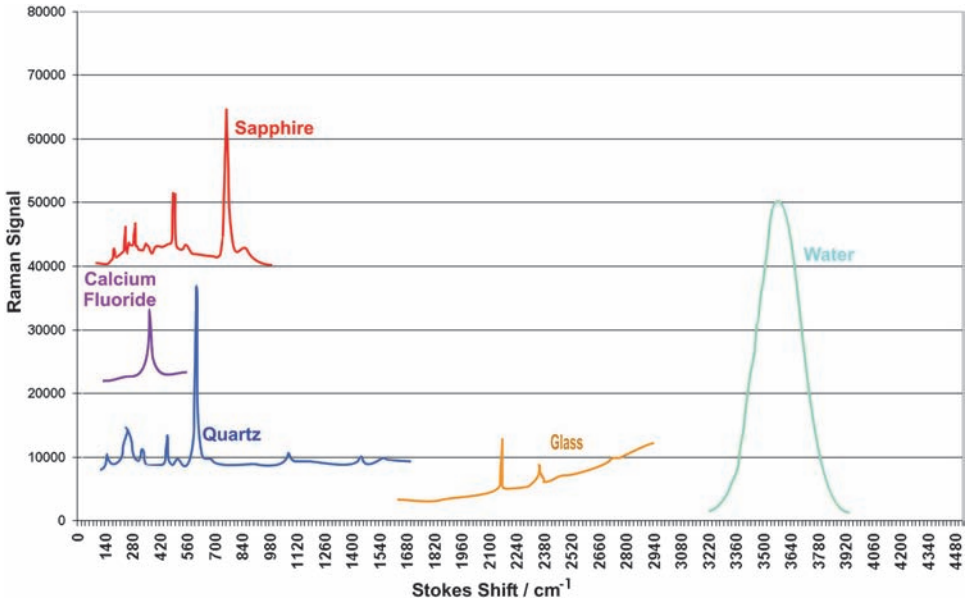

Figure 6.5 Raman spectra of materials, which may appear to interfere.

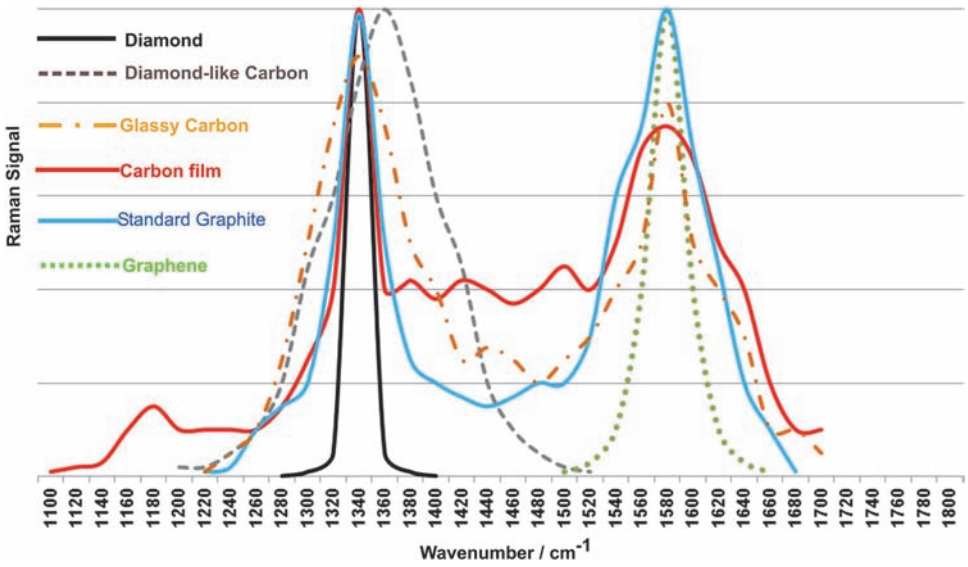

Figure 6.6 Raman spectra of some solid versions of carbon.

"fingerprint" of the latter. It is also popular to characterize nanolayers, e.g., the red curve. Glassy carbon (blue) typically provides only the two major peaks, whereas the single structure of graphene only responds with the peak at 1580 cm^{-1}. Figure 6.6 concentrates in the main range between 1100 and

1700 cm^{-1}, while fine structures of the multiple carbon and graphite versions are found outside that range to allow more discrimination.

6.5 Design or Selection of Raman Spectrometers

During design or selection, three parameters are important:

- What are the desired excitation wavelengths? (This is strongly defined by the projected samples.)
- How close to the Rayleigh line must the Raman data be acquired?
- In what time frame should the measurement be performed?

6.5.1 The wavelength of excitation

If the wavelengths can be freely chosen (Table 6.1), those between 450 and 650 nm are preferable for several reasons: The interval of 4500 cm^{-1} corresponds to ~130 to 170 nm in the wavelength domain. It is easy to find gratings of optimal efficiency in that range and interval. The types of detectors in question are close to their maximum efficiency. If parallel detection is used, it is easy to find suitable gratings for the required interval. The excitation beam—with all precautions—is easily viewed and adjusted. The range is spiked with strong, well-collimated lasers that provide a high beam quality, such as argon ion lasers, providing many lines to choose from. The line used should be as narrow as possible (single mode) because the width of the excitation is found in the Raman signals. If there are no major reasons for the side of the sample to require a different excitation wavelength, it is the best-suited range.

Table 6.1 A selection of frequently used lasers for Raman excitation in the UV–Vis–NIR range.[1]

Wavelength [nm]	Wavenumber [cm^{-1}]	Type of laser	Typical power [W]	Output
244	40,984	Argon	0.01	cw
248	40,323	Excimer	2.00	5-ns pulses / 500 Hz
266	37,594	Nd:YAG	0.10	5-ns pulses / cw
275	36,364	Argon	0.10	cw
308	32,468	Excimer	2.00	5-ns pulses / 500 Hz
325	30,769	Helium-cadmium	0.02	cw
351	28,490	Krypton	0.25	cw
355	28,169	Nd:YAG	20.00	ps pulses / cw
442	22,624	Helium-cadmium	0.20	cw
488	20,492	Argon	2.00	cw
514.5	19,436	Argon	2.00	cw
534	18,727	Nd:YAG	0.35	5-ns pulses / cw
633	15,798	Helium-neon	1.00	cw
780	12,821	Diode laser	200.00	div pulsed / cw
1064	9,398	Nd:YAG	0.70	5-ns pulses / cw

6.5.2 Applicable distance of Raman signals

6.5.2.1 Single-stage spectrometer with notch filter

Figures 5.5 and 5.6 show materials that do not require the detection of nearby Raman signals and only need analysis at the Stokes side. For these tasks, a single-stage spectrometer will suffice if equipped with a steep notch filter at the Rayleigh line. The detector can be chosen from a single point or CCD. The latter is preferred because it saves time by a factor of 5–20 at comparable bandwidths and SNR.

Figure 6.7 shows a single-stage Raman spectrometer that will solve ~90% of the routine Raman measurements. The laser's excitation signal—the Rayleigh line—is largely suppressed by notch filters (inverted bandfilters, also called frequency traps, shown in the right part of the figure) made of a material that has been treated by holographic methods, leaving 3D structures in the body. For narrow wavelength intervals, the structures produce interferences that strongly quench the selected wavelength range (see also Section 9.3 of *Fundamentals*[2]). The reduction is effected by either reflection or subtractive interference at a specific wavelength in the holographic structure. The full bandwidth, specified at 50% T, varies in the available versions roughly between 700 cm^{-1} (standard notch) and 300 cm^{-1} (super notch). Since about 2012, a version with an even-narrower bandwidth is available: the volume holographic grating (VHG). It reflects only an extremely narrow band out of the spectrum while passing through a wide interval on both sides. A VHG is stacked from several holographic structures and reaches bandwidths as narrow as 30 cm^{-1}, combined with Rayleigh line suppressions

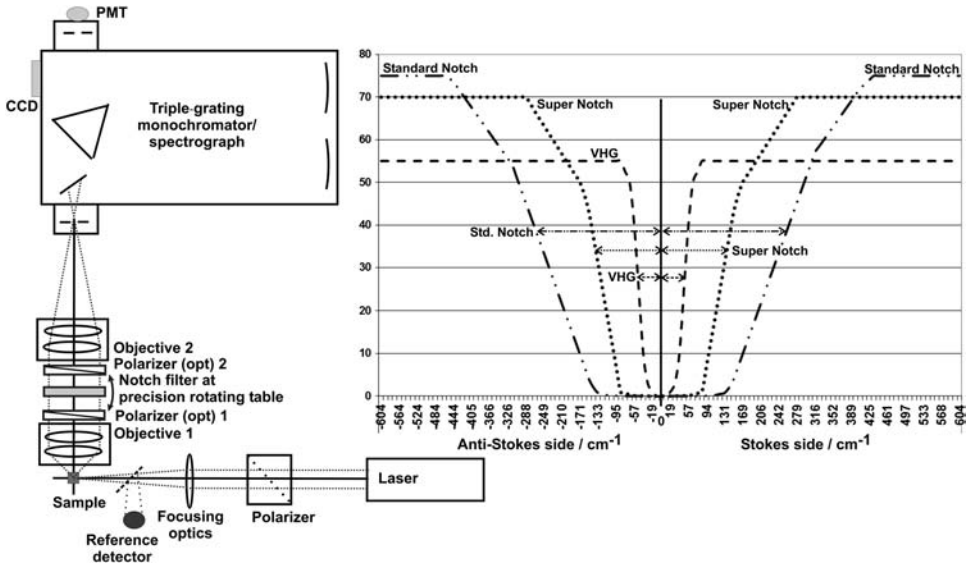

Figure 6.7 Raman spectrometer with a notch filter.

of up to 6 AU. The attenuation curve of all of the filters is symmetric, as shown and marked in the figure. Indeed, half of the bandwidth is important for most Raman measurement, as marked by the arrows. Thus, the specifications of notch filters for Raman always define that half bandwidth. Standard notch filters provide a half bandwidth of $\sim$300 cm^{-1} at signal reductions down to between 10^{-4} through 10^{-6} and transmit $\sim$75% outside the notch band. Super notch filters are narrower and steeper, delivering a half bandwidth of $\sim$100 cm^{-1}. They are also reduced to a factor of 10^{-6} but transmit a smaller percentage outside the notch band, and they are remarkably more expensive. The VHG is even narrower, providing a half FWHM down to as little as 15 cm^{-1}, which also reduces the Rayleigh line to a factor of 10^{-6} at the expense of further reduced transmission (at an increased price).[2]

Notch filters ultimately require illumination by collimated and polarized light to function properly. The center wavelength of the notch band can be moved by several nanometers by turning the filter around its vertical axis, which modifies the interference pattern relative to the beam. The result is that a standard notch filter will allow good measurements as close as $\sim$200 cm^{-1} toward the Rayleigh line on the Stokes side, whereas a super notch allows data well below 100 cm^{-1}, and a VHG may provide useful data near 10 cm^{-1}. These limits are adequate for most routine measurements. Because the holographic technique only works in certain materials, holographic Raman notch filters are only offered for 350–1100 nm; the available wavelengths for VHGs are even more limited.

The setup shown in Fig. 6.7 illustrates a standard excitation that is sufficient for the use of notch filters. The Raman signal emitted by the sample is collected by an efficient, color-corrected, photographic objective and sends the collimated light through the notch filter, which is placed in a precision rotary holder. A second lens system refocuses the light under the required angle into the entrance slit of the spectrometer. The two lens systems do not need to be identical but should provide the same cross-section (see Sections 6.2 and 6.4.3.4 of *Fundamentals*[2]). Beam magnification may be evident with different focal lengths of the two arms (see Section 1.6 of *Fundamentals*[2]). Efficient coupling techniques with mirrors are also available and have often been achieved. A tunable polarizer may be placed between both objectives and the notch filter. The one in front of the notch is used to adjust the (already strongly) polarized Raman signal to the needs of the filter, whereas the second turns the angle again to fit the spectrometer's preferred plane of polarization. The spectrometer may feature a focal length of 300−800 mm, depending on the required dispersion, resolution, and wavelength range. The detector is typically a well-cooled, low-noise, back-illuminated CCD that is often completed by a PMT. The PMT offers improved resolution and stray light suppression to allow measurements closer to the Rayleigh line. The advantage in stray light may be up to a factor of 30. If the full Raman range of 4500 cm^{-1} is required on the Stokes side, the maximum wavelength of the

laser is limited. A PMT will barely work above 900 nm, whereas a CCD will not exceed 1050 nm. That, in turn, limits the laser wavelength to ~750 nm for CCD detection and 640 nm if the PMT is used. Longer wavelengths are reserved for FT-IR systems. InGaAs arrays and similar integrating NIR detectors are very critical because of their high sensitivity to thermal background. InGaAs avalanche diodes work, but they only provide small active areas. In summary, there is no real alternative to FT-IR if NIR excitation is required.

Compare a system with 514.5-nm excitation, a 0.5-m spectrometer with triple gratings, and a CCD with 2048 pixels of 13 μm at a 26.6-mm length. To record 4500 cm^{-1} on the Stokes side (+155 nm) in parallel fashion, a dispersion of 5.83 nm/mm is needed. Theoretically, in a 500-mm spectrometer, the grating should have 320 mm^{-1}, which leads to a 300-mm^{-1} grating. The resulting bandwidth will be 1.9 cm^{-1}, and the resolution ~5.6 cm^{-1}. If a resolution of 1 cm^{-1} is required, a second grating of 1800/mm should be used. The bandwidth will then be 0.25 cm^{-1}, and the resolution will be 0.75 cm^{-1}. Using a PMT at a slitwidth of 20 μm produces a resolution of <0.5 cm^{-1}. A third grating can still be installed, but in the wavelength range reviewed, none with >1800 mm^{-1} are useful. On the anti-Stokes side, the system will work equally well with two limitations: the Raman signals will not be detected as close to the Rayleigh line (because of stronger scatter), and a grating optimized for the range around 350 nm will be used, which might be the third grating. There is a general limitation for anti-Stokes applications: notch filters show increasing absorption below 380 nm, which must be taken into account when planning the excitation and wavenumber interval. In short, the transfer efficiency (of a system like the one described) between the sample and detector is on the order of 20%. Compact, fixed Raman spectrograph systems with notch filters are also available in many variations. Because this book focuses on modular, flexible spectrometer systems, the compact systems are not discussed separately.

6.5.2.2 Double spectrometers versus single-stage systems

Figures 6.5 and 6.6 show the spectra of materials that require Raman data more than 100 cm^{-1} apart from the Rayleigh line and only in the Stokes range. However, many samples carry distinct information in the range between 0 and 100 cm^{-1}. To a remarkable extent, those samples can be analyzed with the help of the new VHG notch filters. The requirement for even-closer measurements is valid, especially in research applications, e.g., the amino acid L-Cystine, showing the Stokes Raman spectrum in Fig. 6.8.

Because a notch-filter-based spectrometer needs the perfect plane of polarization and collimation at the filter, followed by another optimization in front of the spectrometer, a reasonable amount of useful signal may be lost when the polarization and cone angle are adjusted. Assuming a transmission of 50% with a standard notch through all filter components (without

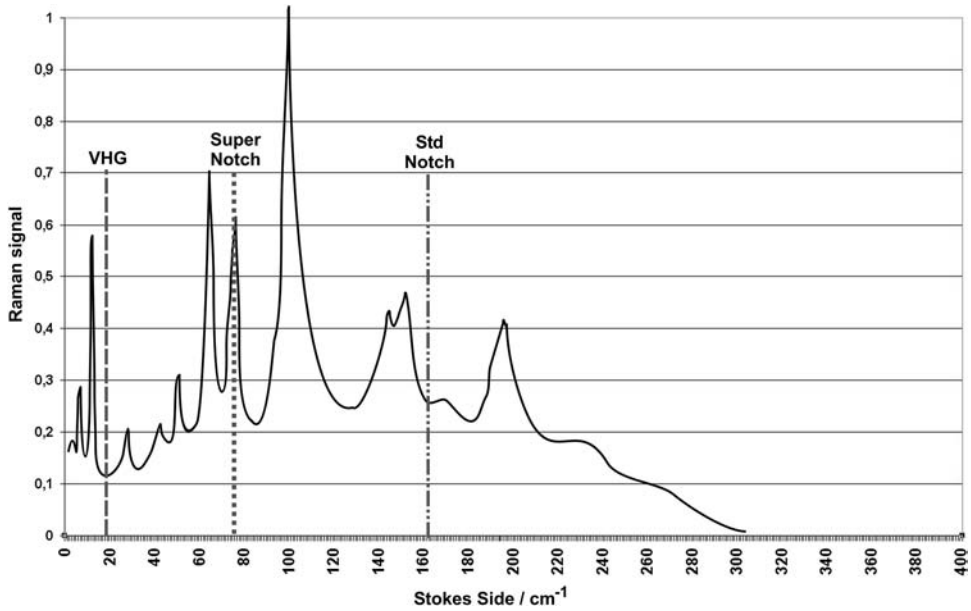

Figure 6.8 The limits of the different notch filters at the Raman spectrum of L-Cystine.

polarizer), and another 50% inside the spectrometer, the result is a total of 25%, which is also assumed for a double spectrometer with all parts required for proper operation. Thus, a double spectrometer may even be faster, especially if the filter must be narrower than the standard version can perform or if it needs optional polarizers.

According to Fig. 6.8, a standard notch filter will miss all important spectral information, whereas a perfectly tuned super notch filter still will block about half of the required spectral data. Even a VHG will not transfer the full spectrum to the spectrometer. If the real, nearby range below $\sim$20 cm^{-1} is required, multistage spectrometers are utilized.

The version shown in Fig. 6.9 is optimized for efficiency because it has a minimum of reflections. The sample excitation is as before, but now the bandwidth of the laser may be important, as may be seen when considering the resolution. The Raman signal emitted by the sample is now collected, transferred, and refocused by fewer components. A typical Raman double spectrometer has a focal length between 500 and 2000 mm, depending on the required dispersion/resolution (0.75 m is the most popular). Again, the favorite detector will be a well-cooled, low-noise CCD, completed by a PMT, because it reaches much closer toward zero wavenumbers. Thus, combined with multistage spectrometers, selected-and-cooled single-point detectors are frequently used despite the popularity of high-performance CCDs. The wavelength/wavenumber limits toward the NIR are like those in Section 6.5.2.1, whereas in the UV regime the limits are not defined by filters. In principle, and if only the Stokes side is required, a 193-nm excimer laser can

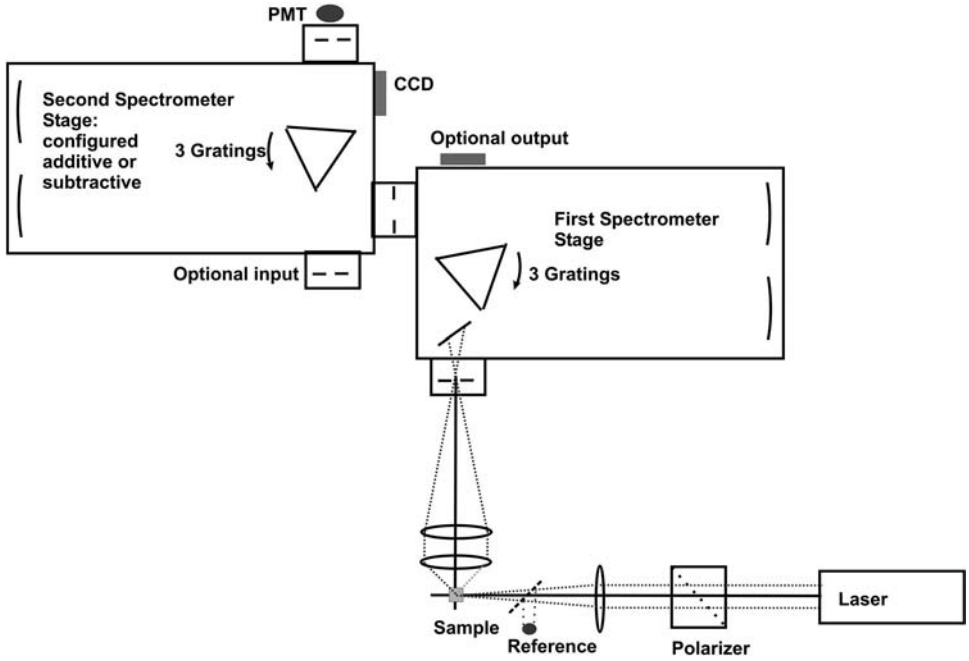

Figure 6.9 One of the many possible double-spectrometer versions.

be used for excitation (the advantages and disadvantages follow). Now compare a system with 514.5-nm excitation, a 1-m additive double spectrometer, and a CCD with 2048 pixels of 13 μm at 26.6 mm. To cover a 4500-cm^{-1} Stokes (or 155 nm) in parallel fashion, a dispersion of 5.83 nm/mm is required. The total focal length of the double system is 2000 mm, and thus gratings of only 80 cm^{-1} are required. These are available, but it does not make much sense to minimize the performance this way. A better solution creates overlapping spectral intervals with an automated chain of exposures. A grating of 300 cm^{-1} will eventually be chosen. Therefore, an interval will cover 1570 cm^{-1}, and three exposures will combine to 4500 cm^{-1}. The bandwidth will be close to 0.8 cm^{-1}, and the resolution will roughly be 2.3 cm^{-1}. In order to allow a high resolution, a second grating (perhaps 1800 cm^{-1}) will be added, which will result in a bandwidth of 0.11 cm^{-1} and produce a 0.33-cm^{-1} resolution. When a PMT is used with a 20-μm slitwidth, the resolution improves to <0.2 cm^{-1}. A third grating can be mounted on demand. On the anti-Stokes side, the system is not restricted and very useful, especially if an additional grating optimized to 350 nm is used.

The following discusses a problem inherent to additive double spectrometers: to illuminate the CCD completely, the required wavelength interval must pass through the intermediate slit. In the presented case, the intermediate slit must open to a width of 13.3 mm, which invites a rather-high stray light level to enter stage two, followed by a strong difference in Raman

performance between the PMT and CCD. In the visible wavelength region, the PMT will reach well below 10 cm^{-1} toward the Rayleigh line, whereas the CCD may only provide useful data down to ~50 cm^{-1}. The transfer efficiency between the sample and detector of a double spectrometer, as shown in Fig. 6.9, will be around 20%, assuming optimized gratings.

6.5.2.3 Stray light consideration

Stray light is a serious problem for all kinds of optical spectroscopy, particularly for methods dealing with scattering effects. (See Chapter 8 in *Fundamentals*[2] for further details.) Some key sources of stray light may be apparent; external stray light may enter from the environment, primarily from the experiment if, for example, the light of the excitation laser may not only reach the sample but also its nearby environment and be reflected or scattered there. The impact can be reduced by optimizing the transfer optics and masking the light path. If liquid samples are the object, care should be taken that no emission from the sample cell walls will enter the spectrometer. Spectrometers themselves create stray light internally, which is highly important for Raman measurements. Optimization of components in the optical path helps keep the contrast high. External and internal stray light is reduced by the following:

- High density of grating lines (the advantage increases roughly with the square function);
- Long focal length (the advantage increases roughly with the cubic function); and
- Serial arrangement of multiple spectrometer stages (the advantage increases exponentially).

Furthermore, small slit areas keep stray light away but at the expense of the luminosity and SNR. One more example: consider a 500-mm single-stage spectrometer with 1800 mm^{-1}, a PMT, and a CCD, looking for a Raman signal 100 cm^{-1} apart from the laser line at 514.5 nm, with a bandwidth of 1 cm^{-1} and a slitwidth of 30 μm. Using the PMT, the stray light level will be $\sim 3 \times 10^{-5}$, whereas the use of a CCD may be distorted by a stray light level of about 5×10^{-3}. Using the same components, combined with an additive double monochromator with 30-μm slits, the PMT measurement may only suffer from stray light of 10^{-7}. However, the CCD, combined with the wide intermediate slit required, may receive a level of 3×10^{-5}, which is depicted in Fig. 6.10.

The data shown in Fig. 6.10 are simulated and relate to an additive double spectrometer with a 1-m focal length, a grating of 1800 mm^{-1}, and a used surface of 100 × 100 mm (*f*/10) in the green spectral range. The *x* axis represents the distance to the laser line. Note that 100 cm^{-1} corresponds to roughly 2 nm only in the green range. The vertical scale is normalized to the linear working range of the different detectors. In monochromator mode, the

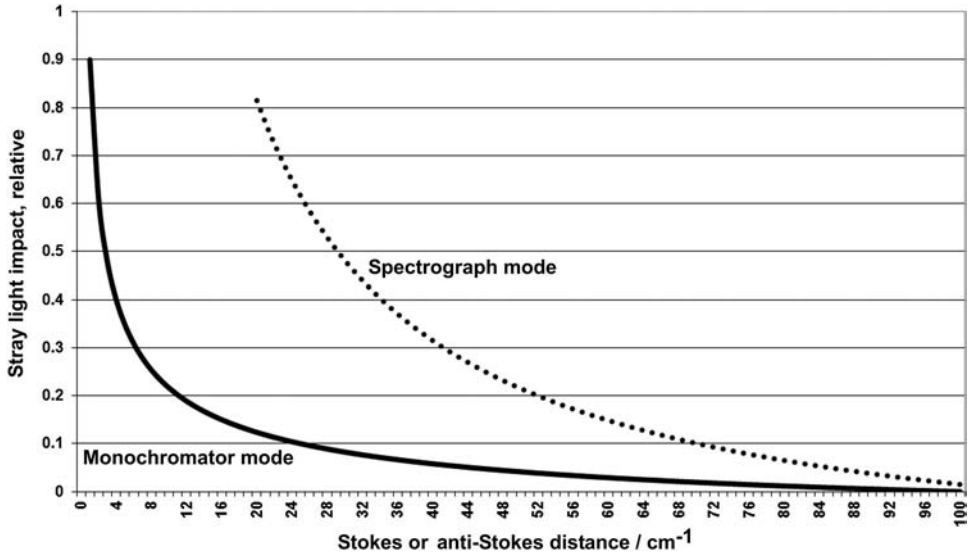

Figure 6.10 General impact of Rayleigh scattering on the signal of interest.

system is well suited to a distance of 10−20 cm^{-1} relative to the excitation. If the system is used as a spectrograph, a substantially larger distance is required. If the Rayleigh line is shifted toward longer wavelengths, both curves shrink to shorter distances. After excitation deeper in the blue or even the UV, the curves will spread significantly to larger distances. The figure shows that, overall, double spectrometers are much better suited to work as a monochromator than as a spectrograph.

6.5.2.4 Spectrometers for measurements extremely close to the Rayleigh line, Brillouin spectrometers

To analyze sample scattering from phonons (the Brillouin signal), data between roughly ±150 cm^{-1} must be recovered, which includes the extra challenge to acquire useful data within ±1 cm^{-1}. In Fig. 6.11, all three spectra have been excited at 514.5 nm but present a different axis in wavenumbers. Whereas the silicon spectrum (left curve) has a range of ±5 cm^{-1} (±0.13 nm), the LiF spectrum (center) only covers ±1 cm^{-1} (±0.025 nm), and the spectrum of ultra-pure water (on right) has an axis of only ±0.3 cm^{-1} (±0.008 nm). With the double spectrometers considered so far, measurements like that are out of reach. One solution to the application is to extend the focal length and combine it with an increase in the effective line density of the grating. If the system also works in double-pass configuration (see Section 4.3.1 in *Fundamentals*), data acquisition to almost zero wavenumbers is possible with both single-point and parallel detectors.

The heart of the system shown in Fig. 6.12 is an Ebert−Fastie double spectrometer with a focal length of 2 m, configured for double-pass operation

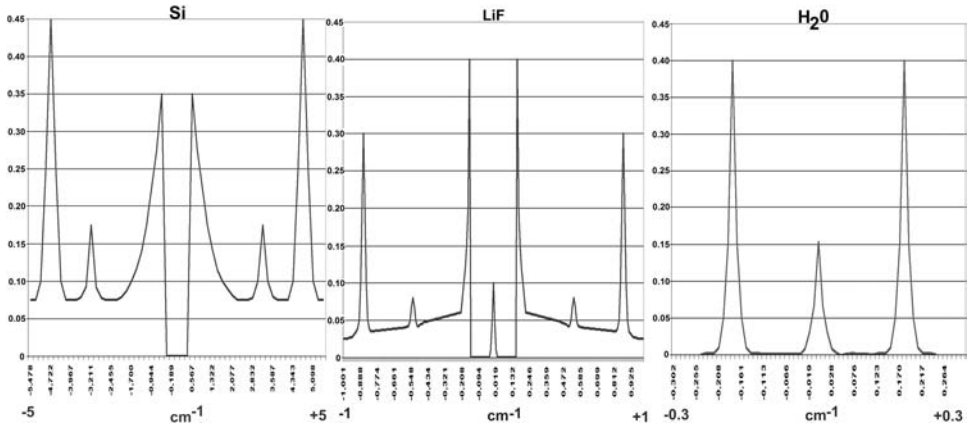

Figure 6.11 Three Brillouin spectra that require different instrument performance. The spectral recordings are reprinted with permission from SOPRA SA, F-92270 Bois-Colombes, France, via instruments in the "DMDP 2000" series.

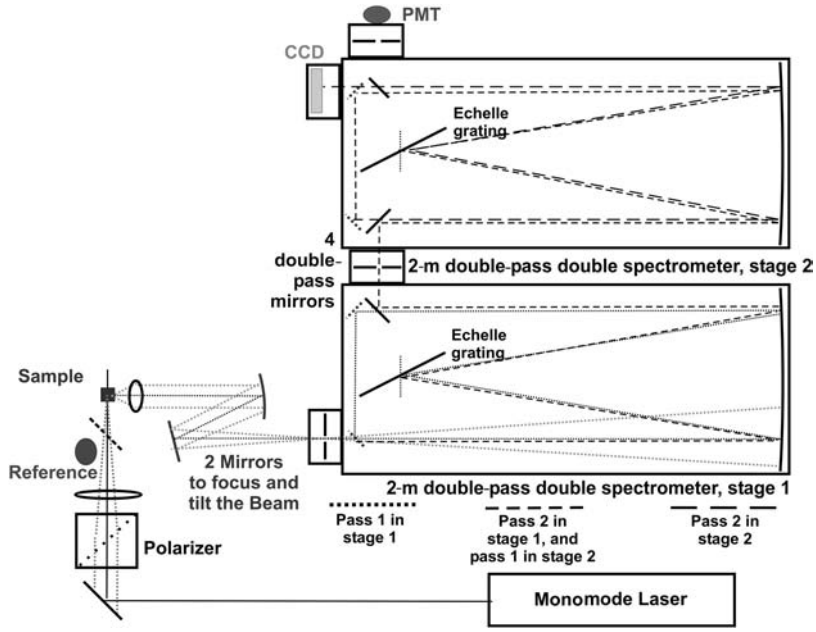

Figure 6.12 High-performance double spectrometer for extremely low wavenumber differences.

and equipped with Echelle gratings. Thus, the total focal length can be set to be 4 m or 8 m. The outcome is a tremendous resolution with extreme stray light suppression; it allows Brillouin spectra below 1 cm^{-1}. The Echelle grating may be chosen, for example, to provide 316 mm^{-1} at a blaze angle of 63 deg. Thus, it will always work very close to the blaze condition and cover

the range of 200−1100 nm, working in spectral orders 29 (UV) through 5 (NIR). At 514.5 nm, it will run in the 11th order, which, in turn, leads to the effective line density of 3476 mm^{-1}. The dispersion in a double spectrometer/single-pass mode then increases to 1.12 cm^{-1}/mm, or 0.03 nm/mm. An additional benefit is improved stray light suppression compared to common systems. The grating's illuminated area is 110 mm × 110 mm, providing an aperture of *f*/18, or $\omega = 0.03$. The silicon spectrum in Fig. 6.11 (left curve) was recorded with a PMT detector in scanning mode. Even though solid state samples distribute an extremely high level of Rayleigh scattering, the shutter (to save the detector) was only closed between ±0.6 cm^{-1} (corresponding to ±15 pm).

The spectrometer features a useful slit height of 40 mm; however, it cannot be utilized in Raman applications due to the lack of suitable detectors and due to the sample illumination, which will not cover that height. However, 20-mm-high PMTs with superb detection limit and sensitivity and low-noise CCDs are available. The slits are curved to provide optimal resolution, which requires special read-out modes for 2D-CCDs, to maintain optimal resolution and efficiency. A system like this will have a transfer efficiency of ∼20% throughout the working range—a benefit of Echelle gratings.

Measurements remarkably closer to the Rayleigh line are produced after the system is switched to double-pass configuration. It then has a total focal length of 8 m. The slit height is reduced to 20 mm, which is no longer in the slit center. The upper half of the slits is occupied by the double-pass mirrors, and therefore both the center of illumination and the detector must move down 10 mm. Because the incoming light beam must still hit the middle of the Ebert mirror, the beam travels upward under an angle of 2.8 deg.

The change from single to double pass (and vice versa) and the changes in beam travel can be organized either manually by micrometer drives or automatically by stepper motors. In either case, after both positions are adjusted, it is a quick and reproducible change.

The central and the right spectra in Fig. 6.11 were recorded in double-pass (DP) mode. The dispersion is 0.4 cm^{-1}/mm (10 pm/mm). The bandwidth, at a slitwidth of 50 μm, is 0.02 cm^{-1} (0.5 pm). The LiF, a strong Rayleigh scattering material, was recorded in the range of ±1 cm^{-1} (±25 pm) with the shutter closed between ±0.15 cm^{-1} (±3.5 pm). After that, and in a different measurement, the maximum of Rayleigh scattering was registered and added to the graph by the small peak in the middle. Its magnitude is 10^{12}-fold over the LiF signal; in other words, the stray light suppression of the system at a distance of 5 bandwidths (0.1 cm^{-1}) from the center of the disturbance is 10^{12}. The spectrometer also works with parallel detection, like a CCD, where it illuminates an area of 20 mm × 20 mm because the intermediate slit can be opened to 10 mm. Due to the high dispersion in double-pass mode, 11 cm^{-1} (0.3 nm) at a very high resolution will reach the detector. In single-pass mode, the interval is 22.5 cm^{-1} (0.6 nm). The ultimate resolution performed by such an instrument in double-pass scanning mode is shown on the right of

Fig. 6.11: the Brillouin spectrum of ultra-pure water, a common test object for instruments of that class. To avoid Rayleigh signals from the walls of the sample cell, the cell was masked on all four sides. The spectrum was recorded with a slitwidth of 20 μm (a bandwidth of 0.008 cm^{-1}, or 0.2 pm). The remaining Rayleigh scattering from the water itself has a footwidth of 0.06 cm^{-1} or covers 6 bandwidths at half height. An Echelle double-pass double spectrometer has a throughput of ~7%. An estimate of the Rayleigh scattering's impact on the signal of interest is shown in Fig. 6.15.

6.5.2.4.1 The free spectral range of Echelle spectrometers

The only identifiable disadvantage of Echelle systems is the overlay of different orders. The free spectral range (FSR) near the 514.5-nm wavelength in the 11th order is ±23.4 nm, according to the following equations:

$$m \times \lambda = k \times (\sin \alpha \pm \sin \beta), \tag{6.1}$$

where m is the spectral order of diffraction; λ is the wavelength; and k is the distance between the structures (inversion of mm^{-1}), also called the "grating constant;"

$$FSR = \lambda/m; \tag{6.2}$$

and, more precisely,

$$FSR = \lambda_2\lambda_1, \text{ and } \lambda_2 = \lambda_1 + (\lambda_1/m), \tag{6.3}$$

where λ_1 is the lowest wavelength with noteworthy light intensity in the system, λ_2 is the highest wavelength without order overlay, and m is the used spectral order.

6.5.2.4.2 Alternative solutions for the ultra-near wavenumber range, and history

After single-mode lasers that allow excitation bandwidths below 0.001 cm^{-1} became available, several different spectrometer approaches were developed for extremely high resolution. All offer adequate performance for the nearby scattering region. In the 1970s, state-of-the-art systems were additive, triple spectrometers or double spectrometers with a 3–4-m total focal length. At that time, Raman measurements were almost only operated in scanning mode, and the standard detector was a cooled, photon-counting PMT. The culmination of that development was the system described so far, with a 4- or 8-m total focal length and a light path of up to 32 m. It was developed and manufactured in France since the mid-1980s and worked with single-point and parallel detectors up to 20 mm wide, which can still be considered "state-of-the-art." Unfortunately, the system has been phased out.

Interference spectroscopy was developed parallel to dispersing instruments, primarily supported by computer-based Fourier-transform infrared (FT-IR). FT-IR has more or less completely replaced dispersing apparatus for molecular analytics above a 2-μm wavelength because they provide a higher

resolution in less time. In NIR Raman spectroscopy, FT-NIR dominates over dispersive techniques. An ultra-high-resolution FT Raman and Brillouin system for low wavenumbers, working in the visible range, is available that delivers similar resolution and contrast as the described Echelle system. The limiting factor that is the general disadvantage of Michelson or Fabry–Pérot interferometers is overlay of spectral orders. To achieve a high resolution comparable to a monochromator, the interferometer requires a long internal pathlength. As opposed to dispersing spectrometers, this feature lets the orders move closer together. With increasing resolution, the problem of order overlay increases, too. High-resolution interferometers provide only a very small FSR and thus a small number of wavenumbers in the visible range. Consequently, the FT system is only used for Brillouin spectroscopy in the range of very small wavenumbers. The order problem is also a major reason why FT interferometers were not successfully marketed in the UV–Vis range.

6.5.2.4.2.1 The multi-Echelle grating spectrometer A similar yet remarkably different construction of the double-pass double monochromator (DPDM) is the "multi-Echelle grating apparatus" (MEGA), designed by a group of Swedish scientists. It also realizes four diffraction processes. To the knowledge of the author, the design was never actively marketed, but some specimens are used in European research labs. The main difference between the MEGA and DPDM is the absence of both mirrors between the gratings and the intermediate slit. The system has been realized with a 0.5-m (*f*/4.5) and 1-m (*f*/9) focal length, which is also the distance between gratings.

The beam travel illustrated in Fig. 6.13 appears rather simple. The design accepts grating angles between 45 deg (dark-grey position) and 80 deg (light-grey position), which is compatible with Echelle dispersers. The side entrance and exit may be used for grating adjustments because a laser beam introduced from the side will pass through the center axis of grating rotation. The main advantages and disadvantages compared to the DPDM: If the same gratings are used in both designs and operate identically in the same focal length, the dispersion is the same. In an Ebert–Fastie instrument, the resolution and image quality primarily depend on the mirrors. Small flaws in the grating surface are tolerated. In the MEGA, both parameters depend solely on the grating quality. The throughput will be reasonably higher—up to 26% instead of perhaps 7%—because the MEGA only incorporates 6 reflections, compared to 18 with the DPDM. In terms of stray light, the DPDM is the clear winner. It features two separate compartments, the intermediate slit, and the rays need to travel longer distances, which increases the probability of unwanted rays leaving the accepted path.

6.5.2.5 Triple spectrometers, the work horses of Raman and Brillouin spectroscopy

Not every laboratory will be equipped with climate control and anti-vibration equipment, which are required for the optimal operation of a system for ultra-

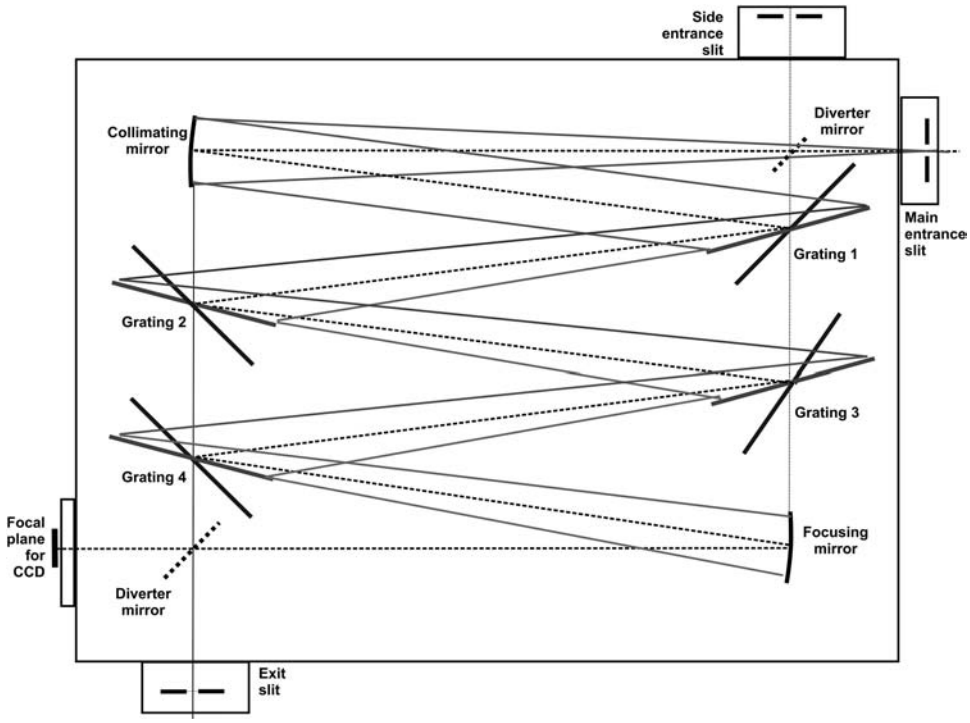

Figure 6.13 Beam travel in the multi-Echelle grating spectrometer.

near scatter applications. On the other hand, the basic measurements for interference-free data within ± 1 cm^{-1} can be given to labs with the machinery. For all other Raman and Brillouin experiments, the best-suited system is a flexible and universal triple spectrometer. Figure 6.14 shows an actual high-performance system that perfectly matches the modes of a spectrograph and monochromator.

This system features the choice of configuring the first two stages for additive or subtractive dispersion. The focal length of the stages is typically 0.5−0.75 m, whereas the pre-stages may have a shorter length than the third one. This discussion here begins with stage three. In the optimal case, it will have an extra entrance that may be used for a fiber optic light guide and notch filter for measurements beyond 100 cm^{-1}. By reducing the number of reflections inside the spectrometer, the throughput and SNR will strongly increase. The main detector will be a highly efficient 2D-CCD completed by a PMT for the highest-resolution measurements or acquisitions that are ultimately close to the Rayleigh line. Depending on the applications, the three gratings may support the wavelength range from 200−1100 nm. The optimal selection could be 2400 mm^{-1} for 200−450 nm, 1800 mm^{-1} for 400−800 nm, and 1200 mm^{-1} for 700−1100 nm. If only one excitation wavelength will be used (e.g., 514.5 nm), the alternative grating selection

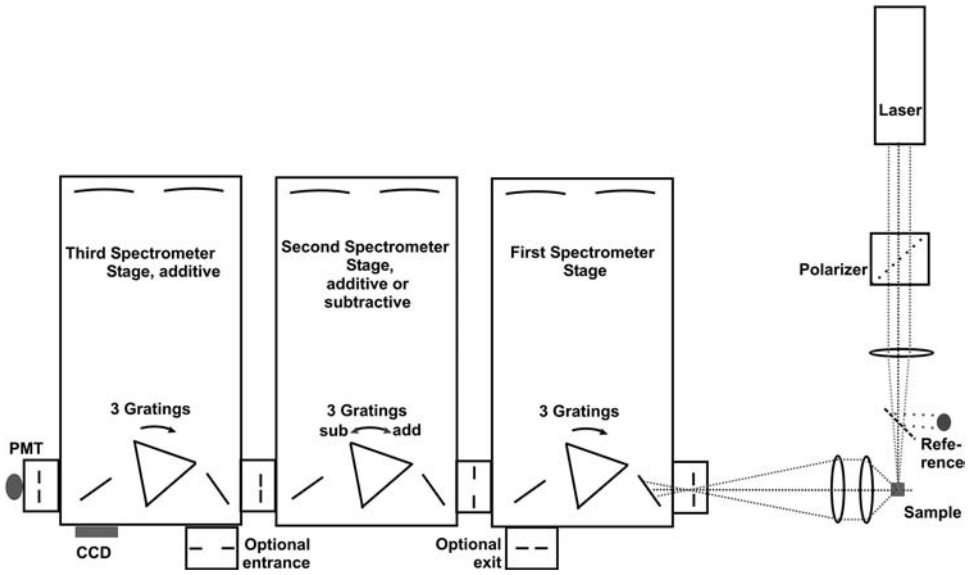

Figure 6.14 A modern, flexible triple spectrometer, equally suited for use as a spectrograph and a monochromator.

could be chosen for three different dispersions. With a focal length of 75 cm for all three stages and subtractive operation,

- 1800-mm^{-1} gratings: reciprocal dispersion RD = 0.61 nm/mm, or 23 cm^{-1}/mm (with a 25.4-mm interval, 580 cm^{-1});
- 600-mm^{-1} gratings: RD = 2.06 nm/mm, or 77.7 cm^{-1}/mm (with a 25.4-mm interval, 1970 cm^{-1}); and
- 150-mm^{-1} gratings: RD = 8.35 nm/mm, or 314 cm^{-1}/mm (with a 25.4-mm interval, 8000 cm^{-1}).

Thus, 150-mm^{-1} gratings would allow one to acquire the Stokes and anti-Stokes simultaneously at a relatively low resolution. The two pre-stages are prepared for alternating tasks. In additive mode, they best reduce the stray light and help produce the maximum resolution. In subtractive mode, they will illuminate the final stage the best for CCD detection. First, consider all three stages equipped with identical gratings for the green range and additive mode for PMT detection. The following typical parameters are found for a set of 1800-mm^{-1} gratings: RD = 0.2 nm/mm, or 7.6 cm^{-1}/mm. At slitwidths of 25–50 μm, the resolution will be 9.3 pm, or 0.35 cm^{-1}. The system will then allow data acquisition as close as 0.5 cm^{-1} toward the Rayleigh line, as shown by the dashed green curve in Fig. 6.16. If the scan crosses the Rayleigh line, the shutter will be closed to protect the detector. For operation with parallel detection, the two pre-stages will be configured subtractively.

Not all triple spectrometers on the market are designed for both modes, or else the reconfiguration may be complicated. This fact might affect the decision at purchase. Furthermore, the reviewed system can be used as single-stage spectrograph. In addition to general applications, it acts as a Raman system with a notch filter at the extra entrance. In any case, the detector considered here has 1340 pixels 20 μm wide and 400 pixels tall, making an area of 26.8 mm × 8 mm. The resulting parameters are a recovered interval of 16 nm, or 612 cm^{-1}, and a resolution of 36 pm, or 1.3 cm^{-1}. The entrance slit of the spectrograph stage will lead to the optimal resolution at a slitwidth of 40 μm. The slits of the pre-stages are set such that slightly more than an interval of 612 cm^{-1} enters stage three. If a wider range than the 600 cm^{-1} must be acquired, the system will automatically do that with a "step and combine" mode that moves the spectrometers accordingly and fits the acquired data. It will not often hurt the CCD if the Rayleigh line comes into view because CCDs have a high tolerance level. Indeed, in the CCD, the quantum wells may break down in strong-overload situations. In that case, the pixels will distribute their charge carriers not only toward the register but in all directions, which is called "blooming" and produces useless data. Although one or two "clean" cycles will repair the disturbance without residual, it is much better to avoid dangerous illumination. An example is presented in Fig. 6.15, taken with the triple system reviewed. The subtractive spectrograph mode with gratings of 1800 mm^{-1} provides useful data as close

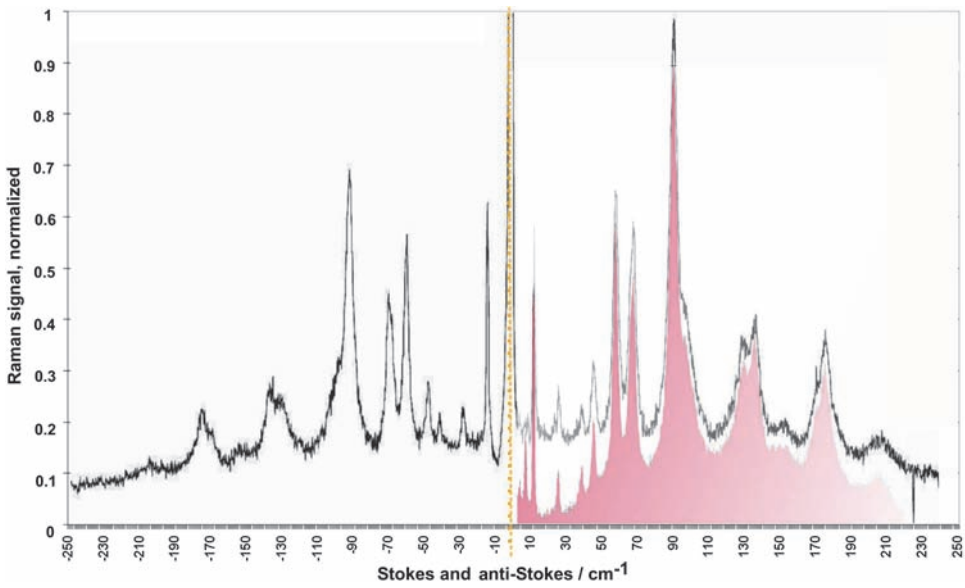

Figure 6.15 Performance of a modern triple spectrometer recording both wings at once. The L-Cystine spectra are reprinted with permission from Spectroscopy & Imaging (S&I) GmbH, D-59581 Warstein, Germany, via instruments in the "Tri-Vista" series.

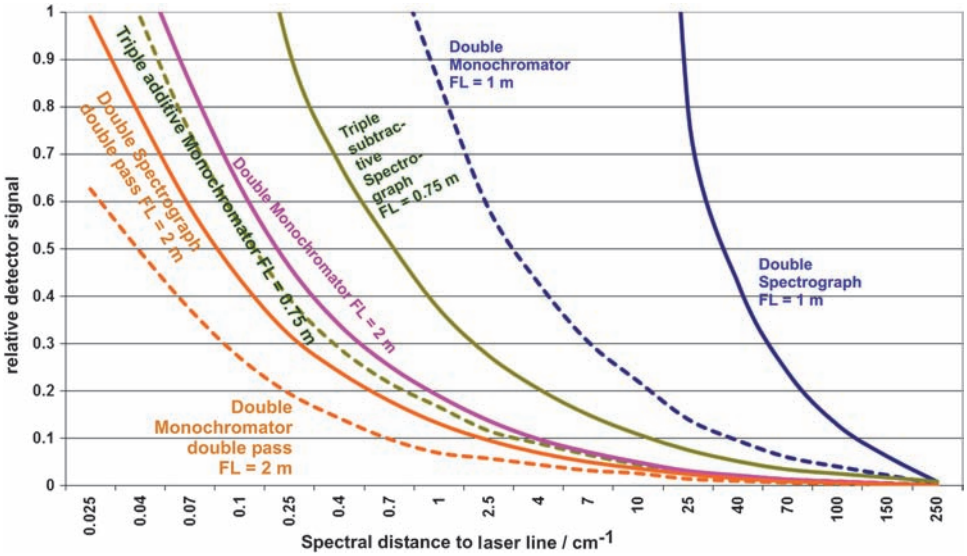

Figure 6.16 Estimations of the impact of Rayleigh scatter in some typical Raman spectrometer configurations.

as ~3 cm^{-1} relative to the Rayleigh line. A triple spectrometer in the "side-to-side" configuration shown in Fig. 6.13 has a throughput of ~8%.

L-Cystine is a dimetric amino acid that is suitable for testing Raman spectrometers because the Stokes and anti-Stokes wings differ slightly: the spectrum has strong and narrow structures, requiring a high resolution. The wanted scattered signals reach as close as 3 cm^{-1} beside the Rayleigh line on the Stokes side. Furthermore, a small, nonspecific, wideband Raman background from the solvent is present. Both spectra have been excited at 488 nm and are recorded by a 750-mm subtractive triple CCD spectrometer, as described earlier. With the 1800-mm^{-1} grating, the parallel-detected interval is 660 cm^{-1} at a resolution of 1 cm^{-1}. While measuring the red curve, the spectral adjustment of the slits is such that the Rayleigh line is kept just out of the interval, which is transferred into the third stage. The spectral lock-out distance was 2 cm^{-1}. The measurement of the white curve, covering the anti-Stokes and Stokes wings, was performed by a single CCD exposure. The Rayleigh line (yellow dashed line) scatters within ± 2 cm^{-1}, and the shoulders of the Rayleigh peak quickly return to the baseline. Nevertheless, and despite its manifold overload signal, the residual does not disturb the regions of interest. The different Raman background of the two data sets is due to the different sample preparation, not a malfunction. It has been proven that the continuum under the peaks is Raman or Brillouin (not a fluorescence signal) because of its presence on both sides. If it were fluorescence, it would be absent in the anti-Stokes wing, drawn to the left from center.

6.5.2.6 Estimation on the impact of Rayleigh scattering in different systems

The curves in Fig. 6.16 demonstrate the error in the output signal due to Rayleigh scattering. In other words, as soon as the value is above 0.5, no reasonable measurement can be expected. All curves are estimations that result from one's own measurements and experience, publications of instrument manufacturers, and user reports. The curves are valid for the wavelength region between 450 and 650 nm. If the excitation wavelength (and hence the Rayleigh signal) moves toward the UV, the shape of the curves will remain but reach critical values already at more distant wavenumbers because of the increasing photon energy. At 300-nm excitation, the distances will probably experience growth by a factor of 8. If the Rayleigh line is shifted toward the NIR, the distance in the wavenumber regime will decrease with the function of photon energy. At 750 nm, the curves may appear five times closer to the Rayleigh line.

The solid blue curve represents a 1-m double spectrograph with 1800-mm^{-1} gratings and an intermediate slit 10 mm wide. The dotted blue curve is the same instrument in a monochromator configuration. The solid green line shows a 0.75-m triple spectrograph with subtractive pre-stages, whereas the dotted green one presents the same system in additive triple monochromator mode, again equipped with 1800-mm^{-1} gratings. The solid pink curve shows a 2-m Echelle double monochromator in a single-pass setup; the 316-mm^{-1} gratings are in the 11^{th} order. The solid orange curve is the 2-m Echelle double spectrograph in double-pass mode (a total of 4 passes) with an intermediate slit 10 mm wide. Finally, the dotted orange curve represents the 2-m Echelle double system in the ultimate four-pass monochromator setup.

6.6 Special Raman Methods

6.6.1 Raman versus fluorescence

Unfortunately, the Raman and fluorescence overlay each other rather often. Many biologically and chemically relevant substances are excitable for luminescence in the wavelength range between 200 and 600 nm; the emission is often found between 400 and 700 nm. Thus, if Raman is excited below 600 nm, a good chance exists to find luminescence signals in the Stokes Raman window. If they appear, they are often stronger than the Raman signals.

Discrimination is possible by several methods. Luminescence emission is stationary in wavelength, independent from the excitation wavelength. The shape of the curve and the magnitude may vary, but the center wavelength will remain. If a laser with several lines is used, one can separate both effects with deconvolution algorithms. It is also helpful that in 99% of cases the luminescence will not be found in the anti-Stokes spectrum [exceptions are luminescence signals based on the two-photon effect (upward conversion)].

A common method to avoid luminescence is elusion into the NIR. Still, in spite of the declining Raman signal toward the IR, some materials fluoresce there, e.g., the luminescence and Raman of III-V compounds. They are excited and emit in the NIR range, and create very narrow-banded luminescence spectra that may easily be interpreted as Raman. It may sound paradoxical, but there are ranges in the UV that allow luminescence-free Raman measurement. The scenario needs some comparison of luminescence data, but it can be worth the effort (see Section 6.6.3).

6.6.2 NIR Raman

A popular method to avoid disturbance by luminescence is to shift the excitation into the NIR. Suitable diode lasers are available between 670 and 780 nm. How far the excitation can be moved into the NIR is defined by the maximum Stokes wavenumber difference required for recording. The SNR will suffer from the fact that Raman intensity follows the excitation photon energy with eV^4. Changing from 514.5 nm to 775 nm results in a signal reduction by about a factor of 5. On the contrary, the spectrometer will benefit because the relative bandwidth (nm per cm^{-1}) increases (wider slits for the same resolution), whereas the Rayleigh scattering decreases by the same amount as the signal itself. Nevertheless, there are still luminescent phenomena in the NIR. Lanthanides are excited between 600 and 800 nm and emit up to ~1200 nm. The fluorescence of 3/5 semiconductor materials, such as indium-gallium-arsenide (InGaAs), reach even further into the NIR. Both material families create sharp emission signals with a narrow bandwidth, which are easily confused with Raman. Thus, in case of suspicion, it is advantageous to correlate the data from different excitation wavelengths and record the anti-Stokes signal, too. Almost all manufacturers of FT-IR spectrophotometers offer accessories for Raman applications; the common excitation source is a 1064-nm Nd:YAG laser. With increasing wavelength, the probability of luminescence decreases, but the Raman signal also drops. In comparison to 514.5 nm, the Raman intensity at 1064 nm shrinks to ~1/15. Further aggravating the situation, the efficiency and the detection limit of NIR detectors is far less than that of a PMT and CCD. Finally, interference spectrometers work with smaller entrance apertures compared to dispersive instruments. In short, it results in longer measurement times and reduced detection limits.

6.6.3 UV Raman

Raman in the UV has the obvious advantage of radically increasing the Raman intensity due to the eV^4 increase, which at 250 nm produces a factor of ~20, compared to 500 nm. Unfortunately, the same is true for the Rayleigh intensity. A severe problem is that the slitwidth (to get the same bandwidth in cm^{-1}) of a grating with the same line density must be cut into halves, which leads to a strong loss in luminosity. Thus, UV-optimized spectrometers

feature longer focal lengths, and gratings of 2400 mm^{-1} or more, or Echelles. All instruments, shown in different figures, are UV compatible except Fig. 6.7, the notch filter system. UV excitation features some advantages. There is a good chance of achieving resonance Raman conditions (Section 6.6.5) or finding a "fluorescence gap," i.e., the wavelength interval between the luminescence excitation and the emission departure. Many substances start emitting above 330 nm. 4500 cm^{-1} at an excitation wavelength of 300 nm corresponds with ~45 nm. In short, fluorescence-free conditions are often found at Raman excitations below 300 nm.

6.6.4 Raman microscopy

Raman microscopy is more of an imaging method[3] than a spectroscopic one. In most cases, a hyperspectral system will be used (see Section 4.5 of *Fundamentals*[2]), which can record spectra, as well as an imaging method to recover the distribution of signals within a small wavenumber interval (a Raman band) over the sample surface. In the first step, a notch filter in front of a single-stage spectrometer with relatively low resolution will be set such that the CCD at its output will record the spectral distribution from the surface. The size of the area is defined by the microscope objective and probably additional cover blades. Best-suited CCDs are square shaped for that application. After the spectrum has been recorded, the user chooses the wavenumber range that would be analyzed for its spatial distribution. At this time, two technical solutions are offered. In the first version, the system moves the spectrometer out of the beam and replaces it with a bandfilter, which transmits the selected wavenumber range directly to the CCD. Therefore, the spatial distribution of the selected band will be imaged at the CCD. In the second version, the system keeps the spectrometer in place and modifies its settings. The entrance slit will be replaced by a square aperture. The grating ensures that only the rays of a certain spectral interval hit the CCD, whereas the spatial distribution in the entrance is transferred 1:1 to the detector. In that case, the horizontal position is convolved with the wavelength distribution.

6.6.4.1 Confocal Raman microscopy

A confocal system, such as that shown in Fig. 6.17, is based on aligning several optical apertures to the same axes, which effects a strong suppression of light signals outside the viewed area and an extremely reduced depth of focus. Thus, the field of interest is closely defined. Several different designs have been created to reach that goal; the one provided here is one example. A confocal system designed for Raman is also useful for luminescence, in principle.

6.6.4.1.1 Principle of confocal Raman systems

In order to analyze the Raman answer of a very small area with extreme sharpness and concentration on the evaluated area, a confocal technique is

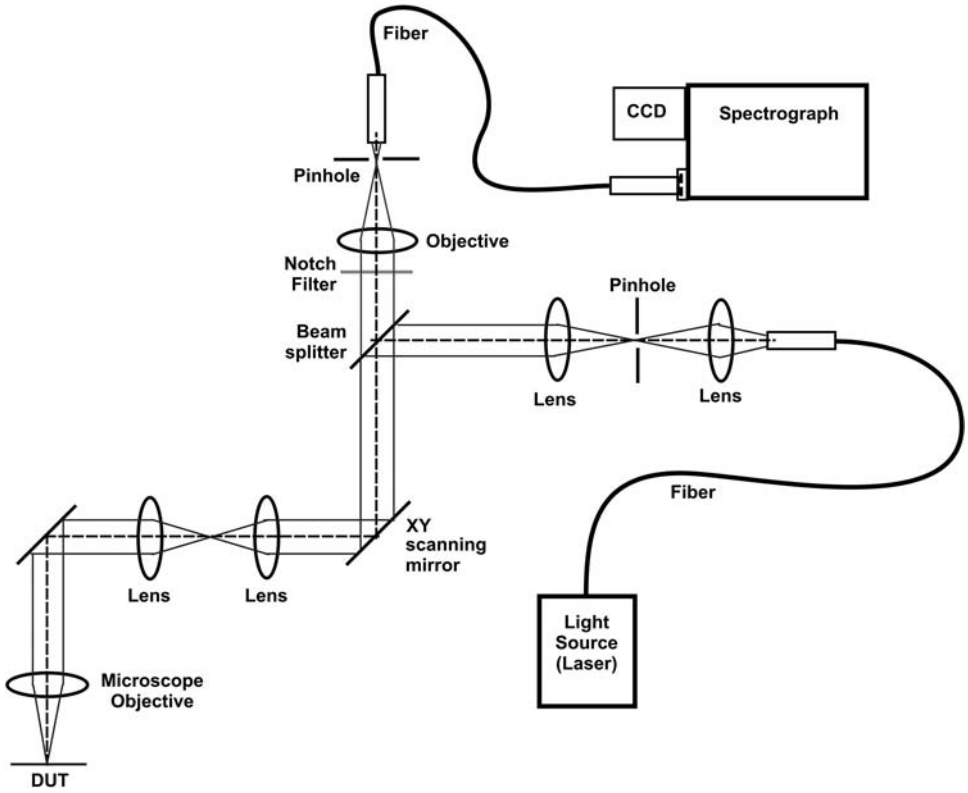

Figure 6.17 Confocal scanning microscopy Raman spectrometer.

applied. The confocal effect reduces the influence of light outside the wanted area twice. A precise transfer of the illumination light via pinholes ensures the reproduction of the viewed spot on the sample surface. The diameter typically is a few microns. The light source of choice is a laser because it allows the best refocusing and the required light density. Typical laser light allows parallel light transfer and a high optical numerical aperture, which guarantees an extremely short depth of field at the sample. The signal emitted by the sample is transferred along the same path until it reaches the beamsplitter. After that is passed, the signal hits the output pinhole before it reaches a fiber line to the spectrograph. Both pinholes are perfectly aligned to the identical optical axis and have the same size, which provides extremely sharp geometric filtering in all three dimensions on the sample surface. The scan over the surface of the sample is realized by a stepper-motor-driven mirror that deflects the beam in both axes. Naturally, only a rather small area can be addressed, defined by the optical performance of the objective systems. Due to the high spatial resolution, a large number of spectra can be created from a sample. Each may provide a Raman spectrum; if not, the system only looks for one or a few spectral lines. Between the beamsplitter

and refocusing objective is a notch filter to remove the excitation line from the measured spectrum. It is understandable that the recovered Raman signals are very weak. If a CCD is used for detection, rather long integration times may be required. If single-point analysis is preferred, photon-counting and correlation techniques for background suppression are commonly used. Confocal Raman systems are suitable for other applications with rather little modification, e.g., fluorescence, correlation techniques, applications with capillaries, reflection, etc.

6.6.5 Resonance Raman (RR)

If the excitation wavelength is near the absorption maximum of the substance under investigation, the intensity of the Raman signal will rise drastically. Signal enhancements of up to 10^6 have been reported. The reason is the increased molecular vibration in the sample during the absorption process. Thus, two effects of excitation support each other and lead to enhanced emission. Because the absorption bands of the different substances are distributed over the whole spectrum, RR is found in the whole range, most likely in the UV.

6.6.6 Surface-enhanced Raman scattering (SERS)

The enhancement effect occurs in microscopically small solid state substrates, which include a very small concentration of the material of interest. The basic principle is supported by the assumption that a solid conglomerate of low concentration remains in an inert substrate. If the excitation is provided by intense laser light, an electronic communication between the single atoms will occur. The plasmons will be excited much more easily than in bulk layers and therefore respond more strongly. Measurements of single molecules have been reported. According to the published data, the signal increase (compared to bulk material) can reach up to 10^6. When the scene of excitation expands from the surface deeper into the sample, the response will become "normal" after only a few molecular layers.

6.6.7 Coherent anti-Stokes Raman spectroscopy (CARS)

CARS is a nonlinear method that is only applied to gases. It permits contactless temperature measurement in small sample volumes, inside a cloud of gas. CARS[4] was developed around 1970 and was the standard method for 20–30 years in the research of thermal processes in flames and combustions. Practically all car and motor manufacturers had a "glass motor" for CARS applications. Since the mid-1990s, the method was increasingly replaced by laser-induced fluorescence (LIF), which works with a simpler setup and requires less data crunching for comparable results. A CARS system needs

- two laser excitation beams,
- beam steering to control and change the place of excitation within the sample,

- collection optics for the Raman light,
- a spectrograph with a gated line or area detector, and
- special data-reduction programs.

The signals from the two lasers must be pulsed and must impinge the volume of interest at the same time. Some systems use a 355-nm excimer laser with a 10-ns pulsewidth; its signal is called the pump signal. It pumps the sample molecules and the second source, a dye laser, as well. The dye laser's emission is shifted toward longer wavelengths. It also has a 10-ns duration and is called a probe beam. By varying the optical pathlengths of the two beams, the coherent arrival inside the sample volume is arranged, which leads to nonlinear effects that create Raman signals. These effects are found at higher photon energies than both lasers—on the anti-Stokes side of the pump laser. The detector is gated synchronously, and thus it is only illuminated during the 10-ns period. Complex algorithms calculate the temperature. In addition, the gas components and compounds present in the volume are analyzed. Because the experiments are turbulent, one data point is usually created by an average number of single measurements. The pulse rep rate is in the millisecond regime. For applications that involve explosions, the progress of the explosion itself must be correlated with the pump laser and the detector gate to acquire the required point of time.

References

1. P. W. Milonni and J. H. Eberly, *Lasers*, John Wiley and Sons, New York (1988).
2. W. Neumann, *Fundamentals of Dispersive Optical Spectroscopy Systems*, SPIE Press, Bellingham, WA (2014) [doi: 10.1117/3.1002528].
3. E. Smith and G. Dent, *Modern Raman Spectroscopy: A Practical Approach*, John Wiley & Sons, New York (2009).
4. S. Mukamel, *Principles of Nonlinear Optical Spectroscopy*, Oxford University Press, Oxford, UK (1999).

Chapter 7
Spectrometry of Laser Light

7.0 Introduction

This chapter deals with lasers as a light source and tool, not their design, construction, or specifics. It also does not address any specific application performed with lasers as the primary light source. Both issues are supported by a wealth of literature, including an easy-to-read introduction.[1,2] Therefore, the lasers are reviewed with respect to their future use and application details. Because the product group of lasers provides very different parameters, different equipment may be required to analyze their emitted light. Large variations are found in all parameters:

- the wavelength range reaches from the vacuum UV into the far-IR;
- the number of discrete emissions can be a single line, lots of lines, or so many lines that they melt together;
- the bandwidth of the signals reaches from subpicometers to several hundred nanometers;
- the signal may be steady state or pulsed (if pulsed, the pulsewidth can reach from subpicoseconds into the microsecond regime);
- the rep rate of pulsed lasers may be found to be less than 1/s, up to megahertz;
- the optical power covers microwatts through mega- or even gigawatts;
- the spectral distribution of the signals may be Gaussian, Lorentzian, or a different shape;
- the area illuminated by a laser may be tiny and circular, cover a rather-large circle or square, or show different dimensions in both directions (slab-shaped); and
- the homogeneity, the collimation, and the polarization of the light may be very different and change within the first millimeters after leaving the primary laser source (near field/far field).

Reviewing that rough list shows that rather-different spectroscopic instrumentation may be required to measure the parameters wanted. Table 7.1 lists a subset of laser parameters.

Table 7.1 Some key parameters of popular lasers.

Laser Type	Operation	Prominent Wavelengths [λ/nm]	Typical Beam Cross-Section [mm]	Typical Bandwidth*** [ν/λ]
Excimer (F_2)	pulsed	157	50 × 50	0.7 GHz / 0.1 nm
Excimer (Ar-F)	pulsed	193	50 × 50	0.7 GHz / 0.15 nm
Excimer (Kr-F)	pulsed	248	50 × 50	0.7 GHz / 0.2 nm
Excimer (Kr-Cl)	pulsed	308	50 × 50	0.7 GHz / 0.25 nm
Excimer (Xe-F)	pulsed	351	50 × 50	0.7 GHz / 0.3 nm
He-Cd	cw	325	2	0.2 GHz / 0.06 nm
	cw	442	2	0.2 GHz / 0.1 nm
Argon-Ion, DUV	cw	248–275 (some)	0.5–2.0	0.1 GHz / 0.2 nm
Argon-Ion, UV	cw	333–370 (some)	0.5–2.0	50 MHz / 0.05 nm
Argon-Ion	cw	488	0.5–2.0	10 MHz / 8 pm
	cw	514.5	0.5–2.0	10 MHz / 7 pm
	cw	647.1	0.5–2.0	10 MHz / 12 pm
Copper-Vapor	pulsed	510	0.5–2.0	10 MHz / 7 pm
He-Ne	cw	632.8	< 1	1 MHz / 2 pm
Ruby	cw	694.3	2 × 2	0.3 MHz / 0.1 pm
Rh6G-Dye	cw	*	< 2	*
Ti-Sa	pulsed	700–1000	< 2	>1 THz / >200 nm
Solid state	cw /pulsed	**	< 2	MHz to GHz
Nd:Yag	pulsed	1064	< 10	10 kHz / 0.3 pm
CO_2	pulsed	10600	> 3 × 3	50 MHz / 1 nm
Notes	* = depends on the pump laser and dye ** = depends on the laser material		*** = mainly multimode	

7.0.2 Near field and far field

Close to the origin, electromagnetic waves change characteristics. With respect to lasers, this affects the intensity distribution, shape, and collimation. Because the near-field area for most systems lies within micrometers, the near-field behavior is not important for the application of lasers to practical tasks. All measurements described hereafter deal with far-field signals.

7.0.3 Considerations

The term "laser" is an abbreviation for "light amplification by stimulated emission of radiation." The bandwidth of laser signals is often defined in Hertz instead of wavelength, and the conversion is calculated by $\nu = c_0/\lambda$. Bandwidths are calculated by $[\delta\nu/\nu] = [\delta\lambda/\lambda]$.

The deviation of laser beams is primarily defined in milliradians (mrad). The rad defines the arc measure of an angle; a full circle of 360 deg consists of 6.283 rad (2π, rounded). One degree equals to 0.174533 rad, and 1 rad equals to 57.29578 deg. One mrad corresponds with 0.0573 deg. The deviation of laser beams may be different in the vertical and the horizontal axis. If so, it is normally defined by the supplier.

The spectral purity (monochromaticity) of laser light is defined by the system's mode selection. If only one mode is coupled out and enters the beam, it is called single mode or TEM_{00}. The linewidth of that beam will be in the

range of kHz to MHz at the expense of power. The combination of several very nearby or overlaid modes into a narrow band produces a spectral signal in the upper MHz range or more. Single-mode lasers provide the best collimation and smallest beam size. Continuous wave models typically show narrower output signals compared to pulsed systems: the shorter the pulse is, the wider the bandwidth.

Required measurements depend on the future applications planned. The spread and power distribution of the laser lines may be important, or the exact position of the examined line and its shape, polarization, and bandwidth. That can be done by stationary spectral analysis. The spatial distribution is another task, requiring 2D data collection, and/or hyperspectral data acquisition. The behavior of a single pulse in comparison with the average may be important. Those three different applications require different equipment. Some of the parameters may exceed the access of dispersive spectrometer systems.

7.1 Measurements in the UV–Vis–NIR Range

7.1.1 Spectral analysis of lasers with single or rather distant lines, and small beam cross section (like He-Ne, argon ion, or other gas lasers)

The lower the repetition frequency and the pulsewidth of a laser is, the better defined the pump/emission processes. The number of modes that create a "laser line" drops to the minimum at cw operation. The bandwidth will be minimal if TEM_{00} is selected. In those cases, the beam cross-section is smaller than a millimeter and shows little divergence. However, it may contain high light density —even the total power distribution may be in the milliwatt range. One spectroscopic problem may be that the beam size and its divergence do not fit any spectrometer or imaging systems. Every kind of optical beam widening and fit to the requirements of the measurement system may modify the true beam behavior. A general solution to that dilemma is a setup like that shown in Fig. 7.1.

Laser beams with a small diameter and negligible divergence angles cannot easily be coupled into spectrometers without a remarkable change of characteristics because the conversion from a thin collimated beam into the cone—required by the spectrometer for proper performance (see Chapter 2 in *Fundamentals*[3])—would call for beam widening and refocusing under the spectrometer's acceptance angle. A good solution is fiber coupling with a tapered entrance. For beams below a 2-mm cross-section, a taper providing a 10:1 reduction can be applied (see Section 6.7.5.1 in *Fundamentals*[3]). As shown in Fig. 7.1, the fiber's entrance angle will be tilted to the requirements of the fiber material according to the following equation:

$$n_0 \times \sin\alpha = (n_2^2 - n_1^2)^{1/2}, \tag{7.1}$$

where n_0 is the refractive index of the external medium (most likely, air = 1), α is the maximum accepted angle of entry light with regard to the center axis

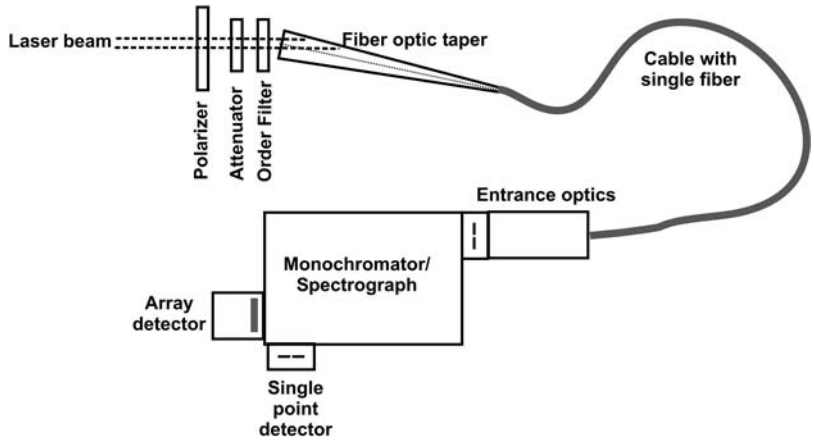

Figure 7.1 Typical setup for the spectral analysis of laser beams.

of the core, n_1 is the refractive index of the core material, and n_2 is the refractive index of the cladding material.

The resulting 200-μm single fiber delivers the light into the spectrometer via coupling optics. Because the polarization of the original signal will often be of interest, a polarizer will be the first component in the chain. A neutral attenuator will follow, which protects the fiber and spectroscopy system from excess power. An order-sorting or band filter will prevent obscure signals from reaching the spectrometer. A setup like this will not maintain any spatial information in the laser beam; it will represent the summarized signal. Alternative collection systems, such as integrating spheres, will behave similarly.

7.1.1.1 Required working range and bandwidth/resolution of the spectrometer

With some exceptions, the bandwidth of laser signals are as narrow as or narrower than the bandwidth of midclass dispersive spectrometers. The examples in Table 7.1 present some multimode systems with 0.1−1-nm bandwidths emitting in the VUV through NIR range. If the exact position of the lines is the goal, the bandwidth of the spectrometer must be at least 5 times narrower, leading to a 0.02–0.2-nm experimental bandwidth. With single-point detectors, that is the typical performance of a half-meter monochromator. Attaching a 2D-CCD with 13-μm pixels to widen the application range and shorten the experiment time will require a 0.75- or 1-m spectrometer if bandwidths below 0.05 nm are targeted. A single-stage system equipped with a UV−Vis and an NIR detector, will cover <200−1600 nm, or even more, probably with two fiber sets. If VUV lasers are analyzed, the entire system may sit in vacuum or a purged environment. If so, the detector should be cooled by water circulation and equipped with a scintillator. The light guide could be a major problem. The standard fiber must be replaced with a solid

and fixed VUV model. Above 1100 nm, purging is also advantageous to avoid misinterpretation of spectra, disturbed by water absorption. If 2500 nm are exceeded, a NIR and IR fiber material may be required (see Section 6.7.2 in *Fundamentals*[3]).

7.1.1.2 High-resolution, single-stage spectrometer limits

Analysis of the spectral distribution of a single peak requires another class of spectrometers. An unknown line shape calls for at least 20 data points across the "line" bandwidth (see Section 2.6.6.2, Fig. 2.17 of *Fundamentals*[3]). The analysis of a 0.1-nm FWHM peak needs a spectrometric bandwidth of 5 pm, whereas single-mode signals create much narrower lines. The limiting resolution of a grating is defined by $R = m \times W/k$. For a grating with 1800 mm^{-1} and $W =$ 120 mm, $R = 2 \times 10^5$ (rounded). At 500 nm, that would be 2.5 pm, which is not enough to resolve most TEM_{00} lines. Therefore, the longest commercially available single-stage dispersing spectrometers is considered here, comprising a 1.5-m focal length, double pass, and Echelle gratings (i.e., 316 mm^{-1} and a blaze of 63 deg). A 220-mm-wide Echelle in the 11^{th} order has a limiting resolution of $R =$ 7.65×10^5, which results in 0.6 pm in single-pass operation. Running in double pass with a single-point detector at 10-μm slits, the minimum spectrometer bandwidth will be ~0.08 pm at 200 nm in 29^{th} order, ~0.34 pm at 500 nm in 11^{th} order, ~0.48 pm at 800 nm in seventh order, and ~2 pm at 1600 nm in third order. Even that bandwidth will not be enough to fully analyze single-mode laser signals. If the CCD mentioned earlier is applied, the measured bandwidth numbers will increase by a factor of 3–4. For a higher resolution, several solutions can be considered.

7.1.1.3 Ultra-high-resolution spectrometers

Littrow and Ebert spectrometer concepts allow structures with rather large focal lengths. For instance, if the Echelle used for calculations earlier were utilized in a 10-m Littrow or Ebert, it would provide between a 0.03-pm (at 200 nm) and 0.19-pm (at 800 nm) bandwidth within a 13-μm slit or pixel size. That arrangement will satisfy many or even most single-mode signals, but not all. Such a system will, of course, require an extremely quiet and thermally stable environment; it is not suitable for standard labs or factories. The aperture ratio of a 10-m system with 110-mm standard optics would be ~*f*/100, or 0.63 deg (roughly 11 mrad), which may either fit the laser beam or need a little beam treatment. Spectrometer systems originally designed for Brillouin spectroscopy, as described in Section 6.5.2.4, may also perform full analysis of monomode laser signals. Compared to very long single-stage spectrometers, they have advantages and disadvantages, and require a dedicated environment.

7.2 Fabry–Pérot Interferometer

The Fabry–Pérot interferometer (FPI) is, in principle, identical to a laser cavity. Two parallel semi-transmitting mirrors create constructive/destructive

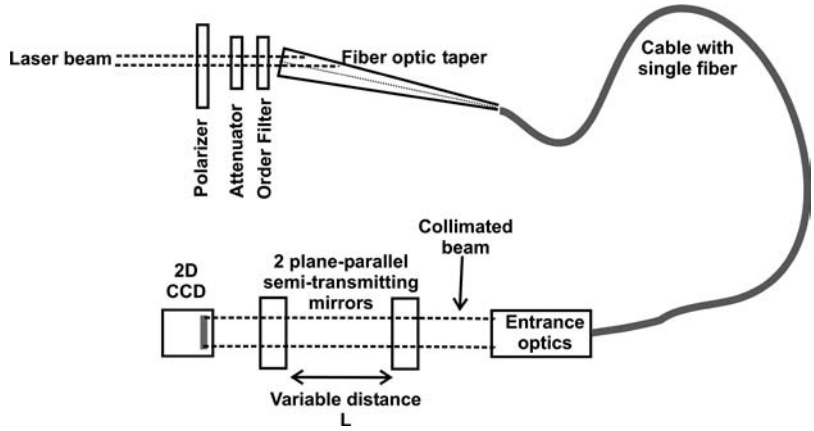

Figure 7.2 Typical interferometer for narrow laser signals.

interference patterns on the incoming collimated light on the screen opposite the entrance. Measurement and data reduction of the patterns allows one to define the spectral position and bandwidth.

The system (Fig. 7.2) utilizes the same entrance optics as the spectrometer system, but instead of requiring refocused light in front of the analyzing setup, it provides a collimated entrance beam to the FPI. The interferometer consists of two semi-transparent mirrors, creating the interference pattern that finally illuminates a 2D-CCD detector. The distance L between the mirrors is controlled by a stepper motor and sets them at a distance that provides the strongest (sharpest) interference pattern. The longer distance L is, the better the resolution. The distance represents the frequency between two constructive interferences. The front-end filtering must ensure that no second line can obscure the patterns. The wider the diameter of the collimated beam is, the better the contrast.

Along the red line in Fig. 7.3, the intensity data are converted into the curve. A line array at the right position would suffice, but a 2D detector is much more convenient because it presents the full pattern. The parameter F defines the "finesse," which is calculated from the ratio of distance between the patterns and their resolution at FWHM. The parameter Δf represents the limiting resolution. It is given by the speed of light c, the refractive index (RI) of the mirror material or its coating, and the distance L. Assume an FWHM bandwidth of 1 kHz, L of 1 m, and RI of 2.5:

$$\Delta f = (3 \times 10^8\,\mathrm{m/s})/(2 \times 2.5 \times 1\,\mathrm{m}) = 3/5 \times 10^8\,\mathrm{s}^{-1}, \text{ or } 800\,\mathrm{MHz}.$$

This number is the "internal frequency" of the FP cavity. 500 nm is equivalent to 30 GHz, and $(30 \times 10^8$ /s) / $(1 \times 10^3$ /s) leads to a resolution of 3×10^6, or 0.15 pm. Again, that level will satisfy many single-mode laser lines but not all. The performance is close to that of the single spectrometer described earlier, with a smaller footprint and lower costs but more-

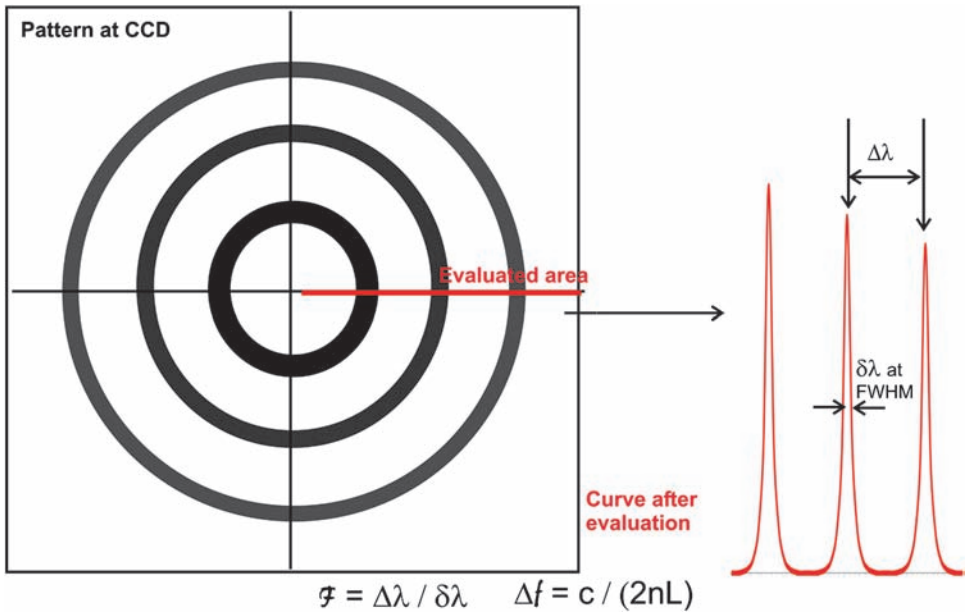

Figure 7.3 Typical circular interference pattern at the CCD.

complicated filtering. A better resolution would require wider optics and longer distance, which requires excessive work toward precision and stability.

7.3 Spectral Measurements of Large Laser Images

If the laser beam illuminates an area with a diameter wider than ~3 mm, it is rather easy to widen the beam and refocus it into the spectrometer or put it into a wide parallel shape for an interferometer. This setup can be achieved by classical lens or mirror systems, removing the fiber optics from the system; the other components will remain. The considerations of spectral resolution remain the same.

7.4 Imaging Analysis

A 2D detector with a 13-μm pixel size requires an illuminated area with a ~1−1.5-mm cross-section, which will divide the area into ~100 data points in both dimensions. If that number is sufficient, the front-end optics, such as the polarizer and filters, may be kept, while the laser beam can travel straight through. For beams larger than the detector surface of 26 mm × 26 mm, a linear compression is required by applying standard optics. This kind of imaging analysis provides the intensity distribution of the beam within the bandwidth of the front-end filter. Beams with a rather small cross-section (which do not require fine spectral analysis) may be collected by a honeycomb fiber system (see Section 5.4, Fig. 5.5 of *Fundamentals*[3]), comprising optical

channels with a 10-μm diameter or even less. The Rayleigh diffraction limit [Eq. (2.23 of *Fundamentals*[3])] must be respected at the entrance. Because the detector pixels may be wider, either the data may be convolved or the fiber bolt may be made of tapered material to widen the output aperture.

7.5 Hyperspectral Analysis

If, in multimode or wide-bandwidth laser beams, both the wavelength and intensity vary over the illuminated area, then hyperspectral analysis can be the analysis tool, as described in Section 4.5 of *Fundamentals*[3]. At this point, the beam management plays a key role. The taper/single-fiber light transfer described thus far will not maintain the spatial information. Beams wider than about a 1-mm diameter can be widened or compressed in linear fashion by precision optics. For diameters below 0.3 mm, three solutions can be considered. Special commercial imaging systems are offered by manufacturers as an accessory to commercial lasers. Moving pinholes, providing spatial resolution close to the Rayleigh diffraction limit, may be precisely placed into the beam between the source and the entrance optics, while the rest of the system works according to Fig. 7.1. The spectra taken at each spatial position combine the spectral distribution and intensity.

7.5 Commercial Analysis Systems

For many commercial laser systems, dedicated analysis systems for both spectroscopy and imaging are offered as accessories. If that is the case, it may be a good idea to consider such equipment even if they may not be useful for general spectroscopy.

References

1. P. W. Milonni and J. H. Eberly, *Lasers*, John Wiley and Sons, New York (1988).
2. W. T. Silfvast, "Lasers," *Handbook of Optics*, Michael Bass, ed., OSA, Washington, D. C. (1995).
3. W. Neumann, *Fundamentals of Dispersive Optical Spectroscopy Systems*, SPIE Press, Bellingham, WA (2014) [doi: 10.1117/3.1002528].

Index

Wilfried Neumann was born in 1945 in a small township south of Frankfurt, Germany. After graduating from high school, he was educated in radio and TV electronics. After working in the R&D department of Hottinger-Baldwin-Messtechnik GmbH (in the field of mechanical stress analysis), he attended a college for electronics, high-frequency technology, and computer hardware and software. He earned a degree as an approved technician in 1973.

Neumann based his career on signal recovery and optical spectroscopy. He worked in the service, application, sales, and marketing of several pertinent international companies. Early on, he worked in service and applications at Perkin-Elmer (analytical instruments) and Varian (optical spectroscopy, now part of Agilent). Between 1977 and 1989, he was an area sales representative at EG&G Instruments (signal recovery and optical spectroscopy). In 1989, he managed the new division of optical spectroscopy at LOT-Oriel GmbH, a distribution company in the field of technical optics and lasers. One of the companies he marketed in Germany was SOPRA, Inc. (Paris, France), a spectroscopy company; the division developed quickly, and in 1991, Neumann became the founder, shareholder, and CEO of a new branch called SOPRA GmbH. In 2000, he joined Roper Scientific GmbH, the German branch of Roper's CCD and optical imaging and spectroscopy business, headed by Princeton Instruments. He served as area sales and product manager for special, research-oriented spectroscopy systems.

After his retirement from regular work in 2005, Neumann started a consulting office, offering spectrometer system maintenance and service, as well as consultation, justification, design, and construction for optical spectroscopy and radiometry. To support this endeavour, and because comprehensive literature on the basics of dispersive optical spectroscopy did not exist, he created a website (www.spectra-magic.de) that has since become a popular online resource.